# FEEDER RECONFIGURATION SCHEME WITH INTEGRATION OF RENEWABLE ENERGY SOURCES USING A PARTICLE SWARM OPTIMISATION METHOD

**By**

GIRESSE FRANCK NOUDJIEP DJIEPKOP

**Thesis submitted in partial fulfilment of the requirements for the degree Master of Engineering:** Electrical Engineering

**In the Faculty of** Engineering

**At the Cape Peninsula University of Technology**

**Supervisor :** Dr. Senthil Krishnamurthy
**Co-supervisor:** Prof. Raynitchka Tzoneva

**Bellville**
September 2018

# DECLARATION

I, Giresse Franck Noudjiep Djiepkop, declare that the content of this thesis represents my own unaided work and that this thesis has not been previously submitted for academic examination towards any qualification. Furthermore, it represents my own opinions and not necessarily those of the Cape Peninsula University of Technology.

**Signed** **Date**

# ABSTRACT

A smart grid is an intelligent power delivery system integrating traditional and advanced control, monitoring, and protection systems for enhanced reliability, improved efficiency, and quality of supply. To achieve a smart grid, technical challenges such as voltage instability; power loss; and unscheduled power interruptions should be mitigated. Therefore, future smart grids will require intelligent solutions at transmission and distribution levels, and optimal placement & sizing of grid components for optimal steady state and dynamic operation of the power systems. At distribution levels, feeder reconfiguration and Distributed Generation (DG) can be used to improve the distribution network performance. Feeder reconfiguration consists of readjusting the topology of the primary distribution network by remote control of the tie and sectionalizing switches under normal and abnormal conditions. Its main applications include service restoration after a power outage, load balancing by relieving overloads from some feeders to adjacent feeders, and power loss minimisation for better efficiency. On the other hand, the DG placement problem entails finding the optimal location and size of the DG for integration in a distribution network to boost the network performance. This research aims to develop Particle Swarm Optimization (PSO) algorithms to solve the distribution network feeder reconfiguration and DG placement & sizing problems. Initially, the feeder reconfiguration problem is treated as a single-objective optimisation problem (real power loss minimisation) and then converted into a multi-objective optimisation problem (real power loss minimisation and load balancing). Similarly, the DG placement problem is treated as a single-objective problem (real power loss minimisation) and then converted into a multi-objective optimisation problem (real power loss minimisation, voltage deviation minimisation, Voltage stability Index maximisation). The developed PSO algorithms are implemented and tested for the 16-bus, the 33-bus, and the 69-bus IEEE distribution systems. Additionally, a parallel computing method is developed to study the operation of a distribution network with a feeder reconfiguration scheme under dynamic loading conditions.

**Keywords**: Feeder reconfiguration, distribution network, Distributed Generation, Power loss minimisation, Load balancing, Optimization methods, Particle Swarm Optimization, Parallel computing, and Smart grid

## ACKNOWLEDGEMENTS

My foremost and tremendous appreciation goes to my supervisor, **Dr. Senthil Krishnamurthy**, for his guidance, advice, and contribution to this research work.

Also, I would like to express my gratitude to **Prof. Raynitchka Tzoneva** and **Prof. Alexander Apostolov**, for their feedback and suggestions were instrumental in improving this research work.

I am grateful to my family and friends for their patience, support, and motivation.

I am thankful to my colleagues from the Centre for Substation Automation and Energy Management Systems (CSAEMS), CPUT staff members, librarians, and laboratory technicians for their assistance for the successful completion of this thesis.

Lastly but not least, I am thankful for the financial support from ESKOM TESP, DST/NRF, the and CPUT.

# TABLE OF CONTENTS

**CHAPTER FOUR:** OPTIMAL PLACEMENT AND SIZING OF DISTRIBUTED GENERATORS IN DISTRIBUTION SYSTEMS

## LIST OF FIGURES

## LIST OF TABLES

## LIST OF APPENDICES

## ACRONYMS

| | |
|---|---|
| A* | : A star. It is a special case of the Best-First Search optimisation method. |
| ABC | : Artificial Bee Colony |
| ACO | : Ant Colony Optimization |
| AFC | : Alkaline Fuel Cells |
| AI | : Artificial Intelligence |
| AIS | : Artificial Immune Systems |
| ALU | : Arithmetic Logic Unit |
| AMPL | : A Mathematical Programming Language |
| AMPSO | : Adaptive Mutation Particle Swarm Optimization |
| ANN | : Artificial Neural Networks |
| APSO | : Adaptive Particle Swarm Optimization |
| BeFS | : Best First Search |
| BIP | : Binary Integer Programming |
| BPSO | : Binary Particle Swarm Optimization |
| BrFS | : Breadth First Search |
| CCHP | : Combined Cooling, Heat and Power |
| CGA | : Clonal Genetic Algorithm |
| CHP | : Combined Heat and Power |
| CPM | : Capacity Planning Model |
| CPU | : Central Processing Unit |
| DE | : Differential Evolution |
| DeLS | : Depth-Limited Search |
| DEPSO | : hybrid of Differential Evolution and Particle Swarm Optimization |
| DFS | : Depth-First Search |
| DG | : Distributed Generation |
| DLP | : Data Level Parallelism |
| DMFC | : Direct Methanol Fuel Cells |
| DP | : Dynamic programming |
| DQPSO | : Decimal Encoding to Quantum Particle Swarm Optimization |
| DSO | : Distribution System Operator |
| EA | : Evolutionary Algorithm |
| EP | : Evolutionary Programming |
| EPSO | : hybrid of Evolutionary programming and Particle Swarm Optimization |
| ES | : Expert System |
| FAPSO | : Fuzzy Adaptive Particle Swarm Optimization |
| FC | : Fuel Cells |

| | |
|---|---|
| FIPSO | : Fully Informed Particle Swarm Optimization |
| FLISR | : Fault Location, Isolation and Service Restoration |
| GA | : Genetic Algorithm |
| GAMS | : General Algebraic Modeling System |
| GA-PSO | : hybrid of Genetic Algorithm and Particle Swarm Optimization |
| HBB-BC | : Hybrid Big Bang-Big Crunch |
| HBMO | : Honey Bee Mating Optimization |
| HSA | : Harmony Search Algorithm |
| IDS | : Iterative Deepening Search |
| IEEE | : Institute of Electrical and Electronic Engineer |
| ILP | : Instruction-Level Parallelism |
| IP | : Integer Programming |
| IPSO | : Improved Particle Swarm Optimization |
| ISFLA | : Improved Shuffled Frog Leaping Algorithm |
| IWD | : Intelligent Water Drop |
| KBS | : Knowledge-Based System |
| LBI | : Load Balance Index |
| LP | : Linear Programming |
| LSF | : Loss Sensitivity Factor |
| LV | : Low Voltage |
| MATLAB | : Matrix Laboratory |
| MCFC | : Molten Carbonate Fuel Cells |
| MDCE | : MATLAB Distributed Computing Engine |
| MDCS | : MATLAB Distributed Computing Server |
| MHBMO | : Multi-Objective Honey Bee Mating Optimization |
| MIHDE | : Mixed Integer Hybrid Differential Evolution |
| MILP | : Mixed- Integer Linear programming |
| MIMD | : Multiple Instruction Multiple Data |
| MINLP | : Mixed- Integer Nonlinear programming |
| MINOS | : Modular In-core Nonlinear Optimization System |
| MIP | : Mixed Integer Programming |
| MISD | : Multiple Instruction Single Data |
| MJS | : MATLAB Job Scheduler |
| MOLP | : Multi-Objective Linear Programming |
| MONLP | : Multi-Objective NonLinear Programming |
| MOPSO | : Multi-Objective Particle Swarm Optimization |
| N/A | : Not Applicable |
| NSGAII | : Non-dominated Sorting Genetic Algorithm II |

NUMA : Non-Uniform Memory Access

PAFC : Phosphoric Acid Fuel Cells

PCU : Processing Control Unit

PEMFC : Proton Exchange Membrane Fuel Cells

PQ : Real-Reactive Power

PSO : Particle Swarm Optimization

PU : Processing Unit

PV : Photo Voltaic

QP : Quadratic Programming

SA : Simulated Annealing

SEM : Switch Exchange Method

SIMD : Single Instruction Multiple Data

SISD : Single Instruction Single Data

SOFC : Solid Oxide Fuel Cells

SPM : Siting Planning Model

SPMD : Single Program Multiple Data

SSOM : Sequential Switch Opening Method

TLP : Task Level Parallelism

TSD : Technology Standardization Department

UCS : Uniform Cost Search

UDVA : Uniform Voltage Distribution based constructive reconfiguration Algorithm

UMA : Uniform Memory Access

VA : Volt-Ampere

Var : Volt-Ampere Reactive

VSI : Voltage Stability Index

# CHAPTER ONE
# INTRODUCTION

## 1.1. Introduction

Modern electrical power distribution networks face numbers of technical challenges such as voltage instability, power losses, unscheduled power interruptions, and grid reliability. These challenges must be dealt with to ensure optimal operation of the grid, to avoid a poor quality of supply and consequently a financial loss to consumers. The energy demand is continuously growing, and power lines become overloaded. Thus, it is challenging to keep up with the electrical energy demand by building centralised power plants due to financial, environmental or technical limitations. The reconfiguration of distribution networks and the integration of distributed generation at distribution levels can be used to overcome some of the power grid challenges. Feeder reconfiguration is a subsystem of distribution automation, and it consists of deploying switching devices, high-speed communication devices and software scheme to restructure the distribution network for enhanced system reliability and improved customer service. Integrating Distributed Generation at distribution levels is an alternative solution to the ever-expanding energy demand. DG also serves to improve the reliability of the distribution network at end-user points. Many optimisation algorithms have been used to provide optimised feeder reconfiguration and DG placement solutions. Some of such algorithms include the Genetic Algorithm (GA), the Differential Evolution (DE), and the Particle Swarm Optimization (PSO)

This research work develops PSO optimisation algorithms to find the solutions of both the optimal distribution network feeder reconfiguration and the optimal DG placement & sizing problems. This chapter covers the awareness of the research problem, the motivation of the research, the problem statement, the research aim, the objectives of the research, the hypothesis; delimitations and assumptions of the research, and finally the research design and methodology.

## 1.2. Awareness of the research problem

The history of electrical power systems is marked by notable blackouts such as the 1999 Southern Brazil blackout (95 million people affected) (Yu & Pollitt, 2009), the August 18, 2005 blackout in Indonesia (100 million people affected), the July 31, 2012 Northern and Eastern blackouts in India (620 million people affected) and the January 26, 2015 blackout in Pakistan where an estimated 80% of the population (160 million people) were affected. Whatever their causes, these blackouts raise questions about the reliability, the robustness and the security of power grids, and thus prompt the move towards smart grids. The smart grid emphasises the development of a self-healing, auto-balancing, and self-monitoring electrical system for reliable power delivery and with minimal human intervention (Gers, 2013). A smart grid should be able to sense disturbances in its network, to clear those disturbances, to reroute the power to prevent a power outage situation, and to enable real-time communication between the consumers and utilities for optimum energy use. With the global energy demand likely to grow at a rate of 1.4% per year until 2020 (Oluwole, 2016), electrical networks will face increased burden, reduced voltage stability, which may lead to an increased risk of bus or grid collapse. Therefore, there is a need to devise solutions to mitigate such problems, where the importance to develop algorithms for optimal distribution network feeder reconfiguration and optimal placement & sizing of Distributed Generation in distribution networks.

## 1.3. Motivation of the research

Traditionally, electricity is generated at central power plants, far from the points of consumption. Thus, the power system needs an infrastructure to transmit and distribute the electricity to the consumers. The long-distance transmission and the eventual distribution of the electricity to consumers result in large power losses in the power system. The percentage of power lost at distribution levels alone is evaluated to be approximately 13% of the power generated (Darfoun, 2013). Reconfiguring the topology of the distribution networks can reduce the power losses for up to 50%. Moreover, the continuously increasing load demand requires power producers to generate more electricity. However, given that the power grid was designed to operate within certain limits, the increase of the power demand might lead to the overloading of the distribution networks. Additional generation capacities, transmission, and distribution lines may be needed. The building of new power generation, transmission and distribution infrastructure appears to be impracticable, due to economic and environmental constraints. An alternative solution is to integrate DG directly at distribution levels. The connection of DG directly at the point of consumption provides the additional power needed by the consumers, improve the bus voltage levels, and reduce the power loss in the distribution networks. However, power utilities are concerned that the reconfiguration of distribution networks and the integration of DG may negatively impact on the reliability, the security of the distribution networks and the quality of the power supply of the distribution network. Therefore, the incentive of this research is to develop new optimisation algorithms to solve the optimal distribution network feeder reconfiguration and the optimal DG placement & sizing problems.

## 1.4. Problem statement

With the recent developments in hardware, software and communication technologies, a more consistent, healthy and efficient power system with moderate contingency margins is made possible. Computational intelligence methods are being developed to enhance the capabilities of distribution systems and the quality of supply. The reconfiguration of distribution network feeders and the placement Distributed Generation in distribution networks are two important methods to improve the efficiency and the operation of distribution networks. At distribution levels, loads are usually unbalanced due to the presence of asymmetrical line segments and the combination of single and three phase loads in the system. Moreover, these loads have an intermittent nature as they depend on the time, day and weather conditions. Therefore, there is a need to relocate the loads (load balance) from heavily loaded feeders to lightly loaded adjacent feeders and to minimise the real power loss in the distribution network. In addition, DG can be deployed at distribution levels to improve the efficiency and the overall performance of distribution networks.

The research problem is to:

- Develop a Particle Swarm Optimization (PSO) solution algorithm to determine the sequence of switches (tie and section switches) states which correspond to an optimal distribution network topology for both the minimisation of real power loss and load balancing.
- Develop a PSO solution algorithm for optimal allocation and sizing of Distributed Generation in distribution networks.
- Develop a sequential and parallel computing solution for the distribution network feeder reconfiguration problem under dynamic loading conditions.

## 1.5. Research aim and objectives

Distribution automation will play an important role in future smart grids as it will contribute to better performance, more effective communication; measurement; and monitoring at generation, transmission, and distribution levels.

This project aims to develop PSO solution algorithms to improve the operation and the performance of distribution networks through optimal feeder reconfiguration, and optimal deployment & sizing of DG in distribution networks.

Currently, the distribution network topology is restructured through human intervention during planned maintenance by changing the status of the section and tie switches in the distribution system.

The objectives of this research are:

- To review the principles of optimisation, some optimisation methods, and their application to the distribution network feeder reconfiguration and the optimal Distributed Generation placement and sizing problems.
- To mathematically formulate the single-objective distribution network feeder reconfiguration problem for minimisation of the real power loss in distribution networks.
- To mathematically formulate the multi-objective distribution network feeder reconfiguration problem for the minimisation of real power loss and optimal load balancing.
- To develop PSO algorithms to solve the single and multi-objective feeder reconfiguration optimisation problems.
- To mathematically formulate the single-objective optimal Distributed Generation placement & sizing problem for real power loss minimisation.
- To mathematically formulate the multi-objective optimal Distributed Generation placement & sizing problem to minimise the real power loss, to improve the voltage profile, and to maximise the Voltage Stability Index (VSI) of distribution networks.
- To develop a PSO solution algorithm for the single-objective and multi-objective Distributed Generation allocation & sizing problem.
- To compare the effectiveness of distribution network feeder reconfiguration and optimal Distributed Generation placement in minimising the real power loss in distribution networks.
- Investigate the application of parallel computing in distribution network feeder reconfiguration under dynamic loading conditions.

## 1.6. Hypothesis

The operation and the performance of distribution networks can be improved through the reconfiguration of distribution feeders and the deployment of Distributed Generation. A complete feeder reconfiguration scheme should be operated automatically, i.e. with minimal human intervention.

The hypothesis is to develop new PSO optimisation methods which provide an optimal distribution network topology through feeder reconfiguration; and optimal DG placement and sizing to ensure a better voltage profile and minimise the real power loss in the distribution networks.

## 1.7. Delimitation of the research

The following limitations apply to this research project:

- The research work does not cover the capacitor bank placement problem for power loss minimisation in distribution networks.
- Energy management problems such as economic dispatch and voltage stability problems at the generation and transmission levels are not considered.
- Only the Particle Swarm Optimization method is used to solve the distribution network feeder reconfiguration and the optimal DG placement and sizing problems. Other optimisation approaches such as the Differential Evolution (DE), the Genetic Algorithm (GA), and the Simulated Annealing (SA) are not considered in this research work.
- Only the real power losses in the distribution lines are considered. Losses in equipment such as PV generator or Distributed Generation are not considered.
- No DG types are prioritised. The best DG type is only known at the end of the DG placement optimisation.
- The loads in the network can be either static or dynamic.
- The distribution systems used in the case studies are limited to radial networks.
- The testing of the algorithms is strictly done in a simulation environment. No hardware implementation is considered.
- Real-time data are not used in the simulations.
- The Fault Location, Isolation and Service Restoration (FLISR) scheme is not part of this research work

## 1.8. Assumptions

The following assumptions are considered:

- The input data (parameters) of the distribution networks under study are known.
- The distribution lines have a fixed line impedance.
- The MATrix LABoratory (MATLAB) software is used for the development of the PSO algorithms.
- The power loss in switching devices (section and tie switches) and generators (PV, Wind, Diesel…) is negligible.
- The data of the current carrying capability of individual branches in the IEEE 16, 33 and 69-bus distribution networks are not available. Therefore, it is assumed that all the branches in each distribution network have the same power rating
- The reconfiguration scheme is only applied to the primary distribution feeders of the distribution system.

- Only one Distributed Generation can be connected at a given PQ bus during the optimisation process.
- Distributed Generation cannot be placed at the source of the network as placing the DG at the source would no contribute to the minimization of the power loss. A DG can only be placed at a load point of connection.
- The maximum size of the DG is limited to the sum of all the loads in the distribution network.
- The Newton-Raphson power flow approach is used to find the power flow in the distribution networks during the optimisation process.
- The real power loss in the distribution network under dynamic loading conditions is dependent on the load profile of the network.
- The parallel computing application is executed in a Multiple Instructions Multiple Data processor.

## 1.9. Research design and methodology

This project aims to develop PSO solution algorithms to improve the operation and the performance of distribution networks through feeder reconfiguration and the deployment of DG.

The research design and methodology are described as follows:

- **Literature review**: A detailed literature review is carried out on diverse optimisation algorithms and their application in solving the distribution network feeder reconfiguration and the optimal Distributed Generation placement and sizing problems.
- **Formulation of the distribution network feeder reconfiguration and optimal Distributed Generation placement and sizing problems**: The single-objective distribution network feeder reconfiguration problem is formulated to minimise the real power loss in distribution networks. The multi-objective feeder reconfiguration problem is formulated to minimize the real power loss and to balance the loads in the distribution networks. The single-objective optimal DG placement and sizing problem is formulated to minimise the real power loss in distribution networks. The multi-objective optimal DG placement and sizing problem is formulated to minimise the real power loss in the distribution network, improve its voltage profile and to maximise the voltage stability index in the distribution network.
- **Development of the PSO algorithms**: the PSO algorithms are developed for both the single and multi-objective optimal distribution network feeder reconfiguration and DG placement & sizing problems

- **MATLAB software program**: MATLAB programs are developed for implementation of the PSO algorithms to find the solution of the single and multi-objective distribution network feeder reconfiguration and optimal DG placement and sizing problems.
- **Performance analysis of the developed algorithms**: the developed PSO algorithms are implemented in the MATLAB environment to solve the optimal distribution network feeder reconfiguration and the optimal DG placement and sizing problems for the IEEE 16-bus, 33-bus, and 69-bus distribution networks.
- **Development of the parallel computing method**: a data-parallel computing method is developed to determine how the IEEE 16-bus distribution network with a feeder reconfiguration scheme performs under dynamic loading.

The flowchart of the research design is shown in Figure 1.1.

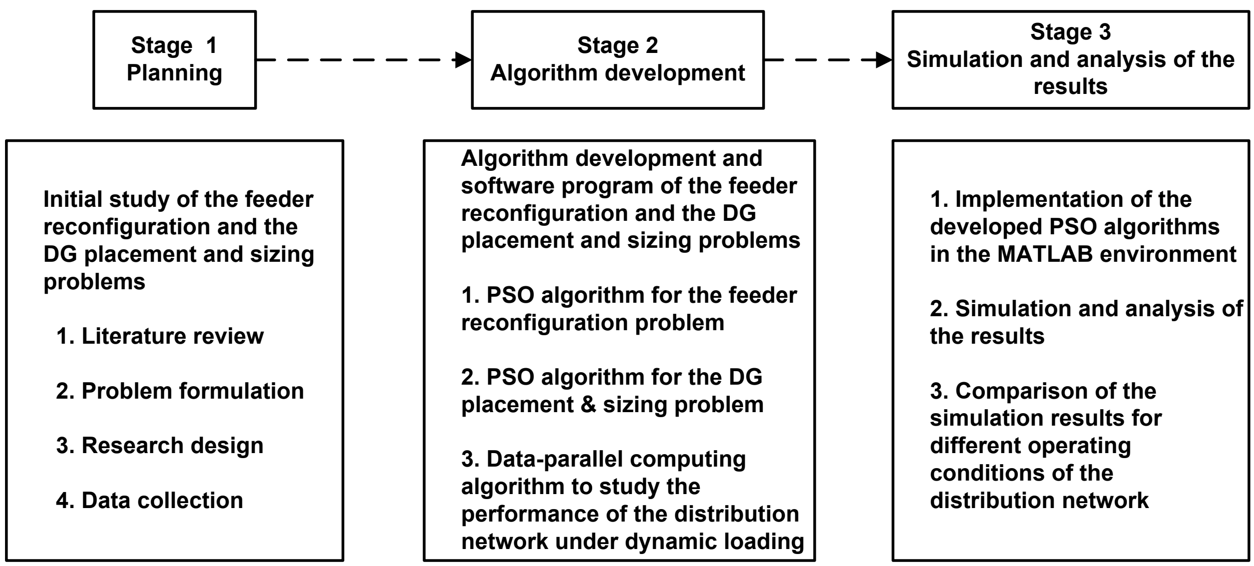


**Figure 1.1**: Research design

## 1.10. Conclusion

This chapter provides the summary of the thesis outline, and the contribution of the thesis such as the PSO algorithm development to solve the distribution network feeder reconfiguration and the Distributed Generation placement and sizing problems; and the development of a parallel computing algorithm to study the distribution network with a feeder reconfiguration scheme under dynamic loading conditions. The overview, the awareness, the motivation, the research problem, the aim and objectives of the research, the hypothesis, the assumptions, and the delimitations of the project are also provided.

The next chapter presents the literature review of the optimisation methods used in power systems applications to solve the optimal distribution network feeder reconfiguration and the Distributed Generation placement and sizing problems.

# CHAPTER TWO
# LITERATURE REVIEW

## 2.1. Introduction

The primary purpose of the reconfiguration of distribution network feeders is to restore as many loads as possible by relocating critical loads from out-of-service feeders to adjacent healthy feeders. The reconfiguration of distribution network feeders is also used to improve the operating conditions of distribution networks, either by balancing the loads or by minimising the power loss. Although many other methods can be used for load balancing of power loss reduction, feeder reconfiguration remains the preferred choice since it does not require the installation of extra equipment and it is cost effective. It involves the switching of tie and section switches to alter the topology of the distribution system while preserving the radial topology of the distribution network. Additionally, Distributed Generation is being investigated to enhance the performance, the efficiency, and the robustness of distribution networks. Optimal allocation of DG is done to find the right DG size and the best location for which the integration of DG would result in improved performance. Placing the DG at a non-optimal position may negatively affect the operation of the distribution network. Some research works have been done to improve the operation and performance of distribution networks using optimal distribution network feeder reconfiguration and DG deployment.

This chapter reviews and analyses the existing knowledge on distribution network feeder reconfiguration and DG placement. It is divided into nine parts, organised as follows:

- Part 1 provides the introduction of the literature review.
- Part 2 provides an overview of the concept of single-objective and multi-objective optimisation.
- Part 3 provides an overview of the different computation techniques and optimisation methods used to find the solution of the distribution network feeder reconfiguration problem.
- Part 4 reviews the existing literature on distribution network feeder reconfiguration.
- Part 5 analyses and compares the literature review on distribution network feeder reconfiguration.
- Part 6 reviews the existing literature on optimal DG placement and sizing.
- Part 7 analyses and compares the literature review on optimal DG placement and sizing.

- Part 8 is a review of existing literature dealing with both the optimal distribution network feeder reconfiguration and optimal DG placement and sizing.
- Finally, part 9 provides a conclusion made about the literature review.

## 2.2. The concept of optimisation

Optimising a problem consists of finding the maximum or the minimum of its objective function by the methodical choice of input variable from an allowed set of variables (Maringer, 2005). Depending on the number of objective functions to be optimised in a problem, optimisation problems can be categorised into two types: single-objective problems and the multi-objective problems.

### 2.2.1. Single-objective optimisation

Single-objective optimisation is a decision-making process that only involves a single-objective. Mathematically, single-objective optimisation problems are formulated as given in Equation 2.1.

$$\mathbf{min\,f(x)} \tag{2.1}$$

Subject to:

$$\mathbf{g(x) \leq 0} \qquad \mathbf{2.1.a}$$

$$\mathbf{h(x) = 0} \qquad \mathbf{2.1.b}$$

$$\mathbf{{x_i}^L \leq x_i \leq {x_i}^U} \qquad \mathbf{2.1.c}$$

Where

$\mathbf{f(x)}$ is the objective function to be optimized.

$\mathbf{x}$ is the decision variable.

$\mathbf{{x_i}^L}$ and $\mathbf{{x_i}^U}$ are the lower bound and the upper bound of $x_i$ respectively.

Equation 2.1 also applies to a maximisation problem. If the objective function and the constraints associated with the problem are linear, then the problem is a linear optimisation problem. However, most real-world problems are non-linear in nature.

A solution $\mathbf{x = [x_1, x_2, \dots, x_i]}$, defined by $\mathbf{i}$ decision variables, is a solution of the single-objective optimization problem if and only if it satisfies the equality and inequality constraints, and it lies within the decision space defined by $\mathbf{[{x_i}^L, {x_i}^U]}$. $\mathbf{{x_i}^L}$ is the lower limit of the decision space and $\mathbf{{x_i}^U}$ is the upper limit.

The set of all feasible solutions is referred to as the search space.

Any solution to the problem that does not belong to the search space is an infeasible solution. Some solutions to the optimisation problem are referred to as local optima, meaning that they are the best solution in their respective vicinity.

So, a solution $\mathbf{x_0}$ is the global optimum or optimal solution if for any variable $\mathbf{x}$ from the search space, Equation 2.2 is satisfied.

$$\begin{cases} \mathbf{f(x_0) \leq f(x)}, & \mathbf{(minimization\ problem)} \\ \mathbf{f(x_0) \geq f(x)}, & \mathbf{(maximization\ problem)} \end{cases} \tag{2.2}$$

### 2.2.2. Multi-objective optimisation

Multi-objective optimisation is a multi-criteria decision-making process involving two or more objectives to be optimised. The multi-objective optimisation algorithm finds the optimal solutions of the multi-objective problems subject to certain constraints.

#### 2.2.2.1. Overview of the multi-objective optimisation

When the objectives to be optimised are non-conflicting, meaning that minimising one of the objectives corresponds to all other objectives being also minimised, the multi-objective optimisation problem is treated as a single-objective optimisation problem.

When the objectives are conflicting, a compromise needs to be made. In this regard, a solution is optimal with respect to all objectives. This can be illustrated by the real-world problem of buying a car. Two objectives are considered in this problem: the price and the comfort of the car. The price ranges from 10 to 100 thousand Dollars while the comfort is in the range 30 to 90%. The cheapest cars are expected to be the least comfortable whereas expensive cars provide a higher level of comfort. Now, which car offers the highest level of comfort for a minimal price? This dilemma is represented in Figure 2.1 (Deb, 2001).

For poor buyers, the concern is the price of the car while the wealthy are more concerned with the comfort. So, from Figure 2.1, the best solution to the car buying problem would be solution A for a poor buyer. Solution E would be the best solution for a wealthy buyer. Between the poorest and the richest, there are middle-class buyers. Depending on their finances and the comfort preferences, middle-class buyers would go for either solution B, C or D. Solutions B, C or D represent a trade-off between the price of the car and its comfort. Amongst A, B, C, D, and E, no solution can be said to be better than the others, since the betterment of a solution in one objective come at the detriment of the other objective (Deb, 2001).

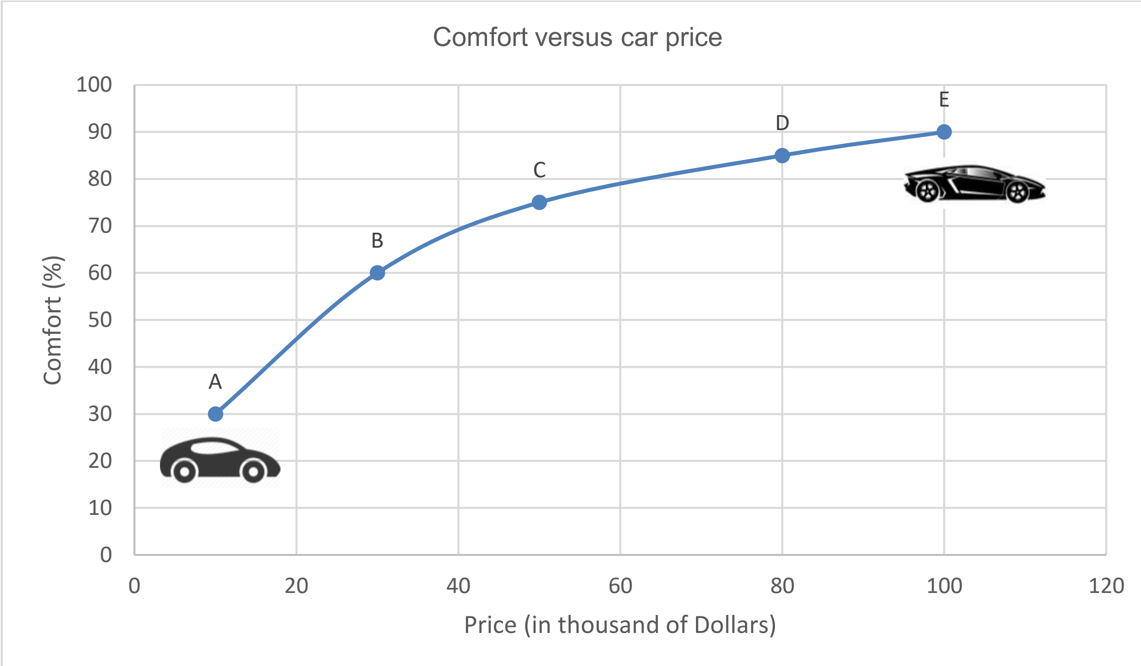


**Figure 2.1**: **Price versus comfort in a car buying decision making (Deb, 2001)**

The car buying problem described is limited to 2 objectives. However, objectives such as the colour of the car, its safety features, fuel consumption could be added to the problem, and they would make the problem even more challenging to solve. Lots of real-world problems are complex in nature, and they may have constraints that limit the solutions of the problem within specific boundaries. When solving such complex problems, most research works try to avoid the intricacy associated with them by using some user-defined parameters to convert the multi-objective optimisation problem into a single-objective problem. The weighted-sum approach can be used to convert the multi-objective problem into a single objective problem. However, this approach requires prior knowledge about the problem and the associated weight factors need to be carefully selected.

#### 2.2.2.2. Mathematical formulation of multi-objective optimisation problems

Multi-objective optimisation problems have several objectives to be minimised or maximised. Mathematically, multi-objective optimisation problems can be formulated as in Equation 2.3.

$$\mathbf{min\, f(x) = [f_1(x), f_2(x), \dots, f_n(x)]} \qquad (2.3)$$

Subject to

$$\mathbf{g_j(x) \leq 0} \qquad \mathbf{j = 1, 2, \dots, J} \qquad \text{(inequality constraint)} \qquad 2.3.\mathrm{a}$$

$$\mathbf{h_k(x) = 0} \qquad \mathbf{k = 1, 2, \dots, K} \qquad \text{(equality constraint)} \qquad 2.3.\text{b}$$

$$\mathbf{x_i{}^L \leq x_i \leq x_i{}^U} \qquad \mathbf{i = 1, 2, \dots, I} \qquad \text{(variables limit)} \qquad 2.3.\text{c}$$

Where

$\mathbf{n}$ is the number of objective functions.

$\mathbf{g_j}$ and $\mathbf{H_k}$ are the inequality and equality constraints respectively.

$\mathbf{I}$, $\mathbf{J}$, and $\mathbf{K}$ are the number of decision variables, the number of inequality constraints and the number of inequality constraints respectively.

If all the objectives and constraints of the multi-objective problem are linear, then the problem is a Multi-Objective Linear Problem (MOLP). Otherwise, the problem is a Multi-Objective Non-Linear Problem (MONLP) (De Weck & Willcox, 2010).

All the solutions of the multi-objective problem in the search space are not optimal. The optimisation of a multi-objective problem with conflicting objectives produces a set of optimal solutions. Therefore, the search space can be divided into two sets: a set $\mathbf{S_1}$ of optimal solutions (non-dominated set) and a set $\mathbf{S_2}$ of non-optimal solutions (dominated set).

The concept of dominance and non-dominance is used by the multi-objective optimisation algorithm to find the optimal solutions.

Any two solutions in $\mathbf{S_1}$ are non-dominated with respect to each other and any solution of $\mathbf{S_2}$ is dominated by at least one solution in $\mathbf{S_1}$.

Let us consider $\mathbf{u = [u_1, u_2, \dots, u_i]}$ and $\mathbf{v = [v_1, v_2, \dots, v_i]}$, two solutions of the search space. $\mathbf{u}$ dominates $\mathbf{v}$ $\mathbf{(u < v)}$ if and only if:

- $\mathbf{u}$ is no worse than $\mathbf{v}$ for all objectives i.e. $\mathbf{f_i(u) \leq f_i(v), \forall\, i = 1, 2, \dots, n}$
- $\mathbf{u}$ is strictly better than $\mathbf{v}$ for at least one objective i.e. $\mathbf{f_i(u) < f_i(v)}$, for at least one $\mathbf{i \in \{1, 2, \dots, n\}}$

The property described above is the **Pareto-dominance**. A solution $\mathrm{u}$ is **Pareto-optimal** if there is no other solution $\mathbf{v}$ in the search space in such a way that $\mathbf{f_i(v) < f_i(u)}$, for all the objectives of the problem.

The set $\mathrm{S_1}$ of all Pareto optimal (non-dominated) solutions is referred to as the **Pareto-optimal set** and the curve formed by joining all the Pareto optimal solutions together is referred to as the **Pareto-optimal front** (Caramia & Dell'Olmo, 2014).

Altogether, when the objectives of an optimisation problem are conflicting, there is no single optimal solution, but a set of solutions all optimal with respect to each other. Given that only one solution is needed for most multi-objective optimisation problems, additional information is often necessary to determine the best solution from the Pareto-optimal set. So, irrespective of the optimisation method used to solve the multi-objective problem, it is recommended first to find the Pareto-optimal set, and then find the best solution in the set by using some additional information.

## 2.3. Overview of the computational techniques and optimisation methods used to solve the distribution network feeder reconfiguration problem

The distribution network feeder reconfiguration can be used to solve the power loss minimisation problem; the voltage stability enhancement problem; the fault location and isolation, service restoration problem; and the load balancing problem (Charlangsut et al., 2012). In mathematical optimisation, these problems are often referred to as objectives. An algorithm or optimisation method is needed to control the reconfiguration process. The aim of the optimisation method is to find the solution that best fits the objectives without violating the constraints associated with the problem. The optimisation problem can have single or multiple solutions depending on the nature of the objective functions. The solution that best fits the criteria for the optimisation problem is the optimal solution. The optimisation methods used to solve the distribution network feeder reconfiguration problem are classified into classical optimisation, heuristic optimisation, metaheuristic optimisation, and hybrid optimisation methods.

The next section provides a summary of those optimisation methods.

### 2.3.1. Classical optimisation methods for the distribution network feeder reconfiguration problem

Classical optimisation methods are generally based on iterative search algorithms. The first feeder reconfiguration scheme using a classical optimisation method was introduced by (Liu et al., 1989) who derived the global optimality conditions for the loss minimisation problem by using the “basic current profile” theory to convert the loss minimisation problem into a quadratic optimisation problem. The most recurring classical optimisation approaches are the Linear Programming, the Quadratic Programming, the Integer Programming, and the Dynamic programming.

#### 2.3.1.1. Linear Programming (LP) methods for the feeder reconfiguration problem

The Linear Programming method is used when the optimisation problem consists of a linear objective function associated with linear equality or inequality constraints (Dantzig, 1998). The general elementary linear programming problem can be expressed as given in Equation 2.4 (Luenberger, 1984).

$$\textbf{minimize } \mathbf{f}(\mathbf{x}) \tag{2.4}$$

Subject to

$$\mathbf{h_i}(\mathbf{x}) = \mathbf{0}, \quad \mathbf{i} \in \mathbb{N}$$
$$\mathbf{g_j}(\mathbf{x}) \leq \mathbf{0}, \quad \mathbf{j} \in \mathbb{N}$$

Where,

$\mathbf{f}$ is the objective function of the optimization problem.

$\mathbf{x}$ is an $\mathrm{n}$-dimentional vector of unknowns. $\mathrm{X} = (\mathrm{x}_1, \mathrm{x}_2, \dots, \mathrm{x}_\mathrm{n})$.

$\mathbf{h_i}$ and $\mathbf{g_j}$ are real-valued functions of the variable $\mathrm{x}$.

Linear programming formulations are popular because the objective function and the constraints are easy to formulate and less difficult to define, in comparison to other optimisation methods. Linear Programming offers reliable convergence properties and can quickly identify if an objective function is feasible (Sierksma, 2001). (Abur, 1996) presented a distribution network feeder reconfiguration method using linear programming to minimise the real power loss in distribution networks. However, the formulation of the linear programming problem was altered to allow for the current/power constraints to be enforced, and for the radial configuration of the distribution network to be maintained. Linear programming can also be used to linearise a nonlinear optimisation problem. (Wagner et al., 1991), using transportation techniques, applied a linear programming method to a small and then to a large distribution network to minimise the real power loss. The authors concluded that the linear programming method was ineffective in minimising the power loss in distribution networks. The conclusion of (Wagner et al., 1991) outlines that linear programming-based techniques are unable to evaluate and minimise the power loss in distribution systems accurately, and consequently, linear programming techniques are ineffective in solving distribution network feeder reconfiguration problems.

#### 2.3.1.2. Quadratic Programming (QP) methods for the distribution network feeder reconfiguration problem

A quadratic objective function with linear equality and inequality constraints characterises a quadratic programming problem. Quadratic Programming is a non-linear programming technique with better accuracy than LP-based methods (Wright & Nocedal, 2006). The quadratic programming problem can be formulated as given in Equation 2.5 (Wright & Nocedal, 2006).

$$\mathbf{mimimize}\ \frac{1}{2}\mathbf{x}^{\mathbf{T}}\mathbf{Q}\mathbf{x}+\mathbf{C}^{\mathbf{T}}\mathbf{x} \tag{2.5}$$

Subject to

$$\mathbf{Ax} \leq \mathbf{b}$$

Where

$\mathbf{x}$ is the decision variable.

$\mathbf{x}^{\mathbf{T}}$ is the vector transpose of $\mathbf{x}$.

$\mathbf{Q}$ is a $\mathrm{n} \times \mathrm{n}$-dimensional real symmetric matrix.

$\mathbf{C}^{\mathbf{T}}$ is the transpose of the real-valued, $\mathrm{n}$-dimensional vector $\mathbf{C}$.

$\mathbf{A}$ is a $\mathrm{m} \times \mathrm{n}$-dimensional real matrix.

$\mathbf{b}$ is a $\mathrm{m}$-dimensional real vector.

Quadratic Programming (QP) problems can be solved using methods such as Primal and Dual Simplex method. The primal simplex method is an iterative optimisation method in which the search starts with a feasible and suboptimal solution and goes through the iterations until the optimal solution is reached. In contrast, the dual simplex method starts with an exceptionally good solution and finds the optimal solution through a series of iterations (Norman, 1993). (Aoki et al., 1990) developed a quadratic programming method to find the best distribution network topology for emergency load re-allocation and service restoration. The authors (Aoki et al., 1990) combined the dual simplex method and the primal simplex method to produce a more coordinated and more efficient algorithm. The dual simplex method alone is inefficient in solving the feeder reconfiguration problem for emergency load re-allocation if the area of the distribution network which is without supply is large. Although good enough in large area service restoration problem, the primal-dual simplex method does not always find the optimal solution.

(Glamocanin, 1990) presented an algorithm for optimal power loss minimization in distribution systems. The author (Glamocanin, 1990) expresses the distribution network feeder reconfiguration problem as a quadratic cost function transhipment problem. The transhipment problem is generally used to find the minimum-cost route in the planning of bulk power distribution. In the method proposed by (Glamocanin, 1990), the power loss function is primarily linearized before the optimization problem is solved. Initially, the line current capacity limits, the transformer current capacity constraints, and the voltage constraints are not taken into. Those constraints are later included in the optimisation problem and a quadratic simplex method is developed to improve the accuracy of the solution. However, the developed QP based algorithm is only suitable if the objective of the distribution network feeder reconfiguration is to minimize the power loss.

(Huddleston et al., 1990) proposed a Quadratic Programming algorithm for distribution network feeder reconfiguration for real power loss minimisation. The QP algorithm is based on a quadratic loss function with linear current constraints. The proposed QP algorithm uses multiple switching pairs at once to reconfigure the distribution network and then gives the optimal distribution network topology for real power loss minimisation without checking for intermediate distribution network configurations.

#### 2.3.1.3. Integer Programming methods for the distribution network feeder reconfiguration problem

The distribution system feeder reconfiguration optimisation problem can also be solved using the Integer Programming (IP) method. Depending on the nature of the objective function and its constraints, there exist several IP based techniques such as Binary Integer Programming, Mixed-Integer Programming (MIP) /Mixed-Integer Linear Programming (MILP) and Mixed-Integer Nonlinear Programming (MINLP) (de Oliveira et al., 2010).

A MILP problem is defined by linear objective function, linear constraints, and some linear boundary conditions. It is generally formulated as in Equation 2.6.

$$\textbf{minimize } \mathbf{C^T x} \tag{2.6}$$

Subject to

$$\begin{aligned}
&\mathbf{A_1 x = b_1}, && \mathbf{i} \in \mathbb{N} \\
&\mathbf{A_2 x \le b_2}, && \mathbf{j} \in \mathbb{N} \\
&\mathbf{l_i \le x \le u_i}, && \mathbf{i = 1, 2, \dots, n}
\end{aligned}$$

where

$\mathbf{C^T x}$ is the objective function of the problem to optimize.

$\mathbf{C}$ is a column vector of constants.

$\mathbf{x}$ is a $\mathbf{n}$-dimentional vector of unknowns. $\mathbf{X} = (\mathbf{x_1}, \mathbf{x_2}, \dots, \mathbf{x_n})$ is the decision variable.

$\mathbf{A_1}$ and $\mathbf{A_2}$ are a $\mathbf{m_1} \times \mathbf{n}$ matrix and a $\mathbf{m_2} \times \mathbf{n}$ matrix respectively.

$\mathbf{l_i}$ and $\mathrm{u_I}$ are the respectively the lower and the upper boundary values.

If the variables can only take the value of 0 and 1 (binary values), the IP is said to be a Binary Integer Programming (BIP). (Sarma & Prakaso, 1995) developed a BIP based algorithm to solve the distribution network feeder reconfiguration problem for real power loss minimisation. Like the method proposed by (Huddleston et al., 1990), the BIP algorithm developed by (Sarma & Prakaso, 1995) uses multiple switching pairs to determine the optimal distribution network topology. However, the BIP algorithm does not stop at the first solution, but it considers if there is any other switching option that would further decrease the real power loss in the distribution network. The application of Integer Programming in distribution network feeder reconfiguration is also covered in the research works by (Chen & Cho, 1993) and (Schmidt et al., 2005).

#### 2.3.1.4. Dynamic Programming methods for the distribution network feeder reconfiguration problem

Dynamic Programming is not really an algorithm. It is rather a concept that consists of solving a problem by dividing it into smaller and simpler sub-problem, and then solving the sub-problems one at the time (Leiserson et al., 2009). The solutions of individual sub-problem are then combined to find the solution to the general problem. Many sub-problems can be computed at the same time using multi-core processors, then allowing a reduction of the computing time (Leiserson et al., 2009). The solution of a sub-problem can be stored in a memory and re-used if the same sub-problem occurs again. (Enrique et al., 2002) used a Dynamic programming-based approach to solve the distribution network feeder reconfiguration problem for real power loss minimisation in large primary distribution systems. (Shariatkhah et al., 2012) developed a distribution network feeder reconfiguration scheme using Dynamic Programming to minimise the costs of power loss, the interruption costs, the switching costs, and to improve the daily load profile. The results indicated that the Dynamic Programming algorithm is more efficient than the other classical optimisation method in solving the distribution network feeder reconfiguration problem.

The next section presents some heuristic search methods used to solve the feeder reconfiguration problem in distribution networks.

### 2.3.2. Heuristic search methods for the distribution network feeder reconfiguration problem

The application of classical optimisation techniques to network reconfiguration problems is faced with many difficulties such as the inability to handle certain constraints and the inability to find the optimal solution. To overcome such difficulties, heuristic search methods have been introduced. Heuristic search methods provide better computational performance when compared to classical optimisation methods. However, in comparison to classical methods, the accuracy of the heuristic solution is low (Gavrilas & Asachi, 2010). This section reviews the different types of heuristic search methods used to solve the distribution network feeder reconfiguration problem.

#### 2.3.2.1. Uninformed or blind search approaches

Blind search approaches are applied with no information on the domain of the objective function (search space). They only use the information provided in the definition of the problem. The most common uninformed search strategies include the Depth-First Search (DFS) and Breath First Search (BrFS), the Uniform Cost Search (UCS), the Depth-Limited Search (DeLS), the Iterative Deepening Search (IDS) and the Bidirectional Search (Pearl, 1984).

(Abul'Wafa, 2011) presented a DFS based heuristic approach for optimal reconfiguration of distribution networks. The DFS is a tree searching algorithm. The DFS explores each branch of the tree, from the root node to the furthest node of the branch before finding the solution of the problem by backtracking (Even & Even, 2011). The DFS tree is illustrated in Figure 2.2. The numbers 1 to 12 represent the order of visit of each node. The approach presented by (Abul'Wafa, 2011) is to find the best switching combinations for power loss minimization with minimal computational burden.

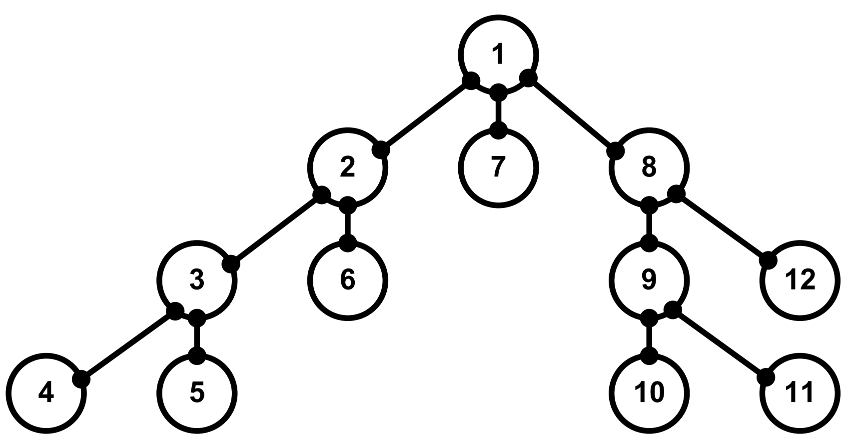


**Figure 2.2**: **Depth First Search pattern**

The Breath First Search (BrFS) is also a tree searching algorithm. But unlike the DFS, the BrFS begins at the root node, first explores the closest nodes, and then moves to the next level nodes. As illustrated in Figure 2.3, numbers 1 to 12 indicate the order in which the nodes are explored. In the distribution networks feeder reconfiguration, this algorithm can be combined with the DFS to accelerate the optimisation process (Song et al., 1997). In fact, by combining the DFS and BrFS, the Iterative Deepening Search (IDS) is created.

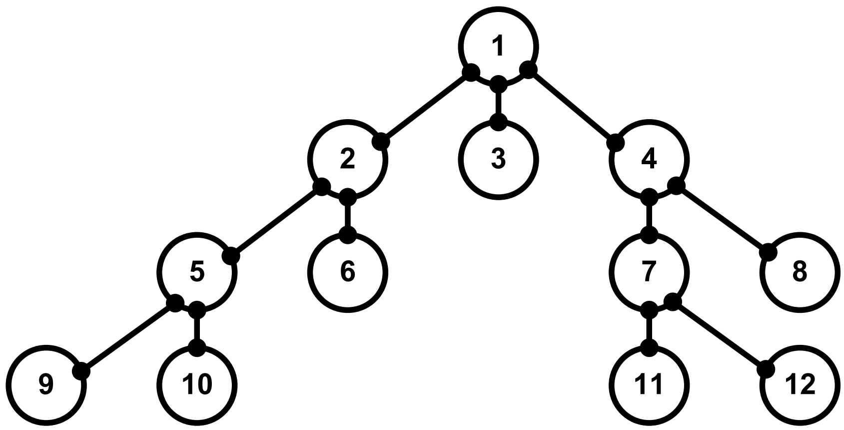


**Figure 2.3:** **Breath First Search Pattern**

The IDS algorithm is used to reduce the storage space and to improve the search efficiency (Reinefeld & Marsland, 1994). (Shirmohammadi & Hong, 1989) developed an IDS based heuristic distribution network reconfiguration method for power loss reduction under normal operating conditions. The authors (Shirmohammadi & Hong, 1989) included the voltage and current constraints in (Back & Merlin, 1975)'s original branch and bound method. (Shirmohammadi & Hong, 1989) considered the distribution network branches as purely resistive. The simulation results showed that the IDS method converges quite quickly and provides a near optimal solution.

#### 2.3.2.2. Informed heuristic approaches

Unlike blind search techniques, informed search approaches use the information related to the problem to solve the objective function. Informed search strategies consist of the Best First Search (BeFS) and the Local Search algorithms.

The Best-First search (BeFS) is one of the most popular heuristic algorithms. It is a graph algorithm that evaluates the paths of the search domain, select the path that is likely to give the optimal solution, and explores all the nodes along that chosen path (Dechter & Pearl, 1984). The Best-First Search is the fastest of heuristic algorithms. However, when using the BeFS, the optimality of the solution is not always assured. The authors (Taylor & Lubkeman, 1990) developed a Best-First Search based method to solve the feeder reconfiguration problem. The developed BeFS based method can process practical operating constraints, and it swiftly eliminates any switching combination that would cause an overload, an overvoltage, or any network abnormality. Variants of the Best-First Search method include the Greedy Search and the A Star (A*) search. The A Star (A*) search is a special case of the BeFS, and it is indeed the most powerful of the heuristic approaches (Zeng & Church, 2009). (Botea et al., 2012) used the A Star (A*) search algorithm to address the distribution network feeder reconfiguration problem for service restoration. Many factors influenced the choice of the A* search algorithm:

- The A* search always finds the optimal solution if the distribution network feeder reconfiguration problem has solutions within the defined domain (search space)
- The computation time is drastically reduced when the A* search is used. The A* never explores a path that does not yield the optimal solution.

#### 2.3.2.3. Others heuristic algorithms

Other heuristic techniques such as the Switch Exchange Method (SEM) and the Sequential Switch Opening Method (SSOM) have been used to solve the distribution network feeder reconfiguration problem.

The Switch Exchange Method (SEM) calculates the power loss reduction that results from a change of switches status in a distribution network. (Civanlar et al., 1988) developed an SEM to solve the distribution network feeder reconfiguration problem for power loss minimization. The authors developed the formula given in Equation 2.7 to calculate the change in power loss in a distribution network after a given reconfiguration. The power loss solutions are recorded and then compared. The distribution network topology that gives the greater power loss reduction is the optimal distribution network topology. The SEM includes a filtering mechanism used to exclude the distribution network topologies that are unlikely to yield a reduced power loss during the configuration exploration process.

$$\mathbf{\Delta P = Re\left[2\left(\sum_{i\in D} I_i\right)(E_m - E_n)^* + R_{loop}\left|\sum_{i\in D} I_i\right|^2\right]} \qquad (2.7)$$

where

$\mathbf{\Delta P}$ is the power loss that occurs after a given switching operation.

$\mathbf{D}$ is the set of buses disconnected from feeder 1 and connected to feeder 2.

$\mathbf{m}$ is the bus of feeder 1 to which loads of feeder 2 are to be connected.

$\mathbf{n}$ is the bus of feeder 2 that will be connected to bus $\mathbf{m}$ via a tie switch.

$\mathbf{I_i}$ is the complex bus current at bus $\mathbf{i}$.

$\mathbf{R_{loop}}$ is the Series resistance of the path between two substation buses of feeder 1 and feeder 2 via closure of a specified tie switch.

$\mathbf{E_m}$ is the voltage at bus $\mathbf{m}$ and it is calculated as $\mathbf{E_m = I_{Bus\ m} * R_{Bus\ m}}$.

$\mathbf{E_n}$ is the voltage at bus $\mathbf{n}$ and it is calculated as $\mathbf{E_n = I_{Bus\ n} * R_{Bus\ n}}$.

$\mathbf{R_{Bus}}$ is the bus resistance matrix of feeder 1 before load transfer.

To improve the Switch Exchange Method (SEM) presented by (Civanlar et al., 1988), (Baran & Wu, 1989) derived two methods to estimate the power loss for network reconfiguration: The Simplified Distflow method and the backwards-forward update of the distflow power flow update. The methods are based on recursive power flow equations in the distribution system when a given switching option is carried out. The developed methods take into consideration the reactive power in the system and can, therefore, be applied to unbalanced distribution networks. Additionally, a Load Balance Index (LBI) is developed, and it is demonstrated that the developed methods are effective in balancing the loads in a distribution network.

The SEM developed by (Gosvami & Basu, 1992) is used to solve the feeder reconfiguration problem for real power loss minimisation. In this SEM, a given tie switch in the network is closed to form a mesh in the network. The tie switch to be closed is the tie switch with a maximum voltage across its terminals. After the power flow computation, a switch in the formed mesh is opened to restore the radial configuration of the network. The switch to open may be the previously closed switch or a different one within the formed mesh.

Another application of the SEM in distribution network feeder reconfiguration is (Borozan et al., 1997)'s approach to minimise the power loss in unbalanced distribution networks. The authors investigated how much influence unbalanced loads had on the solution of distribution network feeder reconfiguration problem. (Borozan et al., 1997)'s approach further extended the utilisation of the SEM to three-phases three-wire distribution systems. (Kashem et al., 2000) developed a minimal tree search-based SEM for optimal network reconfiguration to minimise the power loss in distribution networks. The main advantage of their approach over (Baran & Wu, 1989)'s is that there is no need to perform load flow for every switching action.

Another type of heuristic search method is the Sequential Switch Opening Method (SSOM). The SSOM was first introduced by Back and Merlin in 1975 (Back & Merlin, 1975).

In the SSOM, all the tie switches (Normally open switches) are primarily closed so that the network has a meshed configuration. The switches are then opened in sequence to form a radial network (Ferdavani et al., 2011). The switches are opened in such a way that the current flow in a branch has the lowest possible magnitude, and thus ensuring that the resulting distribution network topology has a minimum power loss (Ferdavani et al., 2011). (Flavio et al., 2005) presents an SSOM based feeder reconfiguration algorithm for power loss minimisation in large radial distribution networks. The proposed SSOM approach is based on the power flow in the branches. The main advantage of (Flavio et al., 2005)'s SSOM approach is that the result obtained is independent of the status of the distribution network switches before the reconfiguration process.

(Peponis et al., 1995) compared the effectiveness of the SEM and the SSOM in solving the distribution network feeder reconfiguration problem. Based on the simulation results, the authors concluded that the SEM is faster than the SSOM. Unlike in the SEM, the solution of the SSOM is not dependent on the initial distribution network topology. Both methods (SEM and SSOM) find the same final solution to the feeder reconfiguration problem.

Although the heuristic search methods presented above may be used to solve the problem of optimal distribution network feeder reconfiguration, they are still limited, and they don't always find the optimal solution. Therefore, there is a need to investigate for more robust and efficient optimisation methods to solve the distribution network feeder reconfiguration problem.

The next section presents some metaheuristic search methods used to solve the distribution network feeder reconfiguration problem.

### 2.3.3. Meta-heuristic search methods

The application of traditional and heuristic optimisation techniques in distribution network feeder reconfiguration is faced with many hurdles. In large distribution systems, these optimisation methods fail more often, especially when the objective function and the constraints associated with the problem are nonlinear (Rao & Savsani, 2012). Therefore, Metaheuristic techniques or Artificial Intelligence (AI) algorithms were introduced to solve non-linear problems.

Artificial Intelligence (AI) based methods simulate either the social intelligence or the human intelligence. Their main characteristics are:

- AI based algorithms find a good solution to the problem, but it is not guaranteed that the solution is optimal.
- Those techniques can solve problems with incomplete or limited information (Blum & Roli, 2003).

Many criteria can be used to compare AI based reconfiguration schemes. These criteria are used as a benchmark when deciding which method to use for a given optimisation problem and they are:

- The complexity of computation (How difficult is it to compute the algorithm?),
- The simplicity of implementation (How easy is it to apply the algorithm to the problem?),
- The speed of convergence (How long does it take to solve the problem?) and
- The reliability (How often does the algorithm find the optimal solution?) (Maringer, 2005).

Meta-heuristic search methods include the Artificial Neural Network (ANN) algorithms, Human intelligence algorithms such as Evolutionary Algorithm (EA); Genetic Algorithm (GA); Evolutionary Programming (EP); and Expert Systems (ES), and social intelligence algorithms such as the Particle Swarm Optimization; the Ant Colony Optimization (ACO) and the Honey Bee Mating Optimization (HBMO).

This section reviews and analyses some metaheuristic optimization methods used to solve the distribution network feeder reconfiguration problem.

#### 2.3.3.1. Artificial Neural Network based algorithms

The Artificial Neural Network (ANN) is an algorithm developed to mimic the central nervous systems of humans. The fact that the human brain can swiftly solve a variety of problems where computerised systems failed incited the research into the design of systems with cerebral capabilities (Tagliarini et al., 1991).

Figure 2.4 is a representation of the ANN architecture. The ANN architecture is a connection of nodes. Each node also referred to as artificial neuron, is equivalent to the biological neuron in the human or animal brain. The connection between the artificial neurons (the equivalent of the synapse) transmit the input signal to the hidden layer and transfer the signal from the hidden layer to the output. The hidden layer is the part of the ANN architecture responsible for computing the inputs of the ANN to produce the desired output.

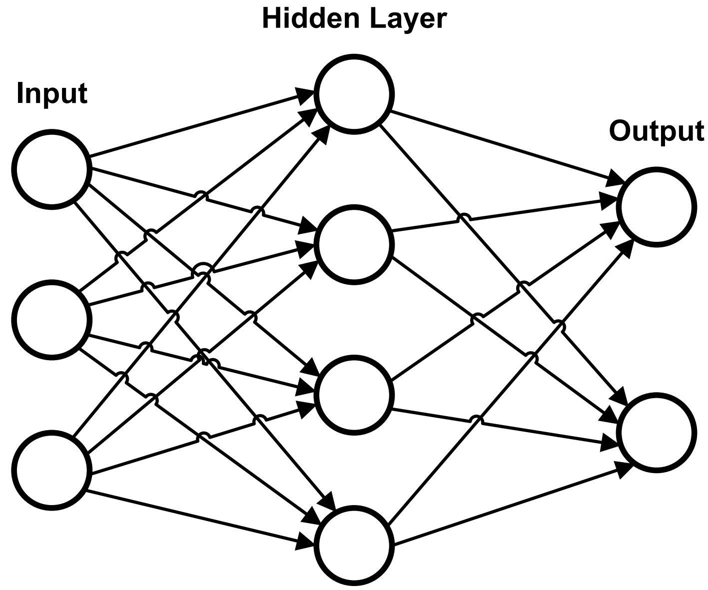


**Figure 2.4:** **Architecture of the Artificial Neural Network (Kashem et al., 1998)**

The effectiveness of ANN lies in its ability to approximate a function based on the observed data. (Kim et al., 1993) proposed a network reconfiguration method for power loss minimisation using the Artificial Neural Network. In their study, the ANN is trained, and the relationship between the load patterns and the corresponding network configurations is recorded. This means that the optimal system topology of a given distribution network is determined by the load patterns in the training knowledge. A two-level ANN algorithm is based on two groups of ANNs:

- The first group of ANN is used to determine the load size
- The second group of ANN is used to find the best distribution network topology based on the information provided by the first group of ANN.

(Kashem et al., 1998) applies the ANN in distribution network reconfiguration for power loss minimisation. Their research was different from (Kim et al., 1993)'s in the way that only a single group of ANN is used to obtain the optimal distribution network topology. Furthermore, the ANN-based algorithm developed by (Kashem et al., 1998) can be applied to any distribution systems with no limitation on the size.

The application of ANN based algorithms allows the finding of the optimal distribution network topology with reduced computation time. However, its use is curbed by difficulties such as:

- The considerable amount of time necessary for ANN training, since an extensive range of training cases is required for real-world applications.

- The fact that any change in the distribution systems must be accounted for means that ANN training is required for each distribution network (Schmidhuber, 2015).
- The data required for ANN training must be accurate to ensure that the final results are correct.
- The large storage and processing resources required to simulate ANN based applications (Schmidhuber, 2015).

#### 2.3.3.2. Evolutionary Algorithms (EA)

Evolutionary Algorithms are based on the mechanisms of natural or biological evolution such as reproduction, mutation, and selection. Evolutionary Algorithms are based on the Darwinian Theory which alleges that: “All species or organisms arise and develop through the natural selection of small, inherited variations that increase the individual’s ability to compete, survive and reproduce” (Wallace, 1889). Although all EA differ at some point, they have nevertheless a common biological process, defined as follows:

- Given an initial random population of individuals (first generation), calculate the fitness of every individual using a fitness function.
- Apply some external conditions to trigger the survival of the fittest (natural selection), which in turn produces a fitter population.
- Individuals with the highest objective value or fitness score (parents) are selected to breed the next generation (offspring) either by mutation or recombination (crossover).
- The offspring become part of the population and compete for survival (based on their fitness/objective value), along with other individuals for a place in the future generation.

This EA biological process described above is repeated until the best result is attained (Back, 1996). At the end of the iterations, many good solutions are obtained rather that an optimal solution. It is then necessary to compare the obtained solutions to determine the optimal solution (Chakradeo et al., 2014).

Several types of Evolutionary Algorithms have been used to solve the feeder reconfiguration problem. The Genetic Algorithm and the Differential Evolution are two of the most common EA.

### a. Genetic algorithm

GA is a random search algorithm used to solve optimisation problems with or without constraints (Nara et al., 1992). GA shares the fundamental principle of EA. The individuals in the population are referred to as chromosomes, and a new population of chromosomes is obtained at each iteration (Goldberg, 1989).

In distribution network feeder reconfiguration, the application of GA has the following disadvantages:

- The GA tends to converge towards the local optima instead of the global optimum.
- The choice of the best solution is relative to other solutions, making it difficult to establish an iteration stop criterion.
- Complex problems and large systems often cause the search space to increase at an exponential rate and thus rendering the simulation process lengthy.

Several variants of GA have been developed to solve the power loss minimisation problem. Some of them are the GA with sequential encoding by (De Macedo Braz & de Souza, 2011), the GA with restricted population and addressed operators by (Mendoza et al., 2006), and the GA based on the Matroid theory by (Enacheanu et al., 2008).

### b. Differential evolution (DE)

DE was developed in 1995 to improve the performance of the GA (Babu & Jehan, 2003). It is easy to use, robust, simple in structure and has a good convergence speed. DE follows the GA's biological process, except for the mutation stage which is perturbed by adding the differential weight of one or more pairs of vectors (individual) to a target vector. DE is widely used in distribution network reconfiguration applications. The popularity of DE lies in its simplicity to code, its straightforward implementation, its low space complexity, and its improved performance (Das & Suganthan, 2011).

EA applied to distribution network feeder reconfiguration are not limited to DE and GA. GA and DE remain the most popular algorithm for distribution feeder reconfiguration applications. The Evolutionary Programming (EP) is another type of EA used in distribution network feeder reconfiguration applications (Song et al., 1997).

#### 2.3.3.3. Swarm intelligence algorithms for network reconfiguration applications

Swarm Intelligence algorithms are based on the social behaviours arising from the interactions between individuals of a colony and between the individuals with their environment. They were inspired by observing the nature's biological systems, in which individuals with limited capabilities come together to achieve a definite goal that requires a higher intelligence (Wang & Beni, 1993). Moreover, Swarm intelligence systems are characterised by their ability to act in a harmonised manner with no centralised control structure. This self-organising ability is governed by four sets of behavioural patterns or rules defined as follows (Garnier et al., 2007):

- Positive feedback results from random behaviours from different individuals to create a structure.
- Negative feedbacks received to balance the positive feedbacks and stabilise the structural patterns.
- The fluctuation of positive feedbacks gathered enables the self-organisation to take place.
- Positive feedbacks based continuous interactions between the individuals of the colony and with their environment are required to sustain the self-organisation, and to elaborate a collective pattern for subsistence against negative feedbacks (Garnier et al., 2007).

The pheromone trail in ant colonies can illustrate this working principle. To find a source of food supply, individuals wander around in a random pattern. If an individual finds a food supply, it returns to the colony (positive feedback). Individuals that did not find a food source also return to the colony (negative feedback). The first group of individuals has been laying pheromone through the search area based on their findings. This pheromone trail affects the path of the next groups of individuals, and subsequently, the path with the best positive feedbacks (greater pheromone laying occurrence) constitutes the best path to the source of supply (structure) (Corne et al., 2012).

This section reviews Swarm intelligence algorithms which have been successfully used to solve the feeder reconfiguration problem. Some of such swarm intelligence algorithms are the Ant Colony Optimization (ACO) and the Particle Swarm Optimization (PSO).

**a. Ant Colony Optimization (ACO) algorithm**

The Ant Colony Optimization (ACO) algorithm is derived from the foraging or the pheromone trail behaviour of ants. Figure 2.5 is a representation of the natural ant behaviour. Figure 2.5.a., the ants are leaving their nest to look for a source of food. In Figure 2.5.b., an obstacle is placed along the path of the ant colony. The colony disperses to find alternative paths to the food source as shown in Figure 2.5.c. Each ant sends a positive or negative feedback to the colony based on its experience and leaves a pheromone trail behind for other ants to follow or not. After a while, the ant colony is directed to the path of greater pheromone strength. The path of greater pheromone strength is the new minimum distance path from the nest to the source of food, and this can be seen in Figure 2.5.d. (Dorigo et al., 1996).

In the ACO algorithm, an artificial ant (a software agent) searches for candidate solutions of a given problem and maps down the shortest path leading to that solution using artificial pheromone. Based on the pheromone trail deposited by forerunner ants, subsequent artificial ants will also find their own solution to the optimisation problem and will update the pheromone, depending on the quality of the solution (Dorigo et al., 1996). The pheromone trail decays over the time. So, the solution with a path of greater pheromone strength is considered as the optimal solution (Dorigo et al., 1996).

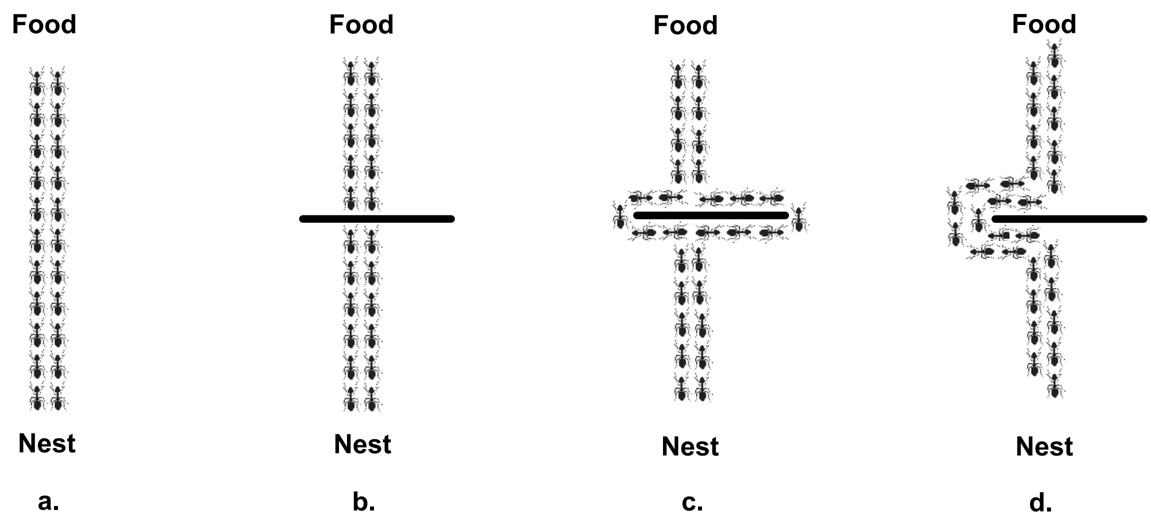


**Figure 2.5:** **Natural behaviour of Ants (Dorigo et al., 1996)**

The ACO has been successfully applied to power systems and particularly in distribution network feeder reconfiguration. (Perreira et al., 2006) and (Hu et al., 2008) proposed an application of ACO in distribution systems to minimise the power loss along the lines, taking into consideration operational constraints such as the voltage limits, the maximum loadability, and the radial configuration of the network. (Carpaneto & Chicco, 2004) and (Khoa & Phan, 2006) also proposed an ACO based method for power loss minimisation in distribution networks through feeder reconfiguration. (Carpaneto & Chicco, 2004) compared the performance of the ACO algorithm with that of Tabu-Search, and Simulated Annealing. (Khoa & Phan, 2006) analysed the performance of the ACO with those of Genetic Algorithm (GA) and Simulated Annealing. Both (Carpaneto & Chicco, 2004) and (Khoa & Phan, 2006) studies concluded that the ACO algorithm performs better in finding the solution of the power loss minimisation optimisation problem, despite the slow convergence characteristic of ACO algorithms.

**b. Particle Swarm Optimization algorithms**

The Particle Swarm Optimization is also an algorithm inspired by nature and derived from the communal demeanour of fish schooling or of birds flocking. It is a population (swarm) based algorithm where the possible solutions (candidate solutions) are referred to as particles (Eberhart & Kennedy, 1995). In the implementation of the PSO algorithm, each particle is given an initial random position and velocity. The particle then moves around the search space, and alters its speed and velocity, depending on its best position and the best positions of other particles in the swarm. The movement of particles is dictated by a fitness function, and over time, all particles finally move to the position with the best fitness value (swarm's best global position) (Parsopoulos & Vrahatis, 2002).

In the PSO algorithm, the velocity and the position of the particles are updated according to Equation 2.8 and 2.9, respectively. Based on the position and velocity update equations, the search mechanism of the PSO algorithm is represented in Figure 2.6.

$$\mathbf{v_{id}(t+1) = w.v_{id}(t) + c_1.R_1.[p_{id}(t) - x_{id}(t)] + c_2.R_2.[p_{gd}(t) - x_{id}(t)]} \tag{2.8}$$

$$\mathbf{x_{id}(t+1) = x_{id}(t) + v_{id}(t+1)} \tag{2.9}$$

where

$\mathbf{w}$ is the inertia weight

$\mathbf{v_{id}}$ is the velocity of the $\mathbf{i^{th}}$ particle in the $\mathbf{d^{th}}$ dimension.

$\mathbf{t}$ is the iteration number.

$\mathbf{c_1}$ and $\mathbf{c_2}$ are positive weighting parameters (constants) to control a particle movement towards its individual as opposed to the global best position.

$\mathbf{p_{id}}$ is the individual best position of the $\mathbf{i^{th}}$ particle in the $\mathbf{d^{th}}$ dimension.

$\mathbf{p_{gd}}$ is the global best position of the swarm.

$\mathbf{x_{id}}$ is the current position of the $\mathbf{i^{th}}$ particle in the $\mathbf{d^{th}}$ dimension.

$\mathbf{R_1}$ and $\mathbf{R_2}$ are randomly selected positive numbers.

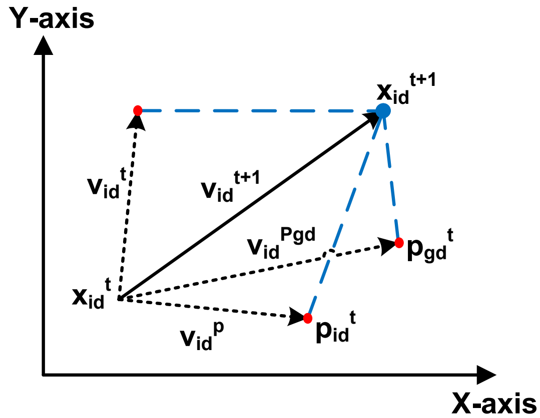


**Figure 2.6**: **Search mechanism of the PSO algorithm**

The application of a typical PSO algorithm in feeder reconfiguration is not a straightforward process. Therefore, the algorithm must be altered to comply with the distribution network operational constraints. As such, the canonical PSO algorithm should be amended before to be used to solve the distribution network feeder reconfiguration problem. (Abdelaziz et al., 2009) modified the population size, the number of iterations of the PSO, and introduced a linearly decreasing inertia weight to expand the search space. In the distribution network feeder reconfiguration, the conventional PSO algorithm tends to converge towards the local optimal rather than the global optima (premature convergence). To elude that inclination, (Kiran et al. 2012) developed an Adaptive Mutation Particle Swarm Optimization (AMPSO), by introducing a mutation operator is in the original PSO algorithm. The simulation results showed that the developed AMPSO finds an improved solution to the distribution network feeder reconfiguration problem with reduced computation time.

#### 2.3.3.4. Hybrid algorithms

Every optimisation algorithm has limitations and depending on the application in which it is used; it may not be able to support the constraints related to the objective function. To overcome this problem, two or more algorithms can be brought together to form a new algorithm referred to as a hybrid algorithm. The benefits of each algorithm are combined, which ensues to an enhanced performance (Ting et al., 2015).

The obtained hybrid algorithm can be used for a single purpose (unified purpose hybrid). A typical example of such an algorithm is the Mixed Integer Hybrid Differential Evolution (MIHDE) algorithm used to solve the distribution network feeder reconfiguration problem in (Su & Lee, 2003). The MIHDE combines the advantage of the Mixed Integer Programming and the Differential Evolution algorithms. The MIHDE is a Parallel direct search algorithm, meaning that the two sub-algorithms run simultaneously and manipulate the same population.

Alternatively, each sub-algorithm of the hybrid algorithm can be used for different purposes (Multipurpose hybrid). The main algorithm is used to solve the optimisation problem whereas the auxiliary algorithm adjusts the parameters of the main algorithm. In (Niknam et al., 2010), the Fuzzy Adaptive Particle Swarm Optimization (FAPSO) and the Ant Colony Optimization (ACO) are combined to solve the distribution network feeder reconfiguration problem. The FAPSO is used to adjust the parameters of the algorithms while the decision-making process is enforced by the ACO.

Although hybrid algorithms provide improved performance while reducing substantial disadvantages, their significant drawbacks remain their complexity; their computational speed; and their difficulty in implementation. The final computation time is longer, since hybrid algorithms are usually longer, more complex, and have more parameters than non-hybrid algorithms. The analysis and troubleshooting of hybrid algorithms are complicated. Therefore, random hybridisation should be discouraged in favour of clever, innovative and effective methods (Ting et al., 2015).

## 2.4. Review of the existing literature in feeder reconfiguration

An intensive literature search has been done using keywords such as feeder/network reconfiguration; feeder/distribution automation; and optimisation methods/algorithms. The published research works, dissertations, and thesis on distribution network feeder reconfiguration span from 1975 to 2018. Figure 2.7 represents the graph of the number of publications found for the distribution network feeder reconfiguration problem per year. The analysis of the histogram in Figure 2.7 shows that 343 publications have been published since the introduction of feeder reconfiguration in 1975. That corresponds to an average of 8 publications per year. Further analysis shows that only a few papers were published in early years. Before 2000, the number of publication per year was below the average. As from 2003, the number of publication per year exceeds the average and reaches its peak in 2014 with 31 publications.

To complete the literature review on the distribution network feeder reconfiguration problem, past research works, conference papers, journals, and thesis were investigated. The survey and the comparison are accomplished using the following criteria:

- **Objective function**: It characterises the nature of the problem to be solved. The objective function can be the power loss minimisation, the load balancing maximisation, the service restoration, the voltage deviation minimisation, or the voltage stability index maximisation.

- **Constraints**: the developed scheme may be subject to operational constraints such as voltage and current limits.
- **Algorithm used**: Classical, heuristic, and meta-heuristic optimisation methods have been successfully used to solve the problem of distribution network feeder reconfiguration.
- **Distribution networks**: To demonstrate their practicability, the developed distribution network feeder reconfiguration schemes are tested on a variety of distribution networks such as the 16-bus, the 33-bus, and the 69-bus IEEE distribution networks.
- **Software**: There is a broad range of available software to simulate and analyse a distribution system. Some of those softwares are MATLAB and GAMS. However, the suitability of a given software is dependent on the problem to solve.

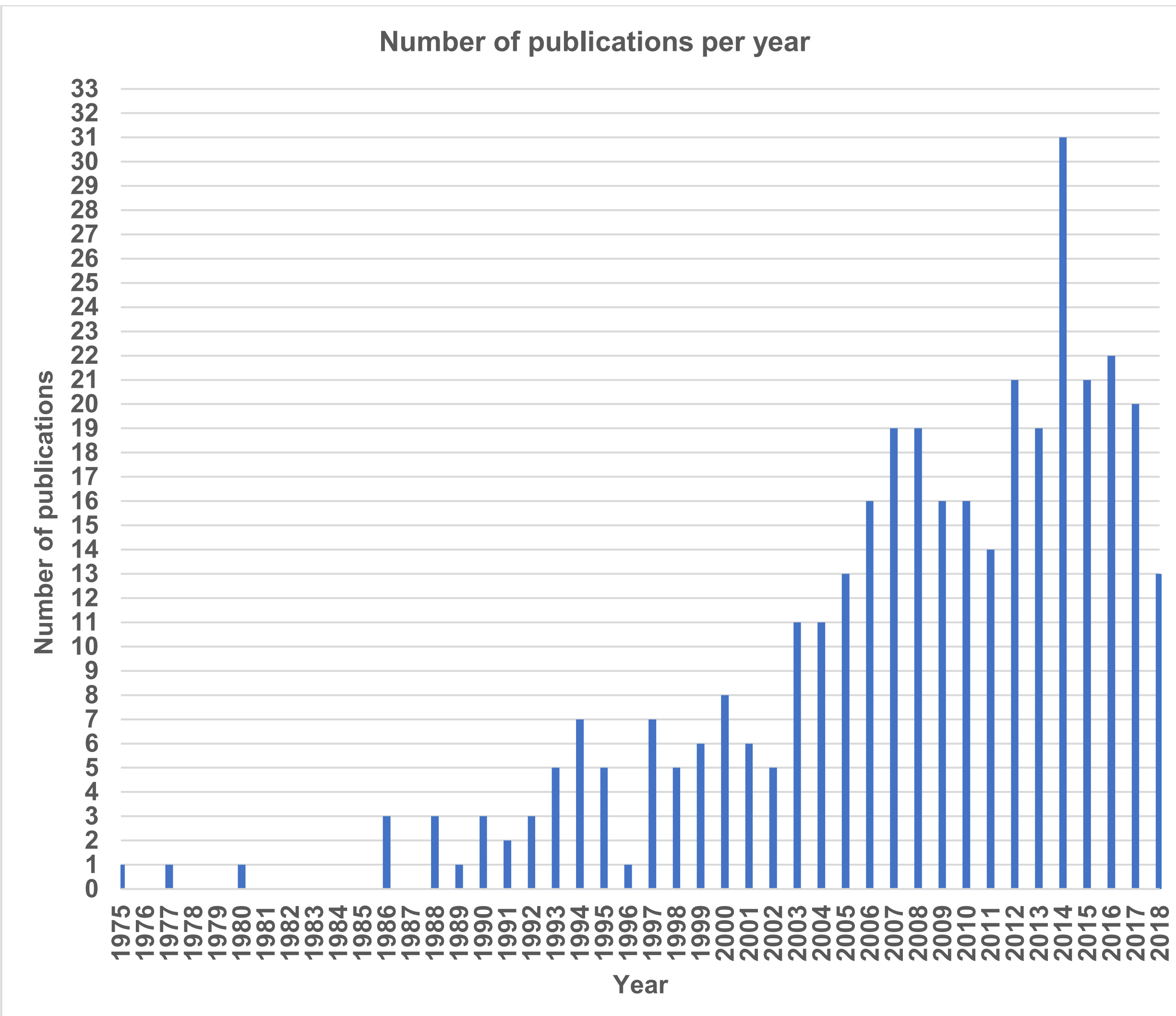


**Figure 2.7: Number of Publications per years**

**Table 2.1**: **Review of optimal feeder reconfiguration**

| Reference paper | Objective function | Constraints | Algorithm | Software used | Distribution system | DG? | Physical implementation? |
|---|---|---|---|---|---|---|---|
| (Back & Merlin, 1995) | Power loss minimization | - Voltage constraint<br>- Current constraint | SSOM | N/A[1] | N/A | No | No |
| (Abur, 1996) | Power loss minimisation | - Branch power constraint.<br>- Topological constraint | - Linear Programming<br>- Modified Simplex method | N/A | IEEE 16-bus distribution system | No | No |
| (Wagner et al., 1991) | Loss reduction | Power balance constraint | Linear Programming methods using a Stepping Stone algorithm | N/A | 16-bus distribution system. Kingston Power Utility Company 44 kV, 150MW distribution system | No | No |
| (Aoki et al., 1990) | Emergency load re-allocation | - Voltage constraint<br>- Current constraint | Quadratic Programming (combined Primal-Dual Effective gradient) | N/A | Real scale 6.6 KV distribution system | No | Yes |
| (Glamocanin, 1990) | Loss reduction | - Branch power limits.<br>- voltage constraints.<br>- topology constraint | Quadratic simplex method | N/A | 10 nodes distribution system | No | No |
| (Huddleston et al., 1990) | System loss minimization | - Current constraint<br>- Topological constraint | Quadratic Programming | IMSL Subroutine QPROG | IEEE 16-bus distribution system | No | No |

| | | | | | | | |
|---|---|---|---|---|---|---|---|
| (Sarma & Prakaso, 1995) | Loss minimization | N/A | Binary Integer Programming | N/A | IEEE 16-bus distribution system | No | No |
| (Chen & Cho, 1993) | Loss minimization | - Voltage constraint<br>- Current Constraint | Binary Integer Programming with branch and bound technique | N/A | Taipower distribution system (four substations and nine feeders) | No | No |
| (Enrique et al., 2002) | Loss minimization | - Voltage constraints<br>- Current constraint<br>- Topological constraint | Algorithm-based on Dynamic Programming, Graph theory and Harmony Search | C+ + language | IEEE 16-bus distribution system | No | No |
| (Shariatkhah et al., 2012) | Power loss minimization | - Voltage limit<br>- Current limit<br>- Topological constraint<br>- Minimal switching operation | Dynamic Programming and Harmony Search | MATLAB | 95-bus distribution network | No | No |
| (Momoh & Caven, 2003) | Service Restoration and load balancing | - Power balance<br>- voltage constraint<br>- Current constraint | Integer interior point linear programming | GAMS<br>MINOS | 32-bus distribution system | No | No |
| (Abul'Wafa, 2011) | Power loss minimisation | - Current constraint<br>- Topological constraint | Depth-First Search | MATLAB | IEEE 33-Bus distribution system | No | No |

| | | | | | | | |
|---|---|---|---|---|---|---|---|
| (Song et al., 1997) | Loss minimization | - Voltage constraint<br>- Current constraint<br>- Topological constraint<br>- Power balance constraint | Fuzzy-controlled Evolutionary Programming. Combined Depth-First and Breadth-First Search strategy (used to speed-up The optimisation) | Turbo C++ | IEEE 16-bus distribution system | No | No |
| (Shirmohammadi & Hong, 1989) | Loss reduction | - Voltage constraint<br>- Current constraint<br>- Topological Constraint | Iterative Deepening Search (IDS) | DISTOP (Distribution Network Optimisation) | small distribution system consisting of 3 radial feeders connected at the station transformer, and a group of switches | No | No |
| (Taylor & Lubkeman, 1990) | Transformer Overload minimisation | - Voltage constraints<br>- Line thermal constraints | Best-First Search | Knowledge Based System (KBS) | IEEE 16-Bus distribution system | No | No |
| (Botea et al., 2012) | Service restoration | - Current constraint<br>- Topological constraint | Informed A Star (A*) search | Java 1.6 | - Small distribution system with 54 circuit-breakers, 139 switches, and 138 lines.<br>- Large distribution system with 81circuit-breakers, 210 switches, and 207 lines. | No | No |

| | | | | | | | |
|---|---|---|---|---|---|---|---|
| (Civanlar et al., 1988) | Loss reduction | N/A | Switch Exchange Method | N/A | IEEE 16-Bus distribution system | No | No |
| (Baran & Wu, 1989) | - Power loss reduction<br>- Load balancing | Voltage constraint | - Branch exchange with Simplified DistFlow method.<br>- Branch Exchange With Backwards and Forward Update of DistFlow | / | 33-bus distribution system. | No | No |
| (Gosvami & Basu, 1992) | Reduction of line losses | - Voltage constraint<br>- Current Constraint<br>- Topological constraint | Switch Exchange Method | N/A | 35-bus distribution system | No | No |
| (Kashem et al., 2000) | Loss minimisation | - Voltage constraint<br>- Current constraint | Minimal tree search based SEM | N/A | 33-bus distribution system | No | No |
| (Peponis et al., 1995) | Power loss reduction | - Voltage constraint<br>- Topological constraint | Switch Exchange Method (SEM)<br>Sequential Switch Opening Method (SSOM) | N/A | Five 20kV feeders, with 63 nodes; 80 branches and 50 branch switches | No | No |
| (Kim et al. 1993) | Loss reduction | Topological constraint | Artificial Neural Network | FORTRAN | 16-bus distribution system | No | No |
| (Kashem et al., 1998) | Real power loss reduction | N/A | Artificial Neural Network | FORTRAN | 16-bus distribution system | No | No |

| | | | | | | | |
|---|---|---|---|---|---|---|---|
| (Nara et al., 1992) | Loss minimum | - Voltage constraint<br>- Current constraint | Genetic Algorithm (GA) | FORTRAN | 106 sectionalizing switches system<br><br>1692 switches real scale urban distribution system. | No | No |
| (Mendoza et al., 2006) | Real power loss minimization | - Voltage constraint<br>- Current constraint<br>- Topological constraint | Genetic Algorithm with restricted population and addressed operators | MATLAB | - 16-Bus distribution system.<br>- Hypothetical 12.66 kV system with a 2-feeder substation, 32 buses and 5 tie-lines | No | No |
| (Enacheanu et al., 2008) | Loss minimization | - Voltage constraint<br>- Current constraint<br>- Topological constraint | Genetic Algorithm based on the Matroid Theory | MATLAB | - 16-Bus distribution system.<br>- Hypothetical 12.66 kV system with a 2-feeder substation, 32 buses and 5 tie-lines.<br>- 11-kV radial distribution system with 2 substations, 4 feeders, 70 nodes, and 78 branches | No | No |

| | | | | | | | |
|---|---|---|---|---|---|---|---|
| (de Oliveira et al., 2014) | Power losses minimization | - Voltage constraint<br>- Current constraint<br>- Topological constraint | Artificial Immune Systems (AIS) | MATLAB | 14-bus distribution system | No | No |
| (Su & Lee, 2003) | Power loss reduction<br><br>Voltage profile improvement | - Voltage constraint<br>- Current constraint | Mixed-Integer Hybrid Differential Evolution (MIHDE) | MATLAB | - 16-bus Distribution system.<br>- TaiPower company distribution system (11 11.4 kV feeders, 83 section switches, and 13 tie-switches) | No | No |
| (Hu et al., 2008) | Power loss minimisation | N/A | ACO | N/A | 69-bus distribution system | No | No |
| (Su et al., 2005) | Power loss minimization | - Voltage constraint<br>- Current constraint | ACO | MATLAB | - 16-bus distribution system<br>- 11.4 kV Taipower distribution system with 11 feeders, 83 section switches, and 13 tie switches | No | No |
| (Jin et al., 2004) | Load balancing | - Voltage constraint<br>- Topological constraint | Binary Particle Swarm Optimisation (BPSO) | N/A | 16-bus Distribution system | No | No |

| | | | | | | | |
|---|---|---|---|---|---|---|---|
| (Abdelaziz et al., 2009) | Power loss minimization | - Voltage constraint<br>- Current constraint<br>- Topological constraint | Modified Particle Swarm Optimisation | MATLAB 6.5 | - 33-bus Distribution system.<br>- 69-bus Distribution system | No | No |
| (Wu & Tsai, 2008) | Load balancing | - Voltage constraint<br>- Topological constraint | Binary Coding Particle Swarm Optimisation | Java | 4-feeder distribution system with 24 section switches, 8 tie-switches and 28 load-zones | No | No |
| (Voropai & Bat-Undraal, 2012) | Power loss minimization<br>Power supply reliability. | - Voltage constraint<br>- Current constraint | Hybrid ACO-successive concessions method | N/A | Simplified distribution system of the central Power system of Mongolia with 4 thermal power plants of DG size | Yes | No |
| (Olamaei et al., 2008) | Real power loss minimization.<br>DG Generated real power minimisation | - Voltage deviation constraints.<br>- Number of Switching operations | Particle Swarm Optimisation | MATLAB | 31-bus distribution system with 3 feeders and 4 tie-switches | Yes | No |
| (Niknam, 2011) | Real power Loss Minimisation<br>Number of switching operations minimisation<br>Voltage deviation minimisation | - Branch capacity constraint<br>- Power balance constraint<br>- Topological constraints | Multi-Objective Honey Bee Mating Optimisation (MHBMO) | N/A | - 94-bus distribution system with 2 substations, 11 feeders and 96 switches.<br>- 33-bus distribution system | No | No |

[1] N/A (Not applicable) means that no information was provided

Table 2.1 provides a comprehensive list of some of the surveyed research works on distribution network feeder reconfiguration.

### 2.5. Comparative analysis of the literature review on the distribution network feeder reconfiguration

This section provides an analysis of the literature review on the distribution network feeder reconfiguration problem and the optimisation methods used to solve the problem.

#### 2.5.1. Analysis of the distribution network feeder reconfiguration problem objectives

From the survey, it can be inferred that the application of optimal distribution network feeder reconfiguration has many goals or objectives. The most common objectives are the following:

- **Power loss minimisation**: The energy lost in the power system in general and particularly in the distribution system leads to reduced energy availability and unnecessary operational and management costs. So, minimising the power loss results in surplus power availability and significant cost savings.
- **Load balancing**: The objective of load balancing is to find the best distribution network topology to balance the loads amongst distribution feeders by altering the network topology via switching (ON/OFF) of the tie and section lines. Load balancing allows for the partial relocation of loads from heavily loaded feeders to adjacent lightly loaded feeders.
- **Service restoration:** If a fault occurs in the distribution network, the management system is tasked to locate the fault and identify the type of fault. Successful fault location and identification is followed by an interruption of the service supply at the faulty part of the network. If the fault is temporary (transient faults), the grid management system should restore the power supply to the affected area after the fault is cleared. In the fault persists beyond a certain period, the optimal feeder reconfiguration of the distribution network should allow the power supply to be rerouted accordingly, to minimise the outage time and restore the power to disconnected loads.
- **Voltage profile improvement:** In distribution networks, the low $\frac{R}{X}$ ratio inevitably causes some voltage drop along the lines, from the substation to the end-user points. Reactive power compensation devices and voltage regulators are used to keep the voltage within the recommended margins. Optimal feeder reconfiguration can alter the topology of the network to keep the voltage in the allowable range without the need for additional equipment.

Power loss minimisation remains the most used objective function in optimal distribution network feeder reconfiguration. In some instances, the optimal distribution network feeder reconfiguration problem consists of two or more objectives, as shown in research works by (Niknam, 2011), (Olamaei et al., 2008), and (Voropai & Bat-Undraal, 2012).

The trends suggest that in the research works conducted before 2000, the distribution network feeder reconfiguration problem is formulated as a single-objective problem. As of 2000, the distribution network feeder reconfiguration problem is formulated as both a single-objective and multi-objective problem. However, most of the multi-objective problems are converted into a single-objective problem using the weighted-sum approach. Another popular method to solve the multi-objective distribution feeder reconfiguration problem is by using the Pareto-front approach.

Irrespective of the objective(s), the application of feeder reconfiguration in distribution networks is subjected to some constraints. The most considered constraints are the voltage limit constraint, the current limit constraint (branch capacity) and the topological constraint (network radiality).

### 2.5.2. Analysis of the optimisation methods used in feeder reconfiguration

Classical, heuristic and meta-heuristic optimisation solution algorithms have been suggested to solve the distribution network feeder reconfiguration problem.

Early solution algorithms developed to solve the feeder reconfiguration problem were based on successive load flows (Back & Merlin, 1975). Successive load flow methods have the advantages of providing a near-global optimum solution and a final network topology which is independent of the initial switching configuration. However, successive loads flows-based optimisation methods are not viable for the real-time feeder reconfiguration of distribution networks, due to their computational burden. The fact that a load flow is performed at every iteration and for every possible configuration makes successive loads flow approaches computationally inefficient.

Feeder reconfiguration solution algorithms based on mathematical programming (classical methods) were first introduced in (Liu et al., 1989). Mathematical programming approaches are best suited for problems that fulfil certain conditions, and constraints with specific format type. For instance, the Linear Programming approach is best suited to solve problems with linear objective function and constraints, and it may not be a good approach to solve nonlinear optimisation problems. Therefore, due to the non-linear nature of the distribution network feeder reconfiguration problem, its objective functions and constraints need to be converted into a linear format type before to be solved by a Linear

Programming. Similarly, the objectives and constraints of the distribution network feeder reconfiguration problem should be converted in a quadratic format type before to be solved using a Quadratic Programming approach. As such, given that when using classical optimisation methods to solve the distribution network feeder reconfiguration problem, approximations are made to convert the objective functions and the constraints from a format type to another (e.g. from quadratic to linear), and finding good solutions to the distribution network feeder reconfiguration problem becomes more difficult.
Moreover, mathematical programming-based algorithms are too time-consuming, and thus unsuitable for the feeder reconfiguration problem.

To deal with the shortcomings of classical programming methods in solving the distribution network feeder reconfiguration problem, heuristic algorithms have been used. Heuristic algorithms are deemed more direct, intuitive, and fast enough to be used in the implementation of distribution networks feeder reconfiguration. Heuristic algorithms have the advantages of quickly determining the switches configuration which provides reduced distribution network power losses, although it is not guaranteed that the final solution is optimal. When heuristic algorithms are used to solve the feeder reconfiguration problem, the final solution is dependent on the initial distribution network switches status.

The use of heuristic and classical programming algorithms in distribution network feeder reconfiguration is being phased-out as a new breed of artificial intelligence, or meta-heuristic algorithms is emerging. Metaheuristics algorithms are effective search strategies used to guide the search procedure with the objective to efficiently explore the search space to find the optimal solution. Although **local-search single-solution** algorithms such as Tabu-Search (Zhang et al., 2007) have also been used to solve the feeder reconfiguration problem, the most commonly used metaheuristic algorithms are **population-based global-search** algorithms such as Genetic Algorithm (Enacheanu et al., 2008), Particle Swarm Optimization (Jin et al., 2004), Differential Evolution (Su & Lee, 2003), Ant Colony optimization (Hu et al., 2008), Honey Bee Mating Optimization (Niknam, 2011), etc. If applied adequately, almost all metaheuristic algorithms are suitable for optimisation of large power system networks. They have been proven to be successful in solving small and large distribution network feeder reconfiguration problem. A range of distribution systems has been used in the literature to test the performance of metaheuristic algorithms in feeder reconfiguration. The most recurrent distribution systems are the 16-bus distribution network, the 33-bus distribution network, and the 69-bus distribution network. The most significant distribution system recorded in the literature is the 119-bus distribution system.

Like other optimisation methods, meta-heuristic can get stuck in the local optima (premature convergence). But when applied accordingly, they are more likely to converge to the global optimum. The significant drawbacks of metaheuristic optimisation methods remain the **convergence speed** and **the adequate adjustment of their search parameters**.

## 2.6. Review of the existing literature on optimal Distributed Generation Placement and sizing

The benefits of Distributed Generation in distribution networks cannot be secured if the Distributed Generations are not correctly sized and placed. Independently of the objective function, researchers have developed a number of optimisation algorithms to solve the Distributed Generation placement problem. The major methods used to solve the optimal Distributed Generation placement and sizing problem are classified as follows:

- **Analytical methods**: Analytical methods are based on logical reasoning and analysis. Some research works using analytical methods to solve the optimal Distributed Generation placement & sizing problems include (Acharya et al., 2006) which used a loss sensitivity factor based on the exact loss formula; and (Hung et al., 2010) which uses the Exact loss formula to find the optimal DG location and size
- **Classical optimisation method**: Classical optimisation methods are based on iterative search algorithms. Classical optimisation methods used to solve the optimal DG placement and sizing problem include Dynamic Programming (Khalesi et al., 2010), and Mixed Integer Non-Linear Programming (Kaur et al., 2014)
- **Heuristic and Metaheuristic methods**: the concepts of heuristic and meta-heuristic are intertwined. As such, some heuristic optimisation methods are referred to as metaheuristic methods. Meta-heuristic search methods used to solve the optimal DG placement and sizing problem include Human intelligence algorithms Genetic Algorithm (Borges & Falcao, 2006); and social intelligence algorithms such as Ant Colony Optimization (Abu-Mouti & El-Hawary, 2011), and Particle Swarm optimisation (Aman et al., 2013).

To complete the literature review on the optimal DG placement and sizing problem, past research works, conference papers, journals, and thesis were surveyed and compared. The survey and the comparison are accomplished using the following criteria:

- **Objective function**: It characterises the nature of the problem to be solved. The objective function can be the power loss minimisation, the maximisation of the system loadability, the maximisation of the system reliability, the voltage deviation minimisation, or the voltage stability index maximisation.
- **Constraints**: the developed scheme may be subject to operational constraints such as the DG size limit, the DG placement constraints, the voltage limits, and the current limits.
- **Algorithm used**: Analytical, classical, and meta-heuristic optimisation methods have been successfully used to solve the problem of optimal DG placement and sizing.
- **Distribution networks**: To demonstrate their practicability, the developed distribution network feeder reconfiguration schemes are tested on a variety of distribution networks such as the 16-bus, the 33-bus, and the 69-bus IEEE distribution networks.
- **Software**: There is a broad range of available software to simulate and analyse a distribution system. Some of those softwares are MATLAB and GAMS. However, the suitability of a given software is dependent on the problem to solve.
- **DG type**: DG can be classified into four types, depending on their real and reactive power delivering capabilities.

  Type I DG only injects real power in the distribution systems (Venkatesh, 2014).

  Type II DG only injects reactive power Q in the distribution system (Hung et al., 2010).

  Type III DG can inject both the real and reactive power in the network.

  Type IV DG injects the real power (P) in the network but absorbs reactive power (Q) from the network (Hung et al., 2010).

Table 2.2 provides the summary of some research works on the optimal DG placement and sizing problem.

**Table 2.2**: **Summary of research works on the optimal Distributed Generation placement and sizing problem**

| Reference paper | Objective | constraints | Algorithm | Distribution system | Number of DG | DG type | Software |
|---|---|---|---|---|---|---|---|
| (Moradi & Abedini, 2012) | Power loss minimization<br><br>Voltage profile improvement<br><br>Voltage stability improvement | - Load balance constraint<br><br>- Voltage constraint<br><br>- DG technical constraints<br><br>- Branch capacity constraint | Combined Genetic Algorithm and Particle Swarm Optimisation | - 33-bus distribution network<br><br>- 69-bus distribution network | Three | Type I | MATLAB |
| (Aman et al., 2013) | Power loss minimisation<br><br>Bus voltage stability maximisation<br><br>Line voltage stability maximisation | DG size limit | Weighted Multi-Objective Particle Swarm Optimisation (MOPSO) | - 12-bus distribution network<br><br>- 30-bus distribution network<br><br>- 33-bus distribution network<br><br>- 69-bus distribution network | One | Type I | N/A |
| (Abdi & Afshar, 2013) | Real and reactive power minimisation<br><br>Voltage profile improvement<br><br>System stability Improvement | Voltage limit Constraint<br><br>Branch Capacity constraint | Hybrid Improved Particle Swarm Optimisation (IPSO)/Monte Carlo simulation | 33-bus distribution system | - One<br><br>- Two<br><br>- Three | Type I | N/A |

| | | | | | | | |
|---|---|---|---|---|---|---|---|
| (Acharya et al., 2006) | Power loss minimisation | Power balance Constraint<br><br>DG size limit | Loss sensitivity factor based on the Exact Loss formula | - 30-bus distribution network<br><br>- 33-bus distribution network<br><br>- 69-bus distribution network | One | Type I | MATLAB |
| (Gopiya et al., 2013) | Real power loss minimisation | Voltage Constraint<br><br>current limit constraints<br><br>DG size limit<br><br>Power balance constraint | Real power loss Sensitivity Analysis technique | - 12-bus distribution network<br><br>- 33-bus distribution network | - One<br><br>- Two | Type I<br><br>Type III | MATLAB |
| (Zeinalzadeh et al., 2015) | Real power Loss Minimization<br><br>Voltage Stability Improvement<br><br>Balancing branch current | Power balance Constraint<br><br>Voltage and Branch capacity limit constraint<br><br>DG size limit | Pareto-optimal MOPSO | - 33-bus distribution system<br><br>- Actual 94-bus Portuguese distribution system | Three | Type III | MATLAB |
| (Kansal et al., 2013) | Power loss minimisation | Power balance Constraint<br><br>Voltage and current limit constraints<br><br>DG location constraint | PSO | - 33-bus distribution system<br><br>- 69-bus distribution system | - One<br><br>- Two | Type I, Type II, Type III Indepen-dently<br><br>Type I & Type II Simulta-neously | MATLAB |

| | | | | | | | |
|---|---|---|---|---|---|---|---|
| (Hung et al., 2010) | Power loss minimisation | DG size limit<br><br>Voltage limit constraint | Exact loss formula | - 16-bus distribution network<br><br>- 33-bus distribution network<br><br>- 69-bus distribution network | One | Type III | MATLAB |
| (Khalesi et al., 2010) | Power loss Minimisation<br><br>System Reliability Enhancement<br><br>Voltage profile improvement | DG size limit<br><br>Branch capacity limit<br><br>Voltage limit | Dynamic Programming | Hypothetical 9-bus distribution system | One | Type I | MATLAB |
| (Kaur et al., 2014) | Power loss minimization | Power balance constraint<br><br>Voltage and current limit constraints<br><br>DG size limit constraint<br><br>Number of DG limit | Mixed Integer Non-Linear Programming | - 33-bus distribution network<br><br>- 69-bus distribution network | - One<br><br>- Two<br><br>- Three | Type I<br><br>Type III | MATLAB AMPL |
| (Atwa & El-Saadany, 2010) | Power loss minimisation | Voltage and Branch capacity limit constraints<br><br>DG size limit constraint<br><br>DG penetration level | Mixed Integer Non-Linear Programming | IEEE RTS-96 load transition system | Three | Type IV | GAMS |

| | | | | | | | |
|---|---|---|---|---|---|---|---|
| (Rama Prabha et al., 2015) | Power loss minimization | Power balance Constraint<br><br>Voltage and current limit constraints | Combined Loss Sensitivity Factor (LSF) and Intelligent Water Drop (IWD) algorithm | - 10-bus distribution network<br>- 33-bus distribution network<br>- 69-bus distribution network | - One<br>- Three | Type I | MATLAB |
| (Moravej & Akhlaghi, 2013) | Voltage profile Improvement<br><br>Power loss minimisation | Power balance constraint<br><br>Voltage and Branch capacity limit constraints | Cuckoo search | - 38-bus distribution network<br>- 69-bus distribution network | Four | Type I | MATLAB |
| (Abu-Mouti & El-Hawary, 2011) | Real power Loss minimisation | Power balance Constraint<br><br>Voltage and Branch capacity limit constraint<br><br>DG size limit constraint | Artificial Bee Colony (ABC) algorithm | 69-bus distribution system | - One<br>- Two | Type III | C programming |
| (Kefayat et al., 2015) | Minimisation of power loss, total emission produced by substation & resources, total cost of electrical energy.<br><br>Voltage Stability improvement | Power balance Constraint<br><br>Voltage constraint | Hybrid of Ant Colony Optimisation & Artificial Bee Colony | - 33-bus distribution system<br>- 69-bus distribution system | - One<br>- Two<br>- Three<br>- Four<br>- Five<br>- Six<br>- Seven | Type I | N/A |

| | | | | | | | |
|---|---|---|---|---|---|---|---|
| (Dehghanian et al., 2013) | Minimisation of total imposed costs, total network losses, customer outage costs and private investments | Power balance constraint<br><br>Voltage Constraint<br><br>DG size constraint | NSGAII | 37-bus distribution system | One | Type I | MATLAB |
| (Borges & Falcão, 2006) | Minimize power loss<br><br>Guarantee acceptable reliability level<br><br>Guarantee acceptable voltage profile | Voltage constraint<br><br>DG size limit constraint | GA | 2 Hypothetical distribution systems | Two | Type I | N/A |
| (Murthy & Kumar, 2013) | Minimisation of the cost of power loss<br><br>Minimisation of the cost of power supplied from DG | N/A | - Combined power Loss sensitivity method<br><br>- Index vector Method<br><br>- Voltage sensitivity index | - 33-bus distribution network<br><br>- 69-bus distribution network | One | Type I<br><br>Type III | N/A |

[1] N/A means that no information was provided

## 2.7. Comparative analysis of the literature review on optimal DG placement and sizing

From the literature review, it is observed that most research works on the DG placement and sizing problem are as recent as the year 2000. This may be due to the growing interest in Distributed Generation in the last two decades. Although there is an extensive number of research works in the topic of optimal placement and sizing of DG, only those in Table 2.2 have been retained to illustrate the state of the research on the optimal placement and sizing of DG. Very few research works used classical optimisation or heuristic algorithms to solve the problem of optimal DG placement and sizing. This may be justified by the fact that by 2000, more advanced computational intelligence optimisation approaches were already available. Metaheuristic/artificial intelligence and analytical optimisation are the most used approaches to solve the optimal DG placement and sizing. The objectives used in the literature review includes the power loss minimisation, the load balancing, the system reliability enhancement, the voltage profile improvement, the total cost of DG integration, and voltage stability improvement amongst other. Power loss minimisation remains an undeniable aspect in most of the research works found in the literature.

### 2.7.1. Analysis of the optimisation approaches used in the DG placement and sizing problem

This section provides a review analysis on the analytical, classical and meta-heuristic optimisation algorithms used in to solve the DG placement & sizing problem.

In analytical approaches, the distribution system is modelled by a mathematical expression, and a systematic approach is developed to determine the optimal solution of the problem. Analytical approaches are more suited for small distribution systems, with a limited number of parameters. In terms of accuracy and computational speed, analytical optimisation methods are only as accurate as the mathematical formulation of the problem and the developed system approach allows. The performance of analytical optimisation approaches in large and complex systems is mediocre (Viral & Khatod, 2012).

The most common analytical methods are the index-based method, the Point Estimation method and the sensitivity index-based method (Prakash & Khatod, 2016). The index method is based on the deviation of a parameter from its base value. The indexes are measured in terms of the relative deviation (Prakash & Khatod, 2016). An application of the index based analytical method is found in the research works by (Kuroda et al., 2012). Sensitivity index-based methods are built on the belief that varying a parameter affects the objective variable. (Gopiya et al., 2012) used the voltage sensitivity index to find the optimal position of the DG in the distribution network. After calculation of the Voltage Stability Index

(VSI) at each bus, the authors identified the bus with the lowest VSI as the location for DG placement. (Murthy and Kumar, 2013) used a combined loss sensitivity to determine the candidate position for DG placement in the distribution network. The combined loss sensitivity method is derived from the fact that the installation of the Distributed Generation in the distribution network does not only affect the real/reactive power loss but can affect both the real and the reactive power.
Analytical methods are good at finding the optimal location for DG placement, but they fail to find the optimal size of the DG.

(Khalesi et al., 2010) applied a dynamic programming approach to determine the optimal DG location for the minimisation of power loss, the improvement of the stability, and the enhancement of the voltage profile in distribution networks. Their research work only focused on finding the best DG location. The DG sizing was handled by varying the DG size as a percentage of the peak load. The dynamic programming approach developed by (Khalesi et al., 2010) was only tested in a small distribution system, and its performance and reliability in medium and large distribution systems were not examined.
(Atwa & El-Saadany, 2010) and (Kaur et al., 2014) solved the DG allocation problem using Mixed Integer Non-Linear Programming (MINLP) approaches. In their research, (Atwa & El-Saadany, 2010) used a probabilistic approach to allocate and size a wind-based DG. The developed MINLP approach takes into consideration the DG uncertainties (such as wind speed) the load variations. The research work by (Kaur et al., 2014) subdivided the problem of optimal DG placement & sizing into two sub-problems: The Siting Planning Model (SPM) to find the DG location, and the Capacity Planning Model (CPM) to determine the optimal DG size. The method used loss sensitivity factors to determine the candidate buses for DG placement. The sizing is obtained by using a combination of Sequential Quadratic Programming and branch & bound methods. The proposed techniques were successfully applied to a range of distribution systems and are deemed efficient by the authors.

Classical optimisation techniques lack the flexibility required to solve the DG allocation problem (Jordehi, 2015). Heuristic search algorithms are mostly pathfinding algorithms and therefore unsuited for the DG allocation problem. So, most of the research works used meta-heuristic methods to solve the optimal DG placement and sizing problem. The meta-heuristic approaches used in the literature range from single-objective algorithm such as the Particle Swarm Optimization (PSO) (Kansal et al., 2013); and the Artificial Bee Colony (Abu-Mouti & El-Hawary, 2013), to multi-objective algorithms such as the Non-Dominated

Sorting Genetic Algorithm II (NSGAII) (Dehghanian et al., 2013) and the Multi-Objective Particle Swarm Optimization (MOPSO) (Zeinalzadeh et al., 2015). Metaheuristics have been proven efficient in solving the DG allocation problem (Prakash & Khatod, 2016). They are flexible and well suited for single and multi-objective DG placement and sizing problems.

Although efficient, some metaheuristic approaches may have drawbacks. GA, for instance, is computationally expensive and it takes a long processing time to solve the DG allocation problem. To circumvent their shortcomings, two or more algorithms may be combined to form a new and more powerful algorithm referred to as a hybrid algorithm. (Moradi & Abedini, 2012) used a combination of GA and PSO in their research. (Abdi & Afshar, 2013) and (Kefayat et al., 2015) used a hybrid ACO/ABC and a hybrid PSO/Monte Carlo Simulation, respectively for multi-objective DG allocation problems.

Another drawback of metaheuristic approaches is that they might be trapped in the local optima and then give an inaccurate solution. So, intensive research is being undertaken to devise mechanisms to avoid premature convergence in the DG allocation problem (Jordehi, 2015).

### 2.7.2. Analysis of the DG types and the distribution systems used in the optimal DG placement and sizing problem

The most used DG types in the literature are Type I DG, Type II DG and Type 3 DG. One salient characteristic of the research works in the literature is that the DG type is predefined before the optimisation process starts. Some research works such as (Acharya et al., 2006) and (Hung et al., 2010) focused on the optimal placement and sizing of a single DG, while others such as (Aman et al., 2014) and (Abdi & Afshar, 2013) also looked at multi-DG placement and sizing. Further details about the different DG types are given in Chapter Four, section 4.2.1. Research works focusing on the optimal placement and sizing of Type IV DG such as (Atwa & El-Saadany, 2010) are rare and not commonly found in the literature.

The distribution systems used in the literature to test the effectiveness of the algorithms developed to solve the problem of optimal DG placement and sizing range from a hypothetical 5-bus distribution network to the 94-bus distribution network. Most of the research works use two or more distribution systems in their case studies. However, the most recurrent distribution systems used in the literature are the 33-bus distribution network and the 69-bus distribution network.

## 2.8. Review of the existing literature involving both the optimal distribution network feeder reconfiguration and the optimal DG placement and sizing problem

The research works analysed so far dealt with either the optimal distribution network feeder reconfiguration problem or the optimal DG placement and sizing problem independently. However, in some research works, both the optimal distribution network feeder reconfiguration problem and the optimal DG placement and sizing problem are considered. Table 2.3 provides the summary of some research works which consider both the optimal distribution network feeder reconfiguration problem or the optimal DG placement and sizing problem. The summary is accomplished using the following criteria:

- **Objective function**
- **Constraints**
- **Algorithm used**
- **Distribution networks**
- **Software**
- **Number of DG**

A characteristic common in these research works is that they all deal with multi-DG placement and sizing.

Research works by (Chidanandappa et al., 2015), (Ma et al., 2015), (Cailian et al., 2014), (Hao et al., 2014) and (Guan et al., 2015) propose a solution algorithm for optimal feeder reconfiguration problem in distribution networks with Distributed Generation. To solve this optimisation problem, the authors used the Genetic Algorithm (GA), the Improved Hybrid Clonal Genetic Algorithm/Tabu-Search, the Immune Genetic Algorithm, the Improved Adaptive Genetic Algorithm, and the Decimal Encoding to Quantum Particle Swarm Optimization (DQPSO), respectively. In the research works above, the location and the size of the DG are predefined, meaning that the proposed algorithms are used only to solve the feeder reconfiguration problem. It is also noted that the distribution systems used in these research works are IEEE distribution systems which do not have DG in their original design. The DG location and size in the IEEE distribution systems are different for all the research works above, and it is unknown if the IEEE distribution systems were subjected to any optimisation to determine the respective DG location and size.

**Table 2.3**: **Review of literature works which consider both the optimal feeder reconfiguration and Distributed Generation placement**

| Reference paper | Objectives | Algorithm | | Distribution system | Number of DG | Comments |
|---|---|---|---|---|---|---|
| | | Feeder reconfiguration | DG allocation | | | |
| (Rao et al., 2013) | Real power loss minimisation<br><br>Voltage improvement | Harmony Search Algorithm (HSA) | Sensitivity analysis | - 33-bus distribution system<br>- 69-bus distribution system | Three | Sensitivity analysis used to determine the candidate buses for DG location.<br><br>HSA used for simultaneous DG sizing and feeder reconfiguration. |
| (Chidanandappa et al., 2015) | Power loss minimisation<br><br>Number of Switching minimisation | GA | N/A | 33-bus distribution system | Five | No mention of the algorithm used for DG placement.<br><br>DG allocation takes place before feeder reconfiguration |
| (Ma et al., 2015) | Power loss minimisation | Improved hybrid Clonal Genetic Algorithm (CGA)/ Tabu Search | N/A | 33-bus distribution system | Four | Type 3 DG with predefined location and size |
| (Cailian et al., 2014) | Power loss minimisation | Immune Genetic Algorithm | N/A | 33-bus distribution system | Four | DG of type I, II, III Location and size predefined |
| (Hao et al., 2014) | Power loss Minimisation<br><br>Improvement of the utilisation of renewable energy resources (PV and wind) to reduce the demand for traditional energy consumption | improved Adaptive Genetic Algorithm | N/A | 33-bus distribution system | Two | PV and wind turbine |

| | | | | | | |
|---|---|---|---|---|---|---|
| (Bayat et al., 2015) | Maximum power loss reduction | Uniform Voltage Distribution based constructive reconfiguration Algorithm (UVDA) | | 33-bus distribution system | Three | UDVA used for DG allocation and feeder reconfiguration |
| (Guan et al., 2015) | Real power loss minimisation | Decimal Encoding to Quantum Particle Swarm Optimisation (DQPSO) | N/A | - 33-bus distribution system<br>- 69-bus distribution system | - Four for 33-bus distribution system<br>- Two for 69-Bus distribution system | DQPSO has a mechanism that prevent entrapment in local optima and guaranty convergence |
| (Imran et al., 2014) | Power loss Minimisation<br><br>Voltage stability enhancement | Fireworks Algorithm | | - 33-bus distribution system<br>- 69-bus distribution system | Three | DG allocation and Feeder reconfiguration |
| (Das et al., 2017) | Real power loss reduction | GA | Sensitivity analysis | - 33-bus distribution system<br>- 69-bus distribution system | Three | Sensitivity analysis used to determine the candidate buses for DG location.<br><br>GA used for DG sizing followed by feeder reconfiguration. |
| (Sedighizadeh et al.,2014) | Power loss minimisation Voltage stability Improvement<br><br>DG cost Minimisation<br><br>Greenhouse gas Emissions Minimisation | Hybrid Big Bang-Big Crunch (HBB-BC) | | - 33-bus distribution system<br>- 22-bus distribution system | Two | DG allocation and Feeder reconfiguration |

[1] N/A means that no information was provided

In the research work by (Das et al., 2017), the DG location and sizing is not predefined before the optimisation process. The authors (Das et al., 2017) use the sensitivity analysis method for the optimal DG placement, while the optimal DG sizing and the optimal distribution network feeder reconfiguration process is done using the Genetic Algorithm.

The research works by (Rao et al., 2013), (Inram et al., 2014), (Sedighizadeh et al., 2014), and (Bayat et al., 2015) simultaneously solved both the optimal DG allocation and the feeder reconfiguration problems. In the research works above, five case studies were used to evaluate the performance of the developed algorithms:

- **Case 1**: The proposed algorithm is used to reconfigure the distribution system without DG present.
- **Case 2**: DG are installed in the non-reconfigured distribution system
- **Case 3**: The optimal distribution network feeder reconfiguration process occurs before the optimal DG placement and sizing
- **Case 4**: The optimal DG placement and sizing process occurs before the optimal distribution network feeder reconfiguration.
- **Case 5**: The optimal feeder reconfiguration and DG allocation processes both take place simultaneously.

(Rao et al., 2013) used the Harmony Search Algorithm (HSA) to solve the optimal distribution network feeder reconfiguration problem, and the sensitivity analysis is used to solve the optimal DG placement and sizing problem. The research works (Inram et al., 2014), (Sedighizadeh et al., 2014), and (Bayat et al., 2015) proposed the Fireworks Algorithm, the Hybrid Big Bang-Big Crush (HBB-BC) algorithm and the Uniform Voltage Distribution based constructive reconfiguration Algorithm (UVDA) to solve both the optimal distribution network feeder reconfiguration and the optimal DG placement and sizing problems.

After a comparison of the results obtained from the above five case studies, the research works by (Rao et al., 2013), (Inram et al., 2014), (Sedighizadeh et al., 2014), and (Bayat et al., 2015) all support that the case study 4 (the optimal distribution network feeder reconfiguration process occurs before the optimal DG placement and sizing) yields better results.

## 2.9. Conclusion

This chapter reviews and analyses the concept of optimisation and the existing knowledge on the application of optimisation algorithms in the optimal distribution network feeder reconfiguration and the optimal DG placement and sizing problems. It follows that utilities and network operators are forced to adjust the operation of the power grid, to comply with the growing energy demand and with new regulations in the power engineering field. As such, the shift away from fossil fuels, the integration of Distributed generations, the implementation of effective demand response mechanisms, and the improvement of the electrical grid reliability; stability; robustness and flexibility are vital issues to address. At the grid's distribution levels, distribution automation will play an important role and enable advanced monitoring, management and protection functionalities necessary for the optimal operation of the smart grid. Therefore, there is a need for new algorithms and control schemes to be designed to achieve the functionalities of distribution automation.

This thesis develops new algorithms to find the optimal topology of distribution networks, and to find the optimal location and size of Distributed Generation to be placed in distribution networks.

In the next chapter, **Particle Swarm Optimization** (PSO) algorithms are developed to solve the single and multi-objective distribution network feeder reconfiguration problems.

# CHAPTER THREE
# DEVELOPMENT OF THE PSO ALGORITHM FOR THE DISTRIBUTION NETWORK FEEDER RECONFIGURATION PROBLEM

## 3.1. Introduction

The particle swarm optimisation method was introduced in 1995 by Eberhart and Kennedy. It is a stochastic search algorithm inspired by the behavioural interaction of a flock of birds or a school of fish. It has since then been used to solve linear, non-linear, non-convex, continuous, and discrete type problems. The PSO algorithm is simple and easy to implement. It has a limited number of parameters to be tuned and a limited dependence on the initial set points. The PSO algorithm is similar to the Genetic algorithm (GA) in the sense that it starts by a random initialisation of a population (initial solution) and searches for the optimum (optimal solution) through a series of updated generations.

This chapter provides more information about the operation of the PSO, the different variants of PSO and its application in solving the distribution network reconfiguration problem.

## 3.2. Standard Particle Swarm Optimization

Optimising a function $\mathbf{f}$ consists of finding the set $\mathbf{X}^*$ such as the function $\mathbf{f}(\mathbf{X}^*)$ is either a minimum or a maximum of function $f$ in the search space. The function to optimize can be linear or non-linear, convex, or non-convex, continuous, or discrete. Depending of the search space, the optimization can be: an unconstrained optimization if there are no restrictions on the values that the variables of the optimization problem can take; a constrained optimization if the variables of the optimization problem are subjected to some limitations; and a dynamic optimization if the objective function of the problem change over time in such a way to change to the optimum. Many approaches have been developed to solve optimization problems. The Particle Swarm Optimization (PSO) is one of such approaches and, it has been used to solve diverse optimization problems.
This section presents the background or origin of the PSO algorithm, the most important parameters of the PSO and its operating principle.

### 3.2.1. Background of the PSO algorithm

The Particle Swarm Optimization (PSO) algorithm was first introduced in 1995 by Eberhart and Kennedy. It is a stochastic search algorithm inspired by the behavioural interaction of a flock of birds or a school of fish (Eberhart & Kennedy, 1995). The concept of PSO is best described by a flock of birds circling over an area where they can smell a hidden source of food. The bird closest to the food source chirps the loudest, and the other birds fly towards him. If any other bird comes closer to the food that the previous, it will chirp louder, and all the other birds will veer towards him. This process continues until the food source is reached (Kennedy & Eberhart, 1995).

In PSO algorithms, the flock of birds is represented by a set or swarm of particles $\mathbf{P} = (\mathbf{p_1}, \mathbf{p_2}, \dots, \mathbf{p_n})$, where $\mathbf{p_1}$ to $\mathbf{p_n}$ are the search agents or particles. The food source is the optimization target or optimal solution. The objective function $f$ defines the optimization problem. The position of the birds are the candidate or possible solutions to the optimization problem and they are termed particles position. The speed at which a bird is flying is represented by the velocity of the particle. Just like the bird's flying speed dictates its next position after the bird closest to the food source chirps, the velocity of a particle is an indication of how much the particle's position should be changed to match the target. The particle's velocity is dependent on the distance between the particle and the target: the bigger the distance between them, the larger the velocity value. The position $\mathbf{x_i}$ and the velocity $\mathbf{v_i}$ of particle $\mathbf{p_i}$ change over time. The closest a particle (bird) has ever come to the target (food source) is the particle's personal best position $\mathbf{pbest_i}$. Therefore, in the PSO algorithm, each particle consists of the following:

- **Position** that represents a possible solution
- **Velocity** which indicates the rate of change of the particle position
- **Personal best value** which indicates the closest the particle has ever come to the target.

The next part of this section covers the parameters of the PSO algorithm.

### 3.2.2. Parameters of the PSO algorithm

One of the advantages of the particle swarm optimisation algorithm is the fact that it has only a few parameters. Some of these parameters have a significant effect on the PSO algorithm, and if not carefully selected they can negatively impact on the efficiency and performance of the PSO algorithm. Some of the PSO algorithm parameters include the number of particles, the dimension of the search space, the range of the particles, the stopping criteria, and the learning factors or acceleration coefficients

#### 3.2.2.1. Number of particles or swarm size

The number of particles in the swarm should be selected accordingly for the PSO algorithm to perform optimally. The larger the swarm size, the higher the computation time taken by the PSO algorithm to find the optimal solution. The smaller the swarm size, the smaller the computation time taken by the PSO algorithm to find the optimal solution. However, a large swarm size covers large parts of the search space and increase the chance of finding the optimal solution. In contrast, a small swarm size won't cover the whole search space, and consequently, the probability of the particle to be trapped in the local optima is increased. In most practical applications, the number of particle lies in the range [20, 60] although a swarm of 10 particles is large enough for some problems.

#### 3.2.2.2. Dimension of the search space

The dimension of the search space is problem dependent. The search space is a delimited area within which the optimal solution lies. The particles have a better chance to find the optimal solution if they don't wander out of the search space during the search process, and therefore the particles' positions should be constrained within the search space.

#### 3.2.2.3. Range of the particles

The range of a particle is dependent on the problem to be optimised. It represents all the possible positions the particle can occupy without leaving the search space. The particle should be constrained within the domain $[\mathbf{x}_{\mathbf{min}}, \mathbf{x}_{\mathbf{max}}]$, where $\mathbf{x}_{\mathbf{min}}$ and $\mathbf{x}_{\mathbf{max}}$ are the minimum and maximum position respectively that the particle can occupy in the search space.

#### 3.2.2.4. Stopping criteria

In the PSO algorithm, the particles have no intelligence on their own, and they are not able to stop the search process on their own. Therefore, a stopping criterion should be established to terminate the PSO iterative search process. Many criteria can be used to stop the search (Engelbrecht, 2007). They are:

- **The maximum number of iteration**: the PSO search process is terminated when the maximum number of iteration is reached. Precautions should be taken when choosing the maximum number of iterations, as a small number of iterations can prematurely end the search process, meaning that the search process can stop before the optimal solution is reached. In contrast, a high number of iterations only increases computation the time taken by the PSO algorithm to find the optimal solution.

- **The stagnant global best position**: When the global best position does not improve over a certain number of iterations, the PSO search process can be stopped. This is often illustrated by the velocity keeping a value of zero over several iterations.

#### 3.2.2.5. Velocity

The velocity update equation has three components:

- $\mathbf{v_i}^{\mathbf{k}}$ is the velocity of the particle $\mathbf{i}$ at iteration $\mathbf{k}$. This component prevents an abrupt change in the particle direction and force the particle to keep moving in its current direction.
- $\mathbf{c1} * \mathbf{rand1} * \left(\mathbf{Pbest_i} - \mathbf{x_i}^{\mathbf{k}}\right)$ is a measure of the particle's current performance relative to its past experience. This term is often referred to as the cognitive component.
- $\mathbf{c2} * \mathbf{rand2} * \left(\mathbf{Gbest_i} - \mathbf{x_i}^{\mathbf{k}}\right)$ or $\mathbf{c2} * \mathbf{rand2} * \left(\mathbf{Lbest_i} - \mathbf{x_i}^{\mathbf{k}}\right)$ is a measure of the particle's current performance relative to its neighbours' (Local Best PSO) or the other particles in the swarm (Global best PSO). This term is referred to as the social component.

The following observations are made about the components of the velocity update equation.

- The cognitive and the social components of the velocity update equation are used to change the particle's velocity. In the absence of those terms, the movements of the particle would be unidirectional, i.e. the particles would move in the same direction until they reach the limits of the search space (Shi & Eberhart, 1998).
- If the cognitive component alone is zeroed, all the particles will be attracted to a unique point: the local/global best point.
- In contrast, if it is the social component that is zeroed, all particles would be independent, i.e. a particle's position would not be affected by other particles in the swarm or neighbourhood (Shi & Eberhart, 1998).
- If it is the first term that is absent, the particles will converge to their personal or global best values, as the velocity would only be dependent on the particle's current and best positions (Shi & Eberhart, 1998).

The range of the particles $[\mathbf{x_{min}}, \mathbf{x_{max}}]$ usually determines the maximum velocity which can be calculated using Equation 3.1.

$$\mathbf{v_{max}} = \boldsymbol{\varepsilon}\left(\mathbf{x_{max}} - \mathbf{x_{min}}\right) \tag{3.1}$$

where

$\boldsymbol{\varepsilon}$ is a random constant in the interval ]0, 1[.

#### 3.2.2.6. Learning factors

Also referred to as acceleration coefficients, the learning factors $\mathbf{c1}$ and $\mathbf{c2}$ preserve the unpredictable effect of the cognitive and social components of the velocity. $\mathbf{c1}$ is a characteristic of how confident a particle is about itself, whereas $\mathbf{c2}$ highlights the confidence of a particle in its neighbours. In practise, $\mathbf{c1}$ and $\mathbf{c2}$ are usually selected in the range [0, 4] (Van Den Bergh, 2002).

If $\mathbf{c1} \gg \mathbf{c2}$, the particles are more leaning towards their personal best positions. This results in the particles wandering excessively without being able to reach the optimal solution.

In the case where $\mathbf{c1} \ll \mathbf{c2}$, the movement of the particles is more inclined towards the global best or local best position, and often resulting in premature convergence (Van Den Bergh, 2002).

The appropriate value for the learning factors is 2 (Kennedy & Eberhart, 1995). For $\mathbf{c1} = \mathbf{c2} = \mathbf{2}$, all particles in the swarm move towards the average personal best position and global/local best position.

### 3.2.3. Mode of operation of the PSO algorithm

The operating principle of the PSO algorithm is as follows.

- **Initialisation of the parameters of the PSO algorithm**. The PSO algorithm starts by the setting of the PSO parameters such as the acceleration constants $\mathbf{c1}$ and $\mathbf{c2}$; the dimension of the search space $\mathrm{D}$; the swarm size, the maximum number of iterations.
- **Initialisation of the particle's components**.
    - **Initialise the particles' position**. The position of the particles is randomly generated within the search space.
    - **Initialise the particles' velocity**. The velocity can also be randomly generated, but it is usually set to zero to prevent the particles from swinging out of the search space during the first iterations (Clerc & Kennedy, 2002).
    - **Initialise the particles' best positions**. The particles' best positions should also be initialised. In some instances, the particles' best positions are the same as their initial positions, that is if the particles have visited no other position than their initial position.

- **Update the best know position in the swarm**. In the case of a minimisation problem, the best position in the swarm is the position of the particle with the least objective value (fitness value). In a maximisation problem, the position of the particle with the highest objective value (fitness value) is the best position in the swarm.

- **In the main loop,**
    - **Calculate the objective value**: The objective value of each particle is calculated using the objective function.
    - **Update the particles' s best positions**.
    - **Update the best position in the swarm**.
    - **Update the velocity of the particles**. A particle adjusts its velocity according to his own experience and that of its neighbourhood. The velocity update equation is given in Equation 3.2.

$$\mathbf{v_i}^{\mathbf{k+1}} = \mathbf{v_i}^{\mathbf{k}} + \mathbf{c1} * \mathbf{rand1} * \left(\mathbf{Pbest_i}^{\mathbf{k}} - \mathbf{x_i}^{\mathbf{k}}\right) + \mathbf{c2} * \mathbf{rand2} * \left(\mathbf{Gbest}^{\mathbf{k}} - \mathbf{x_i}^{\mathbf{k}}\right) \tag{3.2}$$

Where

$\mathbf{v_i}^{\mathbf{k}}$ is the velocity of the particle $\mathbf{i}$ at iteration $\mathbf{k}$.

$\mathbf{c1}$ and $\mathbf{c2}$ are the acceleration coefficients.

$\mathbf{x_i}^{\mathbf{k}}$ is the position of particle $\mathbf{i}$ at iteration $\mathbf{k}$.

$\mathbf{Pbest_i}^{\mathbf{k}}$ is the best position of particle $\mathbf{i}$ at iteration $\mathbf{k}$.

$\mathbf{Gbest}^{\mathbf{k}}$ is the best position in the swarm at iteration $\mathbf{k}$.

$\mathbf{rand1}$ and $\mathbf{rand2}$ are random numbers between 0 and 1.

- **Update the position of the particles.** The position of a particle is updated using Equation 3.3.

$$\mathbf{x_i}^{\mathbf{k+1}} = \mathbf{x_i}^{\mathbf{k}} + \mathbf{v_i}^{\mathbf{k+1}} \tag{3.3}$$

Where

$\mathbf{x_i}^{\mathbf{k}}$ denotes the position of particle $\mathbf{i}$ at iteration $\mathbf{k}$.

$\mathbf{v_i}^{\mathbf{k}}$ is the velocity of the particle $\mathbf{i}$ at iteration $\mathbf{k}$.

- **Print the results.** At the end of the PSO search process, the optimal solution should be displayed.

In the PSO algorithm, a particle updates its position and velocity according to his own experience and those of its neighbours. Depending on the size of the neighbourhood, two types of PSO can be derived: The Local Best (Lbest) PSO and the Global best (Gbest) PSO. A neighbourhood defines the extent of the social interaction between the particles in the swarm. Figures 3.1.a and 3.1.b represent the neighbourhood topologies for the Global best PSO and the local best PSO respectively, where $\mathbf{p_1}$ to $\mathbf{p_6}$ are the particles.

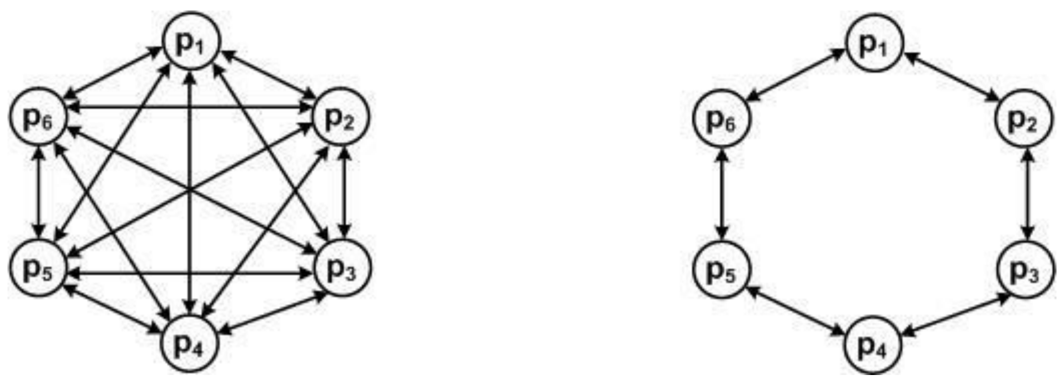


**a. Star neighbourhood topology** **b. Ring neighbourhood topology**

**Figure 3.1: Neighbourhood topologies for the local and global best PSO**

In the local best PSO, each particle only gathers information from its immediate neighbouring particles as illustrated in Figure 3.1.b. So, a particle's position and velocity are just influenced by its own experience and the position of its best performing neighbouring particle which is the particle with least (in the case of a minimisation problem) or highest (in the case of a minimisation problem) objective value (Li & Deb, 2010). The particle's position is updated using Equation 3.3. Its velocity is updated using Equation 3.4.

$$\mathbf{v_i^{k+1} = v_i^k + c1 * rand1 * \left(Pbest_i - x_i^k\right) + c2 * rand2 * \left(Lbest_i^k - x_i^k\right)} \qquad (3.4)$$

Where

$\mathbf{Lbest_i^k}$ is the position best performing particle in the neighbourhood of particle $\mathbf{i}$.

In the global best PSO, each particle gathers information from all the other particles in the entire swarm as illustrated in Figure 3.1.a. So, the position and the velocity of a particle are influenced by its own experience and the position of the best performing particle in the entire swarm (Bratton & Kennedy, 2007). The particle's position is updated using Equation 3.3. Its velocity is updated using Equation 3.2.

Due to the large interconnectivity between the particles, the Global best PSO tends to converge faster than the Local best PSO. The Local best PSO is, however, less likely to be trapped in the local optima (non-optimal solution). In sum, the Global best PSO is recommended when quick results are desired and, the Local best PSO when refined results are desired (Engelbrecht, 2007).

## 3.3. Improvement of the convergence rate of the PSO algorithm

Two features are often used to determine the effectiveness of a Particle Swarm Optimization algorithm. They are:

- The exploration which is the ability of the PSO algorithm to search through diverse parts of the search space to find an excellent optimal solution.
- The exploitation which is the ability of the PSO algorithm to concentrate the search around a search area to refine the optimal solution (Talukder, 2011).

These abilities should be balanced for optimal results. Therefore, many authors have developed diverse approaches to improve the convergence rate of the PSO algorithm.

### 3.3.1. Inertia weight approach

To balance the exploration and the exploitation abilities of the PSO algorithm, a trade-off between the local and global best PSO is established using the inertia weight $\omega$. The inertia weight is to control the PSO search process and to reduce the influence of $\mathbf{v_{max}}$ or even eliminate it completely. The Inertia weight controls the particle's motion by weighing the contribution of the previous velocity. In the inertia weight approach, the velocity update equation is calculated using Equation 3.5.

$$\mathbf{v_i}^{\mathbf{k+1}} = \boldsymbol{\omega} * \mathbf{v_i}^{\mathbf{k}} + \mathbf{c1} * \mathbf{rand1} * \left(\mathbf{Pbest_i} - \mathbf{x_i}^{\mathbf{k}}\right) + \mathbf{c2} * \mathbf{rand2} * \left(\mathbf{Gbest_i} - \mathbf{x_i}^{\mathbf{k}}\right) \tag{3.5}$$

where

$\boldsymbol{\omega}$ is the inertia weight

The inertia weight is calculated using Equation 3.6.

$$\boldsymbol{\omega} = \boldsymbol{\omega}_{\mathbf{max}} - \left(\frac{\boldsymbol{\omega}_{\mathbf{max}} - \boldsymbol{\omega}_{\mathbf{min}}}{\mathbf{t_{max}}}\right) * \mathbf{t} \tag{3.6}$$

where

$\boldsymbol{\omega}_{\mathbf{max}}$ is the maximum inertia weight.

$\boldsymbol{\omega}_{\mathbf{min}}$ is the minimum inertia weight.

$\mathbf{t_{max}}$ is the maximum number of iteration.

$\mathbf{t}$ is the iteration number.

The inertia weight ω is introduced to substitute the maximum velocity. It is multiplied by the previous particle's velocity at every iteration to adjust the importance of the previous velocity in the search process.

If $\boldsymbol{\omega < 0.8}$, the PSO algorithm performs a local search and the global optimum is swiftly found, if it exists in the local search space.

If $\boldsymbol{\omega > 1.2}$, the PSO performs a global search and the particles try to explore new parts of the search space. The odds of finding the global optimum are reduced and the search process is longer.

Appropriate values for the maximum and minimum inertia weight are $\boldsymbol{\omega_{max} = 0.9}$ and $\boldsymbol{\omega_{min} = 0.4}$, respectively.

The inertia weight is efficient at ensuring that the PSO algorithm converges to the optimal solution (Del Valle et al., 2008).

### 3.3.2. Constriction coefficient PSO approach

When the PSO algorithm is executed without any limitations on the particle's velocity, then the velocity quickly escalates to unacceptable levels within a few iterations. To prevent the explosion of the swarm, the authors (Clerc & Kennedy, 2002) introduced the constriction coefficient $\boldsymbol{\chi}$. The constriction coefficient controls the explosion of the swarm, ensures the convergence of the PSO algorithm, and presumably eliminates the need for $\mathbf{v_{max}}$ (Del Valle et al., 2008). In the constriction coefficient approach, the velocity update is calculated using Equation 3.7.

$$\mathbf{v_i^{k+1} = \chi * \{v_i^k + \varphi 1 * rand1 * (Pbest_i - x_i^k) + \varphi 2 * rand2 * (Lbest_i - x_i^k)\}} \qquad (3.7)$$

Where,

$\boldsymbol{\chi}$ is the constriction coefficient

$\boldsymbol{\varphi 1}$ and $\boldsymbol{\varphi 2}$ are the acceleration coefficients

The constriction coefficient is calculated using Equation 3.8.

$$\chi = \frac{\mathbf{2}}{\left|\mathbf{2 - \varphi - \sqrt{\varphi^2 - 4\varphi}}\right|} \qquad (3.8)$$

Where,

$$\boldsymbol{\varphi} = \boldsymbol{\varphi 1} + \boldsymbol{\varphi 2}$$

The typical value of $\boldsymbol{\varphi}$ is 4.1.

If $\boldsymbol{\varphi} > \mathbf{4}$, the particles converge to the optimal solution faster and the convergence is guarantee within the search space.

If $\boldsymbol{\varphi} \leq \mathbf{4}$, the particles will fly towards and around the best solution in the search space without guarantying convergence (Bratton & Kennedy, 2007).

If the particle's personal best position is far from its neighbourhood best, the swarm may not converge.

Although all constricted particles will converge without using $\mathbf{v_{max}}$, studies from the authors (Eberhart & Shi, 2000) illustrate that the constriction coefficient approach performs better when $\mathbf{v_{max}}$ is limited to $\mathbf{x_{max}}$ i.e. $\mathbf{v_{max}} = \mathbf{x_{max}}$.

A comparison between the Inertia Weight approach and the Constrained Coefficient PSO approach reveals that the PSO with the constrained coefficient performs better than the inertia weight approach. The PSO solution algorithms when using the constrained coefficient approach is even better when the maximum velocity is limited to the maximum position of the particle.

## 3.4. PSO variants

The standard PSO algorithm was developed to solve mainly continuous optimisation problems. However, Real life application problems are of a combinatorial nature. Therefore, researchers have developed many variants of the Particle Swarm Optimization algorithms to solve non-continuous optimization problems.

### 3.4.1. Discrete or binary PSO (BPSO)

The binary PSO was first proposed in 1997 by (Kennedy & Eberhart, 1997). Before his introduction, PSO algorithms were only applied in continuous spaces applications. The binary PSO is used for discrete domains applications. The position $\mathbf{x}_{\boldsymbol{i}}$ of a particle can only be either a 0 or a 1. In this case, a particle is said to be static only if none of his bits are changed through an iteration. Hence, the position of the particle belongs to a discrete domain, but the velocity $\mathbf{v}_{\boldsymbol{i}}$ is still a continuous state. The velocity $\mathbf{v}_{\boldsymbol{i}}$ is defined as the rate of change of the position of a particle. Thus, in binary PSO, the value of the velocity $\mathrm{v_I}$ is the probability of the position $\mathbf{x}_{\boldsymbol{i}}$ to change from 0 to 1 or vice-versa. This means that if $\mathbf{v}_{\boldsymbol{i}} = \mathbf{0.30}$, $\mathbf{x}_{\boldsymbol{i}}$ has 70% of chance to change to or stay 0 and 30% to change to or stay a 1.

The velocity update Equation 3.4 is still valid for the BPSO. The particle's position update is now determined according to Equation 3.9.

$$\mathbf{x_i}^{\mathbf{k}} = \begin{cases} \mathbf{1} & \textbf{if } \mathbf{r} < \mathbf{sig}\left(\mathbf{v_i}^{\mathbf{k}}\right) \\ \mathbf{0} & \textbf{if } \mathbf{r} \geq \mathbf{sig}\left(\mathbf{v_i}^{\mathbf{k}}\right) \end{cases} \tag{3.9}$$

Where,

$\mathbf{r}$ is a uniformly distributed random number in the interval [0,1]

$\mathbf{sig}$ is a sigmoid function defined by $\mathbf{sig}(\boldsymbol{\alpha}) = \frac{\mathbf{1}}{\mathbf{1+e^{-\alpha}}}$

The algorithm of the BPSO is the same as the continuous PSO one, except for the position update equation. In continuous PSO, the velocity $\boldsymbol{v_i}$ of the particle is constrained in the interval $[\mathbf{v_{imin}}, \mathbf{v_{imax}}]$ where $\mathbf{v_{imin}}$ and $\mathbf{v_{imax}}$ are the minimum and the maximum particle velocity respectively.
When the Binary PSO is used for practical application, the velocity of particles is restricted to the interval [-4, 4] to prevent the sigmoid function to saturate (Kennedy et al., 2001).

### 3.4.2. Adaptive PSO

The adaptive PSO controls the exploration and the exploitation of the search space by adaptively changing its parameters. The adjusting is done by automatic control of parameters such as:

- Swarm size,
- Neighbourhood size,
- Inertia weight,
- Constriction coefficient, and
- Learning factors.

The authors (Zhang et al., 2009) for instance adjusted the algorithm by controlling the inertia weight $\boldsymbol{\omega}$ and the acceleration coefficients. The authors state that instead of decreasing the inertia weight $\boldsymbol{\omega}$ purely over time, it is more beneficial for the inertia weight $\boldsymbol{\omega}$ to decrease according to the evolutionary function given in Equation 3.10. The acceleration coefficients are adaptively adjusted to force the search process either towards an exploration, an exploitation, or a convergence state. Based on their studies, the authors concluded that the adaptive PSO performs better than the standard PSO.

$$\boldsymbol{\omega}(\mathbf{f}) = \frac{\mathbf{1}}{\mathbf{1 + 1.5e^{-2.6f}}} \tag{3.10}$$

Where

$\mathbf{f}$ is an evolutionary factor. The value of $\mathbf{f}$ belongs to the interval [0, 1].

In (Clerc, 2006) adaptive PSO, the constriction coefficient, the swarm size, and the number of particles in the neighbourhood are adaptively modified. The adaptive adjustment follows these three rules given below:

- A particle is destroyed when it is at his worst and regenerated to perform at his best.
- The constriction factor is increased when good improvements are recorded in the neighbourhood and decreased when poor improvements are noted in the vicinity.
- Best performing particles reduce their swarm size and poorly performing particles increase theirs.

The adaptive PSO in (Clerc, 2006) is different from that of (Zhang et al., 2009) in the fact that the adaptation of the PSO parameters is not carried out at each iteration. Other studies on the applications of Adaptive PSO (APSO) include research works by (Hossen et al., 2009), (Aghababa et al., 2010), (Rezazadeh et al., 2011) and (Alfi & Modares, 2011).

### 3.4.3. Fully informed PSO

The Fully Informed Particle Swarm optimisation (FIPSO) is a variant of PSO introduced in 2004 by (Mendes et al., 2004). The FIPSO is different from the canonical PSO in the fact that it takes into consideration the experience of all the particles in the neighbourhood during the velocity update process (see Figure 3.1.a.). In traditional PSO, a particle is directed only by its own experience and the experience of the best particle in its neighbourhood. The position update of the fully informed PSO is calculated using Equation 3.3. The velocity update is calculated using Equation 3.11.

$$\mathbf{v_{i,j}}^{\mathbf{t+1}} = \boldsymbol{\chi} * \left[\mathbf{v_{i,j}}^{\mathbf{t}} + \frac{\mathbf{1}}{\mathbf{K_i}} . \sum_{\mathbf{n=1}}^{\mathbf{K_i}} \mathbf{U(0,\boldsymbol{\varphi})}.\left(\mathbf{p^t_{N_i(n),j}} - \mathbf{x^t_{i,j}}\right)\right] \qquad (3.11.\mathrm{a})$$

With

$$\boldsymbol{\chi} = \frac{\mathbf{2k}}{\left|\mathbf{2} - \boldsymbol{\varphi} - \sqrt{\boldsymbol{\varphi}^{\mathbf{2}} - \mathbf{4}\boldsymbol{\varphi}}\right|} \qquad (3.11.\mathrm{b})$$

Where

$\mathbf{K_i}$ is the number of particle in the neighbourhood of particle $\mathbf{i}$.

$\boldsymbol{\chi}$ is the constriction factor obtained using Equation 3.11.b.

$\mathbf{U(0,\varphi)}$ is a uniformly distributed random number in the range $[\mathbf{0},\boldsymbol{\varphi}]$.

$\boldsymbol{\varphi}$ is the constant number referred to as acceleration coefficient ($\boldsymbol{\varphi} > \mathbf{4}$).

$\mathbf{N_i(n)}$ is a function returning the index of the $\mathbf{n^{th}}$ neighbord of particle $\mathbf{i}$.

$\mathbf{p^t_{N_i(n),j}}$ is the $\mathbf{j^{th}}$ component of the previous best position of the $\mathbf{n^{th}}$ neighbour of $\mathbf{i}$.

$\mathbf{k}$ is a constant number in the interval $[0,1]$.

The constriction coefficient $\boldsymbol{\chi}$ limit the explosion of the velocity of the particles, i.e. it prevents the particle's velocity to increase exponentially and cause the particle to wander out of the search space (Montes de Oca & Stützle, 2008).

Compared to the traditional PSO, the FIPSO uses more information to direct the search process. This can be detrimental to its performance as the influence of many particles may cancel each other. Figure 3.1.a shows six particles sharing information among each other in the same neighbourhood. The higher the amount of information shared by the particles during the search, the poorer the performance of the FIPSO algorithm. Therefore, if all particles in the swarm belong to the same neighbourhood and they all share information with each other, then the performance of the FIPSO algorithm will be drastically reduced (Lukasik & Kowalsk, 2014).

### 3.4.4. Other PSO variants

Although the inertia weight PSO approach and the discrete PSO remains the most widely used variant of the traditional PSO in continuous and discrete applications respectively, many other PSO variants have been proposed by researchers to increase the performance of the conventional PSO. Some of such variants include:

- **The Hybrid PSO**: the conventional PSO can be merged with other metaheuristic algorithms with the goal to increase the search space of the particles or to auto-adapt some parameters in the PSO. Some hybrid PSO comprises the hybrid of Genetic Algorithm and PSO (GA-PSO); the hybrid of Evolutionary programming and PSO (EPSO); and the hybrid of Differential Evolution and PSO (DEPSO). The use of Differential Evolution in hybrid PSO is more geared towards the selection of the best parameters for optimal PSO solution. In (Naka et al., 2003), the natural selection mechanism of the GA is used to increase the number of particles with high objective value while eliminating the ones with low objective value, and then increase the probability of the PSO to find the global optimum. The author (Angeline, 1998) leveraged on the tournament selection mechanism used in Evolutionary Programming to increase the effectiveness of the PSO. The author moves the worst performing particles closer to better performing particles at every iteration. This strategy results in a more consistent finding of the global optimum.

- **Multi-objective PSO (MOPSO)**: This type of PSO variants are used only when the application of PSO is subject to multiples non-compatible objectives that need to be solved simultaneously. The Weighted sum PSO, in which all the objectives are converted into a single-objective function using weight factors, remains the simplest MOPSO approach. The deficiency of the Weighted-Sum approach resides in the fact that sometimes, it is impossible to find the appropriate weight function (Del Valle et al., 2008).

Other MOPSO approaches use the concept of Pareto optimality. The selection of the cognitive and social leaders (personal and global best particle respectively) to guide the search process is the major hurdle faced by such approaches. The application of Pareto-frontier PSO often results in multiple Pareto optimal solutions (solutions in which none is better than the others) when only one solution is required.
The Dynamic Neighbourhood PSO (Hu & Eberhard, 2002) and the vector Evaluated PSO (Parsopoulos & Vrahatis, 2002) are some examples of MOPSO.

Section 3.4 provides a comprehensive list of PSO variants. Other variants have been proposed and tested in a range of applications. It is difficult to conclude that a specific PSO variant is superior to other variants, as most PSO variants have somewhat limited performance and applications.

## 3.5. Application of the PSO algorithm in the distribution network feeder reconfiguration

The distribution system is the most intensive part of the power grid. A great deal of power is lost at this level because of the low $\frac{\mathbf{R}}{\mathbf{X}}$ ratio and the low voltage levels. Distribution networks are usually radial in nature and they contain tie (normally open switches) and section switches (Normally closed switches). The reconfiguration of the distribution network is a means of reducing the real power loss and increasing the steady state and dynamic operation of distribution systems.
This section covers the application of the binary PSO solution algorithm to the distribution network feeder reconfiguration problem.

### 3.5.1. Mathematical formulation of the distribution network feeder reconfiguration problem

In this research work, the distribution network feeder reconfiguration is formulated as:

- Single-objective problem, to minimise the real power loss in the distribution system.
- Multi-objective problem, to minimise the real power loss and load balancing in the distribution system.

#### 3.5.1.1. Formulation of the real power loss minimisation problem

The real power loss minimisation problem is mathematically formulated as in Equation 3.12. In this mathematical formulation, the total real power loss in a distribution system is expressed as the sum of the real component of the difference of apparent power between the buses in the distribution system.

**Minimise**

$$\mathbf{P_{loss}} = \sum_{\substack{\mathbf{j=1} \\ \mathbf{k=1} \\ \mathbf{j \neq k}}}^{\mathbf{NB}} \mathbf{real}\left(\mathbf{V_j} \times \mathbf{i_{jk}}^* - \mathbf{V_k} \times \mathbf{i_{jk}}^*\right) \tag{3.12}$$

where

$\mathbf{j}$ is the sending bus of line $\mathbf{j - k}$.

$\mathbf{k}$ is the receiving bus of line $\mathbf{j - k}$.

$\mathbf{V_j}, \mathbf{V_k}$ are the sending and receiving end voltage of the line $\mathbf{j - k}$ respectively.

$\mathbf{i_{jk}}^*$ is the conjugate of the current flow in line $\mathbf{j - k}$.

$\mathbf{P_{loss}}$ is the total power loss in the distribution system.

$\mathbf{NB}$ is the number of busses in the network.

$\mathbf{V_j} \times \mathbf{i_{jk}}^* = \boldsymbol{S_{jk}}$ and $\mathbf{V_k} \times \mathbf{i_{jk}}^* = \boldsymbol{S_{kj}}$.

The real power loss in distribution can also be expressed in terms of the branch current (Zhu, 2009) and branch power (Mori & Komatsu, 2009), as given in Equations 3.13 and 3.14 respectively.

$$\mathbf{P_{loss}} = \sum_{\mathbf{l=1}}^{\mathbf{NL}} \mathbf{k_l R_{jk} I_{jk}}^{\mathbf{2}} \tag{3.13}$$

Where

$\mathbf{l}$ is the branch number of the line $\mathbf{j - k}$.

$\mathbf{I_{jk}}$ is the current in the branch $\mathbf{l}$.

$\mathbf{R_{jk}}$ is the resistance of branch $\mathbf{l}$.

$\mathbf{k_l}$ is the topological status of the branches. $\mathbf{k_l = 1}$ if branch l is closed and $\mathbf{k_l = 0}$ if the branch is open.

$\mathbf{NL}$ is the number of branches in the distribution system.

$$\mathbf{P_{loss}} = \sum_{\mathbf{l=1}}^{\mathbf{NL}} \mathbf{k_l} . \mathbf{R_{jk}} . \left( \frac{\mathbf{P_j}^2 + \mathbf{Q_j}^2}{\mathbf{V_j}^2} \right) \tag{3.14}$$

Where

$\mathbf{l}$ is the branch number of the line $\mathbf{j - k}$.

$\mathbf{V_j}$ is the voltage at node $\mathbf{j}$.

$\mathbf{P_j}$ and $\mathbf{Q_j}$ are the real and the reactive power flow in branch $\mathbf{l}$.

$\mathbf{k_l}$ is the topological status of the branches. $\mathrm{k_l} = 1$ if branch l is closed and $\mathrm{k_l} = 0$ if the branch is open.

$\mathbf{NL}$ is the number of branches in the distribution system.

The single line diagram of the two-bus distribution line in Figure 3.2.

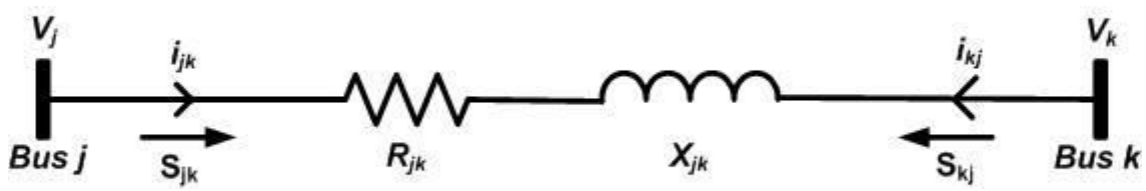


**Figure 3.2**: **Single line diagram of a distribution line**

### 3.5.1.2. Formulation of the load balancing problem

The Load Balancing Index is mathematically formulated and given in Equation 3.15 (Baran & Wu, 1989). The load balancing index $\mathrm{LBI_{sys}}$ should be minimised for optimal load balancing.

**Minimise:**

$$\mathbf{LBI_{sys}} = \frac{\mathbf{1}}{\mathbf{NL}} * \sum_{\mathbf{l=1}}^{\mathbf{NL}} \frac{\mathbf{S_l}}{\mathbf{S_{l\,max}}} \tag{3.15}$$

where,

$\mathbf{l}$ is the branch number of the line $\mathbf{j - k}$.

$\mathbf{S_l}$ is the apparent power loss in the branch $\mathbf{l}$.

$\mathbf{S_{l\,max}}$ is the power rating of branch $\mathbf{l}$.

$\mathbf{LBI_{sys}}$ is the load balance index of the network.

$\mathbf{NL}$ is the number of branches in the distribution system.

Load balancing aims to optimise the use of the network branches, to maximise the branch capacity utilisation, to avoid the overload of a single branch and to use other branches to supply a load. A low value of load balancing index indicates that the distribution system has more capacity reserve in its branches and that the network configuration is safer from an overload condition.

The data of the current carrying capability of individual branches in the IEEE 16, 33 and 69-bus distribution systems are not available. Therefore, it is assumed that all the branches in each distribution system have the same power rating.

#### 3.5.1.3. Constraints on the single and multi-objective problems

The distribution network feeder reconfiguration problem is subject to various operational constraints to satisfy the electrical and the technical requirements (quality of supply, voltage unbalance and fluctuations, steady-state voltage, frequency variation limits, power factor, equipment ratings) of the distribution system. The developed distribution network feeder reconfiguration algorithms are subjected to the following constraints.

##### a. Branch current constraint

The current flowing in any branch $\mathbf{l}$ should be lower than the rated current of the branch. This is mathematically expressed and given in Equation 3.16.

$$|\mathbf{I_l}| \leq \mathbf{I_{l\,max}} \quad \mathbf{l} \in \mathbf{NL} \tag{3.16}$$

Where,

$\mathbf{l}$ is the branch number of the line $\mathbf{j-k}$.

$|\mathbf{I_l}|$ is the magnitude of the current flowing in branch $\mathbf{l}$.

$\mathbf{I_{l\,max}}$ is the maximum current allowed to flow in branch $\mathbf{l}$.

$\mathbf{NL}$ is the number of branches in the distribution system.

The branch current constraint can also be expressed in term of branch power as given in Equation 3.17 and 3.18.

$$|\mathbf{P_l}| \le \mathbf{P_{l\,max}} \quad \mathbf{l} \in \mathbf{NL} \tag{3.17}$$

$$|\mathbf{Q_l}| \le \mathbf{Q_{l\,max}} \quad \mathbf{l} \in \mathbf{NL} \tag{3.18}$$

Where

$|\mathbf{P_l}|$ and $|\mathbf{Q_l}|$ are the actual real and the reactive power flow in branch $\mathbf{l}$ respectively

$\mathbf{P_{l\,max}}$ and $\mathbf{Q_{l\,max}}$ are the maximum real and the reactive power flow in branch $\mathbf{l}$ respectively.

**b. Bus Voltage Constraint**

The voltage at each node $\mathrm{i}$ of the distribution system should be within the recommended limits. This is mathematically formulated and given in Equation 3.19.

$$\mathbf{V_{i\,min}} \le \mathbf{V_i} \le \mathbf{V_{i\,max}} \quad \mathbf{i} \in \mathbf{N} \tag{3.19}$$

Where

$\mathbf{V_{i\,min}}$ and $\mathbf{V_{i\,max}}$ are the minimum and the maximum voltage limits of bus $\mathbf{i}$.

**c. Topological constraint**

The topological constraint is to warrant the radial configuration of the distribution network. The topological constraint is satisfied if:

- There are no isolated nodes in the distribution network.
- There are no closed loops in the distribution network, i.e. that the distribution network should be of radial topology. A network topology is radial if its bus incidence matrix is a square matrix and the rank of the bus incidence matrix is equal to the number of rows in the bus incidence matrix.

### 3.5.2. Binary PSO solution algorithm for the single-objective distribution network feeder reconfiguration problem

The binary PSO algorithm is developed to minimise the real power loss in distribution systems through distribution network feeder reconfiguration. The developed binary PSO algorithm is implemented using the following steps:

**Step 1:** Read the distribution system data such as the number of nodes $\mathbf{NB}$, the number of distribution lines $\mathbf{NL}$, the number of tie lines $\mathbf{NT}$, the bus type ($\mathbf{Slack}, \mathbf{PV}, \mathbf{PQ}$), the load data ($\mathbf{Pd}, \mathbf{Qd}, \mathbf{Bs}, \mathbf{Load_{ID}}$), the generator data ($\mathbf{Pg}, \mathbf{Qg}$) and distribution line data ($\mathbf{bus_i}, \mathbf{bus_j}, \mathbf{r}, \mathbf{x}, \mathbf{sw_{tie}}, \mathbf{sw_{sec}}$).

**Step 2**: Initialize the binary PSO parameters such as the acceleration coefficients $\mathbf{c1}$ and $\mathbf{c2}$; the minimum and the maximum inertia weight ($\mathbf{w_{min}}$ and $\mathbf{w_{max}}$ respectively); the particle's velocity limits ($\mathbf{v_{min}}$ and $\mathbf{v_{max}}$); the number of particles ($\mathbf{Np}$); the dimension of the search space ($\mathbf{D}$) and the stopping criteria (maximum number of iterations $\mathbf{t_{max}}$).

**Step 3:** Initialize the particle position, which is the binary coded representation of the section and tie-switches of the distribution network. The section and tie switches are represented by the binary bit ones (1) and zeros (0) respectively.
A particle is a possible distribution network topology.
A candidate solution is a feasible (comply with the distribution network feeder reconfiguration constraints) distribution network topology.
Figure 3.3 provides the single line diagram of the IEEE 16-bus distribution system. The straight/solid-lines represent the section switches, and the dashed lines represent the tie-switches of the distribution system.

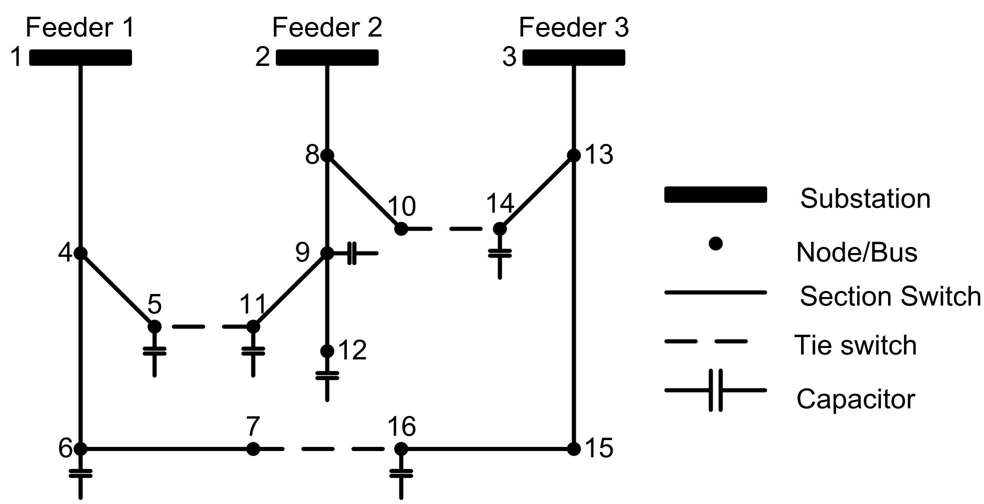


**Figure 3.3**: **Single line representation of the IEEE 16-bus distribution system**

The binary representation into 1's and 0's of the 16-bus distribution system in Figure 3.3 is provided in Table 3.1. From Table 3.1, lines No 14, 15 and 16 represent the tie-switches with the binary bit (status) zeros, and the rest of the lines represent section switches with the binary bit (status) ones.

**Table 3.1**: **Binary representation of the 16-bus distribution network**

| Line No | 1 | 2 | 3 | 4 | 5 | 6 | 7 | 8 | 9 | 10 | 11 | 12 | 13 | 14 | 15 | 16 |
|---|---|---|---|---|---|---|---|---|---|---|---|---|---|---|---|---|
| Sending And receiving bus | 1 - 4 | 4 - 5 | 4 - 6 | 6 - 7 | 2 - 8 | 8 - 9 | 8 - 10 | 9 - 11 | 9 - 12 | 3 - 13 | 13 - 14 | 13 - 15 | 15 - 16 | 5 - 11 | 10 - 14 | 7 - 16 |
| Status | 1 | 1 | 1 | 1 | 1 | 1 | 1 | 1 | 1 | 1 | 1 | 1 | 1 | 0 | 0 | 0 |

A particle's position is the string of bits that represent the open or closed status of the section and tie-switches in the distribution network. For the 16-bus distribution system, a possible particle is by $\mathbf{x_i}^{\mathbf{k}} = [1\ \ 1\ \ 1\ \ 1\ \ 1\ \ 1\ \ 1\ \ 1\ \ 1\ \ 1\ \ 1\ \ 1\ \ 1\ \ 0\ \ 0\ \ 0]$,

where

$\mathbf{i}$ is the particle number.

$\mathbf{k}$ is the iteration number. $\mathbf{k = 0}$ for the initial particle position.

The group of particles in the search space forms a swarm $\mathbf{X^k}$ and is given in the Equation 3.20.

$$\mathbf{X^k} = \left[\mathbf{x_1}^{\mathbf{k}}; \mathbf{x_2}^{\mathbf{k}}; \cdots ; \mathbf{x_{Np}}^{\mathbf{k}}\right] \tag{3.20}$$

Where

$\mathbf{X^k}$ is the swarm or the set of all the particles in the search space at iteration $\mathrm{k}$

$\mathbf{Np}$ is the number of particles.

$\mathbf{k}$ is the iteration number. $\mathbf{k = 0}$ for the initial particle position.

The number of particles is calculated using the Equation 3.21. Parallel lines can be replaced by an equivalent single line and counted as a single line.

$$\mathbf{Np} = \mathbf{NB} * (\mathbf{NL} - \mathbf{NB}) \tag{3.21}$$

Where

$\mathbf{Np}$ is the number of the particles.

$\mathbf{NB}$ is the number of the buses.

$\mathbf{NL}$ is the number of lines.

**Step 4:** Initialize the velocity of the particles which represents the probability for each bit in the particle's position to change its status from open (0) to close (1) or from close (1) to open (0).

Each particle in the search space has a different velocity. The particle's velocity is calculated using Equation 3.22.

$$\mathbf{velocity(i,j)} = \mathbf{v_{min}} + (\mathbf{v_{max}} - \mathbf{v_{min}}) * \mathbf{rand} \tag{3.22}$$

Where

$\mathbf{i}$ is the particle number.

$\mathbf{j}$ is the index of the dimension of the search space.

$\mathbf{velocity(i,j)}$ is the probability of the $\mathbf{j}$-bit of particle $\mathbf{i}$ to change its status from open to close or close to open.

$\mathbf{v_{min}}$ is the minimum velocity.

$\mathbf{v_{max}}$ is the maximum velocity.

$\mathbf{rand}$ is a random number in the range $]0,1[$.

**Step 5:** Find the personal best particles position. In this case, the initial particle position is assumed as the best particle position. Then, calculate the load flow based on the best particles position and find the real power loss using Equation 3.12.

**Step 6:** Find the global best particle position from the set of particles best position given in Step 5. In this case, the global best particle position is the best particle position with the minimal real power loss value.

**Step 7:** Compute the bus incidence matrix of the distribution network**.** The bus incidence matrix is used to identify whether a connection exists between the two nodes or not. This helps to determine whether the network topology is radial or not.

**Start the binary PSO iteration process** and set the iteration counter $\mathbf{t}$ to 1.

**Step 8:** Check the topological constraints after updating the incidence matrix for the candidate network topologies and verify that all the candidate solutions meet the topology constraints. This step ensures that the real power loss is calculated only for feasible distribution network topologies.

**Step 9:** Find The power flow in the distribution network using the Newton-Raphson power flow approach. Then, employ the power flow results to calculate the real power loss of each candidate network topology using Equation 3.12.

**Step 10:** Update the particles' personal best as per the Equation 3.23.

$$\mathbf{Pbest_i}^{\mathbf{t+1}} = \begin{cases} \mathbf{Pbest_i}^{\mathbf{t}}, & \textbf{if } \mathbf{fitness_i}^{\mathbf{t+1}} \geq \mathbf{fitness_{Pbest_i}}^{\mathbf{t}} \\ \mathbf{x_i}^{\mathbf{t+1}}, & \textbf{otherwise} \end{cases} \tag{3.23}$$

Where

$\mathbf{Pbest_i}^{\mathbf{t}}$ is the personal best position of particle $\mathbf{i}$ at iteration $\mathbf{t}$.

$\mathbf{x_i}^{\mathbf{t+1}}$ is the position of particle $\mathbf{i}$ at iteration $\mathbf{t+1}$.

$\mathbf{fitness_i}^{\mathbf{t+1}}$ is the fitness value of particle $\mathbf{i}$ at iteration $\mathbf{t+1}$.

$\mathbf{fitness_{Pbest_i}}^{\mathbf{t}}$ is the fitness value of $\mathbf{Pbest_i}^{\mathbf{t}}$.

**Step 11:** Update the global best in the swarm of particles per the Equation 3.24.

$$\mathbf{Gbest}^{\mathbf{t+1}} = \begin{cases} \mathbf{Gbest}^{\mathbf{t}}, & \textbf{if } \mathbf{fitness_{Pbest_i}}^{\mathbf{t+1}} \geq \mathbf{fitness_{Gbest}}^{\mathbf{t}} \\ \mathbf{Pbest_i}^{\mathbf{t+1}}, & \textbf{otherwise} \end{cases} \tag{3.24}$$

Where

$\mathbf{Gbest}^{\mathbf{t+1}}$ is the global best solution of the swarm at iteration $\mathbf{t+1}$.

$\mathbf{fitness_{Gbest}}^{\mathbf{t}}$ is the fitness value of $\mathbf{Gbest}$ at iteration $\mathbf{t}$.

**Step 12:** Calculate the inertia weight using Equation 3.6 and update the velocity of all particles per Equation 3.5.

$$\mathbf{v_i}^{\mathbf{k+1}} = \boldsymbol{\omega} * \mathbf{v_i}^{\mathbf{k}} + \mathbf{c1} * \mathbf{rand1} * \left(\mathbf{Pbest_i} - \mathbf{x_i}^{\mathbf{k}}\right) + \mathbf{c2} * \mathbf{rand2} * \left(\mathbf{Gbest_i} - \mathbf{x_i}^{\mathbf{k}}\right)$$

Where

$\boldsymbol{\omega}$ is the inertia weight.

The inertia weight is calculated using Equation 3.6.

$$\boldsymbol{\omega} = \boldsymbol{\omega}_{\mathbf{max}} - \left(\frac{\boldsymbol{\omega}_{\mathbf{max}} - \boldsymbol{\omega}_{\mathbf{min}}}{\mathbf{t_{max}}}\right) * \mathbf{t}$$

Where

$\boldsymbol{\omega}_{\mathbf{max}}$ is the maximum inertia weight.

$\boldsymbol{\omega}_{\mathbf{min}}$ is the minimum inertia weight.

$\mathbf{t_{max}}$ is the maximum number of iteration.

$\mathbf{t}$ is the iteration number.

**Step 13:** Update the particles' position as per Equation 3.9.

$$\mathbf{x_i}^{\mathbf{k}} = \begin{cases} \mathbf{1} & \textbf{if } \mathbf{r} < \mathbf{sig}\left(\mathbf{v_i}^{\mathbf{k}}\right) \\ \mathbf{0} & \textbf{if } \mathbf{r} \geq \mathbf{sig}\left(\mathbf{v_i}^{\mathbf{k}}\right) \end{cases}$$

Where

$\mathbf{r}$ is a uniformly distributed random number in the interval [0,1]

$\mathbf{sig}$ is a sigmoid function defined by $\mathbf{sig}(\boldsymbol{\alpha}) = \frac{\mathbf{1}}{\mathbf{1+e^{-\alpha}}}$

**Step 14:** Increment the iteration count of the binary PSO search process and repeat step 8 to step 13 until the stopping criterion is reached.

**Step 15:** Print the results of the search process such as the global best solution (optimal network topology), its corresponding fitness value (minimum real power loss) and the convergence rate of the binary PSO of the algorithm.

The flowchart of the above-described algorithm is shown in Figure 3.4.

The binary PSO algorithm is applied the distribution system to find the distribution network topology that results in a minimum real power loss. Feasible distribution network topologies are evaluated, and their corresponding real power loss is compared with the real power loss of the initial distribution network topology. The candidate network topology should meet the topological constraints of the distribution network. So, right from the start, a sorting strategy is introduced to ensure that only the network topologies meeting the constraints are evaluated. If a candidate solution has better fitness than the global best solution, then this candidate solution is likely to become the new global best solution. The end of an iteration triggers the next iteration. The iterative process continues until the maximum number of iteration is reached.

### 3.5.3. Results of the PSO solution algorithm for the single-objective distribution network feeder reconfiguration problem

To evaluate the performance and the effectiveness of the developed PSO solution algorithm for the single-objective distribution network feeder reconfiguration problem, three distribution systems are used for case studies:

- The IEEE 16 bus distribution system.
- The IEEE 33 bus distribution system.
- The IEEE 69-bus distribution system.

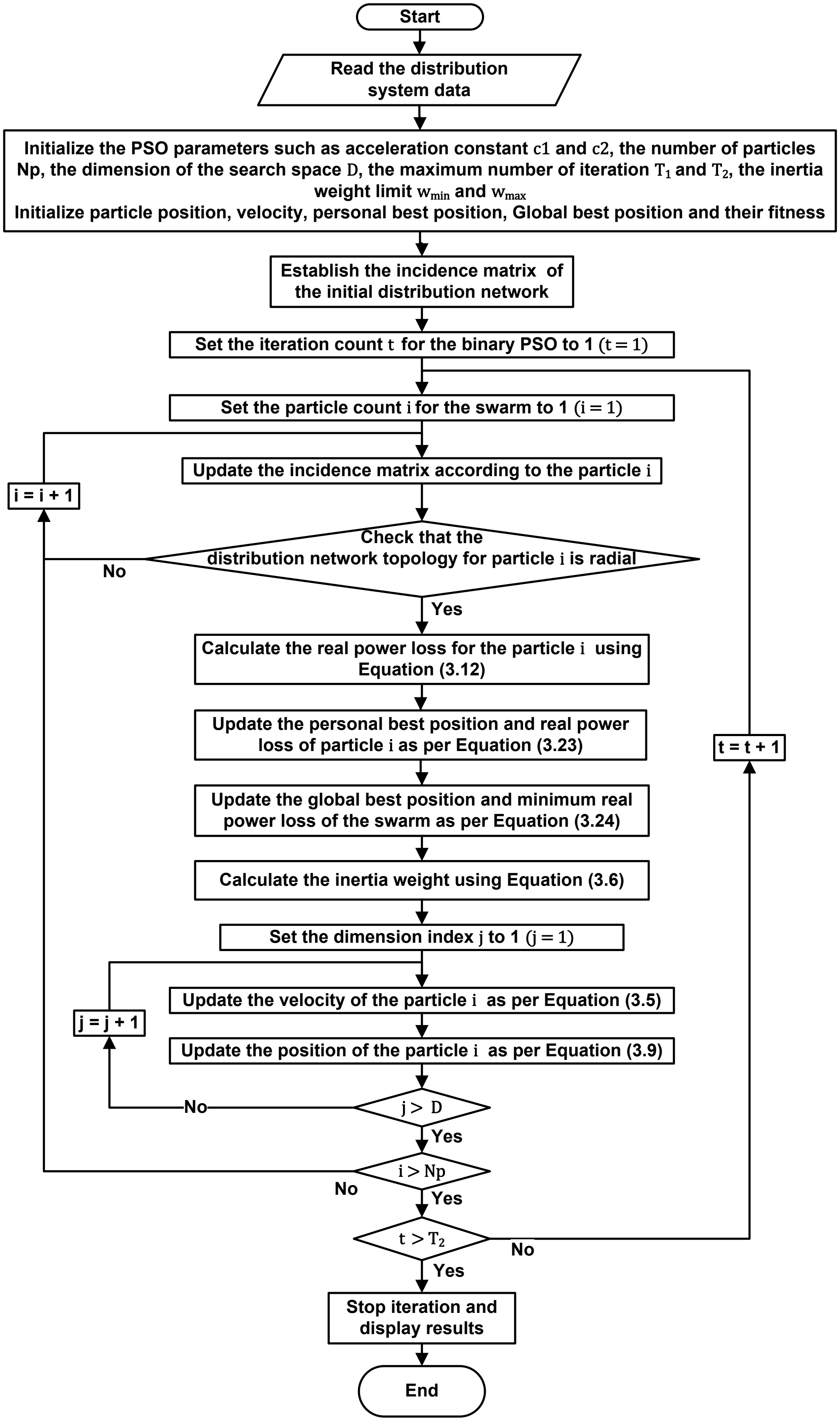


**Figure 3.4**: Flowchart of the PSO algorithm for the single-objective distribution network feeder reconfiguration problem

A comparative analysis of the distribution system before and after reconfiguration is provided in this section. The evaluation is carried out based on the real power loss, the voltage profile and the change in the distribution network topology. The results of the developed binary PSO algorithm are compared with the literature ones. The distribution systems parameters are given in the **Appendices A**, **B**, and **D**, for the 16-bus, 33-bus, and 69-bus distribution systems, respectively. The predefined parameters of the developed binary PSO algorithm are given in Table 3.2. The BPSO solution algorithm is designed in such a way to work on any radial distribution system. Therefore, the number of particles $\mathbf{N_p}$ in the search process changes depending on the number of bus and ties switches in the distribution system, and it is calculated using Equation 3.21.

**Table 3.2: Binary PSO parameters**

| | |
|---|---|
| $w_{min}$ | 0.4 |
| $w_{max}$ | 0.9 |
| Acceleration coefficient ($c1$ and $c2$) | 2 |
| Maximum velocity $v_{max}$ | 4 |

The developed BPSO solution algorithm is implemented in MATLAB R2016b, and the simulations are carried out on a SUPERMICRO computer with 2 Intel Xeon CPU E5-2620 v4 @ 2.10GHz processors and a 16GB RAM.

#### 3.5.3.1. Test case 1: IEEE 16-bus distribution system

The 16-bus distribution system is a $12.66\ \mathrm{kV}$, $100\mathrm{MVA}$ radial distribution network as shown in Figure 3.3. It consists of three main feeders or substation transformers, 13 fixed loads, seven shunt capacitors, and 16 branches. 13 of these branches are section-lines, and 3 are tie-lines. The total real power and the reactive power demands are $\mathbf{28.7Mw}$ and $\mathbf{17.3\ Mvar}$ respectively. The Newton-Raphson method is used to calculate the load flow results of the 16-bus distribution system in the MATLAB platform. The parameters of the IEEE 16-bus distribution system are given in **Appendix A**.

#### a. Simulation results of the 16-bus distribution system before reconfiguration

The power flow results of the 16-bus distribution system before the feeder reconfiguration are given in Table 3.3 and Table 3.4. Table 3.3 provides the bus voltages, the real and the reactive power of both the loads and the generation in the 16-bus distribution network.

**Table 3.3:** Bus voltage, real and reactive power in the 16-bus distribution system before reconfiguration

| Bus number | Voltage | | Generation | | Load demand | |
|---|---|---|---|---|---|---|
| | Mag (p.u) | Ang (deg) | P(MW) | Q(Mvar) | P(MW) | Q(Mvar) |
| 1 | 1.0000 | 0.0000 | 8.5830 | 2.9790 | – | – |
| 2 | 1.0000 | 0.0000 | 15.4901 | 3.9667 | – | – |
| 3 | 1.0000 | 0.0000 | 5.1409 | −0.0050 | – | – |
| 4 | 0.9906 | −0.3672 | – | – | 2.0000 | 1.6000 |
| 5 | 0.9877 | −0.5405 | – | – | 3.0000 | 1.5000 |
| 6 | 0.9859 | −0.6929 | – | – | 2.0000 | 0.8000 |
| 7 | 0.9848 | −0.7000 | – | – | 1.5000 | 1.2000 |
| 8 | 0.9787 | −0.7421 | – | – | 4.0000 | 2.7000 |
| 9 | 0.9703 | −1.4155 | – | – | 5.0000 | 3.0000 |
| 10 | 0.9765 | −0.7487 | – | – | 1.0000 | 0.9000 |
| 11 | 0.9702 | −1.4868 | – | – | 0.6000 | 0.1000 |
| 12 | 0.9682 | −1.7891 | – | – | 4.5000 | 2.0000 |
| 13 | 0.9944 | −0.3262 | – | – | 1.0000 | 0.9000 |
| 14 | 0.9948 | −0.4520 | – | – | 1.0000 | 0.7000 |
| 15 | 0.9917 | −0.5182 | – | – | 1.0000 | 0.9000 |
| 16 | 0.9912 | −0.5851 | – | – | 2.1000 | 1.0000 |
| **Total** | | | **29.21** | **6.94** | **28.70** | **17.3** |

**Table 3.4**: Branch power flow in the 16-bus distribution system before reconfiguration

| Branch number | From Bus | To Bus | From bus injection | | To bus injection | | Loss | |
|---|---|---|---|---|---|---|---|---|
| | | | P(MW) | Q(Mvar) | P(MW) | Q(Mvar) | P(kW) | Q(kvar) |
| 1 | 1 | 4 | 8.5830 | 2.9790 | −8.5211 | −2.8965 | 61.9062 | 82.5416 |
| 2 | 4 | 5 | 3.0075 | 0.4373 | −3.0000 | −0.4269 | 7.5300 | 10.3537 |
| 3 | 4 | 6 | 3.5135 | 0.8592 | −3.5015 | −0.8352 | 11.9992 | 23.9984 |
| 4 | 6 | 7 | 1.5015 | 1.2015 | −1.5000 | −1.2000 | 1.5220 | 1.5220 |
| 5 | 2 | 8 | 15.4901 | 3.9667 | −15.2089 | −3.6855 | 281.2476 | 281.2476 |
| 6 | 8 | 9 | 10.2068 | 0.0834 | −10.1198 | 0.0363 | 87.0199 | 119.6523 |
| 7 | 8 | 10 | 1.0021 | 0.9021 | −1.0000 | −0.9000 | 2.0878 | 2.0878 |
| 8 | 9 | 11 | 0.6007 | −0.4640 | −0.6000 | 0.4647 | 0.6731 | 0.6731 |
| 9 | 9 | 12 | 4.5191 | −1.4424 | −4.5000 | 1.4687 | 19.1210 | 26.2913 |
| 10 | 3 | 13 | 5.1409 | −0.0050 | −5.1119 | 0.0341 | 29.0720 | 29.0720 |
| 11 | 13 | 14 | 1.0020 | −1.0786 | −1.0000 | 1.0812 | 1.9727 | 2.6303 |
| 12 | 13 | 15 | 3.1099 | 0.1445 | −3.1020 | −0.1337 | 7.8419 | 10.7826 |
| 13 | 15 | 16 | 2.1020 | −0.7663 | −2.1000 | 0.7684 | 2.0359 | 2.0359 |
| 14 | 5 | 11 | 0.0000 | 0.0000 | 0.0000 | 0.0000 | 0.0000 | 0.0000 |
| 15 | 10 | 14 | 0.0000 | 0.0000 | 0.0000 | 0.0000 | 0.0000 | 0.0000 |
| 16 | 7 | 16 | 0.0000 | 0.0000 | 0.0000 | 0.0000 | 0.0000 | 0.0000 |
| **Total** | | | | | | | **514.0293** | **592.8887** |

Table 3.4 provides the branch power flow results and the power loss in each branch of the 16-bus distribution system.

It is observed that before the network reconfiguration, the minimum voltage in the 16-bus distribution system is $\mathbf{0.9682\angle-1.7891°\ p.u}$ at **bus 12**. Moreover, the initial network topology has three tie switches: branch $5-11$; branch $10-14$; and branch $7-16$. There is no power flow through those tie switches before the reconfiguration process (see the yellow-highlighted portion of Table 3.4). Branch 5 (branch between nodes 2 - 8) has the highest real power loss ($\mathbf{281.2476\ kW}$) in the 16-bus distribution system. The total real power loss in the initial 16-bus distribution system is $\mathbf{514.0293\ kW}$.

**b. Simulation results of the 16-bus distribution system after reconfiguration**

The developed binary PSO algorithm is applied to the 16-bus distribution system, and the power flow results after reconfiguration of the distribution system are given in Table 3.5 and Table 3.6. Table 3.5 provides the bus voltages, the real and the reactive power of both the loads and the generation in the 16-bus distribution network. Table 3.6 presents the branch power flow results and the power loss in each branch of the 16-bus distribution system.

**Table 3.5:** **Bus voltage, real and reactive power in the 16-bus distribution system after reconfiguration**

| Bus number | Voltage | | Generation | |
|---|---|---|---|---|
| | Mag (p.u) | Ang(deg) | P(MW) | Q(Mvar) |
| 1 | 1.0000 | 0 | 9.1925 | 2.5062 |
| 2 | 1.0000 | 0 | 13.8188 | 3.4329 |
| 3 | 1.0000 | 0 | 6.1570 | 0.9343 |
| 4 | 0.9906 | −0.4230 | − | − |
| 5 | 0.9878 | −0.6576 | − | − |
| 6 | 0.9859 | −0.7486 | − | − |
| 7 | 0.9848 | −0.7557 | − | − |
| 8 | 0.9811 | −0.6672 | − | − |
| 9 | 0.9727 | −1.2764 | − | − |
| 10 | 0.9898 | −0.4827 | − | − |
| 11 | 0.9877 | −0.6831 | − | − |
| 12 | 0.9707 | -1.6490 | - | - |
| 13 | 0.9922 | −0.3317 | − | − |
| 14 | 0.9906 | −0.4804 | − | − |
| 15 | 0.9895 | −0.5243 | − | − |
| 16 | 0.9890 | −0.5913 | − | − |
| **Total** | | | **29.1683** | **6.8733** |

**Table 3.6**: **Branch power flow in the 16-bus distribution system after reconfiguration**

| Branch number | From Bus | To bus | From bus injection | | To bus injection | | Power loss | |
|---|---|---|---|---|---|---|---|---|
| | | | $\mathbf{P(MW)}$ | $\mathbf{Q(Mvar)}$ | $\mathbf{P(MW)}$ | $\mathbf{Q(Mvar)}$ | $\mathbf{P(kW)}$ | $\mathbf{Q(kvar)}$ |
| 1 | 1 | 4 | 9.1925 | 2.5062 | -9.1244 | -2.4154 | 68.0870 | 90.7827 |
| 2 | 4 | 5 | 3.6109 | -0.0437 | -3.6002 | 0.0584 | 10.6306 | 14.6171 |
| 3 | 4 | 6 | 3.5135 | 0.8591 | -3.5015 | -0.8351 | 11.9985 | 23.9971 |
| 4 | 6 | 7 | 1.5015 | 1.2015 | -1.5000 | -1.2000 | 1.5219 | 1.5219 |
| 5 | 2 | 8 | 13.8188 | 3.4329 | −13.5958 | -3.2099 | 223.0195 | 223.0195 |
| 6 | 8 | 9 | 9.5958 | 0.5099 | -9.5191 | -0.4044 | 76.7469 | 105.5270 |
| 7 | 8 | 10 | 0 | 0 | 0 | 0 | 0 | 0 |
| 8 | 9 | 11 | 0 | 0 | 0 | 0 | 0 | 0 |
| 9 | 9 | 12 | 4.5191 | -1.4602 | -4.5000 | 1.4864 | 19.0684 | 26.2190 |
| 10 | 3 | 13 | 6.1570 | 0.9343 | -6.1144 | -0.8916 | 42.6598 | 42.6598 |
| 11 | 13 | 14 | 2.0044 | -0.1606 | -2.0007 | 0.1656 | 3.6965 | 4.9287 |
| 12 | 13 | 15 | 3.1099 | 0.1522 | -3.1020 | -0.1414 | 7.8780 | 10.8322 |
| 13 | 15 | 16 | 2.1020 | -0.7586 | -2.1000 | 0.7606 | 2.0400 | 2.0400 |
| 14 | 5 | 11 | 0.6002 | −0.4851 | -0.6000 | 0.4854 | 0.2442 | 0.2442 |
| 15 | 10 | 14 | −1.0000 | −0.9000 | 1.0007 | 0.9007 | 0.7390 | 0.7390 |
| 16 | 7 | 16 | 0 | 0 | 0 | 0 | 0 | 0 |
| **Total** | | | | | | | $\mathbf{468.3304}$ | $\mathbf{547.1282}$ |

It is observed that after the network reconfiguration, the minimum voltage in the 16-bus distribution system is $\mathbf{0.9707\angle-1.6490°\ p.u}$ at **bus** $\mathbf{12}$. The new tie switches in the distribution system are **branch** $\mathbf{8-10}$; **branch** $\mathbf{9-11}$; and **branch** $\mathbf{7-16}$. There is no power flow through those tie switches before the reconfiguration process (see the yellow-highlighted portion of Table 3.6. Branch 5 (branch between nodes 2 - 8) still has the highest real power loss ($\mathbf{223.0195\ kW}$) in the 16-bus distribution system. The total real power loss in the initial 16-bus distribution system is $\mathbf{468.3304\ kW}$.

## c. Comparative analysis of the results of the 16-bus distribution system before and after reconfiguration

A comparative study of the results of the 16-bus distribution system before and after feeder reconfiguration using the developed binary PSO algorithm is given in Table 3.7. The voltage profile in the distribution system is provided in Figure 3.5. It is observed that the distribution network topology after feeder reconfiguration is different from the initial topology.

**Table 3.7**: Summary of the simulation results of the 16-bus distribution system before and after solving the single-objective feeder reconfiguration problem

| Simulation results | Before reconfiguration | After reconfiguration |
|---|---|---|
| Power generation (MVA) | $29.2140 + j6.9407$ | $29.1683 + j6.8733$ |
| Tie switches | 14 15 16 | 7 8 16 |
| Real power loss | 514.0293 kW | 468.3304 kW |
| Real power loss reduction | – | 8.89033% |
| Minimum voltage | 0.9682 p.u @ bus 12 | 0.9707 p.u @ bus 12 |

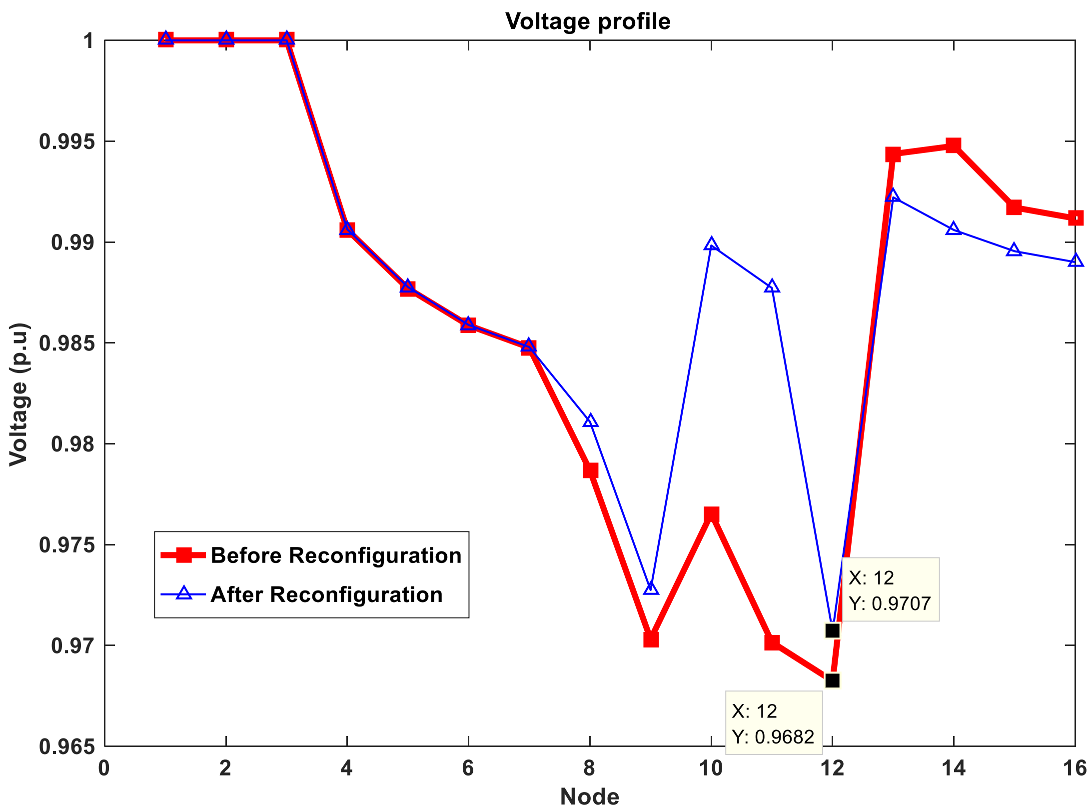


**Figure 3.5:** Voltage profile of the 16-bus distribution system before and after solving the single-objective feeder reconfiguration problem

After the feeder reconfiguration, branches number 7 (branch $8-10$), 8 (branch $9-11$) and 16 (branch $7-16$) are the tie-lines whereas branches number 14 (branch $5-11$), 15 (branch $10-14$) and 16 (branch $7-16$) are the tie-lines before the feeder reconfiguration. This shows that the developed BPSO algorithm effectively reconfigured the network topology. The change in the network topology led to a reduction of the power loss in the 16-bus distribution system. After the feeder reconfiguration, the real power loss in the distribution system is reduced to $\mathbf{468.3304kW}$ from $\mathbf{514.0293kW}$ before the feeder reconfiguration. This corresponds to a real power loss reduction of $\mathbf{8.89\%}$ in comparison with the real power loss in the initial distribution system. The percentage of power loss is calculated using Equation 3.25.

$$\%\mathbf{Ploss} = \frac{\mathbf{Ploss_{After\ reconfiguration}} - \mathbf{Ploss_{Before\ reconfiguration}}}{\mathbf{Ploss_{Before\ reconfiguration}}} \times \mathbf{100\%} \tag{3.25}$$

Where,

$\%\mathbf{Ploss}$ is the power loss reduction in percent (%).

The change in the distribution network topology also improved its voltage profile as shown in Figure 3.5. The minimum voltage in the distribution network is $\mathbf{0.9682\ p.u}$ before the feeder reconfiguration and it is improved to $\mathbf{0.9707\ p.u}$ after the feeder reconfiguration.

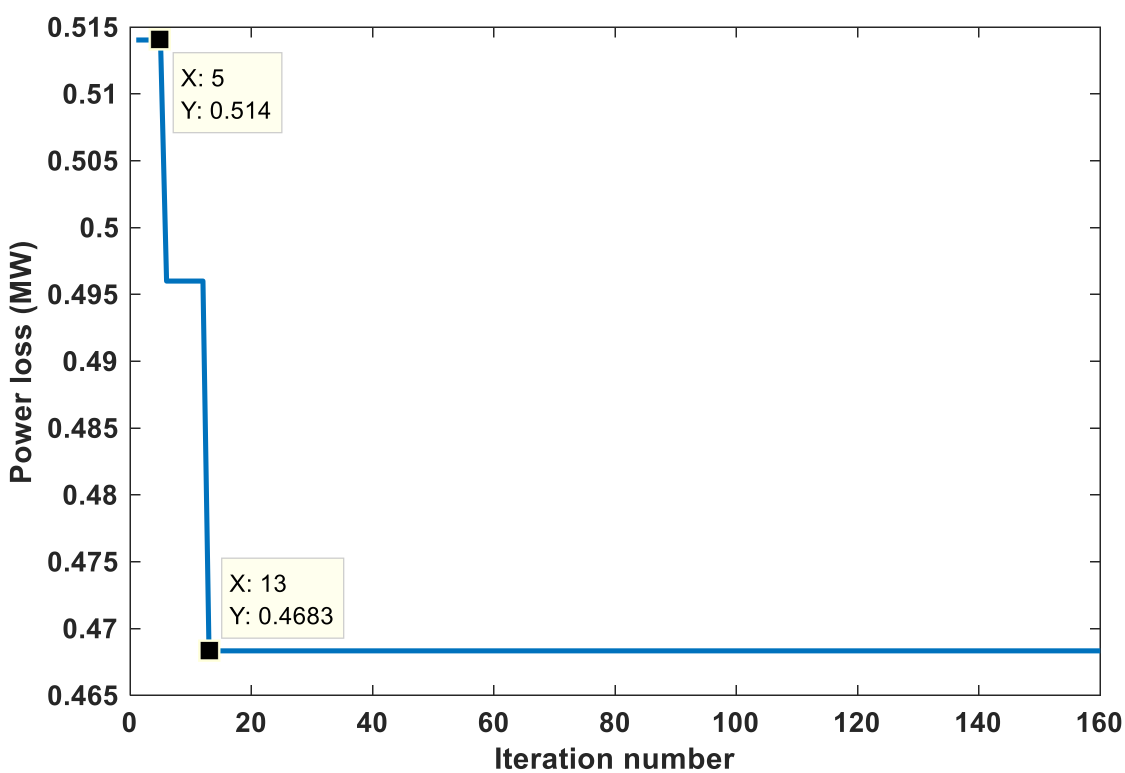


**Figure 3.6**: **Convergence characteristic of the developed BPSO algorithm for the 16-bus distribution system**

The computation performance of the developed BPSO solution algorithm for the distribution network feeder reconfiguration problem is assessed using the success rate.

The success rate defines how many times the developed BPSO algorithm find the optimal network topology for real power loss minimisation in the distribution system. The optimisation process is run 100 times. It results that for the 16-bus distribution system, the developed BPSO algorithm converges to the optimal solution every time, where a 100% success rate. The convergence characteristic for the developed BPSO algorithm is given in Figure 3.6. Initially, the real power loss is $0.514\ \mathrm{MW}$. As the developed PSO algorithm goes through iterations, candidate network topologies with lower real power loss are found. The optimal distribution network topology is found after 13 iterations. It follows that for the 16-bus distribution system, the developed algorithm goes through 160 iterations before the search process is complete, although the optimal solution is found at the thirteenth iteration.

The results of the 16-bus distribution system after the feeder reconfiguration is compared with the literature ones and it is provided in Table 3.8. The comparison study proves that the results of the developed BPSO algorithm are consistent with the literature ones, and the developed BPSO algorithm achieves a higher real power loss reduction compared to the literature. It is also noted that although for both the developed BPSO algorithm and the literature the distribution network topology before and after feeder reconfiguration is the same, their total real power loss is different. The difference in real power loss between the developed BPSO algorithm and the literature results is mainly due to the power flow approach used. The Gauss-Seidal power flow approach is used in the literature whereas the developed BPSO algorithm uses the Newton-Raphson power flow approach for faster convergence and refined results.

**Table 3.8:** **Comparison of the results of the developed BPSO algorithm for the 16-bus distribution system with those provided in the literature**

| **Algorithm** | | **Developed BPSO algorithm** | **ACO (Chiou et al., 2005)** | **MINLP (de Oliveira et al., 2010)** | **SEM (Gomes Et al., 2005)** | **Refined GA (Zhu, 2002)** |
|---|---|---|---|---|---|---|
| Before reconfiguration | Tie switches | 14 15 16 | 14 15 16 | 14 15 16 | 14 15 16 | 14 15 16 |
| | Real power loss (kW) | 514.0293 | 511.4 | 511.44 | – | 511.4 |
| After reconfiguration | Tie switches | 7 8 16 | 7 8 16 | 7 8 16 | 7 8 16 | 7 8 16 |
| | Real power loss (kW) | 468.3304 | 466.1 | 466.13 | 466.13 | 466.1 |
| | Real power loss reduction (%) | 8.8903 | 8.858 | 8.856 | – | 8.858 |

#### 3.5.3.2. Test case 2: IEEE 33-bus distribution system

The developed BPSO algorithm is applied to the 33-bus distribution system to solve the distribution network feeder reconfiguration problem. The 33-bus distribution system is a $12.66\ \mathrm{kV}$, $100\ \mathrm{MVA}$ radial distribution network as shown in Figure 3.7. It consists of 32 fixed loads and 37 branches. 32 of these branches are normally closed branches (section switches), and 5 are normally open (tie switches). The fixed loads account for a total real and reactive power demand of $\mathbf{3.72MW}$ and $\mathbf{2.3\ Mvar}$ respectively. The parameters for the 33-bus distribution system are given in **Appendix B**.

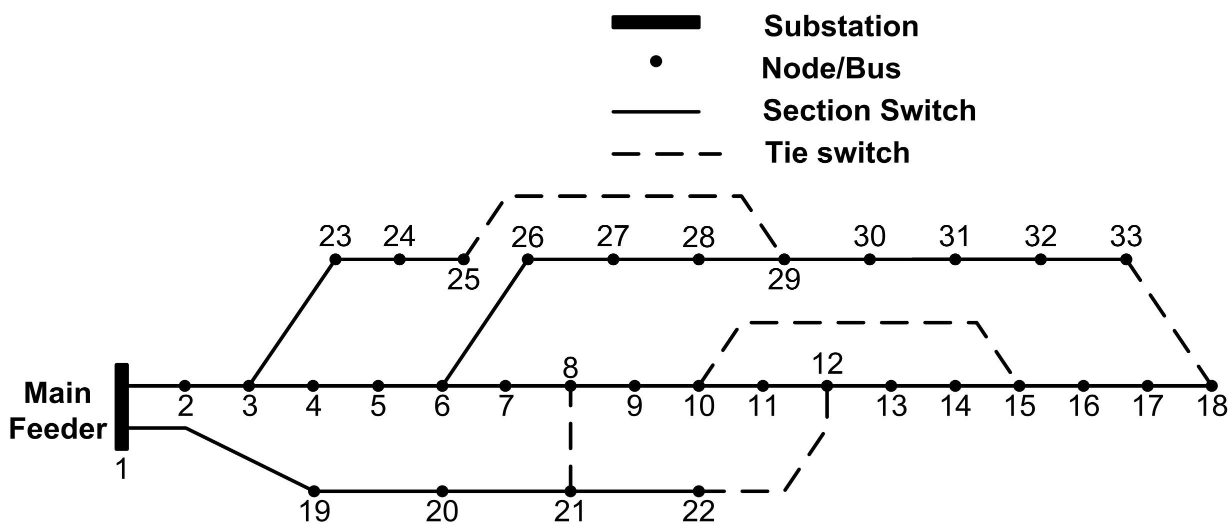


**Figure 3.7: Single line diagram of the 33-bus distribution system**

Initially, the tie switches in the 33-bus distribution system are branch $8-21$; branch $9-15$; branch $12-22$; branch $18-33$; and branch $25-29$. The Newton-Raphson method is used to calculate the load flow of the 33-bus distribution system in the MATLAB platform. The load flow study shows that the 33-bus distribution system has an initial real power loss of $\mathbf{208.4322\ kW}$ and a total power generation of $(\mathbf{3.9234 + j2.4117})\mathbf{MVA}$. It is observed that before the network reconfiguration, the minimum voltage in the 33-bus distribution system is $\mathbf{0.9107p.u}$ at **bus 18**. The load flow results of the 33-bus distribution network are given in **Appendix C1**.

The developed BPSO algorithm is used to find the optimal network topology to minimise the real power loss in the 33-bus distribution system. It is observed that after the network reconfiguration, the new tie switches in the distribution system are: branch $7-8$; branch $9-10$; branch $14-15$; branch $32-33$; and branch $25-29$. The load flow study shows that after the feeder reconfiguration, the 33-bus distribution system has a total real power loss of $\mathbf{138.9105\,kW}$ and a total power generation of $(\mathbf{3.8539 + j2.3917})\mathbf{MVA}$. The minimum voltage in the 33-bus distribution system is now $\mathbf{0.9423p.u}$ at **bus 32**. The comprehensive load flow results of the 33-bus distribution system after the distribution network reconfiguration given in **Appendix C2**.

Table 3.9 gives a comparative analysis of the results of the 33-bus distribution system before and after feeder reconfiguration using the developed binary PSO algorithm.

**Table 3.9**: **Summary of the simulation results of the 33-bus distribution system before and after solving the single-objective feeder reconfiguration problem**

| Simulation results | Before reconfiguration | After reconfiguration |
|---|---|---|
| **Power generation (MVA)** | $3.9234 + j2.4117$ | $3.8539 + j2.3917$ |
| **Tie switches** | 33 34 35 36 37 | 7 9 14 32 37 |
| **Real power loss** | 208.4322 kW | 138.9105kW |
| **Real power loss reduction** | – | 33.3546% |
| **Minimum voltage** | 0.9108 p.u @ bus 18 | 0.9423 p.u @ bus 32 |

Figure 3.8 shows the voltage profile of the 33-bus distribution system before and after the feeder reconfiguration

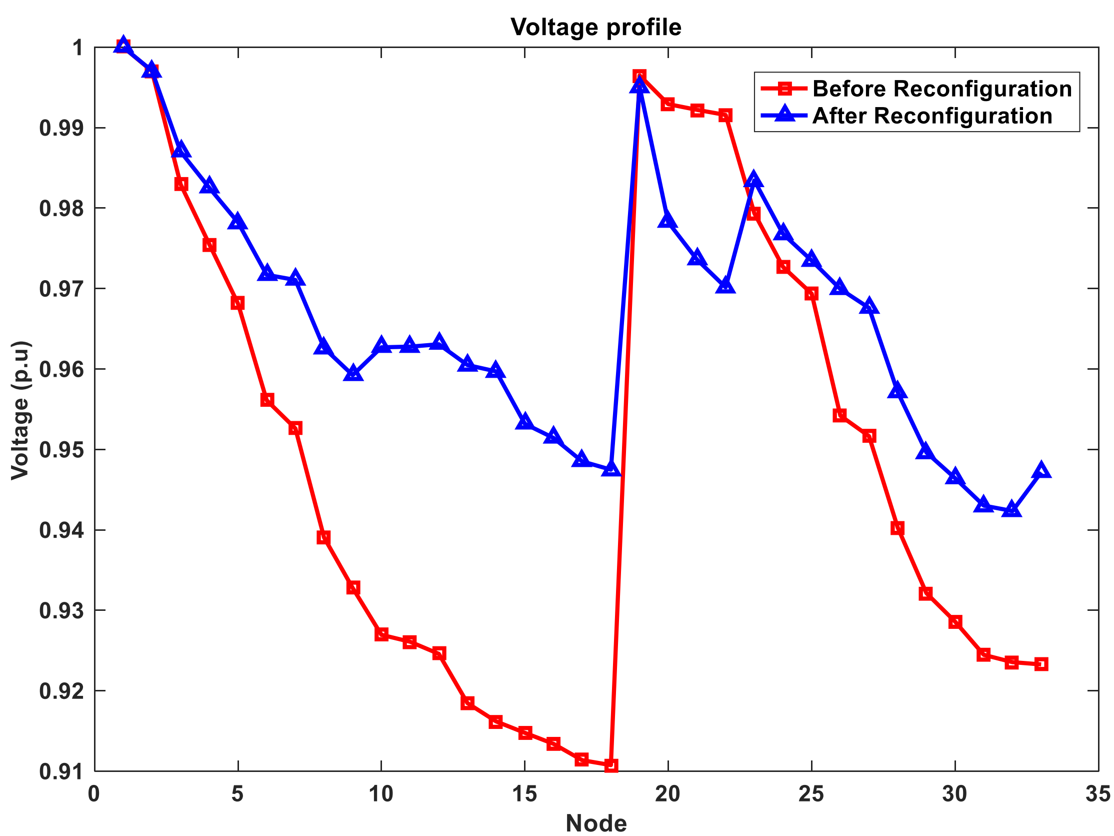


**Figure 3.8**: **Voltage profile of the 33-bus network before and after the feeder reconfiguration**

It is observed that the distribution network topology after feeder reconfiguration is different from the initial topology. Before the feeder reconfiguration, branches number 33 (branch $8-21$), 34 (branch $9-15$), 35 (branch $12-22$), 36 (branch $18-33$) and 37 (branch $25-29$) are the tie-lines whereas branches number 7 (branch $7-8$), 9 (branch $9-10$), 14 (branch $14-15$), 32 (branch $32-33$) and 37 (branch $25-29$) are the tie-lines after the feeder reconfiguration. This shows that the developed BPSO algorithm effectively reconfigured the network topology. The change in the network topology led to a reduction of the power loss in the 33-bus distribution system. After the feeder reconfiguration, the real power loss in the distribution system is reduced to $\mathbf{138.9105\ kW}$ from $\mathbf{208.4322\ kW}$ before the feeder reconfiguration. This corresponds to a real power loss reduction of approximately $\mathbf{33.36\%}$ in comparison with the real power loss in the initial distribution system. The change in the distribution network topology also improved its voltage profile as shown in Figure 3.8. The minimum voltage is $\mathbf{0.9107p.u}$ at **bus 18** before the feeder reconfiguration and it is improved to $\mathbf{0.9423p.u}$ at **bus 32** after the feeder reconfiguration.

A probability study is done to determine how many time the developed PSO algorithm find the optimal network topology for the 33-bus distribution network. The optimisation of the network topology of the 33-bus distribution system is run 100 times. The convergence characteristic for the developed BPSO algorithm is given in Figure 3.9.

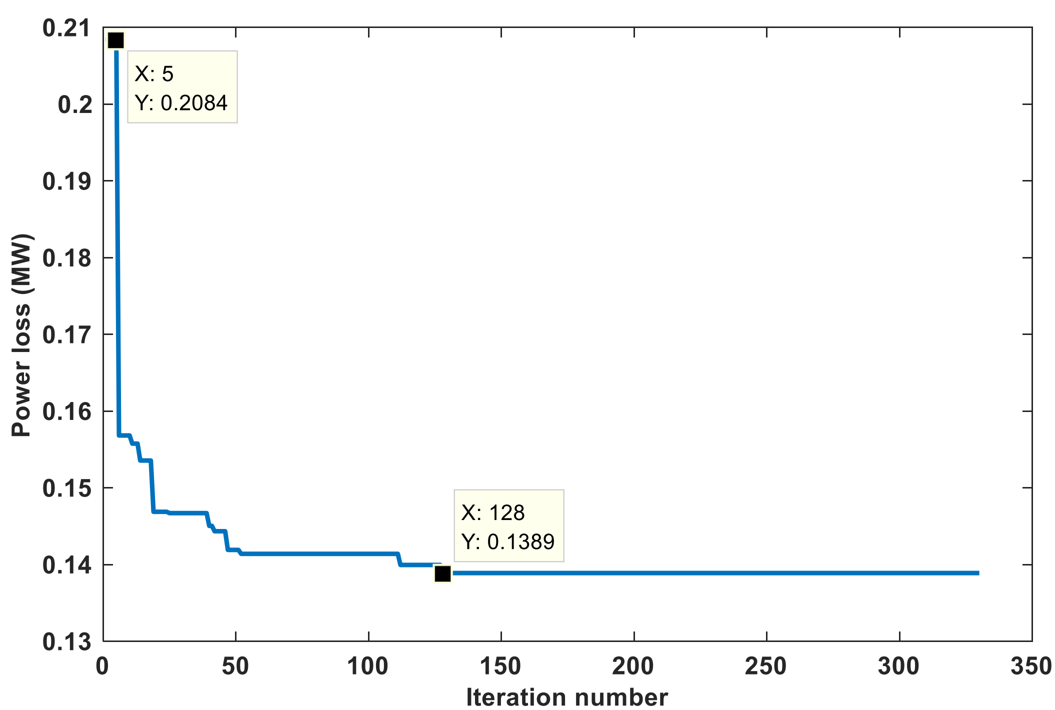


**Figure 3.9**: **Convergence characteristic of the developed BPSO algorithm for the 33-bus distribution system**

It results that for the 33-bus distribution system, the developed BPSO algorithm converges to the optimal solution 92% of the time. The highest value of the real power loss after reconfiguration recorded is $\mathbf{142.1177kW}$. The average power loss after 100 runs is $\mathbf{139.0808kW}$, and therefore, the average percentage of power loss reduction is $\mathbf{33.2729}\%$. Initially, the real power loss is $0.2084\ \mathrm{MW}$. As the developed PSO algorithm go through iterations, candidate network topologies with lower real power loss are found. The optimal distribution network topology is found after 128 iterations. For the 33-bus distribution system, the developed algorithm goes through 330 iterations before the search process is complete, although the optimal solution is found at the $128^{\mathrm{th}}$ iteration.

The results of the 33-bus distribution system after the feeder reconfiguration is compared with the literature ones and it is provided in Table 3.10. The comparison study proves that the results of the developed BPSO algorithm are consistent with the literature ones, and the developed BPSO algorithm achieves a higher real power loss reduction compared to the literature. For both the developed BPSO algorithm and the literature, the distribution network topology before and after feeder reconfiguration is the same. However, their total real power loss is different. The difference in real power loss between the developed BPSO algorithm and the literature results is mainly due to the load flow approach used. The Gauss-Seidal power flow approach is used in the literature whereas the developed BPSO algorithm uses the Newton-Raphson power flow approach for faster convergence and refined results.

**Table 3.10**: **Comparison of the results of the developed BPSO algorithm for the 33-bus distribution system with those provided in the literature**

| **Algorithm** | | **Developed BPSO algorithm** | **SSOM (Afsari et al., 2009)** | **Hybrid PSO-HBMO (Niknam, 2009)** | **ISFLA (Kavousi-Fard & Akbari-Zadeh, 2013)** |
|---|---|---|---|---|---|
| Before reconfiguration | Tie switches | 33 34 35 36 37 | 33 34 35 36 37 | 33 34 35 36 37 | 33 34 35 36 37 |
| | Power loss (kW) | 208.4322 | 202.05 | 202.67 | 202.67 |
| | Minimum voltage (p.u) | 0.9108 @ bus 18 | 0.91365 @ bus 37 | 0.913 | – |
| After reconfiguration | Tie switches | 7 9 14 32 37 | 7 9 14 32 37 | 7 9 14 32 37 | 7 9 14 32 37 |
| | Power loss (kW) | 138.9105 | 139.21 | 139.53 | 139.53 |
| | Minimum voltage (p.u) | 0.9423 @ bus 32 | 0.93796 @ bus 32 | 0.938 | – |
| | Power loss reduction (%) | 33.3546 | 31.1012 | 31.14 | 31.154 |

#### 3.5.3.3. Test case 3: IEEE 69-bus distribution system

The developed BPSO algorithm is applied to the 69-bus distribution system to solve the distribution network feeder reconfiguration problem. The 69-bus distribution system is a $\mathbf{12.66\ kV}$, $\mathbf{100\ MVA}$ radial distribution network as shown in Figure 3.10. It consists of 1 main feeder, 48 fixed loads and 73 branches, 5 of which are tie-lines. The fixed loads account for a total real and reactive power demand of $\mathbf{3.8019\ MW}$ and $\mathbf{2.6946\ Mvar}$ respectively. The parameters for the 69-bus distribution system are given in **Appendix D**.

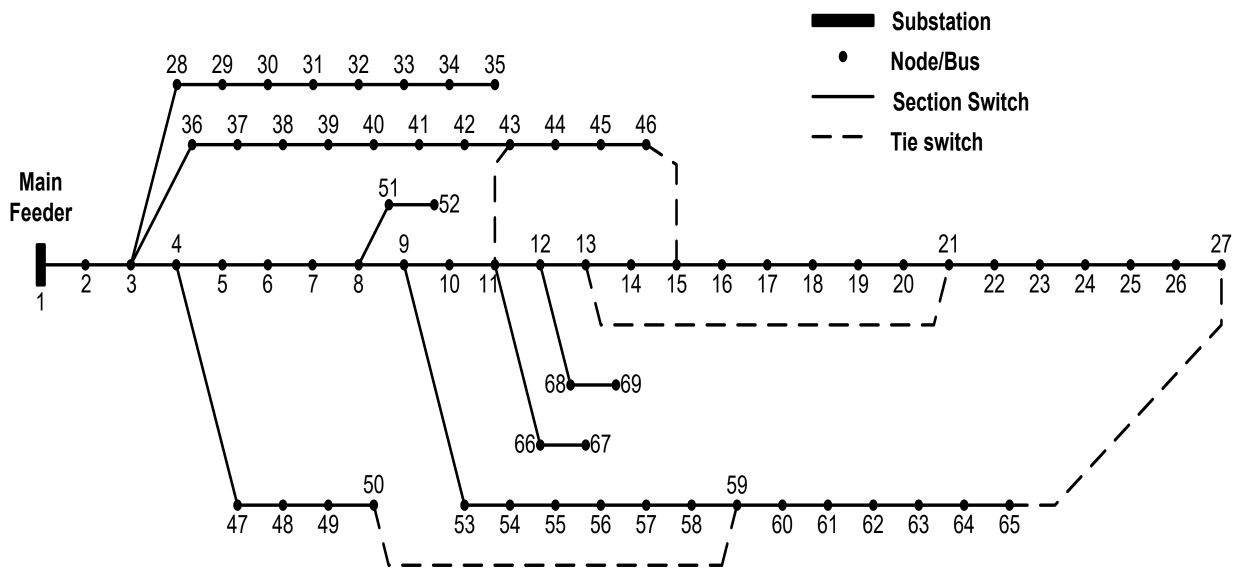


**Figure 3.10**: **Single line diagram of the 69-bus distribution system**

Initially, the tie switches in the 69-bus distribution system are branch $11-43$; branch $13-21$; branch $15-46$; branch $50-59$; and branch $27-65$. The Newton-Raphson method is used to calculate the load flow of the 69-bus distribution system in the MATLAB platform. The load flow study shows that the 69-bus distribution system has an initial real power loss of $\mathbf{224.9804\ kW}$ and a total power generation of $(\mathbf{4.0268+j2.7968})\mathbf{MVA}$. It is observed that before the network reconfiguration, the minimum voltage in the 69-bus distribution system is $\mathbf{0.9092p.u}$ at **bus 65**. The complete load flow results are given in **Appendix E1**.

The developed BPSO algorithm is used to find the optimal network topology to minimise the real power loss in the 69-bus distribution system. It is observed that the developed BPSO algorithm find four possible optimal network topologies as follows:

- **Network topology 1**: the tie switches for this network topology are branch number 14 (branch $14-15$); 55 (branch $55-56$); 61 (branch $61-62$); 69 (branch $11-43$); 70 (branch $13-21$).

- **Network topology 2**: the tie switches for this network topology are branch number 14 (branch $14-15$); 56 (branch $56-57$); 61 (branch $61-62$); 69 (branch $11-43$); 70 (branch $13-21$).
- **Network topology 3**: the tie switches for this network topology are branch number 14 (branch $14-15$); 57 (branch $57-58$); 61 (branch $61-62$); 69 (branch $11-43$); 70 (branch $13-21$).
- **Network topology 4**: the tie switches for this network topology are branch number 14 (branch $14-15$); 58 (branch $58-59$); 61 (branch $61-62$); 69 (branch $11-43$); 70 (branch $13-21$).

The load flow study shows that for all the four possible optimal network topologies, the 69-bus distribution system has a total real power loss of $\mathbf{98.5952\ kW}$ and a total power generation of $(\mathbf{3.9004 + j2.7866})\mathbf{MVA}$. The minimum voltage in the 69-bus distribution system is now $\mathbf{0.9495 p.u}$ at **bus 61**. The comprehensive load flow results of the 69-bus distribution system after the distribution network reconfiguration given in **Appendix E2**.

**Table 3.11: Summary of the simulation results of the 69-bus distribution system before and after solving the single-objective feeder reconfiguration problem**

| Simulation results | Before reconfiguration | After reconfiguration |
|---|---|---|
| Power generation in (MVA) | $4.0268 + j2.7968$ | $3.9004 + j2.7866$ |
| Tie switches | 69 70 71 72 73 | 14 55 61 69 70 |
| Real power loss | 224.9804 kW | 98.5952 kW |
| Real power loss reduction | − | 56.1488% |
| Minimum voltage | 0.9092 p.u @ bus 65 | 0.9495 p.u @ bus 61 |

Table 3.11 gives a comparative analysis of the results of the 69-bus distribution system before and after feeder reconfiguration using the developed binary PSO algorithm. It is observed that there are four possible optimal distribution network topologies after feeder reconfiguration, all different from the initial topology. This shows that the developed BPSO algorithm effectively reconfigured the network topology. The change in the network topology led to a reduction of the power loss in the 69-bus distribution system. After the feeder reconfiguration, the real power loss in the distribution system is reduced to $\mathbf{98.5952\ kW}$ from $\mathbf{227.9804\ kW}$ before the feeder reconfiguration. This corresponds to a real power loss reduction of approximately $\mathbf{56.1488}\%$ in comparison with the real power loss in the initial distribution system. The change in the distribution network topology also

improved its voltage profile as shown in Figure 3.11. The minimum voltage is $\mathbf{0.9092\ p.u}$ at **bus 65** before the feeder reconfiguration and it is improved to $\mathbf{0.9495 p.u}$ at **bus 61** after the feeder reconfiguration.

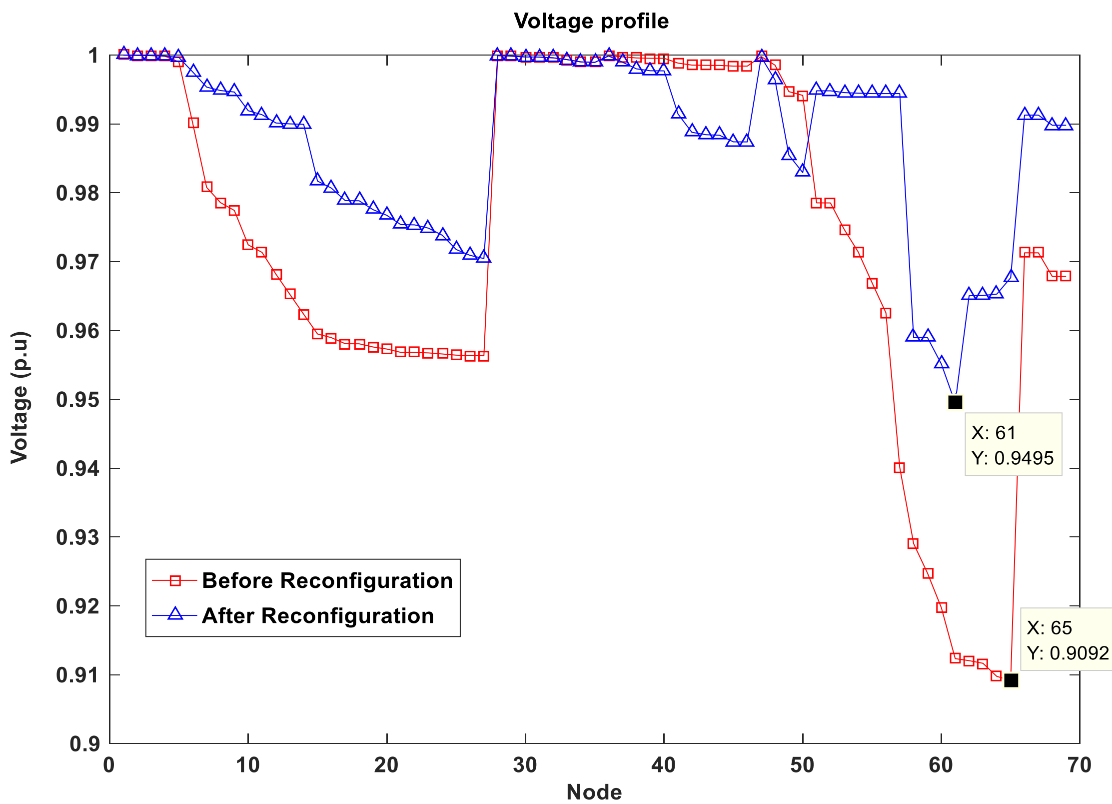


**Figure 3.11**: **Voltage profile of the 69-bus distribution system before and after solving the single-objective feeder reconfiguration problem**

In term of the success rate, for 100 runs, it results that for the 69-bus distribution system, the developed BPSO algorithm converges to the optimal solution 70% of the time. However, most of the local optima recorded have a real power loss close to $\mathbf{98.5952\ kW}$. In fact, the average real power loss after 100 runs is $\mathbf{99.1014\ kW}$, a $\mathbf{0.511\%}$ difference from the real power loss of the optimal distribution network topology. The highest value of the real power loss after reconfiguration recorded is $\mathbf{112.7221\ kW}$, which still is approximately $\mathbf{49.897}\%$ power loss reduction. The success rate of the developed BPSO algorithm can be increased by increasing the number of particles or the number of iterations in the algorithm. But, the computation time it would take to find the optimal solution would also be increased.

The results of the 69-bus distribution system after the feeder reconfiguration is compared with the literature ones and it is provided in Table 3.12. The comparison study proves that the results of the developed BPSO algorithm are consistent with the literature ones, and the developed BPSO algorithm achieves a higher real power loss reduction ($\mathbf{56.1488\ \%}$) in comparison to the literature ones.

**Table 3.12**: **Comparison of the results of the developed BPSO algorithm for the 69-bus distribution system with those provided in the literature**

| **Algorithm** | | **Develop BPSO algorithm** | **Fuzzy multi-objective approach Savier & Das, 2007)** | **HAS (Rao et al., 2013)** | **SPSO (Khalil & Gorpinich, 2012)** |
|---|---|---|---|---|---|
| Before reconfiguration | Tie switches | 69 70 71 72 73 | 69 70 71 72 73 | 69 70 71 72 73 | 69 70 71 72 73 |
| | Real power loss $(\mathrm{kW})$ | 224.9804 | 224.9517 | 225 | 224.96 |
| | Minimum voltage $(\mathrm{p.u})$ | 0.9092 @ bus 65 | 0.9092 @ bus 65 | 0.9092 @ bus 65 | – |
| After reconfiguration | Tie switches | 14 55 61 69 70<br>14 56 61 69 70<br>14 57 61 69 70<br>14 58 61 69 70 | 14 56 63 69 70 | 13 18 56 61 69 | 14 56 63 69 70 |
| | Real power loss $(\mathrm{kW})$ | 98.5952 | 99.5944 | 99.35 | ~98.9824 |
| | Minimum voltage $(\mathrm{p.u})$ | 0.9495 @ bus 61 | 0.9483 @ bus 63 | 0.9428 @ bus 63 | – |
| | Real power loss reduction | 56.1488 % | 55.7263 % | 55.85 % | ~56 % |

### 3.5.4. Solution algorithm for the Multi-objective distribution network feeder reconfiguration problem

The BPSO solution algorithm for the multi-objective distribution network feeder reconfiguration problem is similar to the single-objective distribution network feeder reconfiguration problem's given in section 3.5.2. The most significant differences between the single and multi-objective BPSO solution algorithms are:

- **The objectives functions**: the multi-objective problem consists of two objectives (real power loss minimisation and load balancing index minimisation) instead of one objective (real power loss minimisation) for the single-objective problem.
- **The personal best position update approach**: In the multi-objective BPSO algorithm, the update of the personal best position takes into consideration the real power loss and the load balancing index values of each particle. In the single-objective, only the real power loss of the particle is considered.

- **The global best position update approach**: In the multi-objective BPSO algorithm, a candidate solution has two fitness values: the real power loss and the load balancing index. Consequently, when selecting the global best position, care must be taken to ensure that the chosen candidate solution is in no way dominated by any other particle in the search space.

The Discrete PSO based solution algorithm for the multi-objective feeder reconfiguration problem is implemented using the following steps:

**Step 1:** Read the distribution system network data such as the number of nodes $\mathbf{NB}$, the number of distribution lines $\mathbf{NL}$, the number of tie lines $\mathbf{NT}$, the bus type ($\mathbf{Slack}, \mathbf{PV}, \mathbf{PQ}$), the load data ($\mathbf{Pd}, \mathbf{Qd}, \mathbf{Bs}, \mathbf{Load_{ID}}$), the generator data ($\mathbf{Pg}, \mathbf{Qg}$) and distribution line data ($\mathbf{bus_i}, \mathbf{bus_j}, \mathbf{r}, \mathbf{x}, \mathbf{sw_{tie}}, \mathbf{sw_{sec}}$).

**Step 2**: Initialize the binary PSO parameters such as the acceleration coefficient $\mathbf{c1}$ and $\mathbf{c2}$; the minimum and the maximum inertia weight ($\mathbf{w_{min}}$ and $\mathbf{w_{max}}$ respectively); the particle's velocity limits ($\mathbf{v_{min}}$ and $\mathbf{v_{max}}$); the number of particles ($\mathbf{Np}$); the dimension of the search space ($\mathbf{D}$) and the stopping criteria (maximum number of iterations $\mathbf{t_{max}}$).

**Step 3:** Initialize the particle position which is the binary coded representation of the section and tie-switches of the distribution network, as defined in section 3.5.2.

**Step 4:** Initialize the velocity of the particles which represents the probability for each bit in the particle's position to change its status from open (0) to close (1) or from close (1) to open (0).
Each particle in the search space has a different velocity. The particle's velocity is calculated using equation 3.22 given in section 3.5.2.

$$\mathbf{velocity(i, j) = v_{min} + (v_{max} - v_{min}) * rand}$$

**Step 5:** Find the personal best particles position. In this case, the initial particle position is assumed as the best particle position. Then calculate the load flow based on the best particles position and find the real power loss and the load balancing index using Equations 3.12 and 3.15.

$$\mathbf{P_{loss}} = \sum_{\substack{\mathbf{j=1} \\ \mathbf{k=1} \\ \mathbf{j \neq k}}}^{\mathbf{NB}} \mathbf{real}\left(\mathbf{V_j \times i_{jk}}^* - \mathbf{V_k \times i_{jk}}^*\right)$$

where

$\mathbf{j}$ is the sending bus of line $\mathbf{j-k}$.

$\mathbf{k}$ is the receiving bus of line $\mathbf{j-k}$.

$\mathbf{V_j, V_k}$ are the sending and receiving end voltage of the line $\mathbf{j-k}$ respectively.

$\mathbf{i_{jk}}^*$ is the conjugate of the current flow in line $\mathbf{j-k}$.

$\mathbf{P_{loss}}$ is the total power loss in the distribution system.

$\mathbf{NB}$ is the number of busses in the network.

$$\mathbf{LBI_{sys} = \frac{1}{NL} * \sum_{l=1}^{NL} \frac{S_l}{S_{l\,max}}}$$

where,

$\mathbf{l}$ is the branch number of the line $\mathbf{j-k}$.

$\mathbf{S_l}$ is the apparent power loss in the branch $\mathbf{l}$.

$\mathbf{S_{l\,max}}$ is the power rating of branch $\mathbf{l}$.

$\mathbf{LBI_{sys}}$ is the load balance index of the network.

$\mathbf{NL}$ is the number of branches in the distribution system.

A particle' s personal best position has two individual fitness values, representing the real power loss and the load balancing index for the particle's personal best position. The fitness of a given particle $\mathbf{i}$ is therefore defined as follows:

$$\mathbf{fitness_i = [fitness1_i, fitness2_i]} \tag{3.26}$$

Where

$\mathbf{fitness_i}$ is the fitness of particle $\mathbf{i}$.

$\mathbf{fitness1}$ is the real power loss for the particle's position.

$\mathbf{fitness2}$ is the load balancing index for the particle's position.

**Step 6:** Find the global best particle position from the set of particles best position given in Step 5. In this case, the global best particle position is the best particle position with the minimal real power loss and load balancing index values.

**Step 7:** Compute the bus incidence matrix of the distribution network**.** The bus incidence matrix is used to identify whether a connection exists between the two nodes or not. This helps to determine whether the network topology is radial or not.

**Start the binary PSO iteration process** and set the iteration counter $\mathbf{t}$ to 1.

**Step 8:** Check the topological constraints after updating the bus incidence matrix for the candidate network topologies and verify if all the candidate solutions meet the topology constraints. This step ensures that the real power loss and the load balancing index is calculated only for feasible distribution network topologies.

**Step 9:** Find the power flow in the distribution network using the Newton-Raphson load flow approach. Then, employ the power flow results to calculate the real power loss and the load balancing index of each candidate network topology using Equations 3.12 and 3.15 respectively.

**Step 10:** Update the particles' personal best as per Equation 3.27.

$$\mathbf{Pbest_i}^{\mathbf{t+1}} = \begin{cases} \mathbf{x_i}^{\mathbf{t+1}}, & \mathbf{if\ fitness1_i}^{\mathbf{t+1}} < \mathbf{fitness_{Pbest1_i}}^{\mathbf{t}} \mathbf{and\ fitness2_i}^{\mathbf{t+1}} < \mathbf{fitness_{Pbest2_i}}^{\mathbf{t}} \\ \mathbf{Pbest_i}^{\mathbf{t}}, & \mathbf{otherwise} \end{cases} \quad (3.27)$$

Where

$\mathbf{Pbest_i}^{\mathbf{t}}$ is the personal best position of particle $\mathbf{i}$ at iteration $\mathbf{t}$.

$\mathbf{x_i}^{\mathbf{t+1}}$ is the position of particle $\mathbf{i}$ at iteration $\mathbf{t+1}$.

$\mathbf{fitness1_i}^{\mathbf{t+1}}$ is the real power loss of particle $\mathbf{i}$ at iteration $\mathbf{t+1}$.

$\mathbf{fitness2_i}^{\mathbf{t+1}}$ is the load balancing index of particle $\mathbf{i}$ at iteration $\mathbf{t+1}$.

$\mathbf{fitness_{Pbest1_i}}^{\mathbf{t}}$ is the real power loss of $\mathbf{Pbest_i}^{\mathbf{t}}$ at iteration $\mathbf{t}$.

$\mathbf{fitness_{Pbest2_i}}^{\mathbf{t}}$ is the load balancing index of $\mathbf{Pbest_i}^{\mathbf{t}}$ at iteration $\mathbf{t}$.

**Step 11:** Update the global best in the swarm of particles as per Equation 3.28.

$$\mathbf{Gbest}^{\mathbf{t+1}} = \begin{cases} \mathbf{Pbest_i}^{\mathbf{t+1}}, & \mathbf{if\ fitness_{Pbest1_i}}^{\mathbf{t+1}} < \mathbf{fitness_{Gbest1}}^{\mathbf{t}}\ \mathbf{and\ fitness_{Pbest2_i}}^{\mathbf{t+1}} < \mathbf{fitness_{Gbest1}}^{\mathbf{t}} \\ \mathbf{Gbest}^{\mathbf{t}}, & \mathbf{otherwise} \end{cases} \quad (3.28)$$

where

$\mathbf{Gbest}^{\mathbf{t+1}}$ is the global best solution of the swarm at iteration $\mathbf{t+1}$.

$\mathbf{fitness_{Gbest1}}^{\mathbf{t}}$ is the real power loss of $\mathbf{Gbest}$ at iteration $\mathbf{t}$.

$\mathbf{fitness_{Gbest2}}^{\mathbf{t}}$ is the load balancing index of $\mathbf{Gbest}$ at iteration $\mathbf{t}$

**Step 12:** Calculate the inertia weight using Equation 3.6 and update the velocity of all particles per Equation 3.5.

$$\mathbf{v_i^{k+1} = \omega * v_i^k + c1 * rand1 * \left(Pbest_i - x_i^k\right) + c2 * rand2 * \left(Gbest_i - x_i^k\right)}$$

**Step 13:** Update the particles' position as per Equation 3.9.

$$\mathbf{x_i^k = \begin{cases} 1 & \text{if } r < sig\left(v_i^k\right) \\ 0 & \text{if } r \geq sig\left(v_i^k\right) \end{cases}}$$

Where

$\mathbf{r}$ is a uniformly distributed random number in the interval [0,1]

$\mathbf{sig}$ is a sigmoid function defined by $\mathbf{sig(\alpha) = \frac{1}{1+e^{-\alpha}}}$

**Step 14:** Increment the iteration count of the binary PSO search process and repeat step 8 to step 13 until the stopping criterion is reached.

**Step 15:** Print the results of the search process such as the global best solution (optimal distribution network topology), its corresponding fitness values (real power loss and load balancing index).

The flowchart of the BPSO solution algorithm for the multi-objective feeder reconfiguration problem is shown in Figure 3.12.

The personal best position and the global best position are updated using Equations 3.27 and 3.28 respectively, to ensure that the final solution of the search process is not dominated by any other possible solution in the search space. This is to conform to the Pareto-dominance principle which stipulates that: "Given two solutions $\mathbf{u} = [\mathbf{u_1}, \mathbf{u_2}, \dots, \mathbf{u_I}]$ and $\mathbf{z} = [\mathbf{z_1}, \mathbf{z_2}, \dots, \mathbf{z_I}]$ in the search space, $\mathbf{u}$ dominates $\mathbf{z}$ $\mathbf{(u < z)}$ if and only if:

- $\mathbf{u}$ is no worse than $\mathbf{z}$ for all objectives i.e. $\mathbf{f_i(u) \leq f_i(z);\ \forall\ i = 1, 2, \dots, n}$
- $\mathbf{u}$ is strictly better than $\mathbf{z}$ for at least one objective i.e. $\mathbf{f_i(u) < f_i(z)}$, for at least one $\mathbf{i} \in \{\mathbf{1, 2, \dots, n}\}$."

So, a particle $\mathbf{i}$ is the best solution of a minimization problem if there is no other particle $\mathbf{k}$ in the search space such as the objective value of particle $\mathbf{k}$ is strictly inferior to the fitness of particle $\mathbf{i}$ for all objectives in the problem.

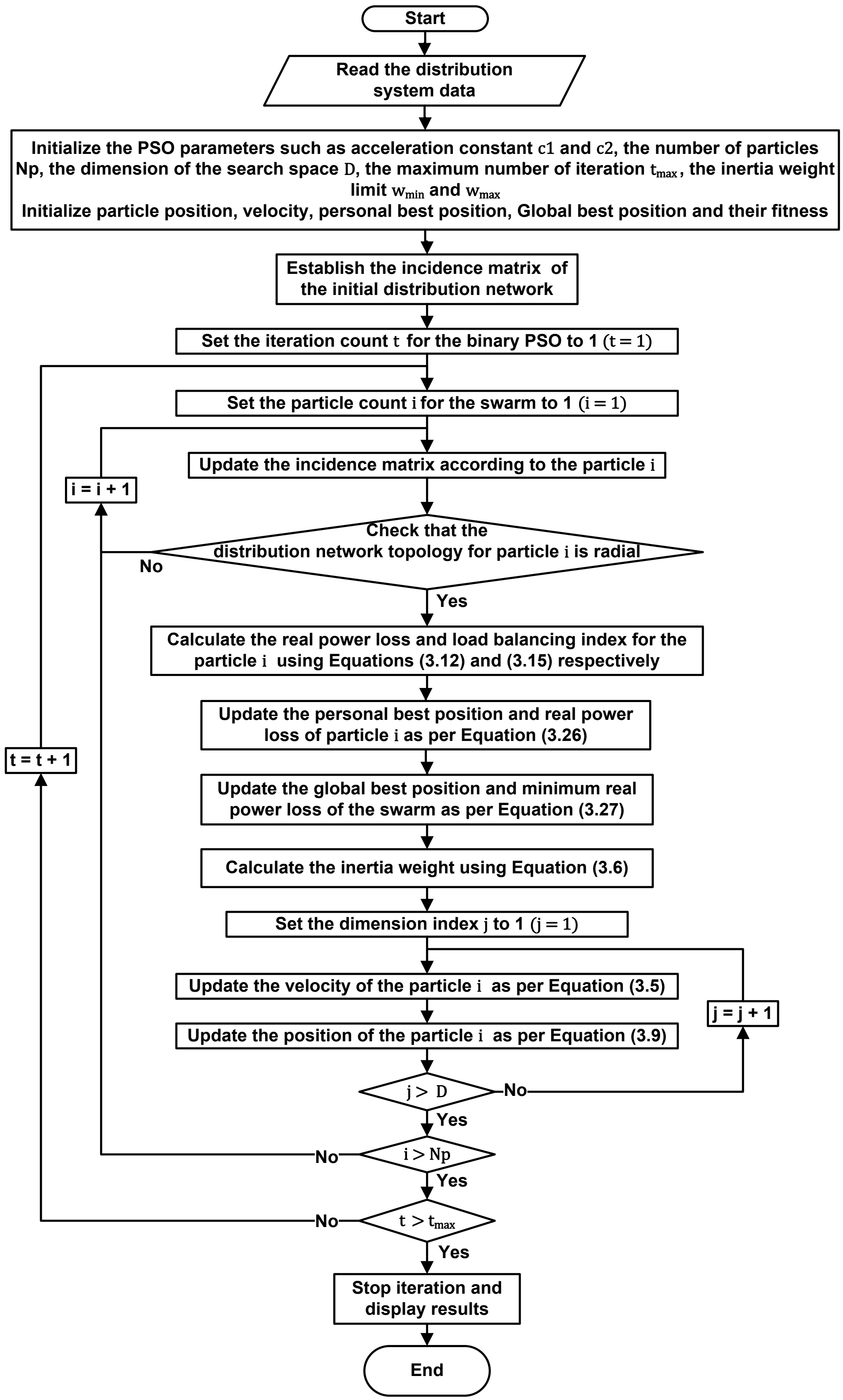


**Figure 3.12**: Flowchart of the developed PSO algorithm for the multi-objective distribution network feeder reconfiguration problem

### 3.5.5. Results of the PSO solution algorithm for the multi-objective distribution network feeder reconfiguration problem

To evaluate the performance and the effectiveness of the developed multi-objective BPSO solution algorithm for the single-objective distribution network feeder reconfiguration problem, three distribution systems are used for case studies: the IEEE 16 bus distribution system; the IEEE 33 bus distribution system; and the IEEE 69-bus distribution system.

A comparative analysis of the distribution system before and after the distribution network reconfiguration is provided in this section. The evaluation is carried out based on the real power loss, the load balancing index, the voltage profile and the change in the distribution network topology. The results of the developed multi-objective BPSO algorithm are compared with the literature ones. The predefined parameters of the developed multi-objective BPSO algorithm are given in Table 3.2. The multi-objective BPSO solution algorithm is designed to work on any radial distribution system. Therefore, the number of particles in the search process changes depending on the number of bus and ties switches in the distribution system, and it is calculated using Equation 3.21.

#### 3.5.5.1. Test case 1: IEEE 16-bus distribution system

The developed multi-objective BPSO algorithm is used to find the optimal network topology to minimise the real power loss and the load balancing index in the 16-bus distribution system. It is observed that after the network reconfiguration, the new tie switches in the distribution system are: branch $8-10$; branch $9-11$; and branch $7-16$. The load flow study shows that after the feeder reconfiguration, the 16-bus distribution system has a total real power loss of $\mathbf{468.3304\,kW}$ and a total power generation of $(\mathbf{29.1683+j6.8733})\mathbf{MVA}$. The minimum voltage in the 16-bus distribution system is now $\mathbf{0.9707\ p.u}$ at **bus 12**.

Table 3.13 gives a comparative analysis of the results of the 16-bus distribution system before and after feeder reconfiguration using the developed multi-objective BPSO algorithm. It is observed that the distribution network topology after feeder reconfiguration is different from the initial topology. Before the feeder reconfiguration, branches number 14 (branch $5-11$), 15 (branch $10-14$) and 16 (branch $7-16$) are the tie-lines whereas branches number 7 (branch $8-10$), 8 (branch $9-11$) and 16 (branch $7-16$) are the tie-lines after the feeder reconfiguration. This shows that the developed multi-objective BPSO algorithm effectively reconfigured the network topology. The change in the network topology led to a reduction of the real power loss and load balancing index in the 16-bus distribution system. After the feeder reconfiguration, the real power loss in the distribution system is reduced to $\mathbf{468.3304\ kW}$ from $\mathbf{514.02932\ kW}$ before the feeder reconfiguration; the load balancing index is reduced to $\mathbf{2.7676 \times 10^{-3}}$ from $\mathbf{2.9812 \times 10^{-3}}$. This corresponds to a real power loss reduction of approximately $\mathbf{8.89033\%}$ and an $\mathrm{LBI}$ improvement of $\mathbf{7.166\%}$, in comparison with the real power loss and the load balancing index of the initial distribution system respectively. The change in the distribution network topology also improved its voltage profile as shown in Figure 3.13. The minimum voltage is $\mathbf{0.9682\ p.u}$ at **bus 12** before the feeder reconfiguration and it is improved **to** $\mathbf{0.9707\ p.u}$ at **bus 12** after the feeder reconfiguration.

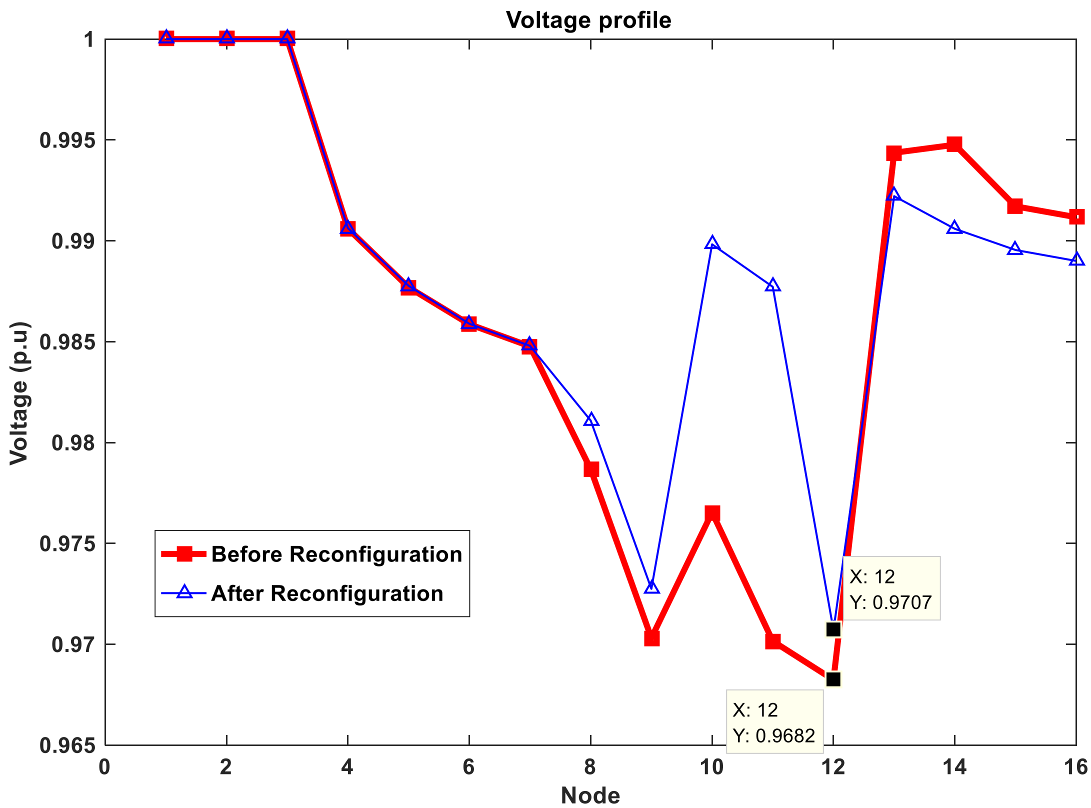


**Figure 3.13: Voltage profile of the 16-bus network before and after solving the multi-objective feeder reconfiguration problem**

The developed multi-objective algorithm is run 100 times on the 16-bus distribution system. And for the 100 times, the developed multi-objective BPSO algorithm converged to the same solution every time. This means that for the 16-bus distribution system, there is no better solution to the multi-objective distribution network feeder reconfiguration problem than the one provided in Table 3.13. The results indicate that a real power loss reduction of $\mathbf{8.89033\%}$ and a load balance improvement of $\mathbf{7.166\%}$ are achieved using the developed multi-objective BPSO method.

**Table 3.13**: **Summary of the simulation results of the 16-bus distribution system before and after solving the multi-objective feeder reconfiguration problem**

| Simulation results | Before reconfiguration | After reconfiguration |
|---|---|---|
| Tie switches (branch number) | 14 15 16 | 7 8 16 |
| Real power loss | $514.02932$ kW | $468.3304$ kW |
| Real power loss reduction | – | $8.89033\%$ |
| Load balancing index (LBI) | $2.9812 \times 10^{-3}$ | $2.7676 \times 10^{-3}$ |
| Load balance improvement | – | $7.166\%$ |
| Minimum voltage | $0.9707$ p.u | $0.9682$ p.u |

### 3.5.5.2. Test case 2: IEEE 33-bus distribution system

The developed multi-objective BPSO algorithm is used to find the optimal network topology to minimise the real power loss and the load balancing index in the 33-bus distribution system. Table 3.14 gives a comparative analysis of the results of the 33-bus distribution system before and after feeder reconfiguration using the developed multi-objective BPSO algorithm. It is observed that unlike in the 16-bus distribution system, the application of the multi-objective feeder reconfiguration algorithm to the 33-bus distribution system does not return the same solution every time the algorithm is run. This may be an indication that there are many Pareto-optimal solutions to the problem instead of a single solution. To ascertain whether the obtained solutions are Pareto-optimal or not, the developed multi-objective BPSO algorithm is run 500 times and the solutions obtained are analysed. Based on the Pareto-dominance principle as defined in section 2.3.2.2., it follows that the application of the developed multi-objective BPSO algorithm to the 33-bus network for optimal feeder reconfiguration has 3 Pareto-optimal or non-dominated network topologies solution:

- **Network topology 1**: the tie switches for this distribution network topology are branches number 7 (branch $7-8$), 9 (branch $9-10$), 14 (branch $14-15$), 32 (branch $32-33$) and 37 (branch $25-29$). For this network topology, the real power loss is $\mathbf{138.9105\ kW}$ and the load balancing index is $\mathbf{1.4503} \times \mathbf{10^{-4}}$. This corresponds to a real power loss reduction of approximately $\mathbf{33.3546}\,\%$ and an LBI improvement of $\mathbf{29.2125}\,\%$, in comparison with the real power loss and load balancing index in the initial distribution system respectively. This network topology has the lowest real power loss in the search space. So, in term of real power loss, network topology 1 dominates all the candidate network topologies in the search.

- **Network topology 2:** the tie switches for this distribution network topology are branches number 7 (branch $7-8$), 9 (branch $9-10$), 14 (branch $14-15$), 28 (branch $28-29$) and 31 (branch $31-32$). For this network topology, the real power loss is $\mathbf{144.1694\ kW}$ and the load balancing index is $\mathbf{1.3487} \times \mathbf{10^{-4}}$. This corresponds to a real power loss reduction of approximately $\mathbf{30.8315}\ \%$ and an $\mathrm{LBI}$ improvement of $\mathbf{34.1697}\ \%$, in comparison with the real power loss and load balancing index in the initial distribution system respectively. This network topology has the lowest load balancing index in the search space. So, in term of load balancing index, network topology 2 is non-dominated in the search space.

- **Network topology 3:** the tie switches for this distribution network topology are branches number 7 (branch $7-8$), 9 (branch $9-10$), 14 (branch $14-15$), 28 (branch $28-29$) and 32 (branch $32-33$). For this network topology, the real power loss is $\mathbf{139.9645\ \ kW}$ and the load balancing index is $\mathbf{1.3751} \times \mathbf{10^{-4}}$. This corresponds to a real power loss reduction of approximately $\mathbf{32.8489}\ \%$ and an $\mathrm{LBI}$ improvement of $\mathbf{32.88251}\ \%$, in comparison with the real power loss and load balancing index in the initial distribution system respectively.

**Table 3.14: Summary of the simulation results of the 33-bus distribution system before and after solving the multi-objective feeder reconfiguration problem**

| Simulation results | Before reconfiguration | After reconfiguration | | |
|---|---|---|---|---|
| | | Topology 1 | Topology 2 | Topology 3 |
| Tie switches | 33 34 35 36 37 | 7 9 14 32 37 | 7 9 14 28 31 | 7 9 14 28 32 |
| Real power loss | 208.4322 kW | 138.9105 kW | 144.1694 kW | 139.9645 kW |
| Real power loss reduction | – | 33.3546% | 30.8315% | 32.8489% |
| Load balancing index ($\mathrm{LBI}$) | $2.0488 \times 10^{-4}$ | $1.4503 \times 10^{-4}$ | $1.3487 \times 10^{-4}$ | $1.3751 \times 10^{-4}$ |
| Load balance improvement | - | 29.2125% | 34.1697% | 32.88251% |
| Minimum voltage | 0.9108p. u @ bus 18 | 0.9423 p. u @ bus 32 | 0.9239 p. u @ bus 32 | 0.9413 p. u @ bus32 |

The real power loss of the network topology 3 ($\mathbf{139.9645kW}$) is higher than that of the network topology 1 ($\mathbf{138.9105\ kW}$) and the load balancing index of the network topology

1 ($\mathbf{1.4503} \times \mathbf{10^{-4}}$) is higher than that of the network topology 3 ($\mathbf{1.3751} \times \mathbf{10^{-4}}$). Likewise, the real power loss of the network topology 2 ($\mathbf{144.1694\ kW}$ ) is higher than that of the network topology 3 ($\mathbf{139.9645\ kW}$) and the load balancing index of the network topology 2 ($\mathbf{1.3487} \times \mathbf{10^{-4}}$) is lower than that of the network topology 3 ($\mathbf{1.3751} \times \mathbf{10^{-4}}$). So, based on the pareto-optimality principle in section 2.3.2.2., the solution network topologies 1, 2 and 3 are pareto-optimal and non-dominated with respect to each other. However, like with most real-world problems, only one solution is needed for as our final network topology. therefore, a higher-level information is needed to split the Pareto-optimal network topologies. The minimum bus voltage is used as the higher-level information.

From Table 3.14, the network topology 2 has the lowest voltage level ($\mathbf{0.9239\ p.u}$) amongst the set of optimal solution. And considering a voltage deviation of $\pm\mathbf{6}\%$, the minimum voltage in the network topology 2 even fall below the recommended standard. Although the network topology 3 has a minimum voltage within the standard, its minimum voltage magnitude ($\mathbf{0.9413\ p.u}$) is still lower than that of the network topology 1 ($\mathbf{0.9423\ p.u}$). So, the network topology 1 emerges as the preferred optimal solution to the multi-objective feeder reconfiguration problem for the 33-bus distribution system.

#### 3.5.5.3. Test case 3: IEEE 69-bus distribution system

The developed multi-objective BPSO algorithm is used to find the optimal network topology to minimise the real power loss and the load balancing index in the 69-bus distribution system. To ascertain whether it has Pareto-optimal solutions or not, the developed multi-objective BPSO algorithm is run 500 times and the solutions obtained are analysed. It is observed the application of the multi-objective feeder reconfiguration algorithm to the 69-bus distribution system does not return the same solution every time the algorithm is run and there is a handful number of non-dominated solution network topologies. Table 3.15 gives a comparative analysis of the results of the 69-bus distribution system before and after feeder reconfiguration using the developed multi-objective BPSO algorithm. The non-dominated solutions are grouped into two sets:

- **Set 1** represents the set of solution network topologies with $\mathbf{98.5952\ kW}$ of real power loss and a load balancing index of $\mathbf{1.5479} \times \mathbf{10^{-4}}$.
- **Set 2** is the set of solution network topologies with $\mathbf{101.2961\ kW}$ of real power loss and a load balancing index of $\mathbf{1.5295} \times \mathbf{10^{-4}}$.

**Table 3.15**: Summary of the simulation results of the 69-bus distribution system before and after solving the multi-objective feeder reconfiguration problem

| Simulation results | Before reconfiguration | After reconfiguration | |
|---|---|---|---|
| | | Set 1 | Set 2 |
| Tie switches (branch number) | 69 70 71 72 73 | 14 55 61 69 70<br>14 56 61 69 70<br>14 57 61 69 70<br>14 58 61 69 70 | 12 18 56 61 69<br>12 18 57 61 69<br>12 18 58 61 69<br>12 19 55 61 69<br>12 20 55 61 69<br>12 20 57 61 69 |
| Real power loss | 224.9804 kW | 98.5952 kW | 101.2961 kW |
| Real power loss reduction | – | 56.1761% | 54.9756% |
| Load balancing index (LBI) | $2.0488 \times 10^{-4}$ | $1.5479 \times 10^{-4}$ | $1.5295 \times 10^{-4}$ |
| Load balance improvement | - | 35.6355% | 36.4006% |
| Minimum voltage | 0.9092 p.u @ bus 65 | 0.9495 p.u @ bus 61 | 0.9495 p.u @ bus 61 |

Any solution network topology from set 1 has a lower real power loss, but a higher load balancing index than a solution network topology from set 2. So, the solutions network topologies in the two sets are Pareto-optimal with respect to each other. Moreover, any solution network topology chosen from the two sets leads to a minimum voltage magnitude of 0.9495 p.u at bus 61: the minimum voltage magnitude cannot be used as the higher-level information to determine which set of solutions is better. The importance of the objectives dictates which set of solutions is better. When the real power loss function is the primary concern, any solution in set 1 can be considered as the optimal solution. Likewise, when the load balancing is the primary concern, any solution in the set 2 is the optimal solution.

### 3.5.6. Discussion on the simulation results of the single-objective and multi-objective feeder reconfiguration problem

The developed BPSO feeder reconfiguration algorithms do not consider the current limits of the distribution system. If the distribution system is lightly loaded or loaded within the required margins, then the application of the feeder reconfiguration algorithm might increase the loading capability and improve the voltage profile of the distribution system.

In the case of a heavily loaded distribution system, an overload condition may occur and cause the voltage to drop outside the minimum limit. Therefore, a feeder reconfiguration scheme might relieve the distribution system overload and improve the voltage profile by reducing the real power loss. The distribution network feeder reconfiguration is however not a solution for distribution system overload mitigation voltage improvement. The improvement of the voltage profile in the distribution system after the network reconfiguration is merely the result of the reduced real power loss. The feeder reconfiguration transfers loads from the heavily loaded portions of the initial distribution system to lightly loaded portions.

The developed BPSO feeder reconfiguration algorithms provide the optimal solutions for the single and multi-objective feeder reconfiguration problem. It is noticed that by increasing the number of particles and the number of iterations, the success rate of the developed algorithms is undoubtedly improved. In the single-objective feeder reconfiguration approach, the personal and global best positions are each updated if a candidate network topology has a lower real power loss. In the multi-objective algorithm, the personal and global best positions are updated if a candidate network topology has a lower real power loss and a lower load balancing Index than each best position. Thus, only the best particles are used to direct the search process.

## 3.6. Conclusion

In this chapter, BPSO optimisation algorithms were developed to solve both the single-objective and multi-objective distribution network feeder reconfiguration problem. The basics of the PSO, its operating principle and some variants of PSO were presented.

The single-objective feeder reconfiguration problem aimed to minimise the real power loss in the distribution systems. The objectives of the multi-objective feeder reconfiguration problem were to minimise the real power loss and the load balancing index of the distribution system. The multi-objective feeder reconfiguration algorithm uses the Pareto-optimality principle to find the optimal distribution system topology. The IEEE 16-bus, the 33-bus, and the 69-bus distribution system were used to test the performance and the efficiency of the developed BPSO algorithms. The simulation results proved that the developed BPSO algorithms are efficient in solving the feeder reconfiguration problem.

The next chapter presents the optimal placement and sizing of Distributed generation (DG) in distribution systems using the BPSO method.

# CHAPTER FOUR

# OPTIMAL PLACEMENT AND SIZING OF DISTRIBUTED GENERATORS IN DISTRIBUTION SYSTEMS

## 4.1. Introduction

With the ever-increasing energy demand, the power grid is faced with hurdles such as increasing power losses, voltage instability, and decreasing reliability. To meet the power demand economically, reliably and efficiently has become a challenge. Moreover, due to high construction and operating costs, environmental concerns, depleting conventional energy sources (coal, water, gas), and the advances in technology, the need for centralised traditional power plants is less and less justified: where the development in Distributed Generation. Distributed Generation (DG) refers to the use of small-scale technologies for power generation at end-user points. Unlike conventional power plants, DG can be disconnected from the grid. And if properly placed and sized, DG can operate autonomously, can strengthen the grid resilience, help to mitigate grid disturbances and eliminates the cost, complexity, and inefficiencies associated with transmission and distribution systems.

This chapter first presents some DG technologies and their impacts on distribution networks. Secondly, the chapter covers the issues encountered in planning the size and location of DG in distribution systems. Then, the development and the testing of a single-objective optimal DG placement and sizing are presented. Finally, the development and the testing of a multi-objective optimal DG placement and sizing are presented. The single-objective optimal DG placement and sizing optimisation is done to minimise the real power loss in the distribution networks, while the multi-objective optimal DG placement and sizing optimisation has for objectives the minimisation of the real power loss, the minimisation or the bus voltage deviation and the maximisation of the bus voltage stability index.

## 4.2. DG technologies

DG offers numerous benefits over traditional power stations. Some of such benefits include increased efficiency, improved reliability and quality of supply, and deferred Transmission & Distribution upgrades among others. The percentage of DG generation in newly constructed power generation has reached the 30%, and it is projected to keep rising in the future (Acharya et al., 2006). Depending on their size, DGs are referred to as micro DG (1kW – 5kW), small DG (5kW – 5MW), medium DG (5MW – 50MW) or large DG

(50MW – 300MW) (Jordehi, 2015). This section covers the different types of DG technologies and the contributing factors to the adoption of DG.

### 4.2.1. Types of DG

It is a widespread belief that DG are only renewable energy technology such as solar and wind. However, technologies such as internal combustion engines, diesel engines, and microturbines are also DG technologies. Irrespective of whether they are renewable or not, DG can be categorised in 4 types, depending on their real and reactive power delivering capabilities: type I DG, type II DG, type III DG and type IV DG.

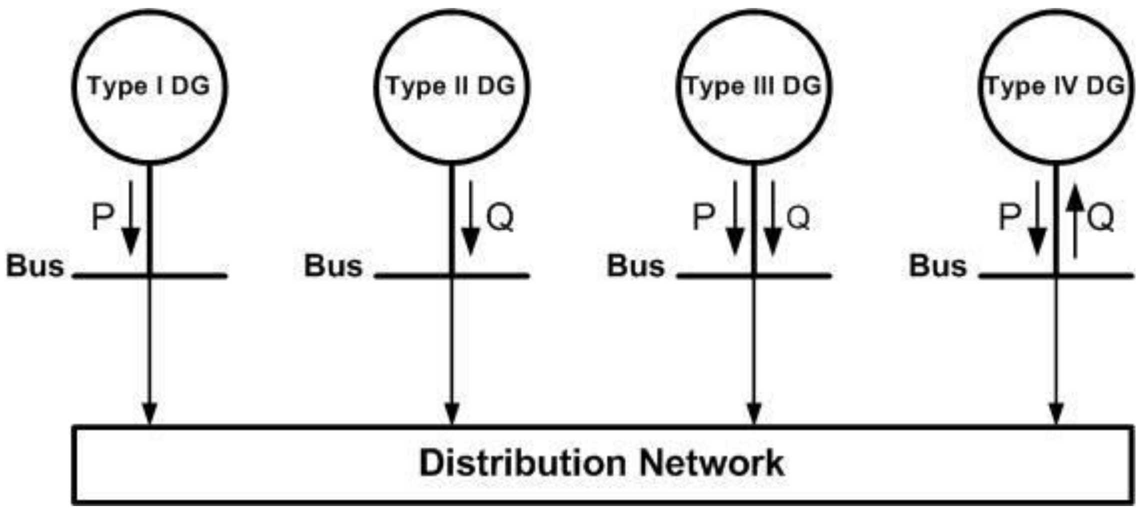


**Figure 4.1**: Types of DG

#### 4.2.1.1. Type I DG

This type of DG only injects real power in the distribution systems. Good examples of type I DG include technologies connected to the grid via a power inverter/converter such as PV, microturbines and fuel cells (Venkatesh, 2014).

- **Photovoltaic (PV) systems**: PV systems are used to harvest sunlight and convert it into electricity. The typical PV system size for residential applications is about 10kW while commercial and industrial applications may reach Megawatts of size. The energy conversion efficiency of PV systems is about 17%. This efficiency is however gradually increasing while the initial capital cost of PV systems is continuously decreasing. The installed capacity of PV systems is projected to double every couple of years.
- **Microturbines**: Microturbines are small combustion engines of size varying from 20kW – 500kW. Their combustible can be natural gas, propane or fuel oil. They operate at fast speed, lower temperature, and lower pressure than in conventional combustion

turbines (El-Khattam & Salama, 2004). Microturbines have gained widespread acceptance as a DG technology due to the advance in power electronics.

- **Fuel cells**: Fuel cells (FC) convert into electricity the chemical energy from a fuel through electrochemical reactions. They are comparable to batteries, although it is not necessary to charge them. Fuel cells produce energy as long as the fuel is supplied. Some fuel cell types include Alkaline FC (AFC), Proton Exchange Membrane FC (PEM/PEMFC), Phosphoric Acid FC (PAFC), Molten Carbonate FC (MCFC), Solid Oxide FC (SOFC) and Direct Methanol FC (DMFC) (El-Khattam & Salama, 2004).

#### 4.2.1.2. Type II DG

Type II DG only injects reactive power Q in the distribution system (Hung et al., 2010). Synchronous compensators are an excellent example of Type II DG. They are used not to produce electric power, but to improve network conditions such as the voltage profile and power factor. Typical applications of type II DG include voltage regulation and power factor correction. Although capacitor banks can inject reactive power in distribution networks, they are not considered as DG since the amount of reactive power injected into the network cannot be continuously fine-tuned.

#### 4.2.1.3. Type III DG

Type III DG can inject both the real and reactive power in the network. Good examples of type III DG technologies include cogeneration and small hydro.

- **Cogeneration/trigeneration:** Cogeneration or Combined Heat and Power (CHP) is the simultaneous generation of electricity and useful heat from fuel combustion at a power station. In small CHP plants, high-temperature steam turbines or natural gas-fired fuel cells are used to produce electricity. The waste heat from the CHP plant is harvested and used for heating of spaces, water or buildings. In trigeneration or Combined Cooling, Heat and Power (CCHP), both electricity and useful heat are also produced simultaneously. However, the harvested heat can be used for both heating and cooling.
- **Small hydro systems:** Small hydro systems are small-scale hydro turbines used to produce electricity to serve a small community. They are linked to the electrical distribution system as a low-cost renewable energy system. Their typical size varies from 1kW to 20MW.
- **Small wind turbines:** small wind turbines with synchronous generators falls under type III DG.

**Table 4.1**: Characteristics of DG technologies (Ackermann et al., 2001), (Viral & Khatod, 2012)

| Technology | DG type | Renewable | Fuel/Source | Typical size (kW) | Electrical efficiency (%) | Reliability |
|---|---|---|---|---|---|---|
| PV systems | Type I and III | Yes | Sun | 0.02-1000⁺ | ~15 - 17 | No- dependent on insolation |
| Wind | Type III and IV | Yes | Wind | 0.2-3000 | ~44 - 48 | No- dependent on the wind speed & direction |
| Biomass gasification | Type III | Yes | Biomass | 100-20000 | 15-25 | No- dependent on the speed of the conversion process |
| Small Hydro Power (SHP) | Type III | Yes | Motion of Water | 5-100000 | ~64 - 90 | Yes |
| Ocean Energy | Type III | Yes | Ocean waves, tides | 100-1000 | 20 - 35 | No- dependent on the wave's speed & tides availability |
| Geothermal | Type III | Yes | Earth internal heat | 5000-100000 | 10-32 | No |
| Reciprocating Engines | Type III | No | Petrol, Diesel, LPG, CNG | 3-6000⁺ | 30-43 | Yes |
| Combustion gas turbines | Type III | No | Coal gas, biogas, landfill, natural gas | 0.5-3000⁺ | 21-40 | Yes |
| Microturbines | Type I | No | Natural gas, propane, fuel oil | 30-1000 | 14-30 | Yes |
| Hybrid fuel cells | Type I | No | Ethanol, hydrogen, propane | 400-20000 | 30-55 | Yes |
| Small fuel cells | | No | | 1-300 | | |
| Automotive fuel cells | | No | | 30-60 | | |
| Micro-CHP | Type III | No | Natural gas, hydrogen, LPG, Biomass, Solar thermal | 1-10 | 30⁺ | Yes |

#### 4.2.1.4. Type IV DG

Type IV DG injects the real power (P) in the distribution network but absorbs reactive power (Q) from the network. Wind turbines with induction generator are good examples of type IV DG (Hung et al., 2010). The reactive power drawn from the network is used to maintain the air flux gap in the induction machine. The active power delivered is a function of the slip above the synchronous speed, and it is only produced when the speed of the generator is above the synchronous speed.

Table 4.1 provides some characteristics of diverse DG Technologies. It can be observed that not all DG technologies are renewables. Non-renewable DG technologies are more reliable than most of their renewable counterparts. This is mainly because most renewable DG are of intermittent nature. PV systems depend on the daily insolation; wind systems are dependent on the wind speed and direction, and ocean energy-based DG have a power output subjected to the sea waves speed. DG sizes vary from a handful of watts to hundredths of Megawatts.

### 4.2.2. Drivers of the DG demand in distribution networks

The advent of DG has been driven by environmental, economic and technical factors. The analysis of these factors is done below.

#### 4.2.2.1. Environmental factors

Due to environmental concerns such as environmental degradation, global warming, and ozone layer depletion, policies are being put in place to reduce the emission of greenhouse gases and mainly the carbon dioxide ($CO_2$) (Pepermans et al., 2005). These policies are the driven force behind the increased demand in DG, as power producers are forced to find more efficient and cleaner energy solutions. As opposed to conventional power plants, DG generates 30% fewer greenhouse gases (Viral & Khatod, 2012). The construction of large power plants requires a large land size. The erection of new transmission and distribution lines is subject to permitting and right of way requirements. So, the building of new centralised power plants is detrimental to ecosystems, hence the backing of Distributed Generation (Lopez et al., 2007).

#### 4.2.2.2. Economic factors

The construction of large power plants and the erection of new transmission and distribution lines are commonly associated with a high capital cost. Small units of DG can be built and installed; the construction times of DG is shorter; the cost of commissioning, operation, maintenance, and decommissioning of DG is reduced. These characteristics make DG technologies a low cost and attractive investment opportunity for investors (Lopez et al., 2007). Additionally, the shift of the energy market from a regulated to a deregulated structure give DG a competitive edge over traditional power plants.

#### 4.2.2.3. Technical factors

From the technical point of view, reliability, quality of supply, energy efficiency and load expansion considerations are the major drivers of the adoption of DG in distribution systems.

- **Reliability and quality of supply:** The electrical power delivery is subject to the power quality, i.e. maintaining sinusoidal voltages and currents within the rated frequency and magnitude margins (Dugan et al., 2012). Disruption of the quality of supply may negatively affect utilities and end-users. The introduction of DG in the distribution system may improve the stability and the quality of supply (Khalesi et al., 2010). DG can also increase the reliability of distribution systems. The reliability of a distribution network is a measure of how much interruptions or power outages the distribution system has sustained over a period. Utilities may invest in DG to increase the overall reliability of the distribution system.

- **Energy efficiency:** Depending on the technology used, optimal sizing and placement of DG in distribution systems may significantly reduce the real power losses, the reactive power losses or even both (Hung et al., 2010). Reduced power losses mean increased power delivered and consequently increased distribution system efficiency.

- **Load expansion:** proper planning of DG can reduce the power loss in distributions systems. This means that more power becomes available to supply the loads. DG can also act as a substitute for transmission and distribution lines expansion. The electricity produced by the DG allows the connection of additional customers locally without the need for erecting further transmission and distribution lines.

### 4.3. DG placement and sizing issues

DG is only beneficial if it is properly planned, installed and operated. Improper planning, installation or operation could fail to secure the projected DG benefits and could even be detrimental to the distribution systems.

The integration of DG in distribution systems faces numerous challenges:

- Distribution networks have been designed to only handle **unidirectional power flow** from utilities to consumers. A high level of DG penetration may lead to bi-directional power flows through distribution lines. This condition can create increased short-circuit levels and affects the performance of protection systems in the distribution system.
- The presence of DG in a distribution network adds the risk of **islanding**. Islanding is a situation in which a part of the distribution system is supplied by a DG, although the electrical supply from the utility gets disconnected. This situation may prove dangerous to personnel (utility workers, public) as they may not know that that part of the distribution system is still energised. Therefore, an anti-islanding system should be installed along with the DG to provide adequate safety in the event of a power outage.
- A distribution system operator (DSO) is charged with the control and the operation of distribution systems. In future smart grids, many of the DG will be customer-owned. A high number of **customer-owned DG** will be challenging to control and monitor (Jordehi, 2015).
- Some DG technologies such as PV and wind systems have an intermittent nature and are **non-dispatchable,** i.e. their output is influenced by external factors and cannot be controlled by operators.
- Some DG technologies are connected to the distribution system via power electronics interfaces such as inverters. They may contribute to the introduction of a high level of harmonics in the network. This situation may result in distorted voltage waveforms and unexpected frequency fluctuations.
- If the distribution system has low voltage (LV) levels, the integration of DG may provide voltage support to the distribution system. Otherwise, the introduction of DG may lead to voltage swells and excessive power losses.

## 4.4. Single-objective DG placement and sizing problem

The single-objective DG placement and sizing problem consists of finding the optimal bus location and DG size to minimise the real power loss of the distribution system.

This section provides the mathematical formulation of the single-objective DG placement and sizing problem, and a PSO based solution algorithm to solve that problem. The developed PSO algorithm is implemented and applied to three distribution systems, namely the IEEE 16-bus system, the IEEE 33-bus system and the IEEE 69-bus system, and the results of the problem are analysed.

### 4.4.1. Formulation of the single-objective DG placement and sizing Problem

The objective of the optimal DG placement and sizing problem is to minimise the total real power loss in the distribution system. The real power loss $\mathbf{P_{Loss}}$ in a distribution system is the sum of the real component of power loss in individual branches of the distribution system and it is given in Equation 4.1.

$$\mathbf{P_{Loss}} = \sum_{\substack{\mathbf{j=1} \\ \mathbf{k=1} \\ \mathbf{j \neq k}}}^{\mathbf{NB}} \mathbf{real}\left(\mathbf{S_{jk}} - \mathbf{S_{kj}}\right) \tag{4.1}$$

where

$\mathbf{S_{jk}} = \mathbf{V_j} \times \mathbf{i_{jk}}^*$ is the sending power in the branch $\mathbf{j - k}$.

$\mathbf{S_{kj}} = \mathbf{V_k} \times \mathbf{i_{jk}}^*$ is the receiving power in the branch $\mathbf{j - k}$.

$\mathbf{V_j}$ and $\mathbf{V_k}$ are the sending and receiving ends voltage of line $\mathbf{j - k}$ respectively.

$\mathbf{i_{jk}}^*$ is the conjugate of the current flow in line $\mathbf{j - k}$.

$\mathbf{j}$ is the sending bus.

$\mathbf{k}$ is the receiving bus.

$\mathbf{NB}$ is the number of busses in the network.

### 4.4.2. Solution algorithm for the single-objective DG placement and sizing problem

The solution procedure of the DG placement and sizing problem takes into consideration the following assumptions:

- DG can only be installed at PQ nodes, and any DG type can be installed at a given PQ bus.
- Only one DG can be installed at a given PQ node at the time.
- The number of DG that can be installed in the network is only limited by the number of PQ buses. This means that for a distribution network with 10 PQ buses, it has ten candidate nodes for a single DG installation.
- The DG size should be limited. The sum of the DGs capacity should be less than the total load demand. Should the DG size be equal to the load demand, then the loads would be supplied locally by DG. This means that all the power generated by the DG to be consumed locally.

The **DG placement sub-problem** is treated as a **discrete problem** while the **DG sizing sub-problem** is treated as **a continuous problem**. The developed solution algorithm is referred to as a hybrid discrete-continuous PSO algorithm. The discrete PSO is used to find the optimal location for the DG placement, and the continuous PSO is used to find the optimal size of the DG. The details about these 2 PSO variants (discrete and continuous) have been given in chapter three (refer to sections 3.3.1. and 3.2.1. respectively).

The PSO based solution algorithm for the single-objective DG placement and sizing problem is implemented as per the following steps:

**Step 1:** Read the distribution system network data such as the number of nodes $\mathbf{NB}$, the number of distribution lines $\mathbf{NL}$, the number of tie lines $\mathbf{NT}$, the bus type ($\mathbf{Slack}, \mathbf{PV}, \mathbf{PQ}$), the load data ($\mathbf{Pd}, \mathbf{Qd}, \mathbf{Bs}, \mathbf{Load_{ID}}$), the generator data ($\mathbf{Pg}, \mathbf{Qg}$), the distribution line data ($\mathbf{bus_i}, \mathbf{bus_j}, \mathbf{r}, \mathbf{x}, \mathbf{sw_{tie}}, \mathbf{sw_{sec}}$) and the DG limit coefficients ($\mathbf{k1}, \mathbf{k2}$).

**Step 2**: Initialize the binary PSO parameters such as the acceleration coefficients $\mathbf{c1}$ and $\mathbf{c2}$, the minimum and the maximum inertia weight ($\mathbf{w_{min}}$ and $\mathbf{w_{max}}$ respectively), the particle's velocity limits ($\mathbf{v_{min}}$ and $\mathbf{v_{max}}$), the number of particles ($\mathbf{Np}$), the dimension of the search space ($\mathbf{D}$) which is equal to the number of PQ buses in the network, and the stop criterions ($\mathbf{t_{1max}}, \mathbf{t_{2max}}$). $\mathbf{t_{1max}}$ and $\mathbf{t_{2max}}$ are used to stop the discrete and continuous PSO search process respectively.

**Step 3:** Initialize the particles' positions. Two swarms are used in the search process:

- Swarm 1 to find the optimal DG location
- Swarm 2 to find the optimal DG size.

The 16-bus distribution system in Figure 3.3 is used to illustrate the coding of the DG status in the distribution network into a string of bit as shown in Table 4.2.

**Table 4.2: DG status of the IEEE 16-bus distribution system**

| **Bus type** | **Slack** | | | **PQ** | | | | | | | | | | | | |
|---|---|---|---|---|---|---|---|---|---|---|---|---|---|---|---|---|
| Bus ID | 1 | 2 | 3 | 4 | 5 | 6 | 7 | 8 | 9 | 10 | 11 | 12 | 13 | 14 | 15 | 16 |
| DG status | – | – | – | 0 | 0 | 0 | 0 | 0 | 0 | 0 | 0 | 0 | 0 | 0 | 0 | 0 |

0 indicates that there is no DG connected to the corresponding PQ bus, and 1 indicates the presence of DG. Initially, there is no DG in the 16-bus distribution system, and that is why there are no 1's in the DG status in Table 4.2. In the first swarm (Swarm 1), a particle's position is the string of bits that represent the DG status in the distribution network. For the 16-bus distribution system, there is initially no DG in the network. So, a particle position can be represented by $\mathbf{x_1}^{\mathbf{k}} = [\mathbf{0} \quad \mathbf{0} \quad \mathbf{0} \quad \mathbf{0} \quad \mathbf{0} \quad \mathbf{0} \quad \mathbf{0} \quad \mathbf{0} \quad \mathbf{0} \quad \mathbf{0} \quad \mathbf{0} \quad \mathbf{0} \quad \mathbf{0}]$, where $\mathrm{k} = 0$ for the initial particle position

Bus 1, 2 and 3 are not PQ buses, so they are omitted when assigning the particle's position $\mathbf{x_1}^{\mathbf{0}}$. So, only the DG status at PQ buses are used when assigning particles in the first swarm. Swarm 1 is a $\mathbf{Np} \times \mathbf{D}$ matrix, where $\mathbf{Np}$ is the number of particles in the swarm and $\mathbf{D}$ the dimension of the search space.

The developed algorithm doesn't discriminate against the type of DG to be used. This means that all DG types are considered, and the DG size is defined by Equation 4.2.

$$\mathbf{S_{DG} = P_{DG} + j.Q_{DG}} \tag{4.2}$$

Where

$\mathbf{S_{DG}}$ is the apparent power of the DG.

$\mathbf{P_{DG}}$ is the real power of the DG.

$\mathbf{Q_{DG}}$ is the reactive power of the DG.

- If $\mathbf{P_{DG} = 0}$, then the DG is of Type II.
- If $\mathbf{Q_{DG} = 0}$, then the DG is of Type I.
- If $\mathbf{P_{DG} > 0}$ & $\mathbf{Q_{DG} > 0}$, then the DG is of Type III.
- If $\mathbf{P_{DG} > 0}$ & $\mathbf{Q_{DG} < 0}$, then the DG is of Type IV.

The maximum DG size $\mathbf{DG_{max}}$ should be less than the total load demand. So, the DG size is limited to the interval $[\mathbf{DG_{min}}, \mathbf{DG_{max}}]$, with $\mathbf{DG_{min}}$ and $\mathbf{DG_{max}}$ defined as in Equation 4.3.

$$\mathbf{DG_{max} < k_1 \times \sum_{i=1}^{nPQ} (P_{di} + jQ_{di})} \tag{4.3.a}$$

$$\mathbf{DG_{min} > k_2 \times \sum_{i=1}^{nPQ} (-j.Q_{di})} \tag{4.3.b}$$

Where

$\mathbf{DG_{min}}$ is the minimum DG size.

$\mathbf{P_{di}}$ and $\mathbf{Q_{di}}$ are the real and reactive power demand respectively at load bus $\mathbf{i}$.

$\mathbf{n_{PQ}}$ is the number of load buses in the distribution network.

$\mathbf{k_1}$ and $\mathbf{k_2}$ are the maximum and minimum DG size limit coefficients respectively.

The DG size limit coefficients represent the penetration levels of the DG in the distribution system.

A particle in the second swarm (Swarm 2) is defined by $\mathbf{x_2}^{\mathbf{0}} = \left[\mathbf{S_{DG_1}}, \mathbf{S_{DG_2}}, \cdots \mathbf{S_{DG_{nPQ}}}\right]$. Swarm 2 is a $\mathbf{Np} \times \mathbf{nDG}$ matrix, where $\mathbf{nDG}$ is the number of DG to be installed in the network.

**Step 4:** Initialize the particles' velocity. The velocity of the first swarm represents the probability for each bit in the particle's position (DG status) to change its status. The velocity in the second swarm represents the rate of change of the particles from their current position to the next position. The velocity in the first swarm is limited to the interval $[-4,\ 4]$ (refer to section 3.3.1.). The velocity in swarm 2 is limited in the interval $[\mathbf{v_{min}}, \mathbf{v_{max}}]$, where $\mathbf{v_{min}}$ and $\mathbf{v_{max}}$ are calculated using Equations 4.4.a and 4.4.b respectively:

$$\mathbf{v_{min}} = -\mathbf{v_{max}} \tag{4.4.a}$$

$$\mathbf{v_{max}} = \boldsymbol{\varepsilon} \times (\mathbf{DG_{max}} - \mathbf{DG_{min}}) \tag{4.4.b}$$

Where,

$\boldsymbol{\varepsilon}$ is a random number in the range ]0,1], and representing the maximum velocity limit factor.

**Step 5:** Find the personal best particles position. The initial personal best position of all particles in swarm 1 corresponds to the string of binary bits representing the DG status a corresponding PQ bus. Initially, there is no DG in the distribution system. So, the initial personal best for all particles in the swarm 2 correspond to the $\mathrm{nDG} \times 1$ matrix whose elements are all zeroed. Initially, all particles have the same objective value, which is equal to the real power loss in the base distribution system.

**Step 6:** Find the global best particle position from the set of particles best position given in Step 5. In this case, the global best particle position is the best particle position whose objective value is minimal.

**Step 7:** Give random DG position(s) for every particle in swarm 1 and the corresponding DG size(s) in swarm 2.

**Start the discrete PSO iteration process** and set the iteration counter $\mathbf{t_1}$ to 1 for the discrete PSO.

**Step 8:** Check that each particle in swarm 1 for which the real power loss should be calculated only has $\mathbf{nDG}$ active distributed generator(s).

**Start the continuous PSO search process** and set the iteration counter $\mathbf{t_2}$ to 1 for the continuous PSO.

**Step 9:** Update the generator data. After analysis of the DG position, the generator data must be updated to include the DG location and size. For the candidate DG position and size solution to be evaluated, find the position of the DG by analysing for which bus ID the DG status is equal to 1. Then, find the corresponding DG size from swarm 2 and update the distribution network generator parameters.

**Step 10:** Perform a Newton-Raphson power flow and calculate the real power loss using Equation 4.1 for the particles in swarm 1.

**Step 11:** Update the personal best position of all particles in swarm 2 as per Equation 3.23 in chapter three, section 3.4.2.

$$\mathbf{Pbest_i}^{\mathbf{t+1}} = \begin{cases} \mathbf{Pbest_i}^{\mathbf{t}}, & \mathbf{if\ fitness_i}^{\mathbf{t+1}} \geq \mathbf{fitness_{Pbest_i}}^{\mathbf{t}} \\ \mathbf{x_i}^{\mathbf{t+1}}, & \mathbf{otherwise} \end{cases}$$

Where

$\mathbf{Pbest_i}^{\mathbf{t}}$ is the personal best position of particle $\boldsymbol{i}$ at iteration $\boldsymbol{t}$.

$\mathbf{x_i}^{\mathbf{t+1}}$ is the position of particle $\boldsymbol{i}$ at iteration $\boldsymbol{t+1}$.

$\mathbf{fitness_i}^{\mathbf{t+1}}$ is the fitness value of particle $\boldsymbol{i}$ at iteration $\boldsymbol{t+1}$.

$\mathbf{fitness_{Pbest_i}}^{\mathbf{t}}$ is the fitness value of $\mathbf{Pbest_i}^{\mathbf{t}}$.

**Step 12:** Update the global best position of swarm 2 as per Equation 3.24 in chapter three, section 3.4.2.

$$\mathbf{Gbest}^{\mathbf{t+1}} = \begin{cases} \mathbf{Gbest}^{\mathbf{t}}, & \mathbf{if\ fitness_{Pbest_i}}^{\mathbf{t+1}} \geq \mathbf{fitness_{Gbest}}^{\mathbf{t}} \\ \mathbf{Pbest_i}^{\mathbf{t+1}}, & \mathbf{otherwise} \end{cases}$$

Where

$\mathbf{Gbest}^{\mathbf{t+1}}$ is the global best solution of the swarm at iteration $\boldsymbol{t+1}$.

$\mathbf{fitness_{Gbest}}^{\mathbf{t}}$ is the fitness value of $\mathbf{Gbest}$ at iteration $\mathbf{t}$.

**Step 13:** Calculate the inertia weight using Equation 3.6 and update the velocity of all particles in swarm 2 as per Equation 3.5.

$$\mathbf{v_i^{k+1} = \omega * v_i^k + c1 * rand1 * \left(Pbest_i - x_i^k\right) + c2 * rand2 * \left(Gbest_i - x_i^k\right)}$$

**Step 14:** Update the position of particles in swarm 2 as per Equation 3.3.

$$\mathbf{x_i^{k+1} = x_i^k + v_i^{k+1}}$$

Where

$\mathbf{x_i^k}$ denotes the position of particle $\boldsymbol{i}$ at iteration $\boldsymbol{k}$**.**

$\mathbf{v_i^k}$ is the velocity of the particle $\mathbf{i}$ at iteration $\boldsymbol{k}$**.**

**Step 15:** Increment the iteration count of the continuous PSO search process and repeat step 9 to step 14 until the stopping criterion is reached.

**Step 16:** Find the real power loss of the particles in swarm 1.
The global best position of the swarm 2 is achieved at the end of the continuous PSO, and it corresponds to the optimal DG size for the DG position from step 8. Consequently, the fitness of the particle in swarm 1 from step 8 is equal to the fitness of the global best position of swarm 2.

**Step 17:** Update the personal best positions in swarm 1 as per Equation 3.23.

**Step 18:** Update the global best in swarm 1 as per Equation 3.24.

**Step 19:** Calculate the inertia weight using Equation 3.6 and update the velocity of all particles in swarm 1 as per Equation 3.5.

**Step 20:** Update the position of the particles in swarm 1 as per Equation 3.9.

$$\mathbf{x_i^k = \begin{cases} 1 & \text{if } r < sig\left(v_i^k\right) \\ 0 & \text{if } r \geq sig\left(v_i^k\right) \end{cases}}$$

Where

$\mathbf{r}$ is a uniformly distributed random number in the interval [0,1]

$\mathbf{sig}$ is a sigmoid function defined by $\mathbf{sig(\alpha) = \frac{1}{1+e^{-\alpha}}}$

**Step 21**: Set the iteration count $t_2$ for the continuous PSO search process to 0 to allow step 7 to step 14 to be repeated for the next iteration of the discrete search process.

**Step 22**: Increment the iteration count $t_1$ of the discrete PSO process and repeat step 6 to step 20 until the stopping criterion is reached.

**Step 23:** Print the results of the search process such as the global best solution (optimal DG position and size), and its corresponding fitness value (minimum real power loss).

The flowchart diagram of the above-defined solution algorithm for the single-objective optimal DG placement and sizing problem is shown in Figure 4.2.

### 4.4.3. Results of the PSO solution algorithm for the single-objective DG placement and sizing problem

Three distribution systems are used to evaluate and test the developed single-objective algorithm used to solve the optimal DG placement and sizing problem:

- The IEEE 16-bus distribution system
- The IEEE 33-bus distribution system
- The IEEE 69-bus distribution system.

For each distribution system, 3 case studies are performed:

- single DG placement and sizing
- Two DG placement and sizing
- Three DG placement and sizing.

The performance of the developed PSO algorithm is analysed for each case study in terms of optimal DG type, optimal DG placement, and DG size. The effects of the introduction of the DG on the distribution network's voltage profile and power loss is also examined.

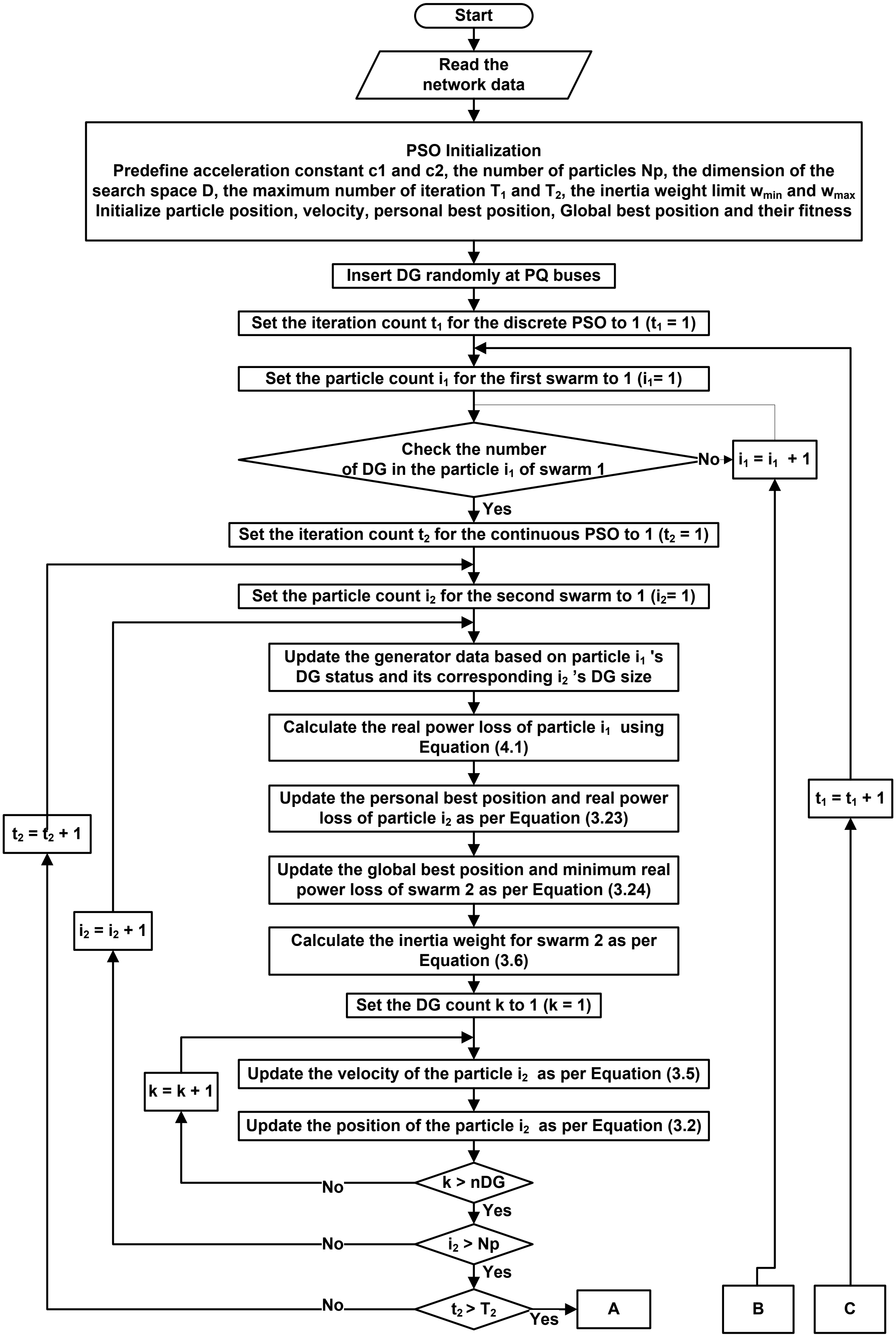
Start
Read the network data
PSO Initialization
Predefine acceleration constant c1 and c2, the number of particles Np, the dimension of the search space D, the maximum number of iteration $T_1$ and $T_2$, the inertia weight limit $w_{min}$ and $w_{max}$
Initialize particle position, velocity, personal best position, Global best position and their fitness
Insert DG randomly at PQ buses
Set the iteration count $t_1$ for the discrete PSO to 1 ($t_1$ = 1)
Set the particle count $i_1$ for the first swarm to 1 ($i_1$= 1)
Check the number of DG in the particle $i_1$ of swarm 1
No
$i_1 = i_1 + 1$
Yes
Set the iteration count $t_2$ for the continuous PSO to 1 ($t_2$ = 1)
Set the particle count $i_2$ for the second swarm to 1 ($i_2$= 1)
Update the generator data based on particle $i_1$'s DG status and its corresponding $i_2$'s DG size
Calculate the real power loss of particle $i_1$ using Equation (4.1)
Update the personal best position and real power loss of particle $i_2$ as per Equation (3.23)
Update the global best position and minimum real power loss of swarm 2 as per Equation (3.24)
Calculate the inertia weight for swarm 2 as per Equation (3.6)
Set the DG count k to 1 (k = 1)
Update the velocity of the particle $i_2$ as per Equation (3.5)
Update the position of the particle $i_2$ as per Equation (3.2)
k > nDG
No
k = k + 1
Yes
$i_2$ > Np
No
$i_2 = i_2 + 1$
Yes
$t_2 > T_2$
No
$t_2 = t_2 + 1$
Yes
A
B
C
$t_1 = t_1 + 1$

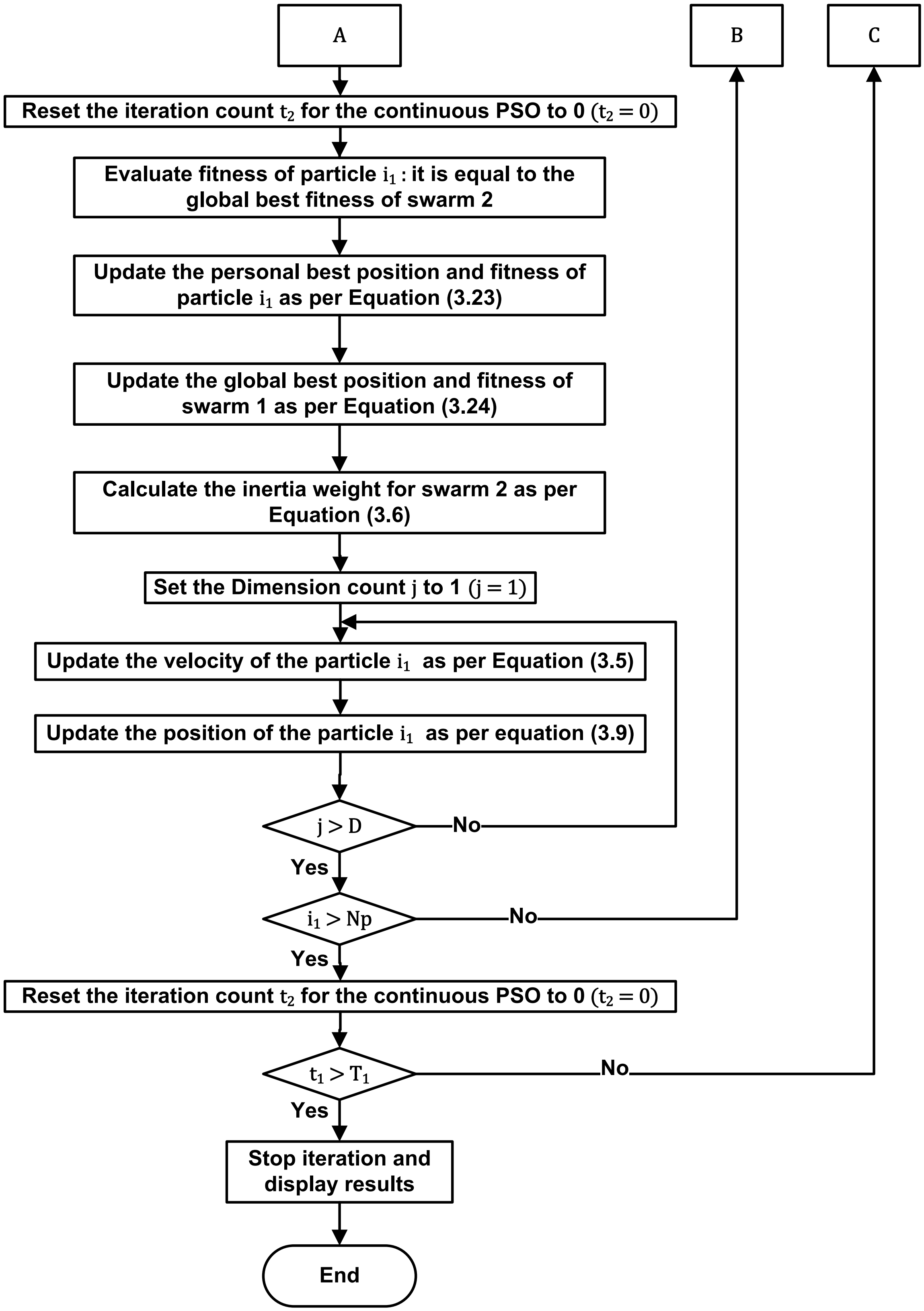


**Figure 4.2**: Flowchart of the developed PSO algorithm for the single-objective DG placement and sizing problem

#### 4.4.3.1. Simulation results of the IEEE 16-bus distribution system

The developed PSO algorithm is used to solve the single-objective DG placement and sizing problem in the IEEE 16-bus distribution system. The parameters of the 16-bus distribution system are given in **Appendix A**.

##### a. Case 1: Single DG placement and sizing problem

The developed PSO algorithm for the single-objective optimal DG placement and sizing problem is applied to the 16-bus distribution system. The solution of the PSO algorithm provides the best location and size for a single DG placement and sizing problem. The simulation results are compiled in Table 4.3.

**Table 4.3**: **Simulation results for the single DG placement and sizing problem of the 16-bus distribution system**

| Simulation results | Before DG placement | After DG placement |
| --- | --- | --- |
| Total generation capacity in ($\mathrm{MVA}$) | $29.2140 + j6.9407$ | $15.8172 + j4.4765$ |
| Transformer power supply in ($\mathrm{MVA}$) | $8.5830 + j2.9790$ @bus 1<br><br>$15.4901 + j3.9667$ @bus 2<br><br>$5.1409 - j0.0050$ @bus 3 | $8.5830 + j2.9790$ @bus 1<br><br>$2.0934 + j1.5025$ @bus 2<br><br>$5.1409 - j0.0050$ @bus 3 |
| Power loss in ($\mathrm{kW}$) | 514.0293 | 162.8352 |
| Power loss reduction (%) | – | 68.3218 |
| Minimum voltage in ($\mathrm{p.u}$) | 0.9682 @bus 12 | 0.9848 @bus 7 |
| Maximum voltage in ($\mathrm{p.u}$) | 1 @ bus 1, 2 & 3 | 1.0007 @bus 9 |
| No of DG | 0 | 1 |
| Optimal DG size ($\mathrm{MVA}$) & location | – | $13.0456 + j1.7526$ @bus 9 |

The simulation results show that for a single DG placement in the 16-bus distribution system, the optimal location is at **bus 9** and the optimal size of the DG is $(\mathbf{13.0456 + j1.7526})$ **MVA**. After DG placement at **bus 9**, the real power loss is reduced to $\mathbf{162.8352\ kW}$ from $\mathbf{514.0293\ kW}$. A power loss reduction of $\mathbf{68.3218}\%$ is achieved after the placement of the obtained single DG in the 16-bus distribution system. The power loss reduction ($\%\mathbf{Ploss}$) is calculated using Equation 4.5. The simulation results also indicate an improvement of the voltage profile of the 16-bus distribution system after DG placement as shown in Figure 4.3. Before the DG placement, the minimum voltage was $\mathbf{0.9682\ p.u}$ at **bus 12**. It is improved to $\mathbf{0.9848\ p.u}$ at **bus 7** after the single DG placement in the 16-bus distribution system.

$$\%\mathbf{Ploss} = \frac{\mathbf{Ploss_{After\ reconfiguration}} - \mathbf{Ploss_{Before\ reconfiguration}}}{\mathbf{Ploss_{Before\ reconfiguration}}} \times \mathbf{100}\% \tag{4.5}$$

Where

$\%\mathbf{Ploss}$ is the power loss reduction in percent (**%**).

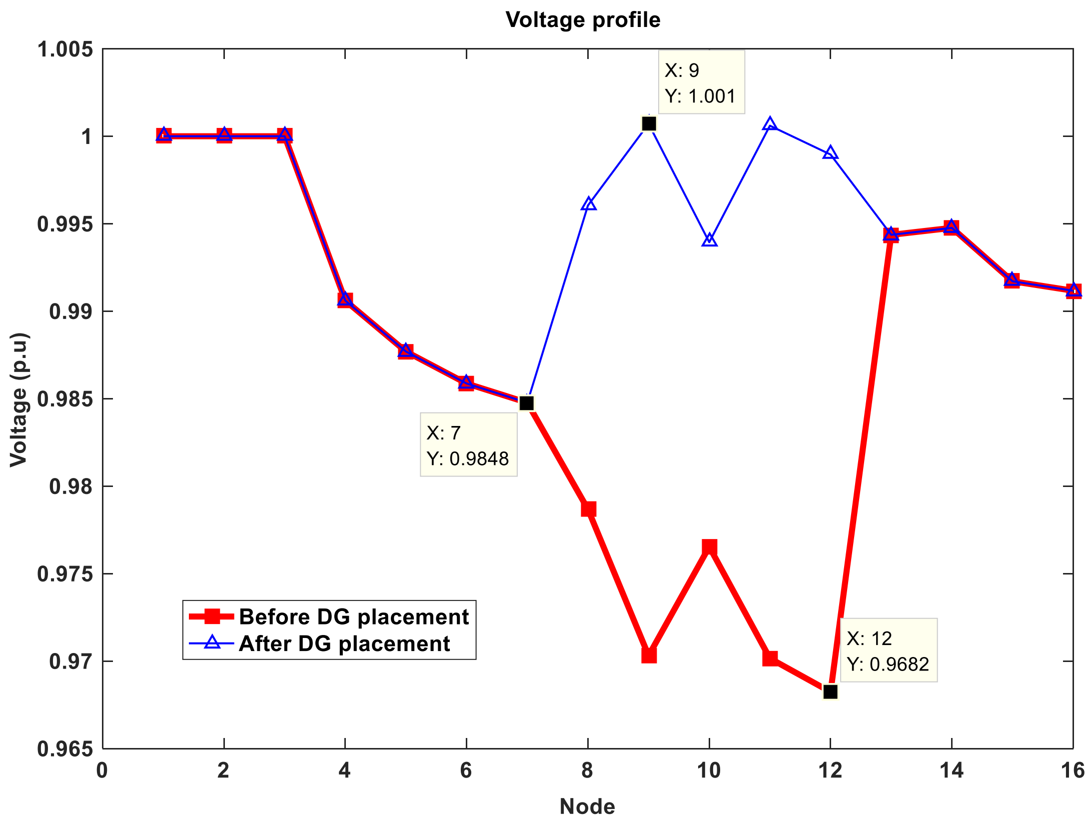


**Figure 4.3**: **Voltage profile of the 16-bus distribution system before and after single DG placement at bus 9**

## b. Case 2: Two DG placement and sizing problem

The developed PSO algorithm for the single-objective optimal DG placement and sizing problem is applied to the 16-bus distribution system to determine the optimal locations to place two DG in the network and to find the optimal size of these two DG. The simulation results are compiled in Table 4.4.

The simulation results indicate that for two DG placement in the 16-bus distribution system, the optimal locations are at **bus 4** and **bus 9**. The optimal sizes of the DG are: $(\mathbf{8.5440 + J2.8834})\ \mathbf{MVA}$ for the DG at **bus 4** and $(\mathbf{13.0456 + j1.7526})\ \mathbf{MVA}$ for the DG at bus 9. After placement of the two DG at **bus 4** and at **bus 9** respectively, the real power loss is reduced from $\mathbf{514.0293\ kW}$ to $\mathbf{100.4816\ kW}$. This corresponds to a real power loss reduction of $\mathbf{80.4522}\%$.

**Table 4.4**: Simulation results for two DG placement and sizing problem of the 16-bus distribution system

| **Simulation results** | **Before DG placement** | **After DG placement** |
|---|---|---|
| Total generation capacity in (MVA) | $29.2140 + j6.9407$ | $7.2109 + j1.4663$ |
| Transformer power supply in (MVA) | $8.5830 + j2.9790$ @bus 1<br>$15.4901 + j3.9667$ @bus 2<br>$5.1409 - j0.0050$ @bus 3 | $-0.0234 - j0.0312$ @bus 1<br>$2.0933 + j1.5025$ @bus 2<br>$5.1409 - j0.0050$ @bus 3 |
| Power loss in (kW) | 514.0293 | 100.4816 |
| Power loss reduction (%) | – | 80.4522 |
| Minimum voltage in (p.u) | 0.9682 @bus 12 | 0.9912 @bus 16 |
| Maximum voltage in (p.u) | 1 @bus 1, 2 & 3 | 1.0007 @bus 9 |
| No of DG | 0 | 2 |
| Optimal DG size in (MVA) & locations | – | $8.5440 + J2.8834$ @bus 4<br>$13.0456 + j1.7526$ @bus 9 |

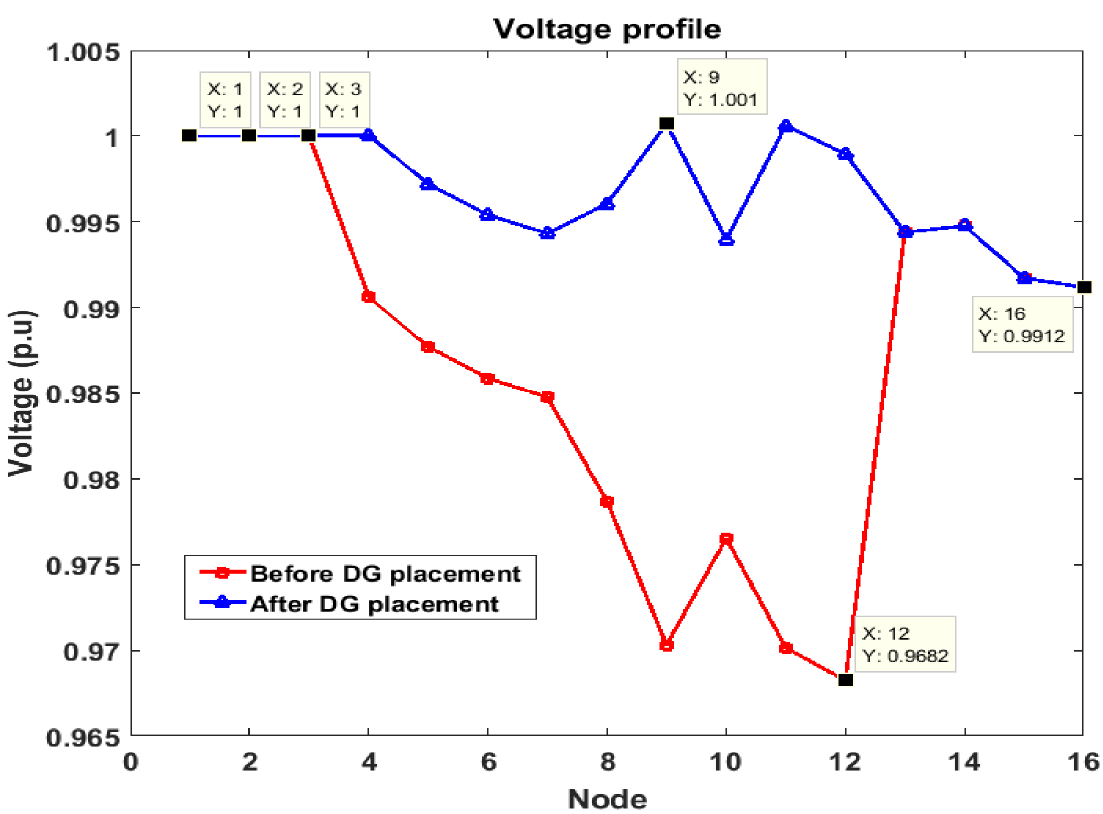


**Figure 4.4**: Voltage profile of the 16-bus distribution network before and after optimal placement of two DG (at buses 4 and 9)

Further analysis of the simulation results shows an improvement of the voltage profile of the 16-bus distribution system after placement of the two DG. As shown in Figure 4.4, Before the DG placement, the minimum voltage in the distribution system was $\mathbf{0.9682\ p.u}$ at **bus 12**. After the placement of the two DG, the minimum voltage is $\mathbf{0.9912\ p.u}$ at **bus 16**.

### c. Case 3: Three DG placement and sizing problem

The developed PSO algorithm for the single-objective optimal DG placement and sizing problem is applied to the 16-bus distribution system to determine the optimal locations to place three DG in the network and to find the optimal size of these three DG. The simulation results are compiled in Table 4.5.

**Table 4.5**: **Simulation results for the three DG placement and sizing problem of the 16-bus distribution system**

| Simulation results | Before DG placement | After DG placement |
|---|---|---|
| Total generation capacity in (MVA) | $29.2140 + j6.9407$ | $3.2889 + j1.5265$ |
| Transformer power supply in (MVA) | $8.5830 + j2.9790$ @bus 1<br><br>$15.4901 + j3.9667$ @bus 2<br><br>$5.1409 - j0.0050$ @bus 3 | $-0.0234 - j0.0312$ @bus 1<br><br>$2.0933 + j1.5025$ @bus 2<br><br>$1.2189 + j0.0551$ @bus 3 |
| Power loss in (kW) | 514.0293 | 65.1744 |
| Power loss reduction (%) | – | 87.3209 |
| Minimum voltage in (p.u) | 0.9682 @bus 12 | 0.9939 @bus 10 |
| Maximum voltage in (p.u) | 1 @bus 1, 2 & 3 | 1.0007 @bus 9 |
| No of DG | 0 | 3 |
| Optimal DG size in (MVA) & locations | – | $8.5440 + J2.8834$ @bus 4<br><br>$13.0456 + j1.7526$ @bus 9<br><br>$3.8867 - j0.1449$ @bus16 |

The simulation results indicate that for three DG placement in the 16-bus distribution system, the optimal locations are at bus 4, bus 9 and bus 16. The optimal sizes of the DG are: $(\mathbf{8.5440 + J2.8834})\ \mathbf{MVA}$ for the DG at **bus 4**, $(\mathbf{13.0456 + j1.7526})\ \mathbf{MVA}$ for the DG at **bus 9**, and $(\mathbf{3.8867 - j0.1449})\ \mathbf{MVA}$ at **bus 16**. After placement of the three DG at **bus 4**, at **bus 9** and at **bus 16** respectively, the real power loss is reduced from

$\mathbf{514.0293\ kW}$ to $\mathbf{65.1744\ kW}$. This corresponds to a real power loss reduction of $\mathbf{87.3209\%}$.

Further analysis of the simulation results shows an improvement of the voltage profile of the 16-bus distribution system after placement of the three DG. As shown in Figure 4.5, Before the DG placement, the minimum voltage in the distribution system was $\mathbf{0.9682\ p.u}$ at **bus 12**. After the placement of the two DG, the minimum voltage is $\mathbf{0.9939\ p.u}$ at **bus 10**.

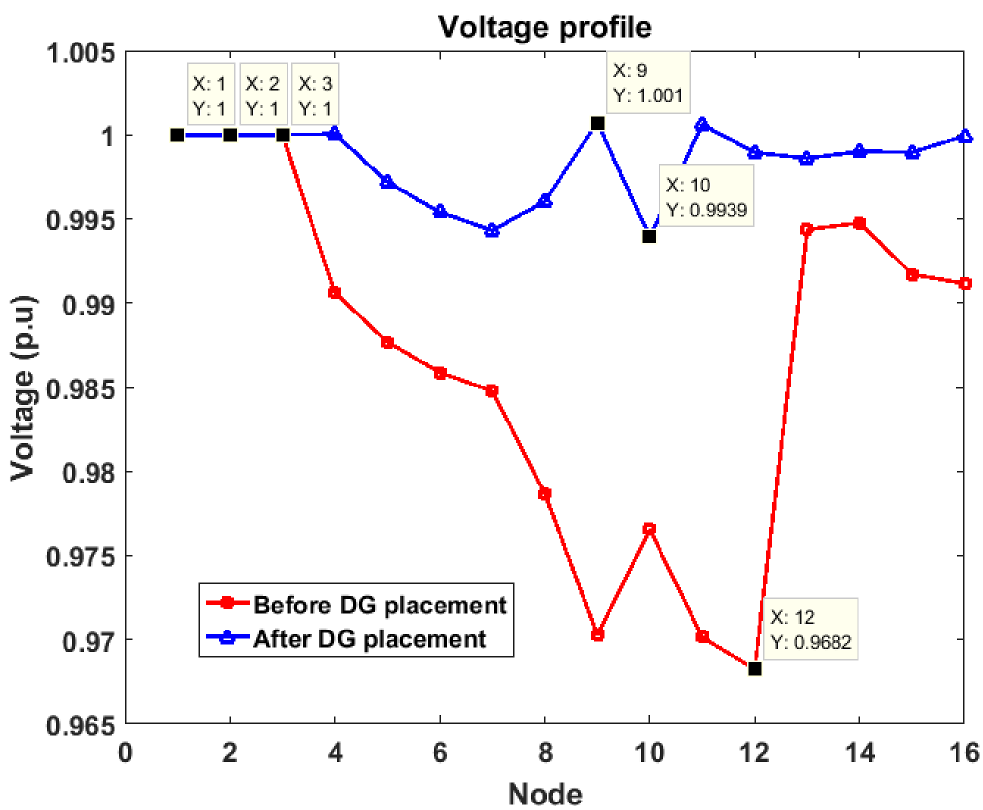


**Figure 4.5**: **Voltage profile of the 16-bus distribution network before and after optimal placement of three DG**

### 4.4.3.2. IEEE 33-bus distribution system results

The developed PSO algorithm is used to solve the single-objective DG placement and sizing problem in the IEEE 33-bus distribution system. The parameters of the 33-bus distribution system are given in **Appendix B**.

#### a. Case 1: Single DG placement and sizing problem

The developed PSO algorithm for the single-objective optimal DG placement and sizing problem is applied to the 33-bus distribution system. The solution of the PSO algorithm provides the best location and size for a single DG placement and sizing problem. The simulation results are compiled in Table 4.6.

**Table 4.6**: **Simulation results for the single DG placement and sizing problem of the 33-bus distribution system**

| Simulation results | Before DG placement | After DG placement |
|---|---|---|
| Transformer power supply in (MVA) | 3.9234 + j2.4117 @bus 1 | 1.2243 + j0.6099 @bus 1 |
| Power loss in (kW) | 208.4322 | 67.9575 |
| Power loss reduction (%) | – | 67.3959 |
| Minimum voltage in (p.u) | 0.9108 @bus 18 | 0.9573 @bus 18 |
| Maximum voltage in (p.u) | 1 @bus 1 | 1.0005 @bus 6 |
| No of DG | 0 | 1 |
| Optimal DG size in (MVA) & location | – | 2.5586 + j1.7440 @bus 6 |

The simulation results show that for a single DG placement in the 33-bus distribution system, the optimal location is at bus 6 and the optimal size of the DG is $(\mathbf{2.5586 + j1.7440})$ $\mathbf{MVA}$. After DG placement at bus 6, the real power loss is reduced to $\mathbf{67.9575\ kW}$ from $\mathbf{208.4322\ kW}$. A power loss reduction of $\mathbf{67.3959\%}$ is achieved after the placement of the obtained single DG in the 33-bus distribution system.

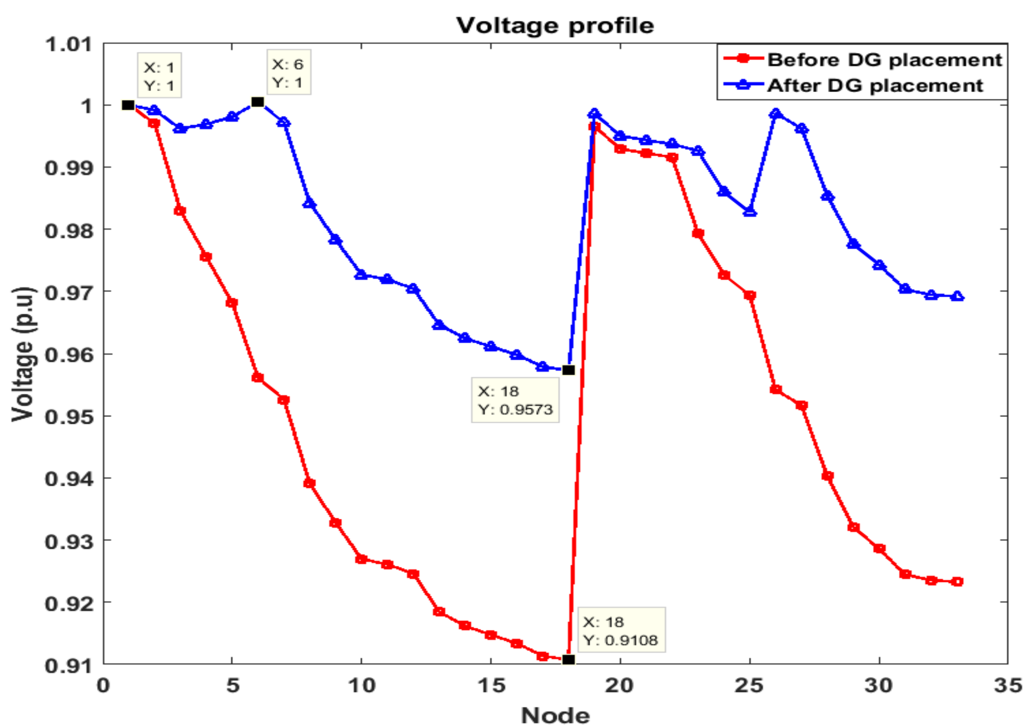


**Figure 4.6**: **Voltage profile of the 33-bus distribution network before and after the optimal placement of a single DG**

The simulation results also indicate an improvement of the voltage profile of the 33-bus distribution system after DG placement as shown in Figure 4.6. Before the DG placement, the minimum voltage was $\mathbf{0.9108\ p.u}$ at **bus 18**. It is improved to $\mathbf{0.9573\ p.u}$ after the single DG placement in the 33-bus distribution system.

**b. Case 2: Two DG placement and sizing problem**

The developed PSO algorithm for the single-objective optimal DG placement and sizing problem is applied to the 33-bus distribution system to determine the optimal locations to place two DG in the network and to find the optimal size of these two DG. The simulation results are compiled in Table 4.7.

**Table 4.7**: **Simulation results for two DG placement and sizing problem of the 33-bus distribution system**

| Simulation results | Before DG placement | After DG placement |
|---|---|---|
| Transformer power supply in (MVA) | $3.9234 + j2.4117$ @bus 1 | $1.7601 + j0.8587$ @bus 1 |
| Power loss in ($\mathrm{kW}$) | 208.4322 | 28.5018 |
| Power loss reduction (%) | – | 86.3256 |
| Minimum voltage in ($\mathrm{p.u}$) | 0.9108 @bus 18 | 0.9803 @bus 25 |
| Maximum voltage in ($\mathrm{p.u}$) | 1 @bus 1 | 1.0011 @bus 30 |
| No of DG | 0 | 2 |
| Optimal DG size in ($\mathrm{MVA}$) & location | – | $0.8456 + j0.3985$ @bus 13<br>$1.1378 + j1.0633$ @bus 30 |

The simulation results indicate that for two DG placement in the 33-bus distribution system, the optimal locations are at **bus 13** and **bus 30**. The optimal sizes of the DG are: $(\mathbf{0.8456 + j0.3985})\ \mathbf{MVA}$ for the DG at **bus 13** and $(\mathbf{1.1378 + j1.0633})\ \mathbf{MVA}$ for the DG at **bus 30**. After placement of the two DG at **bus 13** and at **bus 30** respectively, the real power loss is reduced from $\mathbf{208.4322\ kW}$ to $\mathbf{28.5018\ kW}$. This corresponds to a real power loss reduction of $\mathbf{86.3256}\%$. Further analysis of the simulation results shows an improvement of the voltage profile of the 33-bus distribution system after placement of the two DG. As shown in Figure 4.7, Before the DG placement, the minimum voltage in the distribution system was $\mathbf{0.9108\ p.u}$ at **bus 18**. After the placement of the two DG, the minimum voltage is $\mathbf{0.9803\ p.u}$ at **bus 25**.

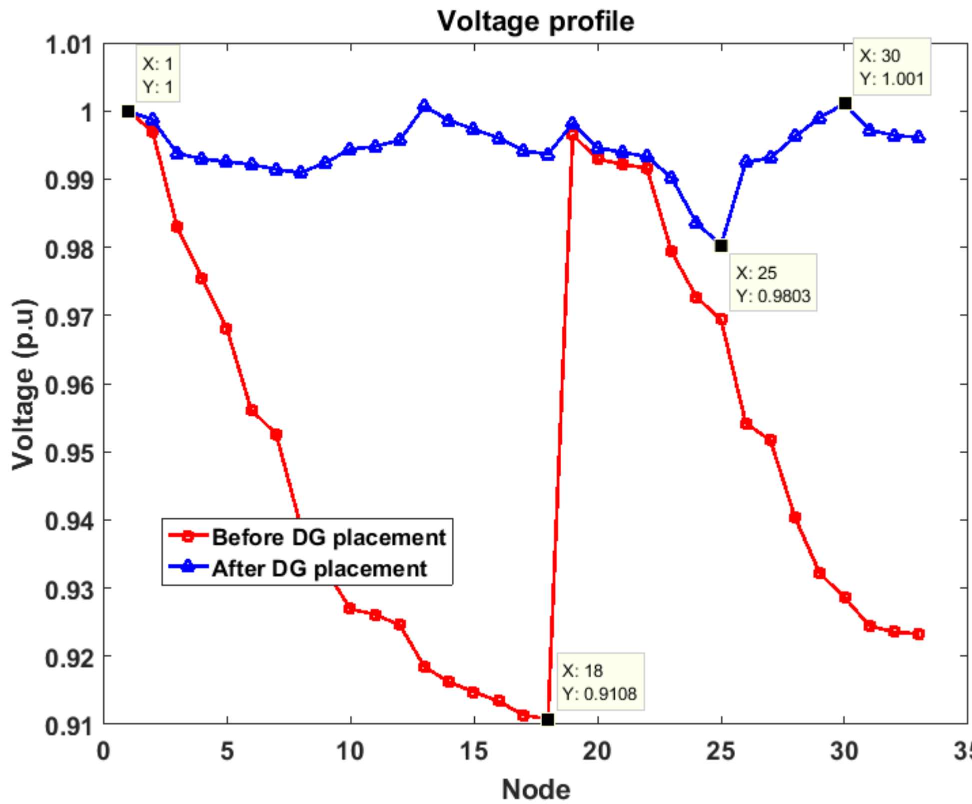


**Figure 4.7**: **Voltage profile of the 33-bus distribution network before and after the optimal placement of two DG**

**c. Case 3: Three DG placement and sizing problem**

The developed PSO algorithm for the single-objective optimal DG placement and sizing problem is applied to the 33-bus distribution system to determine the optimal locations to place three DG in the network and to find the optimal size of these three DG. The simulation results are compiled in Table 4.8. The simulation results indicate that for three DG placement in the 33-bus distribution system, the optimal locations are at **bus 13**, **bus 24** and **bus 30**. The optimal sizes of the DG are: $(\mathbf{0.7923 + j0.3727})$ $\mathbf{MVA}$ for the DG at **bus 13**, $(\mathbf{1.0699 + j0.5174})$ $\mathbf{MVA}$ for the DG at **bus 24**, and $(\mathbf{1.0297 + j1.0104})$ $\mathbf{MVA}$ at **bus 30**. After placement of the three DG at **bus 13**, at **bus 24** and at **bus 30** respectively, the real power loss is reduced from $\mathbf{208.4322\ kW}$ to $\mathbf{11.7335\ kW}$. This corresponds to a real power loss reduction of $\mathbf{94.3706}\%$. Further analysis of the simulation results shows an improvement of the voltage profile of the 33-bus distribution system after placement of the three DG. As shown in Figure 4.8, Before the DG placement, the minimum voltage in the distribution system was $0.9108$ p.u at bus 18. After the placement of the three DG, the minimum voltage is $\mathbf{0.9925\ p.u}$ at **bus 8**.

**Table 4.8**: Simulation results for three DG placement and sizing problem of the 33-bus distribution system

| Simulation results | Before DG placement | After DG placement |
|---|---|---|
| Transformer power supply in (MVA) | $3.9234 + j2.4117$ @bus 1 | $0.8348 + j0.4091$ @bus 1 |
| Power loss in (kW) | 208.4322 | 11.7335 |
| Power loss reduction (%) | – | 94.3706 |
| Minimum voltage in (p.u) | 0.9108 @bus 18 | 0.9925 @bus 8 |
| Maximum voltage in (p.u) | 1 @bus 1 | 1.0009 @bus 30 |
| No of DG | 0 | 3 |
| Optimal DG size in (MVA) & location | – | $0.7923 + j0.3727$ @bus 13<br>$1.0699 + j0.5174$ @bus 24<br>$1.0297 + j1.0104$ @bus 30 |

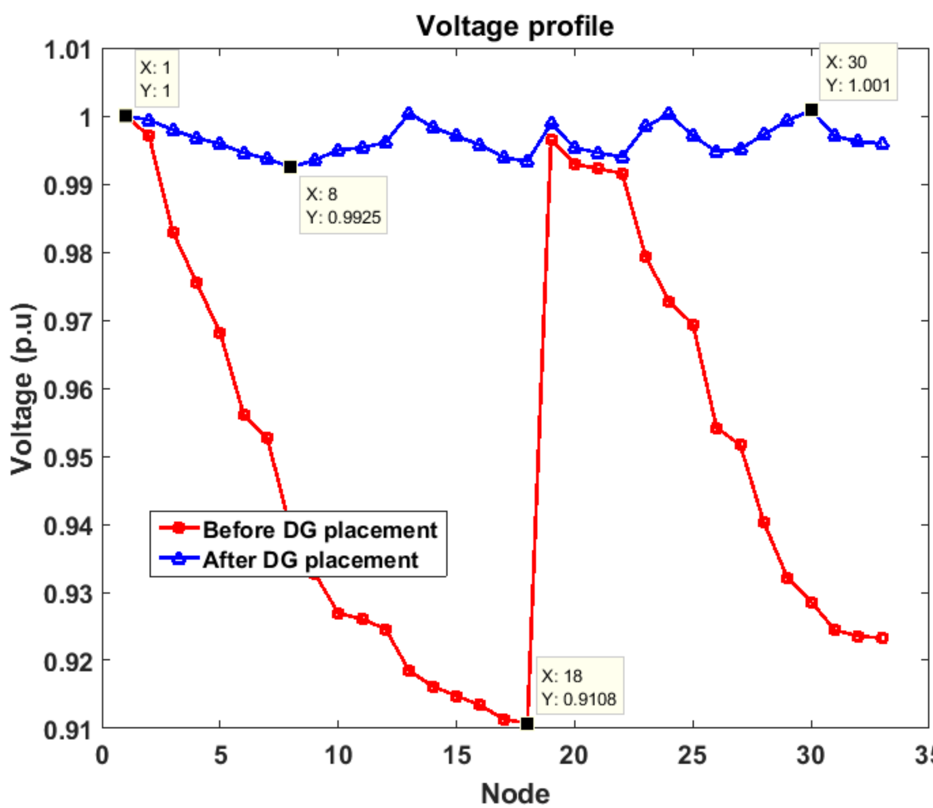


**Figure 4.8**: Voltage profile of the 33-bus distribution network before and after the optimal placement of three DG

### 4.4.3.3. IEEE 69-bus distribution system results

The developed PSO algorithm is used to solve the single-objective DG placement and sizing problem in the IEEE 69-bus distribution system. The parameters of the 69-bus distribution system are given in **Appendix D**.

### a. Case 1: Single DG placement and sizing problem

The developed PSO algorithm for the single-objective optimal DG placement and sizing problem is applied to the 69-bus distribution system. The solution of the PSO algorithm provides the best location and size for a single DG placement and sizing problem. The simulation results are compiled in Table 4.9.

**Table 4.9**: **Simulation results for the single DG placement and sizing problem of the 69-bus distribution system**

| Simulation results | Before DG placement | After DG placement |
|---|---|---|
| Transformer power supply in (MVA) | $4.0268 + j2.7968$ @bus 1 | $1.9973 + j1.4097$ @bus 1 |
| Power loss in (kW) | 224.9804 | 23.1574 |
| Power loss reduction (%) | – | 89.7069 |
| Minimum voltage in (p. u) | 0.9092 @bus 65 | 0.9725 @bus 27 |
| Maximum voltage in (p. u) | 1 @bus 1 | 1 @bus 1 |
| No of DG | 0 | 1 |
| Optimal DG size in (MVA) & location | – | $1.8277 + j1.2993$ @bus 61 |

The simulation results show that for a single DG placement in the 69-bus distribution system, the optimal location is at **bus 61** and the optimal size of the DG is $(\mathbf{1.8277 + j1.2993})$ **MVA**. After DG placement at **bus 61**, the real power loss is reduced to $\mathbf{23.1574}$ **kW** from $\mathbf{224.9804}$ **kW**. A power loss reduction of $\mathbf{89.7069}\%$ is achieved after the placement of the obtained single DG in the 69-bus distribution system.

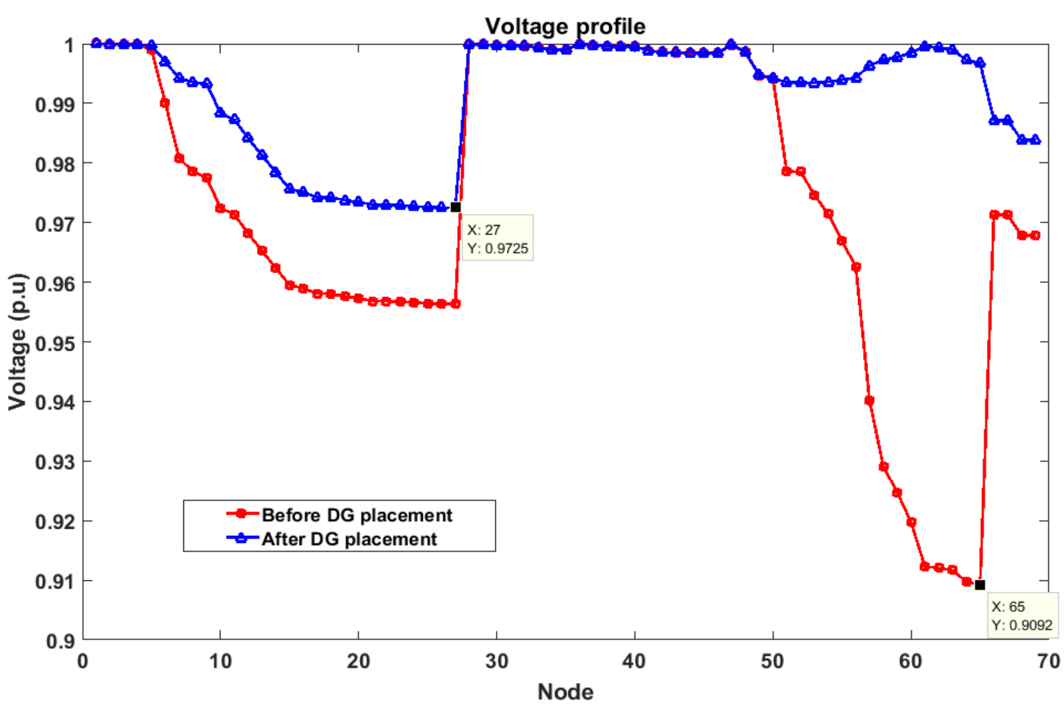


**Figure 4.9**: **Voltage profile of the 69-bus distribution network before and after the optimal placement of a single DG**

The simulation results also indicate an improvement of the voltage profile of the 69-bus distribution system after DG placement as shown in Figure 4.9. Before the DG placement, the minimum voltage was $\mathbf{0.9092\ p.u}$ at **bus 65**. It is improved to $\mathbf{0.9725\ p.u}$ at **bus 27** after the single DG placement in the 69-bus distribution system.

**b. Case 2: Two DG placement and sizing problem**

The developed PSO algorithm for the single-objective optimal DG placement and sizing problem is applied to the 69-bus distribution system to determine the optimal locations to place two DG in the network and to find the optimal size of these two DG. The simulation results are compiled in Table 4.10.

**Table 4.10**: **Simulation results for two DG placement and sizing problem of the 69-bus distribution system**

| Simulation results | Before DG placement | After DG placement |
|---|---|---|
| Transformer power supply in $(\mathrm{MVA})$ | $4.0268 + j2.7968$ @bus 1 | $1.5587 + j1.1168$ @bus 1 |
| Power loss in $(\mathrm{kW})$ | $224.9804$ | $7.2210$ |
| Power loss reduction (%) | $-$ | $96.7904$ |
| Minimum voltage in $(\mathrm{p.u})$ | $0.9092$ @bus 65 | $0.9942$ @bus 69 |
| Maximum voltage in $(\mathrm{p.u})$ | $1$ @bus 1 | $1$ @bus 1 |
| No of DG | $0$ | $2$ |
| Optimal DG size in $(\mathrm{MVA})$ & location | $-$ | $0.5156 + j0.3596$ @bus 17<br><br>$1.7348 + j1.2262$ @bus 61 |

The simulation results indicate that for two DG placement in the 69-bus distribution system, the optimal locations are at **bus 17** and **bus 61**. The optimal sizes of the DG are: $(\mathbf{0.5156 + j0.3596})\ \mathbf{MVA}$ for the DG at **bus 17** and $(\mathbf{1.7348 + j1.2262})\ \mathbf{MVA}$ for the DG at **bus 61**. After placement of the two DG at **bus 17** and at **bus 61** respectively, the real power loss is reduced from $\mathbf{224.9804\ kW}$ to $\mathbf{7.2210\ kW}$. This corresponds to a real power loss reduction of $\mathbf{96.7904}\%$.

Further analysis of the simulation results shows an improvement of the voltage profile of the 69-bus distribution system after placement of the two DG. As shown in Figure 4.10, before the DG placement, the minimum voltage in the distribution system was $\mathbf{0.9092\ p.u}$ at **bus 65**. After the placement of the two DG, the minimum voltage is $\mathbf{0.9942\ p.u}$ at **bus 69**.

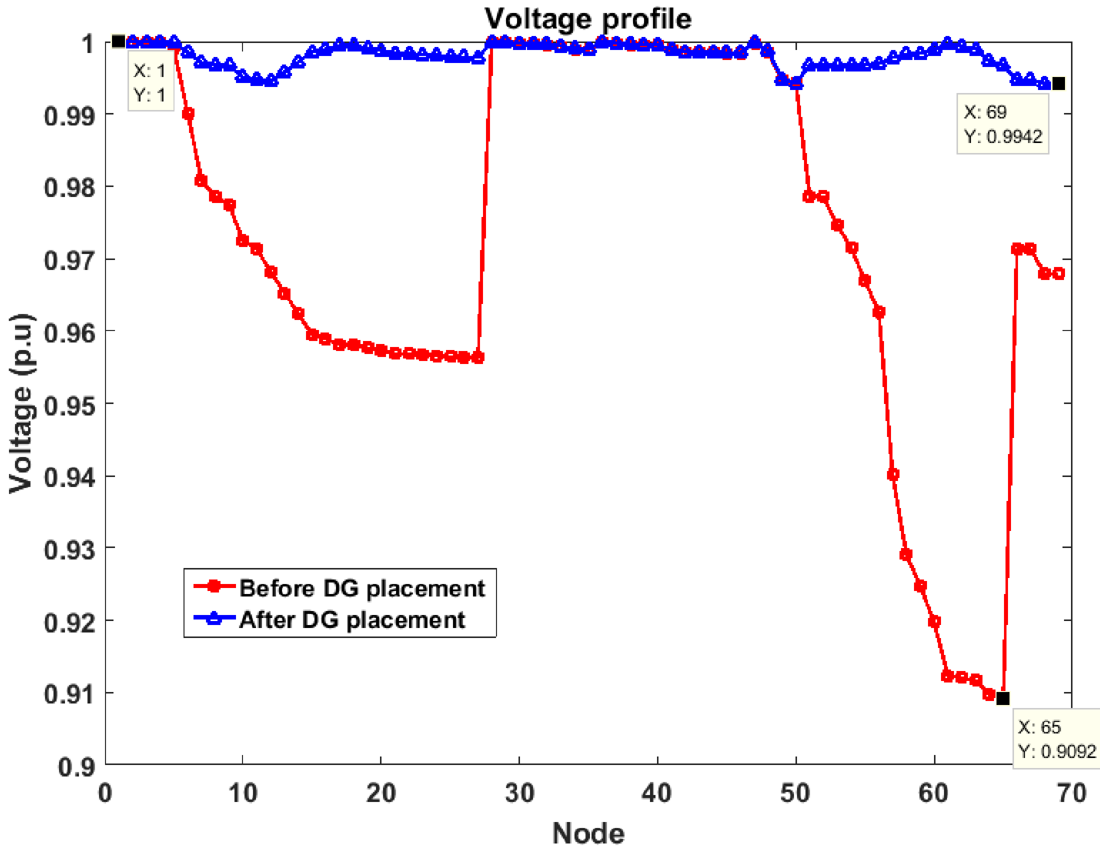


**Figure 4.10**: Voltage profile of the 69-bus distribution network before and after the optimal placement of two DG

### c. Case 3: Three DG placement and sizing problem

The developed PSO algorithm for the single-objective optimal DG placement and sizing problem is applied to the 69-bus distribution system to determine the optimal locations to place three DG in the distribution network and to find the optimal size of these three DG. The simulation results are compiled in Table 4.11.

The simulation results indicate that for three DG placement in the 69-bus distribution system, the optimal locations are at **bus 11**, **bus 21** and **bus 61**. The optimal sizes of the DG are: $(\mathbf{0.5334 + j0.3595})\ \mathbf{MVA}$ for the DG at **bus 11**, $(\mathbf{0.3421 + j0.2296})\ \mathbf{MVA}$ for the DG at **bus 21**, and $(\mathbf{1.6793 + j1.1983})\ \mathbf{MVA}$ at **bus 61**. After placement of the three DG at **bus 11**, at **bus 21** and at **bus 61** respectively, the real power loss is reduced from $\mathbf{224.9804\ kW}$ to $\mathbf{4.2774\ kW}$. This corresponds to a real power loss reduction of $\mathbf{98.0988}\%$.

Further analysis of the simulation results shows an improvement of the voltage profile of the 69-bus distribution system after placement of the three DG. As shown in Figure 4.11, Before the DG placement, the minimum voltage in the distribution system was $\mathbf{0.9092\ \ p.u}$

at **bus 65**. After the placement of the three DG, the minimum voltage is $\mathbf{0.9943\ p.u}$ at **bus 50**.

**Table 4.11**: Simulation results for three DG placement and sizing problem of the 69-bus distribution system

| Simulation results | Before DG placement | After DG placement |
|---|---|---|
| Transformer power supply in (MVA) | $4.0268 + j2.7968$ @bus 1 | $1.2512 + j0.914$ @bus 1 |
| Power loss in (kW) | 224.9804 | 4.2774 |
| Power loss reduction (%) | – | 98.0988 |
| Minimum voltage in (p.u) | 0.9092 @bus 65 | 0.9943 @bus 50 |
| Maximum voltage in (p.u) | 1 @bus 1 | 1.0001 @bus 61 |
| No of DG | 0 | 3 |
| Optimal DG size in (MVA) & location | – | $0.5334 + j0.3595$ @bus 11<br>$0.3421 + j0.2296$ @bus 21<br>$1.6793 + j1.1983$ @bus 61 |

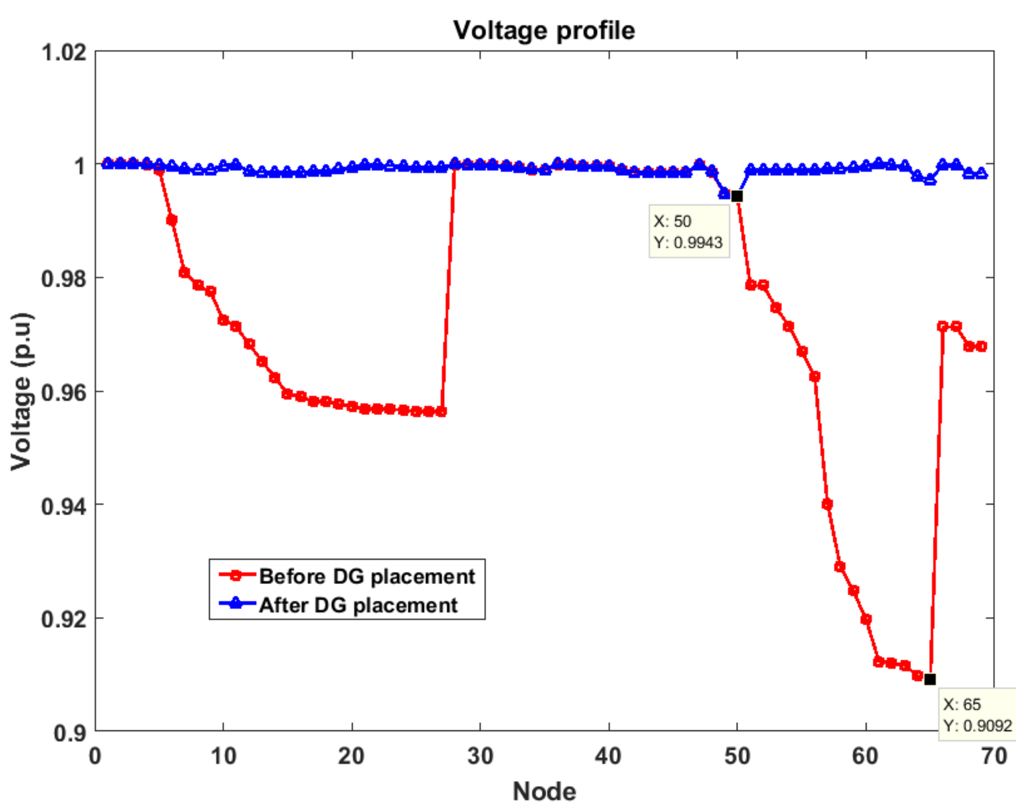


**Figure 4.11**: Voltage profile of the 69-bus distribution network before and after the optimal placement of three DG

### 4.4.4. Discussion of the results of the developed PSO algorithm for the single-objective optimal DG placement and sizing problem

The application of the developed PSO solution algorithm to the single-objective optimal DG placement problem on the distribution system shows that the optimal sizing and placement of a DG in a distribution system results in a reduction of the real power loss along with an improvement of the voltage profile of the system. The percentage of the real power loss reduction increases when multiple DG are optimally sized and placed in the distribution system. The simulation results indicate that for the 33-bus and 69-bus distribution systems, the solution of the real power loss minimisation problem complies with the voltage, power flow, and DG limits constraints of the distribution systems. The simulation results show that after placing multiple DG in the 16-bus distribution system, the source transformer 1 draws the real and reactive power from the downstream network. That means that the solutions from Tables 4.4 and 4.5 may not work in the current state of the power grid. However, these solutions would work in future smart distribution system since the future smart grid will be designed for seamless integration of DG and to accommodate bi-directional power flow in the distribution system.

The placement of multiple DG in the 16-bus distribution system causes a power flow to the grid. This is the evidence that the Distributed Generations create a bidirectional power flow which can affect the power system performance. Therefore, there is a need to add a new constraint to the developed algorithm to prevent the DG power flow to the grid. The alternative solutions for the optimal placement and sizing of 2 and 3 DG in the 16-bus distribution system, resulting from the addition of the new constraint, is provided in Table 4.12. The new voltages profiles after placement of 2 and 3 DG are given in Figure 4.12. From Table 4.12, it is observed that the new real power loss after the placement of 2 and 3 DG in the 16-bus distribution system are: $\mathbf{100.7893\ kW}$ after two DG placement and $\mathbf{65.4821\ kW}$ after three DG placement. The new minimum voltages in the 16-bus distribution system are $\mathbf{0.9912\ p.u}$ at **bus 16** and $\mathbf{0.9939\ p.u}$ at **bus 10**, for the two DG and three DG placement respectively.

The obtained solutions of the optimal DG placement and sizing problem for real power loss minimisation are compared with some results from the literature, and it is given in Table 4.13. It can be deduced that for the case studies considered above, the developed PSO solution algorithm performs better than the algorithms used in the available literature.

**Table 4.12**: Results of the optimal multi-DG placement in the 16-bus distribution network

| **Simulation results** | **After DG placement** | |
|---|---|---|
| No of DG | 2 | 3 |
| Total generation capacity in (MVA) | $9.9605 + j2.5937$ | $5.6624 + j2.5162$ |
| Transformer power supply in (MVA) | $2.7261 + j1.0962$ @bus 1<br><br>$2.0935 + j1.5025$ @bus 2<br><br>$5.1409 - j0.0050$ @bus 3 | $2.7262 + j1.0964$ @bus 1<br><br>$2.0933 + j1.5025$ @bus 2<br><br>$1.2189 + j0.0552$ @bus 3 |
| Power loss (kW) | 100.7893 | 65.4821 |
| Power loss reduction (%) | 80.3923 | 87.261 |
| Minimum voltage (p.u) | 0.9912 @bus 16 | 0.9939 @bus 10 |
| Maximum voltage (p.u) | 1.0007 @bus 9 | 1.0007 @bus 9 |
| DG size (MVA) & position | $5.7948 + j1.7468$ @bus 6<br><br>$13.0454 + j1.7526$ @bus 9 | $5.7947 + j1.7467$ @bus 6<br><br>$13.0456 + j1.7526$ @bus 9<br><br>$3.8867 - j0.1449$ @bus 16 |

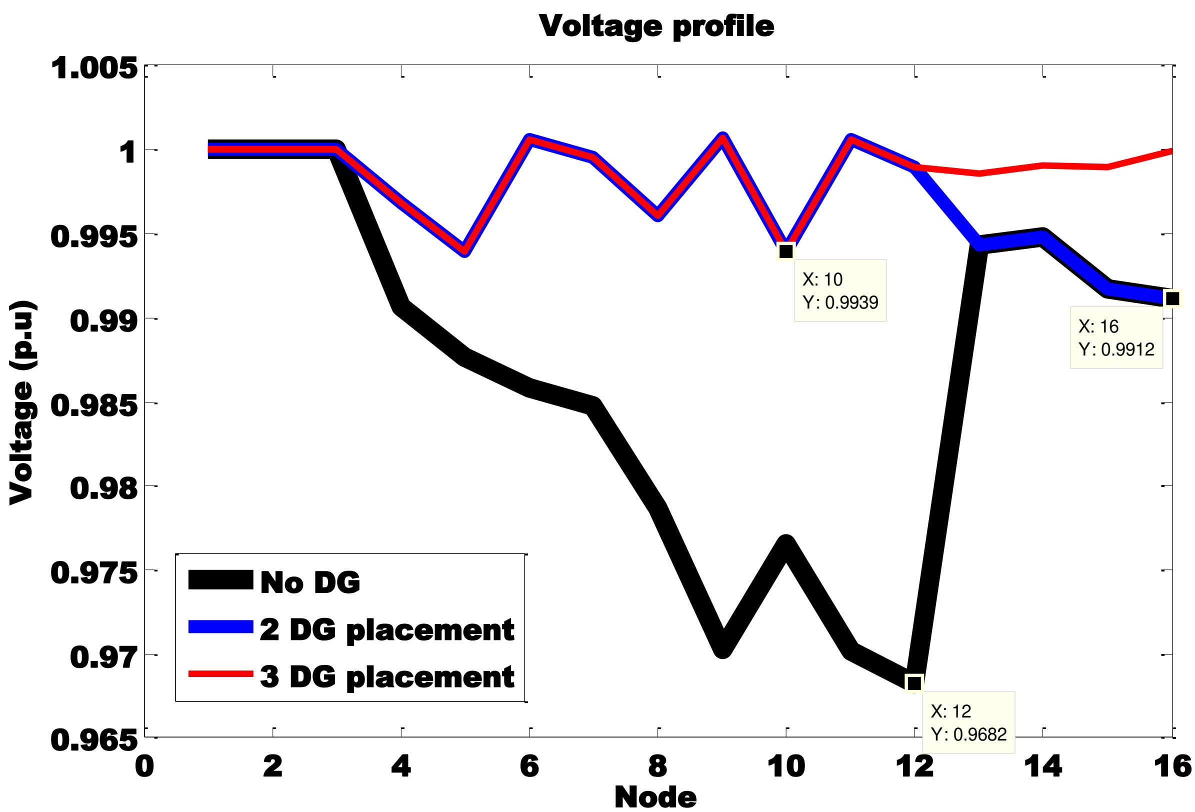


**Figure 4.12**: Voltage profile results for the multi- DG placement in the 16-bus distribution network

**Table 4.13**: Comparison of the developed PSO solution algorithm for the single-objective optimal DG placement and sizing problem with the literature ones

<table>
<tr><td rowspan="7">**16 bus**</td><td>**Algorithm**</td><td colspan="3">**Developed PSO algorithm**</td><td colspan="2">**Improved Analytical (IA) (Hung et al., 2010)**</td><td colspan="2">**Exhaustive Load Flow (ELF) (Hung et al., 2010)**</td></tr>
<tr><td>**No of DG**</td><td colspan="3">1</td><td colspan="2">1</td><td colspan="2">1</td></tr>
<tr><td>**DG type**</td><td colspan="3">III</td><td colspan="2">III</td><td colspan="2">III</td></tr>
<tr><td>**Optimal DG size (MVA) & Location**</td><td colspan="3">13.0456 + j1.7526<br>@bus 9</td><td colspan="2">13.1739 + j0.2276<br>@bus 9</td><td colspan="2">13.1196 + j0.2267<br>@bus 9</td></tr>
<tr><td>**Power loss before DG**</td><td colspan="3">514.0293 kW</td><td colspan="2">511.43 kW</td><td colspan="2">511.43 kW</td></tr>
<tr><td>**Power loss after DG**</td><td colspan="3">162.8352 kW</td><td colspan="2">162.58 kW</td><td colspan="2">162.58 kW</td></tr>
<tr><td>**Percentage of real power loss reduction**</td><td colspan="3">68.3218%</td><td colspan="2">68.2107%</td><td colspan="2">68.2107%</td></tr>
<tr><td rowspan="7">**33 bus**</td><td>**Algorithm**</td><td colspan="3">**Developed PSO algorithm**</td><td colspan="2">**PSO (Kansal et al., 2013)**</td><td>**GA − IPSO (Awodele, 2016)**</td><td>**Modified Fuzzy and Clonal Selection (Murthy & Kumar, 2013)**</td></tr>
<tr><td>**No of DG**</td><td>1</td><td>2</td><td>3</td><td>1</td><td>2</td><td>3</td><td>1</td></tr>
<tr><td>**DG type**</td><td>III</td><td>III</td><td>III</td><td>III</td><td>I & II</td><td>IV</td><td>III</td></tr>
<tr><td>**Optimal DG size (MVA) & Location**</td><td>2.5586 + j1.7440<br>@bus 6</td><td>0.8456 + j0.3985<br>@bus 13<br><br>1.1378 + j1.0633<br>@bus 30</td><td>0.7923 + j0.3727<br>@bus 13<br><br>1.0699 + j0.5174<br>@bus 24<br><br>1.0297 + j1.0104<br>@bus 30</td><td>3.0197 − j0.0432<br>@bus 6</td><td>2.5317 MW<br>@bus 6<br><br>1.2258 Mvar<br>@bus 30</td><td>0.507 + j0.03<br>@bus 18<br><br>0.301 + j0.01<br>@bus 23<br><br>0.707 + j0.002<br>@bus 32</td><td>3.0109 + j0.0473<br>@bus 6</td></tr>
<tr><td>**Power loss before DG**</td><td>208.4322 kW</td><td>208.4322 kW</td><td>208.4322 kW</td><td>211 kW</td><td>211 kW</td><td>211.2 kW</td><td>210.9761 kW</td></tr>
<tr><td>**Power loss after DG**</td><td>67.9575 kW</td><td>28.5018 kW</td><td>11.7335 kW</td><td>67.95 kW</td><td>58.45 kW</td><td>44.60 kW</td><td>70.9072 kW</td></tr>
<tr><td>**Percentage of real power loss reduction**</td><td>67.3959%</td><td>86.3256%</td><td>94.3706%</td><td>67.7962%</td><td>72.2986%</td><td>78.8826%</td><td>66.3909%</td></tr>
</table>

| | Algorithm | Developed PSO algorithm | PSO (Kansal et al., 2013) | Analytical approach (Acharya et al., 2006)) | Exhaustive Load Flow (ELF) (Hung et al., 2010) |
|---|---|---|---|---|---|
| 69 bus | No of DG | 1 | 1 | 1 | 1 |
| | DG type | III | III | I | III |
| | DG size (MVA) & Location | 1.8277 + j1.2993 @bus 61 | 2.2238 + j0.0314 @bus 61 | 1.81 MW @bus 61 | 2.2427 + j0.0321 @bus 61 |
| | Power loss before DG | 224.9804 kW | 225 kW | 219.28 kW | 219.28 kW |
| | Power loss after DG | 23.1574 kW | 23.19 kW | 81.44 kW | 22.62 kW |
| | Percentage of real power loss reduction | 89.7069% | 89.6933% | 62.8603% | 89.6844% |

### 4.5. Multi-objective DG placement and sizing problem using the weighted-sum approach

The optimal placement of DG can be a single-objective or a multi-objective problem, depending on the objectives considered. In this section, a weighted sum based PSO approach is developed to solve a multi-objective problem. The objectives considered are the real power loss minimisation, the voltage deviation minimisation and the maximisation of the bus voltage stability index. The performance of the developed multi-objective solution algorithm is tested for different case studies, and the results are presented in this section.

#### 4.5.1. Problem formulation of the multi-objective DG placement and sizing problem

Sometimes, optimisation problems have more than one objective. These objectives are often conflicting, and therefore, a compromise should be reached when solving a multi-objective optimisation problem. In this research work, the weighted-sum approach is used to solve the multi-objective optimal DG placement and sizing problem.

##### 4.5.1.1. Basics of the weighted-sum approach

The weighted-sum method consists of aggregating a set of objective functions into a single-objective using weight factors. The single-objective function is the sum of all objective functions multiplied by the respective weight factor (Marler & Arora, 2009). It is mathematically formulated as indicated in Equation 4.6.

$$\mathbf{min\,f(x)} = \sum_{\mathbf{i=1}}^{\mathbf{p}} \mathbf{we_i.\,f_i(x)} \tag{4.6.a}$$

Subject to

$$\begin{gathered}\mathbf{we_i \geq 0, \forall i = 1, 2, \cdots, p} \\ \sum_{\mathbf{i=1}}^{\mathbf{p}} \mathbf{we_i = 1}\end{gathered} \tag{4.6.b}$$

Where

$\mathbf{p}$ is the number of objective functions $\mathbf{f_i}$.

$\mathbf{we_i}$ is the weight factor of the objective function $\mathbf{f_i}$

$\mathbf{x}$ is the input data for each function $\mathbf{f_i}$.

The value of the weight factor $\mathbf{we_i}$ of the objective function $\mathbf{f_i}$ depends on the how important the function $\mathbf{f_i}$ is in the problem. As an example, if for two objective functions $\mathbf{f_1}$ and $\mathbf{f_2}$, the solution of $\mathbf{f_1}$ are more important than that of $\mathbf{f_2}$, then, the value $\mathbf{we_1}$ should be greater than $\mathbf{we_2}$'s. The weight factors are usually predefined before the optimization process.

The magnitudes of the objective functions need to be normalised, to obtain a Pareto-optimal solution consistent with the predetermined weight factors. The normalisation of all objective functions ensures that none of the objectives largely dominates others (Marler & Arora, 2009). In this research work, the normalisation approach consists of dividing individual objective function by their respective reference value as indicated in Equation 4.7.

$$\mathbf{f_{i\ norm}(x)} = \frac{\mathbf{f_i(x)}}{\mathbf{|f_{i\ ref}\ (x_0)|}} \tag{4.7}$$

Where

$\mathbf{x}$ is the input data

$\mathbf{f_{i\ norm}}$ is the normalized expression of the objective function $\mathbf{f_i}$ to be optimized.

$\mathbf{f_{i\ ref}}$ is the value of $\mathbf{f_i}$ for the initial input data $\mathbf{x_0}$.

Using Equations 4.6 and 4.7, the weighted-sum based multi-objective problem is formulated as given in Equation 4.8.

$$\mathbf{\min f(x) = we_1 . f_{1\ norm}(x) + we_2 . f_{2\ norm}(x) + \cdots + we_p . f_{p\ norm}(x)} \tag{4.8}$$

Using the normalisation concept above, the objectives functions of the multi-objective DG placement and sizing problem are formulated and presented in the next section of this thesis.

#### 4.5.1.2. Real Power loss formulation

The real power loss $\mathrm{P_{Loss}}$ in a distribution system is the sum of the real component of the power loss in individual branches of the network. It can be mathematically formulated as in Equation 4.1. The normalised power loss formulation $\mathbf{f_{1\ norm}}$ is given in Equation 4.9.

$$\mathbf{f_{1\ norm}(x)} = \frac{\mathbf{P_{Loss}(x)}}{\mathbf{P_{Loss}(x_0)}} \tag{4.9}$$

Where

$\mathbf{x}$ is a distribution network with or without DG.

$\mathbf{P_{Loss}(x_0)}$ is the real power loss in the initial distribution network without DG.

#### 4.5.1.3. Voltage profile improvement

The improvement of the voltage profile in the distribution system is achieved by minimising the Voltage Deviation Index (VDI). The voltage deviation index is a measure of how far the bus voltage has deviated from the reference voltage, and it can be mathematically formulated as in Equation 4.10.

$$\mathbf{VDI} = \sum_{\mathbf{i=1}}^{\mathbf{NB}} |\mathbf{V_i} - \mathbf{V_{rated}}| \tag{4.10}$$

Where

$\mathbf{VDI}$ is the Voltage Deviation Index.

$\mathbf{V_i}$ is the voltage at bus $\mathbf{i}$.

$\mathbf{V_{rated}}$ is the rated voltage and it is equal to $1\ \mathrm{p.u.}$

$\mathbf{NB}$ is the number of buses in the distribution system.

Minimising Equation 4.10 implies that after DG placement, all node voltages should be as close as possible to the rated voltage. The typical voltage rating in primary distribution systems is 1 per-unit with a margin of $\pm 6\%$ (TSD, 2003). Any deviation from this voltage range may indicate either a disturbance or an overload in the distribution system. Therefore, the operating voltage in the distribution system should be kept within the tolerance limit.

The normalised expression for the voltage deviation index objective function is given in Equation 4.11.

$$\mathbf{f_{2\ norm}(x)} = \frac{\mathbf{VDI(x)}}{\mathbf{VDI^0}} \tag{4.11}$$

Where

$\mathbf{VDI^0}$ is the voltage deviation index for the initial distribution system without DG.

#### 4.5.1.4. Voltage stability maximisation

Voltage stability refers to the ability of an electrical network to preserve steady voltages at its nodes after being subjected to a disturbance from a given operating point (Palukuru et al., 2014). Voltage instability may lead to a voltage collapse, characterised by unacceptable levels of voltage at certain nodes. Voltage instability is usually the result of increased load demand and reactive power deficiency (Palukuru et al., 2014). The introduction of a DG in the distribution system can be considered as a small disturbance. So, the Voltage Stability Index (VSI) of the distribution system is likely to be changed. The voltage stability index in radial distribution systems can be obtained using Equation 4.12 (Eminoglu & Hocaoglu, 2007).

$$\mathbf{VSI(j) = 2V_i^2 . V_j^2 - V_j^4 - 2V_j^2 . (P_j . r_{ij} + Q_j . x_{ij}) - |z_{ij}|^2 . (P_j^2 + Q_j^2)} \tag{4.12}$$

Where

$\mathbf{VSI(j)}$ is the voltage stability index at bus $\mathbf{j}$.

$\mathbf{V_i}$ and $\mathbf{V_j}$ are the sending and receiving bus voltages respectively.

$\mathbf{P_j}$ and $\mathbf{Q_j}$ are the real and reactive power demand at bus $\mathbf{j}$ respectively.

$\mathbf{r_{ij}}$, $\mathbf{x_{ij},}$ and $\mathbf{z_{ij}}$ are the resistance, reactance and impedance of branch $\mathbf{i - j}$.

For stable operation of the distribution system, the voltage stability index should be closer to 1. A maximal value of **VSI** means that there is no load connected at the receiving end bus. In that case, if the sending and receiving bus voltages are equal to $1\ \mathrm{p.u}$, then the **VSI** is equal to unity. Increasing the loading of the distribution system will ultimately reduce the stability indexes at all buses. Buses with small voltage stability index values are more prone to be unstable. So, the voltage stability index objective function is a measure of how close to the reference the **VSI** at all buses are. The voltage stability index objective function $\mathrm{VSI_{Dev}}$ is given in Equation 4.13.

$$\mathbf{VSI_{Dev} = \sum_{j=1}^{NB} |1 - VSI_j|} \tag{4.13}$$

Where

$\mathbf{VSI_j}$ is the voltage stability index of bus $\mathbf{j}$.

$\mathbf{VSI_{Dev}}$ is the Voltage Stability Index objective function.

$\mathbf{NB}$ is the number of buses in the distribution system.

The normalised voltage stability objective function is given in Equation 4.14.

$$\mathbf{f_{3\ norm}(x) = \frac{VSI_{Dev}(x)}{VSI_{Dev}{}^0}} \tag{4.14}$$

Where

$\mathbf{VSI_{Dev}}^{\mathbf{0}}$ is the voltage stability index objective value for the initial distribution system without DG.

Therefore, the weighted-sum objective function for the multi-objective optimal DG placement and sizing problem is as given in Equation 4.15.

$$\mathbf{f(x) = we_1 . f_{1\,norm}(x) + we_2 . f_{2\,norm}(x) + we_3 . f_{3\,norm}(x)} \tag{4.15.a}$$

$$\mathbf{f(x) = we_1 . \frac{P_{Loss}(x)}{P_{Loss}(x_0)} + we_2 . \frac{VDI(x)}{VDI^0} + we_3 . \frac{VSI_{Dev}(x)}{VSI_{Dev}{}^0}} \tag{4.15.b}$$

### 4.5.2. Solution algorithm of the weighted sum based multi-objective optimal DG placement and sizing problem

A PSO based algorithm is developed to solve the multi-objective DG placement and sizing problem using the weighted-sum approach.
This section provides the step-by-step procedure of the developed algorithm.

**Step 1:** Read the distribution system network data such as the number of nodes $\mathbf{NB}$, the number of distribution lines $\mathrm{NL}$, the number of tie lines $\mathbf{NT}$, the bus type ($\mathbf{Slack, PV, PQ}$), the load data ($\mathbf{Pd, Qd, Bs, Load_{ID}}$), the generator data ($\mathbf{Pg, Qg}$), the distribution line data ($\mathbf{bus_i, bus_j, r, x, sw_{tie}, sw_{sec}}$) and the DG limits coefficients ($\mathbf{k1, k2}$) which represent the minimum and maximum DG penetration levels.

**Step 2**: Initialize the binary PSO parameters such as the acceleration coefficients $\mathbf{c1}$ and $\mathbf{c2}$, the minimum and the maximum inertia weight ($\mathbf{w_{min}}$ and $\mathbf{w_{max}}$ respectively), the particle's velocity limits ($\mathbf{v_{min}}$ and $\mathbf{v_{max}}$), the number of particles ($\mathbf{Np}$), the dimension of the search space ($\mathbf{D}$) which is equal to the number of PQ buses in the network, and the weight factors ($\mathbf{we_1, we_2, we_3}$) and the stop criterions ($\mathbf{t_{1max}, t_{2max}}$) where $\mathbf{t_{1max}}$ and $\mathbf{t_{2max}}$ are used to stop the discrete and continuous PSO search process respectively.

**Step 3:** Initialize the particles' positions by following the approach defined in section 4.4.2., step 3.

**Step 4:** Initialize the particles' velocity as follows:

- The velocity of the first swarm represents the probability for each bit in the particle's position (DG status) to change its status.
- The velocity in the second swarm represents the rate of change of the particles from their current position to the next position (DG size).

The velocity in the first swarm is limited to the interval $[-4,\ 4]$. The velocity in swarm 2 is limited in the interval $[\mathbf{v_{min}}, \mathbf{v_{max}}]$, where the $\mathbf{v_{min}}$ and $\mathbf{v_{max}}$ are calculated using Equation 4.4.a and 4.4.b, respectively.

$$\mathbf{v_{min}} = -\mathbf{v_{max}}$$

$$\mathbf{v_{max}} = \boldsymbol{\varepsilon} \times (\mathbf{DG_{max}} - \mathbf{DG_{min}})$$

Where

$\boldsymbol{\varepsilon}$ is a random number in the range ]0,1], and representing the maximum velocity limit factor.

**Step 5:** Find the personal best particles position. The initial personal best position of all particles in swarm 1 corresponds to the string of binary bits representing the possible DG status at a load bus. Initially, there is no DG in the network. So, the initial personal best for all particles in the swarm 2 correspond to the $\mathbf{nDG} \times \mathbf{1}$ matrix whose elements are zeros. Initially, all particles are given the same objective value, which is obtained using Equation (4.8) after calculation of the normalized real power loss, voltage deviation index and voltage stability index deviation.

**Step 6:** Find the global best particle position from the set of particles best position given in Step 5. In this case, the global best particle position is the best particle position whose weighted objective value is minimal.

**Step 7:** Give random DG position(s) for every particle in swarm 1 and a corresponding DG size(s) in swarm 2.

**Start the discrete PSO iteration process** and set the iteration counter $\mathbf{t_1}$ to 1 for the discrete PSO.

**Step 8:** Check that each particle in swarm 1 for which the real power loss should be calculated only has $\mathrm{nDG}$ active distributed generator(s). A particle (distribution system) has an active generator if at least one of the binary bits representing the DG status for each bus is the bit 1.

**Start the continuous PSO search process and** set the iteration counter for the continuous PSO to 1.

**Step 9:** Update the generator data. After analysis of the DG position, the generator data must be updated to include the DG location and size. For the candidate DG position and size solution to be evaluated, find the position of the DG by analysing for which bus ID the DG status is equal to 1. Then, find the corresponding DG size from swarm 2 and update the distribution network generator parameters.

**Step 10:** Perform a Newton-Raphson power flow and calculate the normalised real power loss, voltage deviation index and voltage stability index deviation for the particles in swarm 1 using Equations 4.9, 4.11 and 4.14 respectively. Then, calculate the weighted-sum objective value using Equation 4.15.

**Step 11:** Update the personal best position of all particles in swarm 2 as per Equation 3.23 from chapter three, section 3.4.2.

$$\mathbf{Pbest_i}^{\mathbf{t+1}} = \begin{cases} \mathbf{Pbest_i}^{\mathbf{t}}, & \mathbf{if\ fitness_i}^{\mathbf{t+1}} \geq \mathbf{fitness_{Pbest_i}}^{\mathbf{t}} \\ \mathbf{x_i}^{\mathbf{t+1}}, & \mathbf{otherwise} \end{cases}$$

Where

$\mathbf{Pbest_i}^{\mathbf{t}}$ is the personal best position of particle $\mathbf{i}$ at iteration $\mathbf{t}$.

$\mathbf{x_i}^{\mathbf{t+1}}$ is the position of particle $\mathbf{i}$ at iteration $\mathbf{t+1}$.

$\mathbf{fitness_i}^{\mathbf{t+1}}$ is the fitness value of particle $\mathbf{i}$ at iteration $\mathbf{t+1}$.

$\mathbf{fitness_{Pbest_i}}^{\mathbf{t}}$ is the fitness value of $\mathbf{Pbest_i}^{\mathbf{t}}$.

**Step 12:** Update the global best position of swarm 2 as per Equation 3.24 in chapter three, section 3.4.2.

$$\mathbf{Gbest}^{\mathbf{t+1}} = \begin{cases} \mathbf{Gbest}^{\mathbf{t}}, & \mathbf{if\ fitness_{Pbest_i}}^{\mathbf{t+1}} \geq \mathbf{fitness_{Gbest}}^{\mathbf{t}} \\ \mathbf{Pbest_i}^{\mathbf{t+1}}, & \mathbf{otherwise} \end{cases}$$

Where

$\mathbf{Gbest}^{\mathbf{t+1}}$ is the global best solution of the swarm at iteration $\mathbf{t+1}$.

$\mathbf{fitness_{Gbest}}^{\mathbf{t}}$ is the fitness value of $\mathbf{Gbest}$ at iteration $\mathbf{t}$.

**Step 13:** Calculate the inertia weight using Equation 3.6 and update the velocity of all particles in swarm 2 as per Equation 3.5.

$$\mathbf{v_i}^{\mathbf{k+1}} = \boldsymbol{\omega} * \mathbf{v_i}^{\mathbf{k}} + \mathbf{c1} * \mathbf{rand1} * \left(\mathbf{Pbest_i} - \mathbf{x_i}^{\mathbf{k}}\right) + \mathbf{c2} * \mathbf{rand2} * \left(\mathbf{Gbest_i} - \mathbf{x_i}^{\mathbf{k}}\right)$$

**Step 14:** Update the position of particles in swarm 2 as per Equation 3.3.

$$\mathbf{x_i}^{\mathbf{k+1}} = \mathbf{x_i}^{\mathbf{k}} + \mathbf{v_i}^{\mathbf{k+1}}$$

Where

$\mathbf{x_i}^{\mathbf{k}}$ denotes the position of particle $\mathbf{i}$ at iteration $\mathbf{k}$

$\mathbf{v_i}^{\mathbf{k}}$ is the velocity of the particle $\mathbf{i}$ at iteration $\mathbf{k}$

**Step 15:** Increment the iteration count of the continuous PSO search process and repeat step 9 to step 14 until the stopping criterion is reached.

**Step 16:** Find the real power loss of the particles in swarm 1.
The global best position of the swarm 2 is achieved at the end of the continuous PSO, and it corresponds to the optimal DG size for the DG position from step 8. Consequently, the fitness of the particle in swarm 1 from step 8 is equal to the fitness of the global best position of swarm 2.

**Step 17:** Update the personal best positions in swarm 1 as per Equation 3.23.

**Step 18:** Update the global best in swarm 1 as per Equation 3.24.

**Step 19:** Calculate the inertia weight using Equation 3.6 and update the velocity of all particles in swarm 1 as per Equation 3.5.

**Step 20:** Update the position of the particles in swarm 1 as per Equation 3.9.

$$\mathbf{x_i}^{\mathbf{k}} = \begin{cases} \mathbf{1} & \mathbf{if\ r < sig}\left(\mathbf{v_i}^{\mathbf{k}}\right) \\ \mathbf{0} & \mathbf{if\ r \geq sig}\left(\mathbf{v_i}^{\mathbf{k}}\right) \end{cases}$$

Where

$\mathbf{r}$ is a uniformly distributed random number in the interval [0,1]

$\mathbf{sig}$ is a sigmoid function defined by $\mathbf{sig}(\boldsymbol{\alpha}) = \frac{\mathbf{1}}{\mathbf{1+e^{-\alpha}}}$

**Step 21**: Set the iteration count $t_2$ for the continuous PSO search process to 0 to allow step 7 to step 14 to be repeated for the next iteration of the discrete search process.

**Step 22**: Increment the iteration count $t_1$ of the discrete PSO process and repeat step 6 to step 20 until the stopping criterion is reached.

**Step 23:** Print the results of the search process such as the global best solution (optimal DG position and size), and its corresponding fitness value (minimum real power loss).

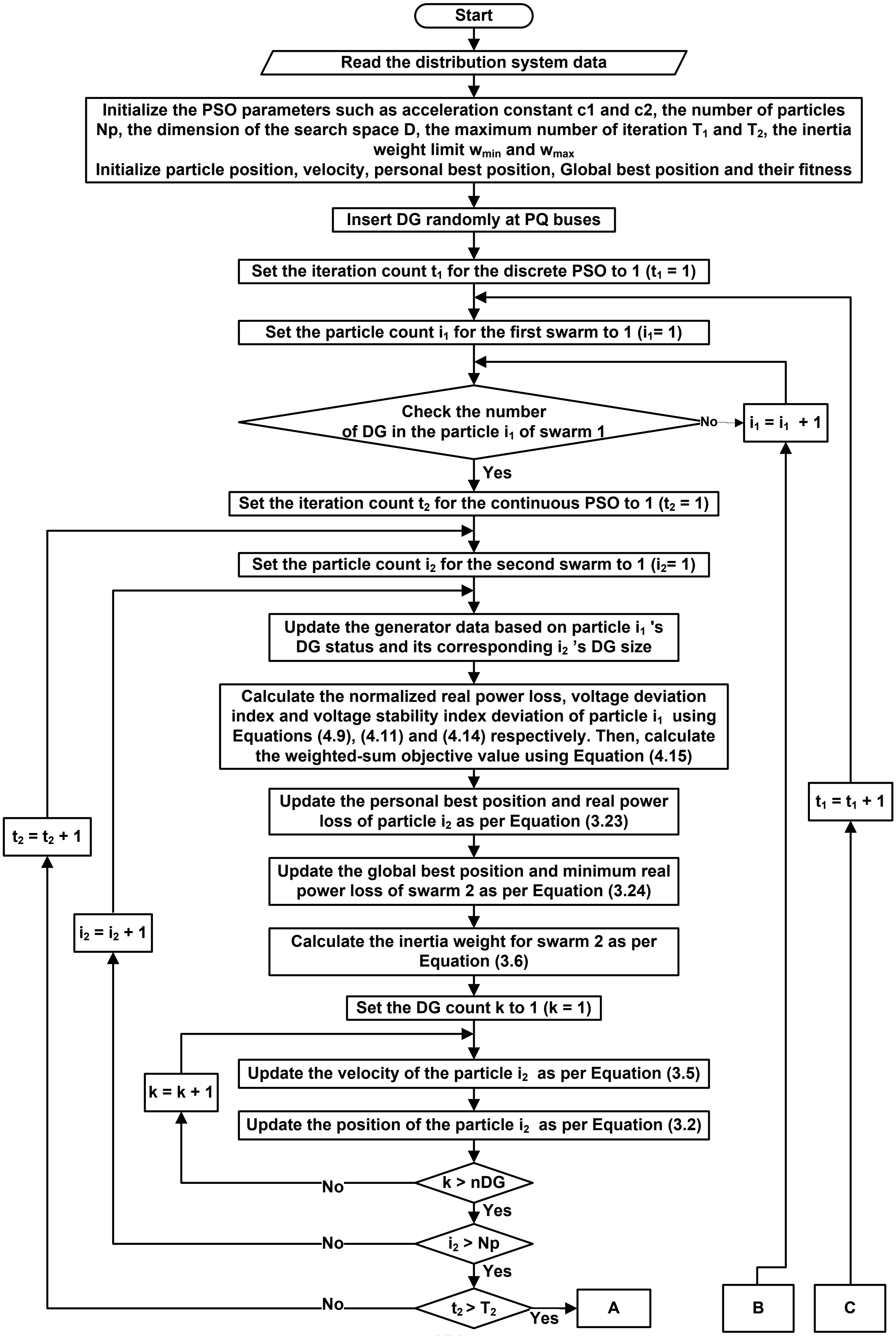
Start
Read the distribution system data
Initialize the PSO parameters such as acceleration constant c1 and c2, the number of particles Np, the dimension of the search space D, the maximum number of iteration T1 and T2, the inertia weight limit wmin and wmax
Initialize particle position, velocity, personal best position, Global best position and their fitness
Insert DG randomly at PQ buses
Set the iteration count t1 for the discrete PSO to 1 (t1 = 1)
Set the particle count i1 for the first swarm to 1 (i1= 1)
Check the number of DG in the particle i1 of swarm 1
No
i1 = i1 + 1
Yes
Set the iteration count t2 for the continuous PSO to 1 (t2 = 1)
Set the particle count i2 for the second swarm to 1 (i2= 1)
Update the generator data based on particle i1 's DG status and its corresponding i2 's DG size
Calculate the normalized real power loss, voltage deviation index and voltage stability index deviation of particle i1 using Equations (4.9), (4.11) and (4.14) respectively. Then, calculate the weighted-sum objective value using Equation (4.15)
Update the personal best position and real power loss of particle i2 as per Equation (3.23)
Update the global best position and minimum real power loss of swarm 2 as per Equation (3.24)
Calculate the inertia weight for swarm 2 as per Equation (3.6)
Set the DG count k to 1 (k = 1)
Update the velocity of the particle i2 as per Equation (3.5)
Update the position of the particle i2 as per Equation (3.2)
k > nDG
k = k + 1
i2 > Np
i2 = i2 + 1
t2 > T2
t2 = t2 + 1
t1 = t1 + 1
No
Yes
A
B
C

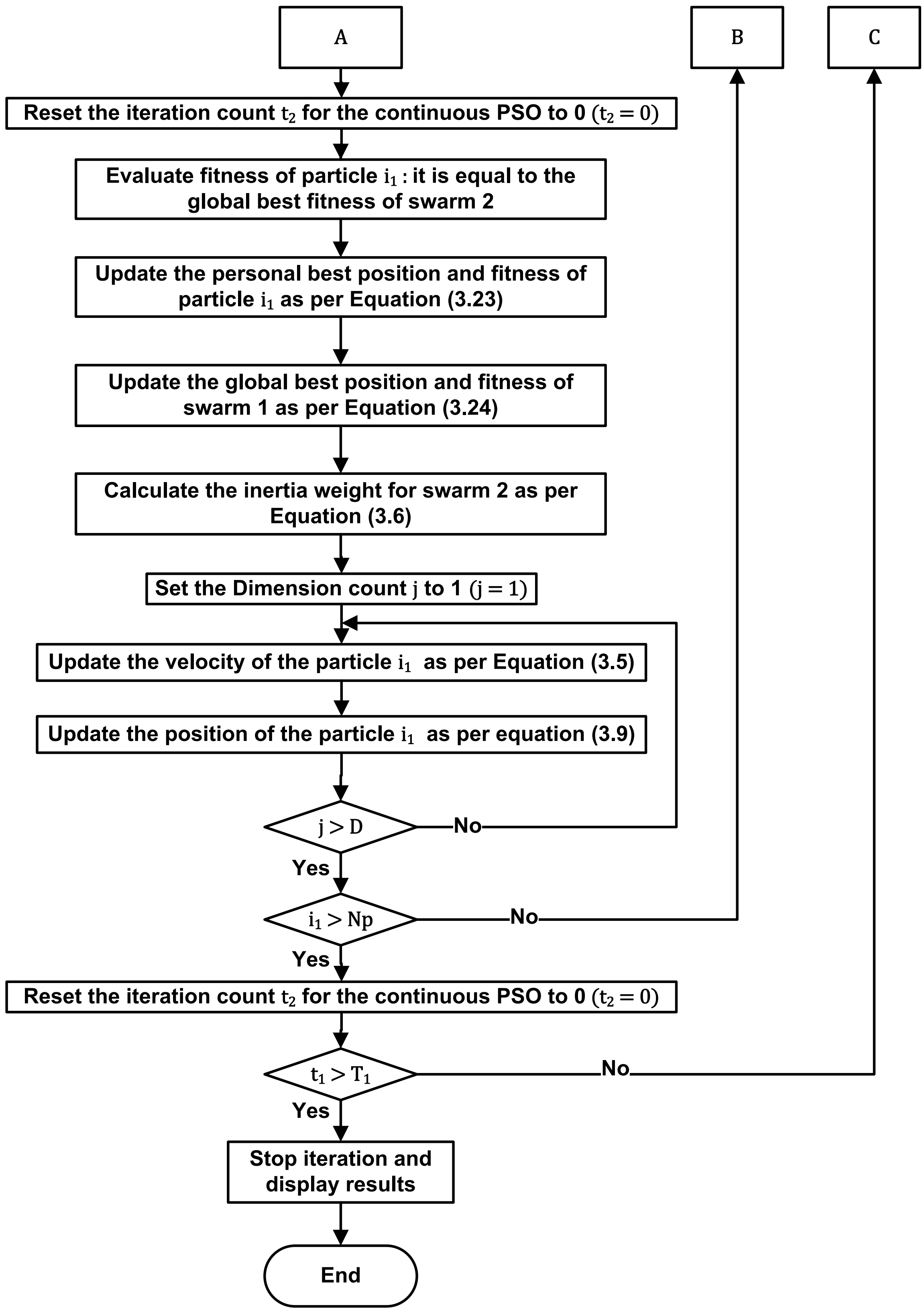


**Figure 4.13**: Flowchart of the developed PSO algorithm for the multi-objective DG placement and sizing problem

. The developed multi-objective algorithm is quite similar to the developed single-objective algorithm. The only difference is the way the objective value is calculated. The developed single-objective algorithm only has one objective which is the real power loss minimisation; the developed multi-objective has three objectives: the real power loss minimisation, the voltage deviation minimisation and the maximisation of the bus voltage stability index. So, in the developed multi-objective algorithm for optimal DG placement and sizing, the individual objective values for real power loss, Voltage Deviation Index, and Voltage Stability Index must be calculated before the weighted-sum objective value is obtained.

The flowchart diagram of the above-defined solution algorithm for the multi-objective DG placement and sizing problem is shown in Figure 4.13.

### 4.5.3. Results of the weighted sum based multi-objective optimal DG placement

The developed PSO algorithm described in section 4.5.2 is used to solve the multi-objective DG placement and sizing problem. The optimal placement and sizing of the DG provides a reduction of the real power loss, an improvement of the voltage profile and voltage stability of the distribution system. The developed weighted sum PSO algorithm is implemented in MATLAB R2016b. The simulation studies are carried out on the 16-bus, 33-bus, and 69-bus distribution systems. For each distribution system, three case studies are considered: single DG placement and sizing, Two DG placement and sizing and Three DG placement and sizing.

However, the values of the weight factors are unknown. So, it is primordial to determine the weight factors for which the weighted-sum objective has the minimum value.

#### 4.5.3.1. Choice of the weight factor of each objective function

The weight factor of each objective function is not known before the execution of the multi-objective optimal DG placement algorithm. So, an analysis is done to determine the combination of the weight factors $\mathbf{we_1}, \mathbf{we_2}$ and $\mathbf{we_3}$ for which the weighted-sum objective value is minimal. The following constraints are considered:

- The weight factors are strictly positive, and their values are limited to one decimal place.
- The sum of all the weight factors must be equal to 1 as per equation 4.6.b.

The 16-bus distribution system is used to examine the effects that the change of weight factors has on the solution of the multi-objective DG placement and sizing problem. The results of the analysis are given in Table 4.14. For any weight factor set $\{\mathbf{we_1}, \mathbf{we_2}, \mathbf{we_3}\}$,

$\mathbf{f}$ is the corresponding optimal weighted-sum value and $\mathbf{Opti_{DG}}$ is the corresponding optimal DG location and size.

**Table 4.14**: **Effects of the weight factors on the weighted sum multi-objective functions for single DG placement in the 16-bus distribution system**

| Weight factors | | | Value of the normalised objective functions for the optimal DG size and position | | | | Optimal single DG Size and location (in MVA) |
|---|---|---|---|---|---|---|---|
| | | | Real power loss | Voltage deviation | Voltage Stability Index | Weighted-sum | |
| $\mathbf{we_1}$ | $\mathbf{we_2}$ | $\mathbf{we_3}$ | $\mathbf{f_{1\ norm}}$ | $\mathbf{f_{2\ norm}}$ | $\mathbf{f_{3\ norm}}$ | $\mathbf{f}$ | $\mathbf{Opti_{DG}}$ |
| 0.1 | 0.1 | 0.8 | 0.3412 | 0.4800 | 0.4641 | 0.4534 | 15.1539 + j3.1924 @bus 9 |
| 0.1 | 0.2 | 0.7 | 0.3338 | 0.4396 | 0.4744 | 0.4534 | 15.1424 + j1.2588 @bus 9 |
| 0.1 | 0.3 | 0.6 | 0.3357 | 0.4314 | 0.4766 | 0.4489 | 15.1423 + j0.8627 @bus 9 |
| 0.1 | 0.4 | 0.5 | 0.3354 | 0.4314 | 0.4766 | 0.4444 | 15.1211 + j0.8808 @bus 9 |
| 0.1 | 0.5 | 0.4 | 0.3319 | 0.4316 | 0.4772 | 0.4399 | 14.9443 + j1.0313 @bus 9 |
| 0.1 | 0.6 | 0.3 | 0.3291 | 0.4227 | 0.4915 | 0.434 | 14.6353 + j0.8510 @bus 9 |
| 0.1 | 0.7 | 0.2 | 0.3268 | 0.4229 | 0.4919 | 0.4271 | 14.4975 + j0.9685 @bus 9 |
| 0.1 | 0.8 | 0.1 | 0.3247 | 0.4231 | 0.4924 | 0.4202 | 14.3554 + j1.0898 @bus 9 |
| 0.2 | 0.1 | 0.7 | 0.3369 | 0.4708 | 0.4664 | 0.4409 | 15.1491 + j2.7526 @bus 9 |
| 0.2 | 0.2 | 0.6 | 0.3232 | 0.4324 | 0.4791 | 0.4386 | 14.3491 + j1.5395 @bus 9 |
| 0.2 | 0.3 | 0.5 | 0.3225 | 0.4325 | 0.4793 | 0.4339 | 14.2796 + j1.5991 @bus 9 |
| 0.2 | 0.4 | 0.4 | 0.3218 | 0.4326 | 0.4795 | 0.4292 | 14.2111 + j1.6577 @bus 9 |
| 0.2 | 0.5 | 0.3 | 0.3206 | 0.4236 | 0.4935 | 0.4240 | 14.0022 + j1.392 @bus 9 |
| 0.2 | 0.6 | 0.2 | 0.3192 | 0.4239 | 0.4941 | 0.4170 | 13.8245 + j1.5443 @bus 9 |
| 0.2 | 0.7 | 0.1 | 0.3188 | 0.4239 | 0.4942 | 0.4099 | 13.7689 + j1.5921 @bus 9 |
| 0.3 | 0.1 | 0.6 | 0.3247 | 0.4481 | 0.4747 | 0.427 | 14.4243 + j2.2332 @bus 9 |
| 0.3 | 0.2 | 0.5 | 0.3203 | 0.4329 | 0.4801 | 0.4227 | 14.0240 + 1.8211 @bus 9 |
| 0.3 | 0.3 | 0.4 | 0.3200 | 0.4333 | 0.4803 | 0.4180 | 13.9662 + j1.8677 @bus 9 |

| | | | | | | | |
|---|---|---|---|---|---|---|---|
| 0.3 | 0.4 | 0.3 | 0.3196 | 0.433 | 0.4805 | 0.4132 | 13.8968 + j1.9273 @bus 9 |
| 0.3 | 0.5 | 0.2 | 0.318 | 0.4241 | 0.4947 | 0.4064 | 13.6207 + 1.7193 @bus 9 |
| **0.3** | **0.6** | **0.1** | **0.3178** | **0.4242** | **0.4949** | **0.3993** | **13.5777 + j1.7563 @bus 9** |
| 0.4 | 0.1 | 0.5 | 0.3193 | 0.4331 | 0.4807 | 0.4114 | 13.8439 + j1.9728 @bus 9 |
| 0.4 | 0.2 | 0.4 | 0.3192 | 0.4332 | 0.4808 | 0.4066 | 13.8088 + j2.0029 @bus 9 |
| 0.4 | 0.3 | 0.3 | 0.3191 | 0.4332 | 0.4809 | 0.4019 | 13.7745 + j2.0324 @bus 9 |
| 0.4 | 0.4 | 0.2 | 0.3175 | 0.4243 | 0.4951 | 0.3958 | 13.4944 + j1.8282 @bus 9 |
| 0.4 | 0.5 | 0.1 | 0.3175 | 0.4244 | 0.4952 | 0.3887 | 13.4625 + j1.8553 @bus 9 |
| 0.5 | 0.1 | 0.4 | 0.3189 | 0.4333 | 0.4810 | 0.3952 | 13.7248 + j2.0751 @bus 9 |
| 0.5 | 0.2 | 0.3 | 0.3188 | 0.4333 | 0.4811 | 0.3904 | 13.6998 + j2.0967 @bus 9 |
| 0.5 | 0.3 | 0.2 | 0.3174 | 0.4244 | 0.4953 | 0.3851 | 13.445 + j1.8704 @bus 9 |
| 0.5 | 0.4 | 0.1 | 0.3174 | 0.4244 | 0.4954 | 0.378 | 13.4036 + j1.9059 @bus 9 |
| 0.6 | 0.1 | 0.3 | 0.3187 | 0.4334 | 0.4813 | 0.379 | 13.6493 + j2.1401 @bus 9 |
| 0.6 | 0.2 | 0.2 | 0.3185 | 0.4326 | 0.4827 | 0.3742 | 13.6046 + j2.1371 @bus 9 |
| 0.6 | 0.3 | 0.1 | 0.3173 | 0.4245 | 0.4955 | 0.3673 | 13.3757 + j1.9300 @bus 9 |
| 0.7 | 0.1 | 0.2 | 0.3186 | 0.4335 | 0.4815 | 0.3627 | 13.5953 + j2.1865 @bus 9 |
| 0.7 | 0.2 | 0.1 | 0.3173 | 0.4245 | 0.4956 | 0.3566 | 13.3465 + j1.9552 @bus 9 |
| 0.8 | 0.1 | 0.1 | 0.3173 | 0.4245 | 0.4957 | 0.3458 | 13.3242 + j1.9743 @bus 9 |

The analysis of the results in Table 4.14 shows that a change in the value of the weight factors results in a different solution for the multi-objective optimal DG placement and sizing problem. However, all the solutions of the multi-objective DG placement and sizing problem in Table 4.14 are non-dominated with respect to each other. Although the set of weight factors $\mathbf{\{we_1 = 0.8,\ we_2 = 0.1\ and\ we_3 = 0.1\}}$ gives the minimal weighted-sum objective value, there is no indication that this set of weight factors results in the minimal weighted-sum objective value for any distribution system other than the 16-bus distribution system. Therefore, for the remaining part of section 4.5.3., it is recommended to use the combination of weight factors which gives a value of weighted-sum objective closest to the average of the minimum and maximum weighted-sum objective value from Table 4.14. it is calculated as in equation 4.16.

$$\mathbf{Avg\ f} = \frac{\mathbf{max\ f} + \mathbf{min\ f}}{\mathbf{2}} = \frac{0.4534 + 0.3458}{2} = 0.3996 \tag{4.16}$$

Where

$\mathbf{max\ f}$ is the maximum weighted-sum objective value from Table 4.14.

$\mathbf{min\ f}$ is the minimum weighted-sum objective value from Table 4.14.

$\mathbf{Avg\ f}$ is the average of the minimum and maximum weighted-sum objective value from Table 4.14.

The $\mathbf{Avg\ f}$ value is $\mathbf{0.3996}$. The set of weight factors which results in a weighted-sum objective value closest to $\mathbf{0.3996}$ is the set $\mathbf{\{we_1 = 0.3,\ we_2 = 0.6,\ we_3 = 0.1\}}$ which corresponds to the weighted sum value $\mathbf{f}$ of $\mathbf{0.3993}$. This set of weight factors is used for the remainder of section 4.5.3.

#### 4.5.3.2. Results of the developed weighted-sum multi-objective algorithm of the 16-bus distribution system

The developed weighted-sum PSO algorithm is applied to the 16-bus distribution system to solve the multi-objective optimal DG placement and sizing problem. The selected weight factors are $\mathbf{we_1 = 0.3}$, $\mathbf{we_2 = 0.6}$ and $\mathbf{we_3 = 0.1}$. The developed algorithm is tested for the single DG, two-DG and three-DG placement. The simulation results are given in Table 4.15 and the voltage profile of the three case studies is given in Figure 4.14.

**Table 4.15**: **Simulation results of the developed weighted sum PSO algorithm for the 16-bus distribution network**

| **No of DG** | **0** | **1** | **2** | **3** |
|---|---|---|---|---|
| **Transformer power supply in (MVA)** | $8.5830 + j2.9790$ @bus 1<br><br>$15.4901 + j3.9667$ @bus 2<br><br>$5.1409 - j0.0050$ @bus 3 | $8.5830 + j2.9790$ @bus 1<br><br>$1.5627 + j1.4882$ @bus 2<br><br>$5.1409 - j0.0050$ @bus 3 | $2.1812 + j1.2523$ @bus 1<br><br>$1.5625 + j1.4883$ @bus 2<br><br>$5.1409 - j0.0050$ @bus 3 | $-1.3653 - j1.8205$ @bus 1<br><br>$1.5623 + j1.4885$ @bus 2<br><br>$0.4418 - j0.1818$ @bus 3 |
| $\mathbf{f_{1\ norm}}$ | 1 | 0.3178 | 0.1982 | 0.1362 |
| $\mathbf{f_{2\ norm}}$ | 1 | 0.4242 | 0.2321 | 0.0967 |
| $\mathbf{f_{3\ norm}}$ | 1 | 0.4948 | 0.2946 | 0.1406 |
| $\mathbf{f}$ | 1 | 0.3993 | 0.2281 | 0.1129 |
| $\mathbf{P_{Loss}\ (kW)}$ | 514.0293 | 163.3697 | 101.8557 | 70.0560 |
| $\mathbf{minV\ (p.u)}$ | 0.9682 @bus 12 | 0.9848 @bus 7 | 0.9912 @bus 16 | 0.9945 @bus 10 |

| | | | | |
|---|---|---|---|---|
| **maxV (p. u)** | 1 @bus 1 | 1.0017 @bus 9 | 1.0017 @bus 9 | 1.0028 @bus 4 |
| **minVSI** | 0.8766 @bus 12 | 0.9426 @bus 7 | 0.9650 @bus 16 | 0.9762 @bus 9 |
| **maxVSI** | 0.9886 @bus 13 | 0.9960 @bus 12 | 1.0022 @bus 7 | 1.0057 @bus 5 |
| **Optimal DG size (in MVA) and location** | – | 13.5768 + j1.7570 @bus 9 | 6.3402 + j1.5914 @bus 6<br><br>13.577 + j1.7569 @bus 9 | 9.8897 + j4.6648 @bus 4<br><br>13.5772 + j1.7567 @bus 9<br><br>4.6644 + j0.0874 @bus 15 |

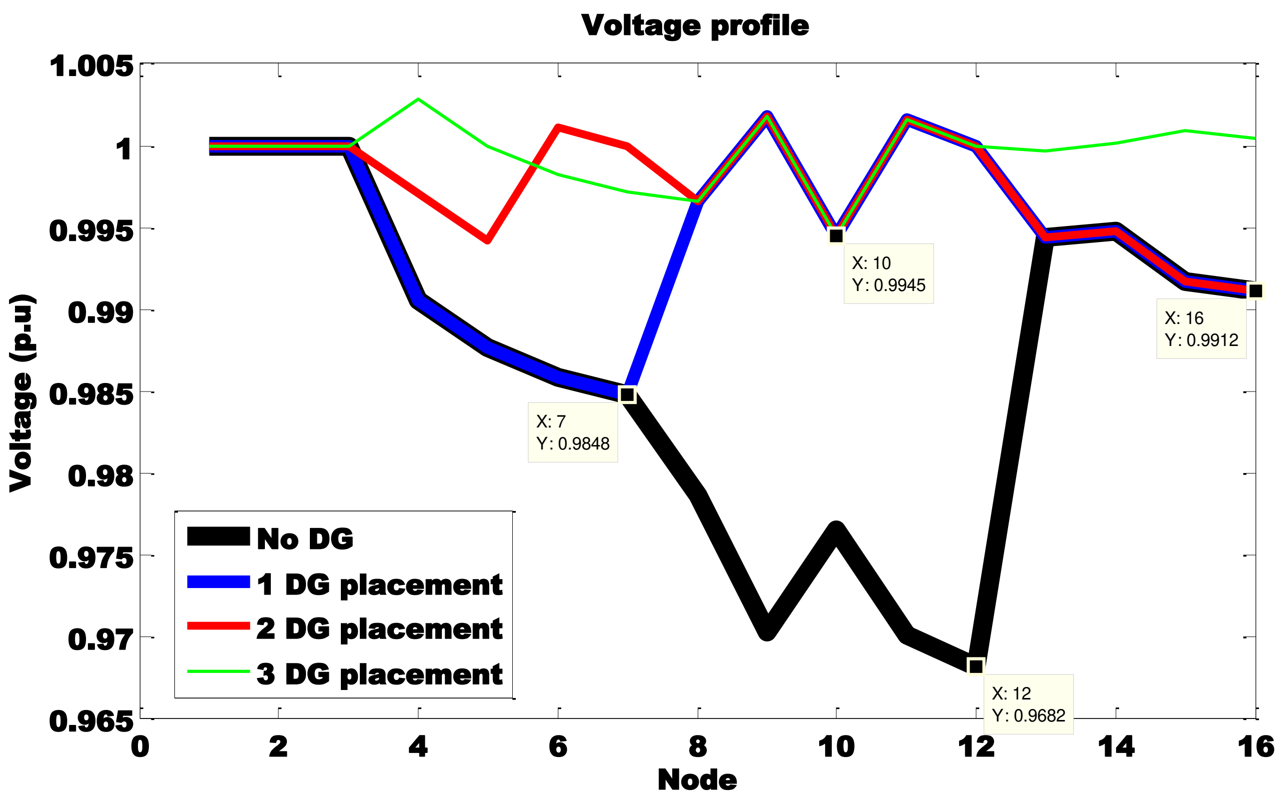


**Figure 4.14**: **Voltage profiles of the 16-bus distribution system for the results of the multi-objective optimal DG placement and sizing problem**

The comparison of the obtained results in Table 4.15 and Figure 4.14 against that of the base case (initial distribution system without DG) shows that the solutions of the developed multi-objective algorithm lead to reduced real power loss, enhanced voltage levels and improved voltage stability in the distribution systems. An increase in the number of DG in the distribution systems results in an increased level of improvements in real power loss, voltage deviation, and voltage stability. This is evidenced by the decrease in the values of $\mathbf{f}_{1\ \mathbf{norm}}$, $\mathbf{f}_{2\ \mathbf{norm}}$ and $\mathbf{f}_{3\ \mathbf{norm}}$ as the number of DG increases. Further analysis of the results from Table 4.15 shows that type III DG are the optimal DG type to solve the multi-objective optimal DG placement and sizing problem.

The optimal DG sizes and locations are:

- $(\mathbf{13.5768 + j1.7570})$ $\mathbf{MVA}$ at $\mathbf{bus\ 9}$ for single DG placement.
- $(\mathbf{6.3402 + j1.5914})$ $\mathbf{MVA}$ at $\mathbf{bus\ 6}$ and $(\mathbf{13.577 + j1.7569})$ $\mathbf{MVA}$ at $\mathbf{bus\ 9}$ for two-DG placement.
- $(\mathbf{9.8897 + j4.6648})$ $\mathbf{MVA}$ at $\mathbf{bus\ 4}$, $(\mathbf{13.5772 + j1.7567})$ $\mathbf{MVA}$ at $\mathbf{bus\ 9}$ and $(\mathbf{4.6644 + j0.0874})$ $\mathbf{MVA}$ at $\mathbf{bus\ 15}$ for the three-DG placement.

### 4.5.3.3. Results of the developed weighted-sum multi-objective algorithm of the 33-bus distribution system

The developed weighted-sum PSO algorithm is applied to the 33-bus distribution system to solve the multi-objective optimal DG placement and sizing problem. The selected weight factors are $\mathbf{we_1 = 0.3}$, $\mathbf{we_2 = 0.6}$ and $\mathbf{we_3 = 0.1}$. The developed algorithm is tested for the single DG, two-DG and three-DG placement. The simulation results are given in Table 4.16. and the voltage profile of the 33-bus distribution system is given in Figure 4.15.

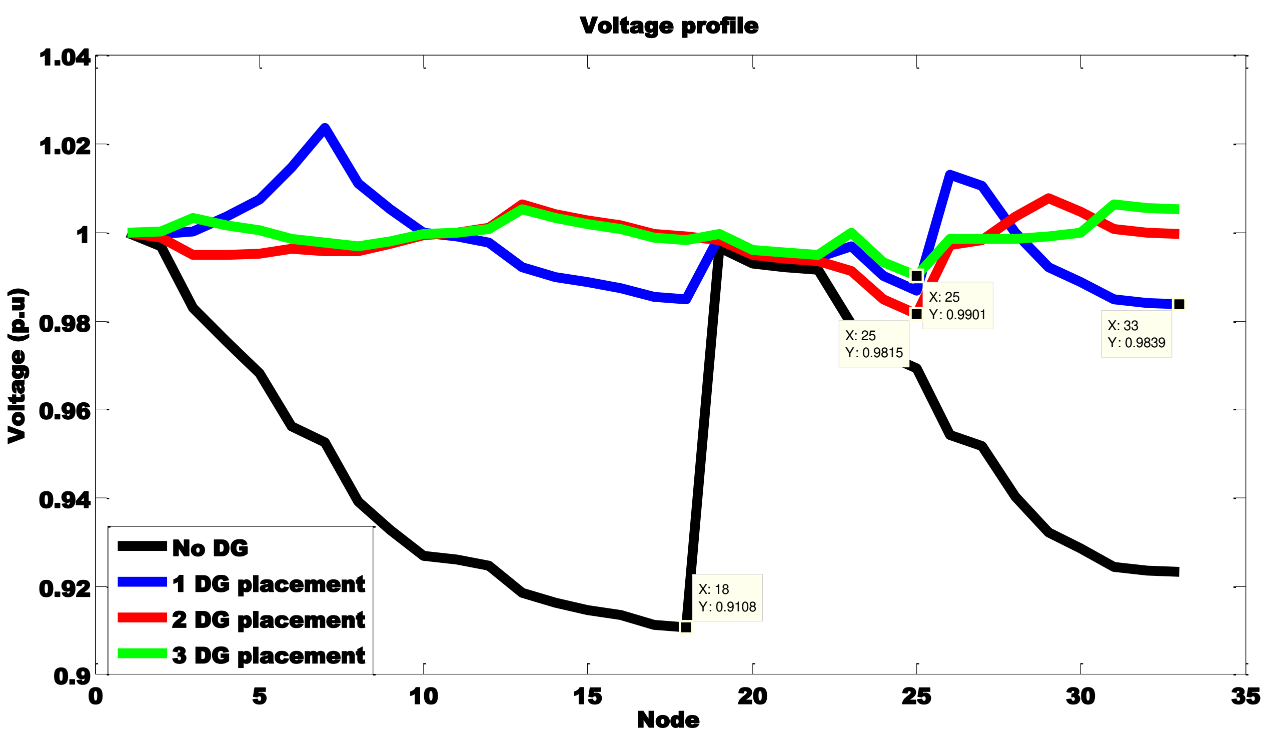


**Figure 4.15**: **Voltage profiles of the 33-bus distribution system for the results of the multi-objective optimal DG placement and sizing problem**

The analysis of the voltage profile in Figure 4.15 shows that the optimisation of DG integration leads to improved voltage levels in the distribution system. The integration of a single DG increases the voltage profile, but the voltage at all buses is closer to the nominal value of 1 p.u only when more DG are integrated into the distribution system.

Table 4.16 provides the results of the optimal placement and sizing of a single-DG, two-DG and three-DG in the 33-bus distribution system. From the table, the optimal DG size and location are as follows:

- $(\mathbf{3.5022 + j2.194})$ $\mathbf{MVA}$ at $\mathbf{bus\ 7}$ for the single DG placement.
- $(\mathbf{0.8698 + j0.4139})$ $\mathbf{MVA}$ at $\mathbf{bus\ 13}$ and $(\mathbf{1.4096 + j1.1294})$ $\mathbf{MVA}$ at $\mathbf{bus\ 29}$ for the placement of two DG.
- $(\mathbf{2.3448 + j1.3862})$ $\mathbf{MVA}$ at $\mathbf{bus\ 3}$, $(\mathbf{0.8119 + j0.3812})$ $\mathbf{MVA}$ at $\mathbf{bus\ 13}$ and $(\mathbf{0.9217 + j0.7873})$ $\mathbf{MVA}$ at $\mathbf{bus\ 31}$ for the placement of three DG.

**Table 4.16**: **Simulation results of the developed weighted sum PSO algorithm for the 33-bus distribution system**

| **No of DG** | **0** | **1** | **2** | **3** |
|---|---|---|---|---|
| **Transformer power supply in (MVA)** | $3.9234 + j2.4117$ @bus 1 | $0.3018 + j0.1875$ @bus 1 | $1.4677 + j0.7801$ @bus 1 | $-0.3393 - j0.2366$ @bus 1 |
| $\mathbf{f_{1\ norm}}$ | 1 | 0.4269 | 0.1542 | 0.1154 |
| $\mathbf{f_{2\ norm}}$ | 1 | 0.1636 | 0.079 | 0.0501 |
| $\mathbf{f_{3\ norm}}$ | 1 | 0.1611 | 0.0869 | 0.0536 |
| $\mathbf{f}$ | 1 | 0.2424 | 0.1023 | 0.07 |
| $\mathbf{P_{Loss}}$ **(kW)** | 208.4322 | 88.9792 | 32.1352 | 24.0519 |
| **minV (p.u)** | 0.9108 @bus 18 | 0.9839 @bus 33 | 0.9815 @bus 25 | 0.9901 @bus 25 |
| **maxV (p.u)** | 1 @bus 1 | 1.0238 @bus 7 | 1.0079 @bus 29 | 1.0064 @bus 31 |
| **minVSI** | 0.6890 @bus 18 | 0.9378@bus 33 | 0.9344@bus 25 | 0.9675 @bus 25 |
| **maxVSI** | 0.9941 @bus 2 | 1.0717 @bus 8 | 1.0254@bus 30 | 1.0242 @bus 32 |
| **Optimal DG size (in MVA) and location** | − | $3.5022 + j2.194$ @bus 7 | $0.8698 + j0.4139$ @bus 13<br>$1.4096 + j1.1294$ @bus 29 | $2.3448 + j1.3862$ @bus 3<br>$0.8119 + j0.3812$ @bus 13<br>$0.9217 + j0.7873$ @bus 31 |

The developed weighted-sum multi-objective PSO algorithm find the optimal DG sizes and locations. The integration of such optimised DG in the 33-bus distribution system leads to an improvement of the voltage deviation, voltage stability and a reduction of real power losses as evidenced by the values of $\mathbf{f_{1\,norm}}$, $\mathbf{f_{2\,norm}}$, $\mathbf{f_{3\,norm}}$ and $\mathbf{f}$ from Table 4.16. In increase of the number of DG leads to further improvements of the operation of the distribution system.

#### 4.5.3.4. Weighted-sum multi-objective algorithm results of the 69-bus distribution system

The developed weighted-sum PSO algorithm is applied to the 69-bus distribution system to solve the multi-objective optimal DG placement and sizing problem. The selected weight factors are $\mathbf{we_1 = 0.3}$, $\mathbf{we_2 = 0.6}$ and $\mathbf{we_3 = 0.1}$. The developed algorithm is tested for the single DG, 2 DG and 3 DG placement. The simulation results are given in Table 4.17 and the voltage profile of the three cases study is given in Figure 4.16.

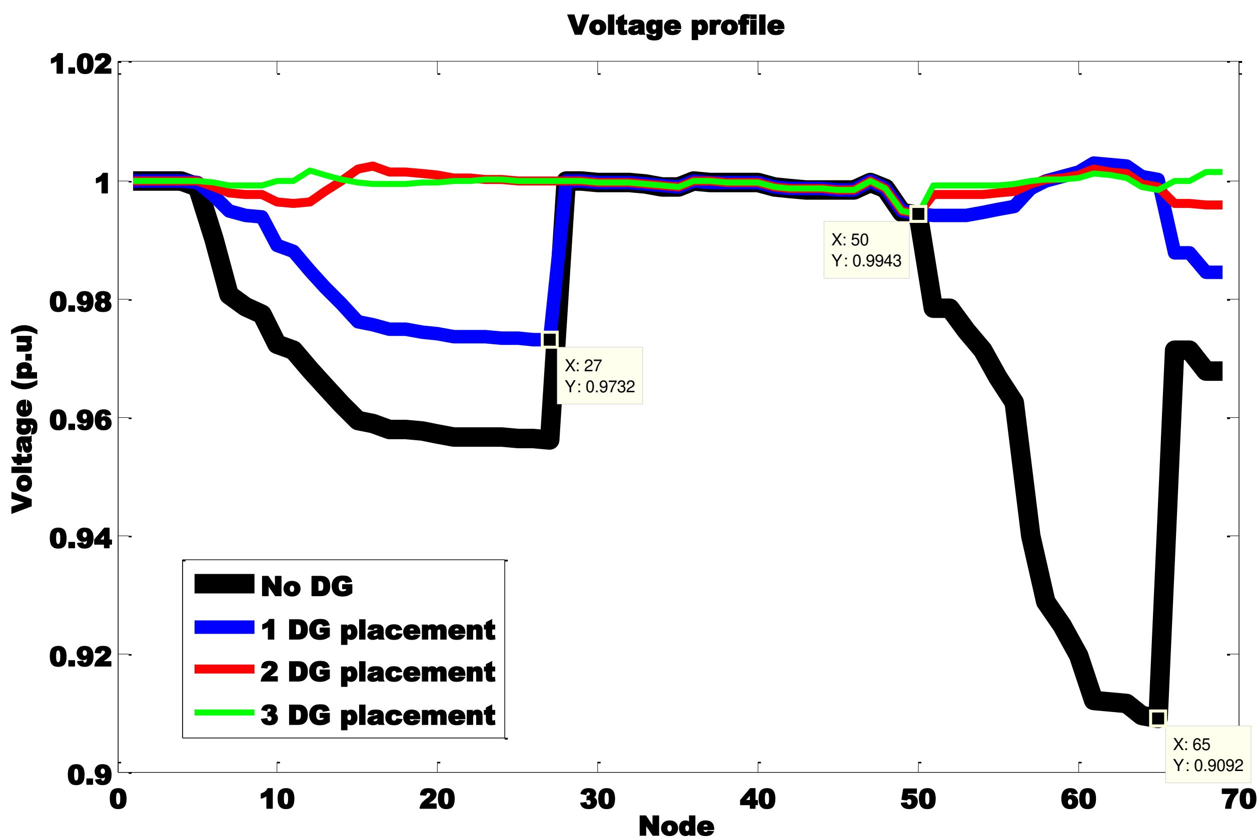


**Figure 4.16**: Voltage profiles of the 69-bus distribution system for the results of the multi-objective optimal DG placement and sizing problem

**Table 4.17**: Simulation results of the developed weighted sum PSO algorithm for the 69-bus distribution network

| No of DG | 0 | 1 | 2 | 3 |
|---|---|---|---|---|
| Transformer power supply in (MVA) | 4.0268 + j2.7968 @bus 1 | 1.9461 + j1.2888 @bus 1 | 1.4532 + j1.0337 @bus 1 | 1.2573 + j0.8405 @bus 1 |
| $f_{1\ norm}$ | 1 | 0.1055 | 0.0339 | 0.0216 |
| $f_{2\ norm}$ | 1 | 0.3045 | 0.0522 | 0.0267 |
| $f_{3\ norm}$ | 1 | 0.3243 | 0.0583 | 0.0273 |
| f | 1 | 0.2468 | 0.0473 | 0.0252 |
| $P_{Loss}$ (kW) | 224.9804 | 23.7253 | 7.62 | 4.8645 |
| minV (p.u) | 0.9092 @bus 65 | 0.9732 @bus 27 | 0.9943 @bus 50 | 0.9943 @bus 50 |
| maxV (p.u) | 1 @bus 1 | 1.0030 @bus 61 | 1.0024 @bus 16 | 1.0017 @bus 12 |
| minVSI | 0.6842 @bus 65 | 0.8970 @bus 27 | 0.9783 @bus 50 | 0.9784 @bus 50 |
| maxVSI | 0.9999 @bus 2 | 1.0116 @bus 62 | 1.0079 @bus 17 | 1.0061 @bus 68 |
| Optimal DG size (in MVA) and location | – | 1.8795 + j1.4202 @bus 61 | 0.5792 + j0.4279 @bus 16<br>1.7771 + j1.2411 @bus 61 | 0.6106 + j0.399 @bus 12<br>0.2552 + j0.1962 @bus 23<br>1.6836 + j1.2659 @bus 61 |

The analysis of the obtained results in Table 4.17 and Figure 4.16 against the base case (initial distribution system with no DG) results shows that just like in the case of the 16-bus and the 33-bus distribution systems, the developed weighted-sum multi-objective algorithm finds the optimal DG sizes and locations for increased performance in the 69-bus distribution systems.

The optimal DG sizes and locations are as follows:

- $(\mathbf{1.8795 + j1.4202})$ **MVA** at **bus 61** for the single DG placement.
- $(\mathbf{0.5792 + j0.4279})$ **MVA** at **bus 16** and $(\mathbf{1.7771 + j1.2411})$ **MVA** at **bus 61** for the placement of two DG.
- $(\mathbf{0.6106 + j0.399})$ **MVA** at **bus 12**, $(\mathbf{0.2552 + j0.1962})$ **MVA** at **bus 23** and $(\mathbf{1.6836 + j1.2659})$ **MVA** at **bus 61** for the placement of three DG.

The integration of multiple DG yields better results than the integration of a single DG. As shown in Table 4.17, the values of the normalised objective functions $\mathbf{f_{1\ norm}}$, $\mathbf{f_{2\ norm}}$,

$\mathbf{f_{3\ norm}}$ and that of the weighted-sum objective value $\mathbf{f}$ decrease as the number of DG increases. Furthermore, Figure 4.16 shows that the 69-bus distribution network with three DG has a better voltage profile in comparison to the other case studies.

### 4.5.4. Discussion of the results of the developed Weighted-sum PSO algorithm for the multi-objective optimal DG placement and sizing problem

The results of the application of the developed weighted sum PSO algorithm to solve the multi-objective optimal DG placement and sizing problem on the 16-bus, the 33-bus and the 69-bus distribution systems provide the optimal DG sizes and positions that result in a reduced real power loss, improved voltage profiles and enhanced voltage stability. These results are given in Tables 4.15, 4.16, and 4.17 respectively. The solutions of multi-objective algorithm show that the more the number of optimally placed DG, the more the level of improvements in the operation of the distribution systems. A change in the value of the weight factors would affect the optimal DG size and probably the optimal position of the DG. Although the change of weight factors in the developed weighted-sum PSO algorithm as seen in Table 4.14 yields no effect on the optimal DG position for the 16-bus distribution system, further studies should be done to ascertain whether a change of the weight factors could affect the optimal DG position in other distribution systems. Based on the analysis of the effects of the weight factors on the solutions of the optimal DG placement and sizing problem for the 16-bus distribution system, it is observed that for any set of strictly positive weight factors $\{\mathbf{we_1}, \mathbf{we_2}, \mathbf{we_3}\}$ where the sum of the weight factors is equal to 1, the solutions of the multi-objective optimal DG placement and sizing problem are non-dominated with respect to each other.

The comparison of the results of the single and multi-objective optimal DG placement and sizing problem shows that the real power loss is minimal for the single-objective DG placement and sizing problem. This can be explained by the fact that since the objectives of the multi-objective optimal DG placement and sizing problem were conflicting, a compromise had to be reached between the objective functions.

## 4.6. Conclusion

In this chapter, PSO optimisation approaches were developed to solve both the single-objective and the multi-objective optimal DG placement and sizing problems. The single-objective problem aimed to minimise the real power loss in distribution systems. The multi-objective problem aimed to minimise the real power loss, minimise the voltage deviation and maximise the bus voltage stability index in radial distribution systems. To solve the multi-objective optimisation problem, the developed PSO based algorithm uses the weighted-sum approach to aggregate the set of objective functions into a single-objective function. For both the single-objective and the multi-objective optimal DG placement and sizing problem, the developed PSO algorithms were tested on the 16-bus, the 33-bus, and the 69-bus distribution systems. The results of the developed PSO algorithms were compared to the results from the literature. It follows that the developed PSO algorithms provide better solutions to both the single-objective and the multi-objective optimal DG placement and sizing problems.

Chapter three and this chapter dealt with the development of PSO based algorithms to solve the optimal distribution network reconfiguration problem and the optimal DG placement & sizing problem, respectively, under constant loading conditions. The next chapter assesses the performance of the developed PSO algorithms under dynamic loading conditions.

# CHAPTER FIVE

# DISTRIBUTION NETWORK FEEDER RECONFIGURATION AND DISTRIBUTED GENERATORS PLACEMENT & SIZING UNDER DYNAMIC LOADING CONDITIONS

## 5.1. Introduction

Feeder reconfiguration and DG deployment are the two main approaches used to minimise the real power loss in distribution networks. In feeder reconfiguration, the real power loss is minimized by altering the status of tie and section switches of the distribution network. When the DG is present in a distribution network, most of the DG power produced is consumed at local points of connections to reduce the amount of power flow in the distribution network and the real power loss. PSO solution algorithms were developed in chapter three and chapter four to solve the optimal distribution network feeder reconfiguration and the optimal DG placement & sizing problems respectively. This chapter compares the performance of both distribution network feeder reconfiguration and DG allocation in minimising the real power losses in distribution networks under constant and dynamic loading conditions.

Based on the results from chapters three and four, the operation of a distribution network with a feeder reconfiguration scheme and a distribution network with DG is compared. Then, sequential and parallel computing solutions are developed to analyse the performance of the distribution network with a feeder reconfiguration scheme for a period of 24 hours under dynamic loading conditions. The sequential programming solution is used to analyse the operation of a distribution network with DG for a period of 24 hours under dynamic loading conditions. Finally, a conclusion is made regarding the use of both the optimal distribution network feeder reconfiguration and the optimal DG allocation to reduce the real power loss in distribution networks under dynamic loading conditions.

## 5.2. Optimal feeder reconfiguration versus DG placement for minimising real power losses in distribution networks under constant loading conditions

Chapter three and chapter four provide the PSO solution algorithms for both the optimal DG placement & sizing and the optimal distribution network feeder reconfiguration problems. The optimisation results obtained in respective chapters three and four for the 16-bus distribution network are given in Table 5.1. The voltage profile results of the 16-bus distribution network under constant loading conditions are shown in Figure 5.1.

**Table 5.1**: DG placement versus feeder reconfiguration optimisation solutions of the 16-bus distribution network under constant loading conditions

| Description | Base case | After reconfiguration | After DG deployment |
|---|---|---|---|
| Total generation (MVA) | $29.2140 + j6.9407$ | $29.1683 + j6.8733$ | $15.8172 + j4.4765$ |
| Source transformer supply (MVA) | $8.5830 + j2.9790$ @bus 1<br>$15.4901 + j3.9667$ @bus 2<br>$5.1409 - j0.0050$ @bus 3 | $9.1925 + j2.5062$ @bus 1<br>$13.8188 + j3.4329$ @bus 2<br>$6.1570 + j0.9343$ @bus 3 | $8.5830 + j2.9790$ @bus 1<br>$2.0934 + j1.5025$ @bus 2<br>$5.1409 - j0.0050$ @bus 3 |
| Tie switches | 14 15 16 | 7 8 16 | 14 15 16 |
| Real power loss (kW) | 514.0293 | 468.3304 | 162.8352 |
| Real power loss reduction (%) | – | 8.89033 | 68.3218 |
| Minimum voltage (p.u) | 0.9682 @bus 12 | 0.9707 p.u @ bus 12 | 0.9848 @bus 7 |
| Maximum voltage (p.u) | 1 @ bus 1, 2 & 3 | 1 @ bus 1 | 1.0007 @bus 9 |
| DG size (MVA) & position | – | – | $13.0456 + j1.7526$ @bus 9 |

The results given in Table 5.1 show that under constant loading conditions, optimal single-DG deployment in the distribution network outperforms the optimal reconfiguration of the distribution networks in reducing the real power losses.

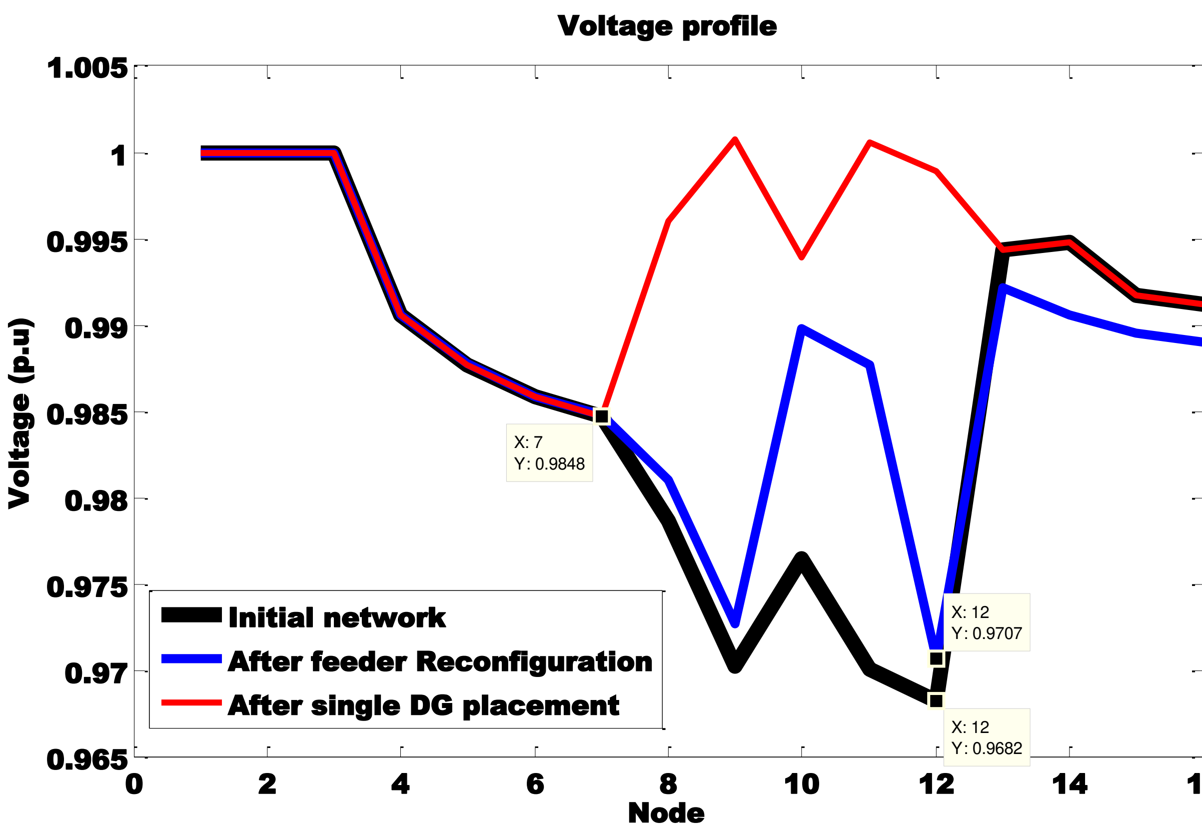


**Figure 5.1**: Voltage profile of the 16-bus distribution network after the optimal feeder reconfiguration and the DG placement under constant loading conditions

The improvement of the voltage profile in the distribution network as shown in Figure 5.1 is more pronounced in the case of optimal DG placement. However, the loads in distribution networks are dynamic in nature, meaning that they vary in function of the weather conditions, time of the day, month and the activity of the end-users. Taking into consideration the dynamic nature of the loads, the research question is: ***"Will the optimal deployment of a single DG still be more efficient than optimal feeder reconfiguration in reducing the real power loss in distribution networks with dynamic loads?"***

The next section of this chapter investigates the daily performance of the distribution network with feeder reconfiguration under dynamic loading conditions

## 5.3. Development of a PSO based algorithm to analyse the performance of a distribution network with feeder reconfiguration under dynamic loading conditions

In the electrical power engineering field, distribution feeder reconfiguration falls under network operation and management, meaning that the optimal network topology at a given period is dependent on the operating load and voltage levels. On the other hand, optimal DG placement falls under electrical network planning. This means that the optimal location and DG size are found beforehand, and once the DG is deployed into the network, its position and maximum size are not changed. Therefore, it is necessary to investigate the impact of dispatchable and non-dispatchable DG in the optimal DG placement and sizing.

### 5.3.1. Description of the power demand profile

The load profile is a representation of the variation of the loads in the distribution network over time. The base load is the minimum power demand in the distribution network over a timeframe while the peak load is the maximum power demand in the same timeframe. Figure 5.2 shows the load profile which is used to assess the performance of distribution network feeder reconfiguration and DG allocation in the 16-bus distribution network under dynamic loading conditions. The total real power demand is measured in $\mathrm{kW}$ for a typical summer and winter day. An analysis of the load profile given in Figure 5.2 shows that the baseload is approximately $\mathbf{25\,MW}$ and $\mathbf{24\,MW}$ for the winter and summer day, respectively. The approximate load demand peaks at $\mathbf{36.5\,MW}$ and $\mathbf{32\,MW}$ in the winter and summer day, respectively. The load profile in Figure 5.2 is for a period exceeding a day. This research work only considers the portion of the load profile that represents a 24-hour load demand.

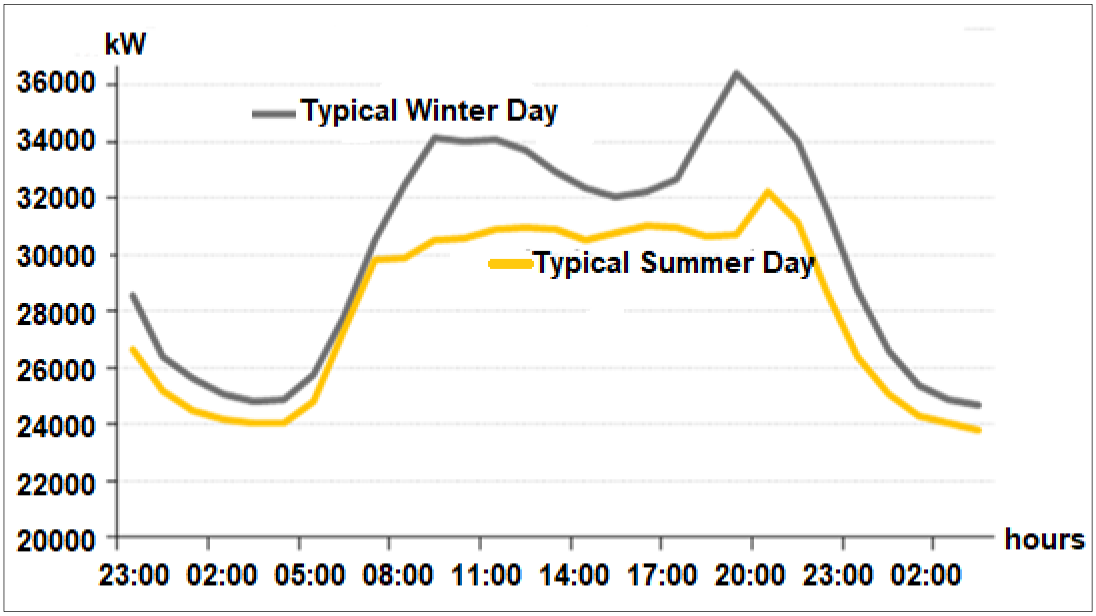


**Figure 5.2**: **Typical summer and winter daily load profile of the 16-bus distribution network (Matona, 2014)**

According to the load profile in Figure 5.2, in the winter day, we observe an increase in the load demand in the early morning up to $09{:}30\ \mathrm{a.m}$. The demand is stable after $09{:}30\ \mathrm{a.m}$ until approximately midday, where it decreases for the whole afternoon. The evening gives rise to the demand until $7\mathrm{p.m}$ where the demand reaches its peak. At night, the load demand decreases continuously, until it reaches its base load.
In the summer day, the load demand increases from 05:00 am throughout the morning. The demand is tight for the rest of the day, and it starts decreasing at night, after $10\ \mathrm{p.m}$.

The difference in loading between the winter and the summer can be explained by the difference in consumers' behaviour, arising as a result of the difference in the weather conditions. Electricity is requested for cooling during the summer while in the winter, it is used for heating. Cooling is usually needed from late in the morning to late in the afternoon whereas, in winter, heating is required for almost the whole day. Additionally, because the daytime is reduced in winter, there is an increased load demand due to the early switch on of lightings.

The winter load profile of the distribution network is used in this study because the loads are more dynamic in winter than in summer. As a consequence of this load dynamism, the power ought to be dispatched to balance the distribution system by matching the power supply to the power demand. In the IEEE 16-bus distribution network, the power is dispatched through source transformers 1, 2 and 3. To match the power demand, generators may be dispatched at time intervals varying from seconds to hours. So, to evaluate the performance of the algorithms for a full day, the day could be divided into time intervals, depending on the load demand. The higher the number of time intervals, the more the numbers of simulations required. As an example, dispatching the power every 15 minutes for a full day results in 96 (24 hours divided by 15 minutes) simulations being done, which is quite time-consuming if the simulations are computed sequentially. **One way to reduce this computational burden is the use of parallel computing**.

The next section presents the sequential computing solution algorithm to assess the daily performance of a distribution network with a feeder reconfiguration scheme and under dynamic loading conditions.

### 5.3.2. Sequential computation of the PSO-based solution algorithm to analyse the performance of a distribution network with a feeder reconfiguration scheme under dynamic loading conditions

The operation of electrical distribution networks is a dynamic process. To estimate the daily real power loss in the distribution network, the power flow needs to be performed and the real power loss calculated at time intervals. The lower the time interval, the more accurate the daily power loss. Given that the distribution lines have a fixed impedance, the power loss in the distribution network is dependent on the loading of the network. The higher the loading, the higher the real power loss in the distribution network. So, to determine the power loss in the distribution network, the real and reactive power demand at each PQ bus should be known. Figure 5.2 shows the total daily winter real power demand in the distribution network. But, it does not provide the power demand at each PQ bus. Therefore, it is necessary to determine the real and reactive power demand at each PQ bus. Equations 5.1 and 5.2 are developed and used to calculate the real and reactive power demand at a given PQ bus, respectively.

$$\mathbf{Pd_i}^{\mathbf{t}} = \mathbf{Rand_i} \cdot \mathbf{P_d}^{\mathbf{t}} \cdot \left(\sum_{\mathbf{i=1}}^{\mathbf{nPQ}} \mathbf{Rand_i}\right)^{-\mathbf{1}} \tag{5.1}$$

$$\mathbf{Qd_i}^{\mathbf{t}} = \mathbf{Pd_i}^{\mathbf{t}} \cdot \frac{\mathbf{Q_{init}}}{\mathbf{P_{init}}} \tag{5.2}$$

Where,

$\mathbf{Pd_i}^{\mathbf{t}}$ and $\mathbf{Qd_i}^{\mathbf{t}}$ are the real and reactive power demand respectively at PQ bus $\mathbf{i}$ at instant $\mathbf{t}$.

$\mathbf{P_d}$ is the total real power demand in the network at instant $\mathbf{t}$.

$\mathbf{P_{init}}$ and $\mathbf{Q_{init}}$ are the initial real and reactive power demand respectively in the network.

$\mathbf{Rand_i}$ is a uniformly distributed random number in the interval ]0,1[.

$\mathbf{nPQ}$ is the number of $\mathbf{PQ}$ buses in the distribution network.

The random element $\mathbf{Rand_i}$ in Equation 5.1 is to ensure that the load demand at each PQ bus stays dynamic. The real and reactive power demand at each PQ bus at a given time $\mathbf{t}$ is calculated using Equations 5.1 and 5.2 respectively, and it is given in Tables 5.3 and 5.4.

The following assumptions are considered:

- The real power demand at each bus is calculated using Equation 5.1, in such a way that the sum of the calculated real power demand at each PQ bus corresponds to the total power demand from the daily winter load profile in Figure 5.2. Figure 5.2 is used as a reference model to create the dynamic loading conditions of the distribution network. Figure 5.3 approximates the reference model in Figure 5.2, and it is plotted using the variation of load demand data given in Table 5.2. The calculated real and reactive power demand at each PQ bus is given in Table 5.3 and 5.4, respectively.

- The real power demand is measured, and the real and reactive powers at each PQ bus are calculated every time there is an increase or decrease of $\pm 500$ kW in the daily winter load from Figure 5.2. The rate of change threshold $\mathrm{dp}$ ($\pm 500$ kW) of the real power demand is only considered for simulation purposes. Power utilities usually use the load profile to determine how much power is needed at a given time.

- An identical real power demand between two distinct points A and B of the winter daily load profile means that at the times $\mathbf{t_A}$ and $\mathbf{t_B}$, the total real power demand is the same. However, the real power demand at individual PQ bus may be different.

The change of load demand in small intervals of time is considered to have no significant impact on the distribution network topology. Likewise, when feeder reconfiguration is performed to minimise the real power loss in the distribution network, it is unlikely that small changes in load demand would impact the result of the feeder reconfiguration process.

The sequential programming solution to evaluate the daily performance of a distribution network with a feeder reconfiguration scheme and under dynamic loading conditions is as follows:

**Step 1**: Read the electrical distribution network data such as the number of nodes $\mathbf{NB}$, the number of distribution lines $\mathbf{NL}$, the number of tie lines $\mathbf{NT}$, the bus type ($\mathbf{Slack}, \mathbf{PV}, \mathbf{PQ}$), the load data ($\mathbf{Pd_i}^{\mathbf{t}}, \mathbf{Qd_i}^{\mathbf{t}}, \mathbf{Bs}, \mathbf{Load\_ID}$), the generator data ($\mathbf{Pg}, \mathbf{Qg}$) and distribution line data ($\mathbf{bus\_i}, \mathbf{bus\_j}, \mathbf{r}, \mathbf{x}, \mathbf{sw\_tie}, \mathbf{sw\_sec}$).

**Step 2**: Set the threshold rate of power change $\mathbf{dp}$. The power demand is dependent on the time of the day. The power demand may be constant or have a flat profile for a period of time. So, it may take a while before any significant real and reactive power demand change occurs at each PQ bus. The rate of power change threshold ($\pm\,\mathbf{500\,kW}$) determines the amount of total real power increase/decrease that should occur in the load profile before the next measurement is done.

**Step 3**: Find the total load demand in the distribution network at each time interval for the 24h period.

Figure 5.2 given in section 5.3.1 has approximately 12 slopes, each slope representing a different rate of change of the power demand over time. Details on the different slopes are given in Table 5.2. The rate of change of the power demand over time of a slope is the difference of the change of power divided by the difference of time of the corresponding period. The number of datasets for each period is the number of times the real and the reactive power demand at each PQ bus is calculated over the corresponding period.

The diagonal downward right arrow (↘) indicates a descending slope, which means that the power is decreasing at the corresponding rate of change and period. The diagonal upward right arrow (↗) indicates an ascending slope, which means that the power is increasing. The right arrow (→) indicates that the power is constant for that corresponding period.

Figure 5.3 provides the approximate winter day load profile.

**Table 5.2**: Change of the total power demand with respect to time

| Slope | Period | | Change of power demand $(MW)$ | | Rate of change of power demand with respect to time $(MW/min)$ | | Number of datasets for each period |
|---|---|---|---|---|---|---|---|
| | From | To | From | To | | | |
| 1 | 23h00 | 00h06 | 28.7 | 26.36 | 39/1100 | ↘ | **5** |
| 2 | 00h06 | 02h00 | 26.36 | 25.1 | 21/1900 | ↘ | **3** |
| 3 | 02h00 | 04h03 | 25.1 | 25 | 1/1230 | ↘ | **1** |
| 4 | 04h03 | 05h00 | 25 | 26 | 1/57 | ↗ | 2 |
| 5 | 05h00 | 06h55 | 26 | 30 | 4/115 | ↗ | 8 |
| 6 | 06h55 | 08h57 | 30 | 34 | 2/61 | ↗ | 8 |
| 7 | 08h57 | 11h00 | 34 | 34 | 0 | → | 1 |
| 8 | 11h00 | 14h57 | 34 | 32 | 2/237 | ↘ | **4** |
| 9 | 14h57 | 17h00 | 32 | 32.73 | 73/12300 | ↗ | 2 |
| 10 | 17h00 | 18h55 | 32.73 | 36.5 | 377/11500 | ↗ | 8 |
| 11 | 18h55 | 20h57 | 36.5 | 34 | 5/244 | ↘ | **5** |
| 12 | 20h57 | 23h00 | 34 | 28.73 | 527/12300 | ↘ | **10** |

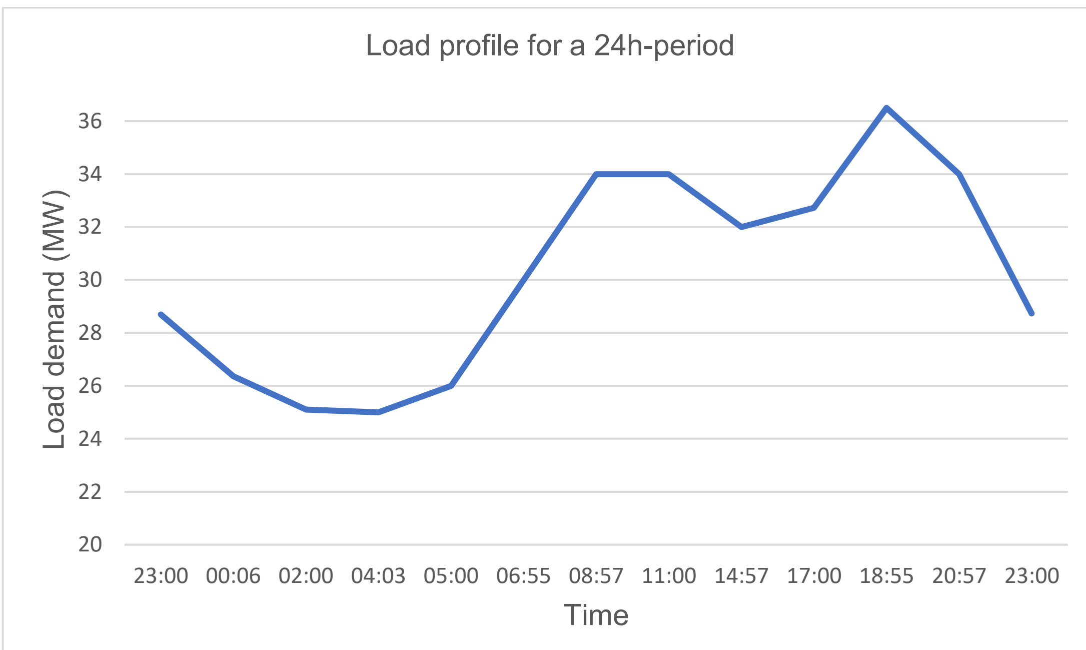


**Figure 5.3**: Plotted winter daily load profile

**Step 4**: Determine the load demand $\mathbf{Pd_i}^{t}$ and $\mathbf{Qd_i}^{t}$ at each PQ bus in the distribution network every time the total real power from Figure 5.2 increases/decreases by $500\text{kW}$. The total real power demand for the different periods was determined in Step 3 (see Table 5.2). Equations 5.1 and 5.2 are used to calculate the real and the reactive power demand

at each PQ bus in the distribution network, and the results are given in Table 5.3 and 5.4 for the real and reactive power demand at each PQ bus, respectively.
The real power results from Table 5.3 and the reactive power results from Table 5.4 are saved in the repertoire $\mathbf{P\_rep}$ and $\mathbf{Q\_rep}$, respectively in the MATLAB coding.

**Start the iteration process** and set the iteration counter $\mathbf{k}$ to 1. The iteration counter counts the number datasets that go through the iterative process.

**Step 5**: Read the real and reactive power demand $\mathbf{Pd_i}^{\mathbf{t}}$ and $Qd_i{}^t$ at each bus at time $\mathbf{t}$ from $\mathbf{P\_rep}$ and $\mathbf{Q\_rep}$, respectively (**dataset** $\mathbf{k}$), and update the load demand in the distribution network.

**Step 6**: The PSO algorithm developed in chapter three, section 3.5.2. to solve the single objective distribution network feeder reconfiguration problem is used to create a function $\mathrm{spmd1}$ which takes the distribution network data (the number of nodes $\mathbf{NB}$, the number of distribution lines $\mathbf{NL}$, the number of tie lines $\mathbf{NT}$, the bus type ($\mathbf{Slack}, \mathbf{PV}, \mathbf{PQ}$), the load data ($\mathbf{Pd_i}^{\mathbf{t}}, \mathbf{Qd_i}^{\mathbf{t}}, \mathbf{Bs}, \mathbf{Load\_ID}$), the generator data ($\mathbf{Pg}, \mathbf{Qg}$) and distribution line data ($\mathbf{bus\_i}, \mathbf{bus\_j}, \mathbf{r}, \mathbf{x}, \mathbf{sw\_tie}, \mathbf{sw\_sec}$)) as inputs, and returns the solution of the distribution network feeder reconfiguration optimization process as outputs.
Using the function $\mathbf{spmd1}$, run the optimal feeder reconfiguration algorithm and determine the real power loss $\mathbf{Ploss\_in}$; the minimum voltage $\mathbf{minV_{in}}$; the maximum voltage $\mathbf{maxV\_in}$ before reconfiguration, and the real power loss $\mathbf{fitness\_Gbest}$; the minimum voltage $\mathbf{Vmin\_Gbest}$; the maximum voltage $\mathbf{Vmax\_Gbest}$ after the reconfiguration process.

**Step 7**: Save the results from Step 6 in the **repertoire** $\mathbf{y}$. The **repertoire y** is created to save the results of Step 6 for each dataset.

**Step 8**: Stop the iteration or increment the iteration counter. If step 5 to step 7 are performed for all data set from step 4, then stop the iterative process. Else, increment the iteration count and repeat step 5 to step 7.

**Step 9**: Print the results of the sequential programming algorithm to evaluate the daily performance of a distribution network with a feeder reconfiguration scheme and under dynamic loading conditions. At the end of the simulations, the results saved in Step 7 should be retrieved and analysed.

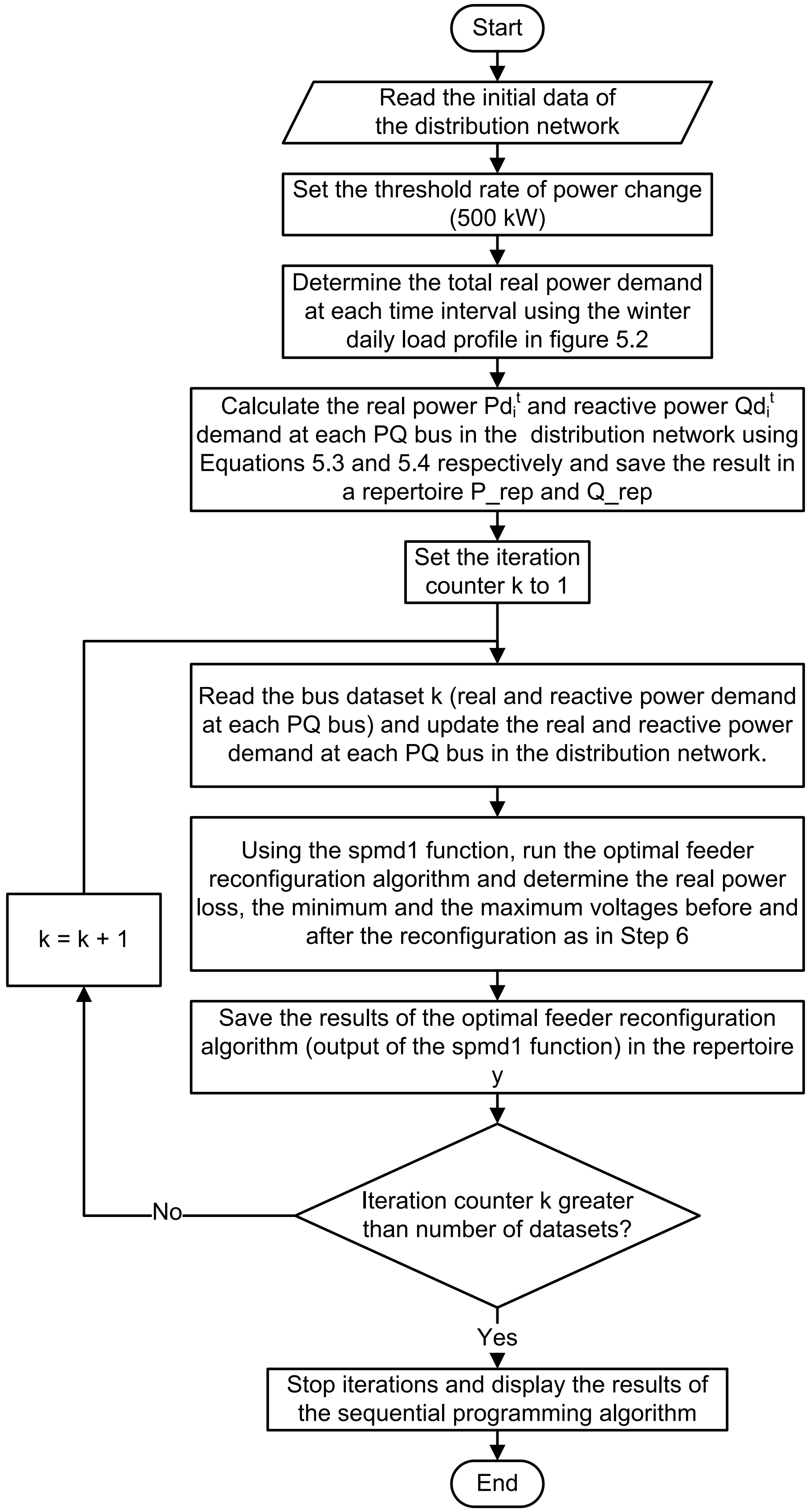


**Figure 5.4**: **Flowchart of the sequential programming solution algorithm to assess the daily winter performance of the distribution network with a feeder reconfiguration scheme under dynamic loading conditions**

**Table 5.3**: **Load bus real power data sets in the repertoire $P\_rep$ calculated using Equation 5.1**

| Bus N°. / Data set N°. | 1 | 2 | 3 | 4 | 5 | 6 | 7 | 8 | 9 | 10 | 11 | 12 | 13 | 14 | 15 | 16 | $\sum Pd_i^t$ |
|---|---|---|---|---|---|---|---|---|---|---|---|---|---|---|---|---|---|
| 1 | 0 | 0 | 0 | 3.2385 | 1.5406 | 3.3821 | 2.0451 | 3.2005 | 2.1372 | 0.0941 | 2.4338 | 4.3120 | 1.5104 | 0.0786 | 2.7889 | 1.9382 | 28.7 |
| 2 | 0 | 0 | 0 | 1.1733 | 2.2446 | 3.7667 | 1.5471 | 2.2456 | 5.0678 | 4.3808 | 0.2420 | 1.7575 | 0.2363 | 0.5193 | 4.8726 | 0.1465 | 28.2001 |
| 3 | 0 | 0 | 0 | 2.8512 | 2.6248 | 2.9452 | 2.4819 | 2.7791 | 2.9754 | 1.6177 | 2.8953 | 0.6893 | 2.0474 | 0.1712 | 2.3721 | 1.2493 | 27.6999 |
| 4 | 0 | 0 | 0 | 0.0909 | 0.4704 | 3.3955 | 0.5234 | 2.8820 | 3.1320 | 0.5920 | 3.0904 | 2.9599 | 2.0192 | 3.1584 | 3.1861 | 1.6999 | 27.2001 |
| 5 | 0 | 0 | 0 | 2.9136 | 2.9995 | 4.8632 | 1.4228 | 2.2620 | 5.0013 | 0.1031 | 0.6083 | 1.8705 | 2.3157 | 0.3237 | 0.6325 | 1.3839 | 26.7001 |
| 6 | 0 | 0 | 0 | 2.5081 | 1.5390 | 2.7180 | 1.9146 | 3.4540 | 0.2965 | 1.0674 | 1.6190 | 2.0538 | 1.4617 | 2.1898 | 2.6323 | 2.9094 | 26.3636 |
| 7 | 0 | 0 | 0 | 2.9704 | 1.2875 | 2.8266 | 2.4234 | 1.2842 | 3.4933 | 0.5220 | 0.2622 | 1.6174 | 1.7654 | 3.2239 | 3.8629 | 0.3244 | 25.8636 |
| 8 | 0 | 0 | 0 | 0.8020 | 2.0245 | 2.8537 | 0.5262 | 4.1591 | 3.3242 | 0.5617 | 3.1486 | 1.6870 | 0.4087 | 2.2623 | 1.1896 | 2.4160 | 25.3636 |
| 9 | 0 | 0 | 0 | 3.2033 | 2.2261 | 0.7800 | 3.3536 | 0.0267 | 1.8366 | 3.9078 | 2.6608 | 1.0425 | 2.3531 | 0.0215 | 2.0848 | 1.6031 | 25.0999 |
| 10 | 0 | 0 | 0 | 1.4852 | 2.7427 | 3.0139 | 3.0800 | 3.1485 | 1.3521 | 1.1816 | 1.6575 | 0.3736 | 1.3031 | 2.7098 | 2.5667 | 0.3853 | 25 |
| 11 | 0 | 0 | 0 | 0.3441 | 1.3326 | 2.0812 | 4.4266 | 0.8169 | 1.3811 | 1.1419 | 3.3279 | 2.3632 | 2.4739 | 3.5341 | 1.7529 | 0.5236 | 25.5 |
| 12 | 0 | 0 | 0 | 3.1347 | 2.1040 | 3.1151 | 0.6773 | 0.7617 | 1.5785 | 0.7000 | 2.2183 | 1.8241 | 0.4304 | 3.4446 | 3.1487 | 2.8628 | 26.0002 |
| 13 | 0 | 0 | 0 | 0.9062 | 2.6279 | 3.7726 | 1.1388 | 2.9447 | 1.7952 | 3.7555 | 1.8119 | 0.2727 | 1.5486 | 2.7947 | 2.8380 | 0.2932 | 26.5 |
| 14 | 0 | 0 | 0 | 0.7272 | 2.3703 | 1.8387 | 3.0308 | 3.1288 | 1.0655 | 2.7572 | 2.6680 | 2.5921 | 2.9854 | 1.0456 | 1.4869 | 1.3036 | 27.0001 |
| 15 | 0 | 0 | 0 | 0.8356 | 0.1659 | 1.0898 | 3.2341 | 1.5830 | 1.0681 | 0.3883 | 3.5796 | 2.9014 | 3.4226 | 3.5318 | 2.5031 | 3.1969 | 27.5002 |
| 16 | 0 | 0 | 0 | 3.3936 | 1.2616 | 0.2166 | 2.2422 | 1.9721 | 3.5403 | 1.4750 | 3.2893 | 3.5881 | 1.3134 | 3.6899 | 0.7560 | 1.2619 | 28 |
| 17 | 0 | 0 | 0 | 1.1730 | 0.1370 | 2.7977 | 1.9638 | 1.4031 | 4.0468 | 2.6381 | 1.4617 | 5.5283 | 2.5490 | 0.0433 | 2.7273 | 2.0309 | 28.5 |
| 18 | 0 | 0 | 0 | 2.0105 | 1.1532 | 1.3525 | 3.3675 | 2.5585 | 3.1930 | 1.1526 | 1.3434 | 3.0437 | 0.6820 | 3.3390 | 2.5689 | 3.2351 | 28.9999 |
| 19 | 0 | 0 | 0 | 3.2574 | 3.2658 | 1.4986 | 2.8242 | 0.4872 | 2.0865 | 2.1304 | 2.2323 | 3.5229 | 3.0272 | 0.0362 | 2.3678 | 2.7635 | 29.5 |
| 20 | 0 | 0 | 0 | 2.1039 | 2.7621 | 3.7217 | 1.1324 | 3.1210 | 3.6687 | 1.1202 | 3.7448 | 3.4519 | 0.0183 | 1.0874 | 1.8494 | 2.2180 | 29.9998 |
| 21 | 0 | 0 | 0 | 3.8085 | 0.0393 | 1.1729 | 2.0830 | 2.1976 | 3.5669 | 0.1232 | 4.1947 | 2.2809 | 3.3446 | 2.7215 | 2.4540 | 2.5130 | 30.5001 |
| 22 | 0 | 0 | 0 | 3.5921 | 2.0870 | 4.4790 | 4.1546 | 1.6927 | 3.5023 | 0.6904 | 2.7274 | 1.2457 | 0.7547 | 0.3666 | 2.1905 | 3.5170 | 31 |
| 23 | 0 | 0 | 0 | 1.8612 | 1.5235 | 3.0183 | 2.6992 | 3.2988 | 3.0108 | 4.3116 | 0.8329 | 1.5538 | 1.6008 | 3.7000 | 1.0852 | 3.0039 | 31.5 |
| 24 | 0 | 0 | 0 | 3.3916 | 4.0911 | 3.4021 | 3.8145 | 1.2680 | 4.3122 | 0.6408 | 0.6390 | 1.8802 | 3.1034 | 2.0806 | 0.2499 | 3.1267 | 32.0001 |
| 25 | 0 | 0 | 0 | 1.0632 | 1.3998 | 0.3611 | 0.9596 | 3.7329 | 3.9034 | 3.8453 | 1.0337 | 2.7448 | 2.4058 | 4.1777 | 4.3794 | 2.4933 | 32.5 |
| 26 | 0 | 0 | 0 | 0.9657 | 1.5812 | 3.5568 | 3.7625 | 2.6392 | 3.1037 | 4.0394 | 2.8907 | 3.4542 | 1.8717 | 1.6161 | 2.8421 | 0.6766 | 32.9999 |
| 27 | 0 | 0 | 0 | 3.6777 | 5.1825 | 4.5425 | 0.6662 | 0.0408 | 4.3502 | 4.9701 | 1.4774 | 1.3585 | 2.9513 | 0.3515 | 0.7292 | 3.2022 | 33.5001 |
| 28 | 0 | 0 | 0 | 0.7735 | 3.5237 | 4.5456 | 4.2499 | 4.3172 | 4.0720 | 3.6115 | 0.1140 | 3.0394 | 1.0134 | 0.2992 | 3.5775 | 0.8631 | 34 |
| 29 | 0 | 0 | 0 | 2.0718 | 4.6317 | 3.4433 | 4.3637 | 2.1722 | 0.9399 | 0.6908 | 0.5090 | 3.1252 | 2.6892 | 2.4224 | 3.2750 | 3.1658 | 33.5 |
| 30 | 0 | 0 | 0 | 1.4924 | 6.2343 | 2.2891 | 0.5983 | 0.5335 | 1.6625 | 2.1610 | 2.5381 | 3.4529 | 3.0872 | 1.6906 | 4.5287 | 2.7315 | 33.0001 |
| 31 | 0 | 0 | 0 | 2.5280 | 0.1894 | 1.9474 | 4.0301 | 0.2417 | 3.5781 | 5.1954 | 5.7623 | 1.9896 | 2.4509 | 0.4121 | 0.5696 | 3.6057 | 32.5003 |
| 32 | 0 | 0 | 0 | 3.8199 | 2.4802 | 4.0356 | 4.0806 | 2.9216 | 2.0335 | 2.0322 | 3.6235 | 0.6203 | 2.1560 | 1.4874 | 2.1870 | 0.5223 | 32.0001 |
| 33 | 0 | 0 | 0 | 6.8444 | 0.9012 | 2.9437 | 1.3628 | 6.7828 | 0.6680 | 1.3548 | 1.8233 | 1.0805 | 3.7198 | 1.3554 | 0.5436 | 3.1197 | 32.5 |
| 34 | 0 | 0 | 0 | 3.1690 | 0.0717 | 2.1027 | 0.2683 | 1.4920 | 5.0112 | 1.5193 | 4.0785 | 2.2562 | 3.0208 | 2.4249 | 4.2879 | 3.0274 | 32.7299 |
| 35 | 0 | 0 | 0 | 3.6761 | 2.4625 | 3.5932 | 3.7721 | 1.6678 | 0.0944 | 1.7491 | 3.0284 | 2.8975 | 3.9349 | 0.3033 | 3.2305 | 2.8202 | 33.23 |
| 36 | 0 | 0 | 0 | 1.8689 | 0.4962 | 2.6611 | 5.0654 | 0.0050 | 4.5734 | 1.7372 | 4.0564 | 2.3704 | 3.4430 | 0.8368 | 1.3330 | 5.2833 | 33.7301 |
| 37 | 0 | 0 | 0 | 0.3178 | 3.8033 | 4.3920 | 2.3711 | 0.2945 | 1.3658 | 3.9648 | 1.7994 | 3.9844 | 1.9302 | 3.2636 | 3.9254 | 2.8177 | 34.23 |
| 38 | 0 | 0 | 0 | 4.0716 | 0.7236 | 1.2250 | 4.1431 | 3.1335 | 4.1609 | 0.5825 | 2.4020 | 1.5991 | 4.1598 | 1.7367 | 4.0217 | 2.7705 | 34.73 |

| | | | | | | | | | | | | | | | | | |
|---|---|---|---|---|---|---|---|---|---|---|---|---|---|---|---|---|---|
| 39 | 0 | 0 | 0 | 2.6624 | 1.8429 | 2.6441 | 1.8835 | 6.2338 | 4.0351 | 0.9480 | 2.5365 | 1.1391 | 3.1486 | 0.8007 | 1.2139 | 6.1414 | 35.23 |
| 40 | 0 | 0 | 0 | 3.5952 | 1.9224 | 3.6262 | 2.9863 | 1.0647 | 1.8863 | 2.2591 | 3.9601 | 2.3906 | 3.4594 | 3.3484 | 0.7449 | 4.4865 | 35.7301 |
| 41 | 0 | 0 | 0 | 0.9863 | 3.6845 | 0.6717 | 1.3706 | 3.7553 | 0.6769 | 4.4101 | 4.6038 | 2.4221 | 4.9808 | 1.0625 | 4.7466 | 2.8587 | 36.2299 |
| 42 | 0 | 0 | 0 | 1.7382 | 4.0022 | 4.6263 | 4.8516 | 1.6151 | 5.1212 | 0.9014 | 0.8382 | 0.0386 | 2.9359 | 0.8599 | 4.7888 | 4.1825 | 36.4999 |
| 43 | 0 | 0 | 0 | 3.0290 | 3.7334 | 2.3276 | 1.7460 | 1.7152 | 3.2128 | 2.6153 | 4.0454 | 4.0099 | 2.4221 | 3.0438 | 1.6230 | 2.4767 | 36.0002 |
| 44 | 0 | 0 | 0 | 4.3259 | 1.6611 | 2.7400 | 2.8972 | 3.7788 | 3.5338 | 3.4036 | 1.3727 | 4.0414 | 2.0088 | 2.8373 | 0.9247 | 1.9747 | 35.5 |
| 45 | 0 | 0 | 0 | 1.1459 | 2.0931 | 0.5584 | 4.3765 | 5.7580 | 0.4281 | 0.9265 | 2.2694 | 6.0609 | 3.2502 | 0.3735 | 6.0364 | 1.7230 | 34.9999 |
| 46 | 0 | 0 | 0 | 3.1305 | 3.0261 | 2.7167 | 2.9977 | 3.4376 | 2.2813 | 3.1316 | 0.7622 | 3.9230 | 1.9249 | 3.8593 | 0.9745 | 2.3346 | 34.5 |
| 47 | 0 | 0 | 0 | 0.5583 | 2.3024 | 4.9378 | 3.5064 | 3.0010 | 0.2819 | 0.6446 | 3.7034 | 3.6805 | 3.2458 | 3.7085 | 0.3225 | 4.1071 | 34.0002 |
| 48 | 0 | 0 | 0 | 2.2413 | 3.0239 | 2.3326 | 0.4417 | 2.4866 | 2.4599 | 3.4260 | 4.3136 | 3.0491 | 1.0711 | 2.8138 | 3.3382 | 2.5021 | 33.4999 |
| 49 | 0 | 0 | 0 | 0.3754 | 0.2929 | 2.5011 | 2.5569 | 4.8145 | 2.6010 | 4.7880 | 1.5151 | 2.9702 | 4.4529 | 0.0423 | 2.7358 | 3.3539 | 33 |
| 50 | 0 | 0 | 0 | 0.7880 | 2.6941 | 2.8352 | 2.0801 | 2.2354 | 1.6491 | 4.1342 | 2.6398 | 1.5255 | 0.2551 | 2.9312 | 1.6835 | 7.0489 | 32.5001 |
| 51 | 0 | 0 | 0 | 3.5846 | 2.2375 | 1.3243 | 1.4463 | 4.1977 | 0.0535 | 4.4446 | 3.1274 | 0.7355 | 0.5289 | 4.3172 | 3.0229 | 2.9798 | 32.0002 |
| 52 | 0 | 0 | 0 | 3.0202 | 0.8478 | 2.2980 | 2.7428 | 3.7457 | 2.8731 | 2.7546 | 1.9005 | 2.0125 | 4.6322 | 3.0118 | 0.4497 | 1.2111 | 31.5 |
| 53 | 0 | 0 | 0 | 0.3272 | 0.4178 | 2.4753 | 2.9253 | 3.5463 | 0.0346 | 3.6743 | 1.3671 | 1.9783 | 2.0178 | 4.9278 | 4.1939 | 3.1144 | 31.0001 |
| 54 | 0 | 0 | 0 | 2.3534 | 3.8374 | 1.9033 | 2.3886 | 3.6111 | 0.5376 | 3.0991 | 3.5028 | 1.4983 | 1.5409 | 2.9219 | 2.3886 | 0.9172 | 30.5002 |
| 55 | 0 | 0 | 0 | 6.0695 | 0.6077 | 0.7469 | 0.9502 | 3.1563 | 0.3751 | 2.0661 | 0.0899 | 2.6821 | 0.5810 | 6.0157 | 5.3081 | 1.3514 | 30 |
| 56 | 0 | 0 | 0 | 3.4981 | 0.1766 | 3.9723 | 1.4591 | 3.1347 | 0.2501 | 1.9993 | 0.2072 | 3.6677 | 3.1151 | 3.0753 | 3.2036 | 1.7408 | 29.4999 |
| 57 | 0 | 0 | 0 | 2.1229 | 1.8505 | 3.0342 | 1.6877 | 1.9060 | 2.4617 | 0.1198 | 1.9150 | 3.0862 | 3.1744 | 0.1902 | 3.9149 | 3.5365 | 29 |

**Table 5.4**: **Load bus reactive power datasets in the repertoire $Q\_rep$ calculated using Equation 5.2**

| Bus N°. / Data set N°. | 1 | 2 | 3 | 4 | 5 | 6 | 7 | 8 | 9 | 10 | 11 | 12 | 13 | 14 | 15 | 16 | $\sum \mathrm{Qd}_i^t$ |
|---|---|---|---|---|---|---|---|---|---|---|---|---|---|---|---|---|---|
| 1 | 0 | 0 | 0 | 1.9521 | 0.9286 | 2.0387 | 1.2328 | 1.9292 | 1.2883 | 0.0567 | 1.4671 | 2.5992 | 0.9105 | 0.0474 | 1.6811 | 1.1683 | 17.3 |
| 2 | 0 | 0 | 0 | 0.7072 | 1.3530 | 2.2705 | 0.9326 | 1.3536 | 3.0548 | 2.6407 | 0.1459 | 1.0594 | 0.1425 | 0.3130 | 2.9371 | 0.0883 | 16.9986 |
| 3 | 0 | 0 | 0 | 1.7186 | 1.5822 | 1.7754 | 1.4961 | 1.6752 | 1.7935 | 0.9751 | 1.7453 | 0.4155 | 1.2342 | 0.1032 | 1.4299 | 0.7531 | 16.6973 |
| 4 | 0 | 0 | 0 | 0.0548 | 0.2835 | 2.0468 | 0.3155 | 1.7372 | 1.8879 | 0.3568 | 1.8629 | 1.7842 | 1.2171 | 1.9038 | 1.9205 | 1.0247 | 16.3957 |
| 5 | 0 | 0 | 0 | 1.7563 | 1.8081 | 2.9315 | 0.8576 | 1.3635 | 3.0147 | 0.0621 | 0.3667 | 1.1275 | 1.3959 | 0.1951 | 0.3812 | 0.8342 | 16.0944 |
| 6 | 0 | 0 | 0 | 1.5119 | 0.9277 | 1.6384 | 1.1541 | 2.0820 | 0.1787 | 0.6434 | 0.9759 | 1.2380 | 0.8811 | 1.3200 | 1.5867 | 1.7538 | 15.8917 |
| 7 | 0 | 0 | 0 | 1.7905 | 0.7761 | 1.7038 | 1.4608 | 0.7741 | 2.1057 | 0.3146 | 0.1581 | 0.9749 | 1.0641 | 1.9433 | 2.3285 | 0.1955 | 15.59 |
| 8 | 0 | 0 | 0 | 0.4835 | 1.2203 | 1.7202 | 0.3172 | 2.5071 | 2.0038 | 0.3386 | 1.8980 | 1.0169 | 0.2463 | 1.3637 | 0.7171 | 1.4563 | 15.289 |
| 9 | 0 | 0 | 0 | 1.9309 | 1.3419 | 0.4702 | 2.0215 | 0.0161 | 1.1071 | 2.3556 | 1.6039 | 0.6284 | 1.4184 | 0.0130 | 1.2567 | 0.9663 | 15.13 |
| 10 | 0 | 0 | 0 | 0.8953 | 1.6532 | 1.8167 | 1.8566 | 1.8979 | 0.8150 | 0.7122 | 0.9991 | 0.2252 | 0.7855 | 1.6335 | 1.5472 | 0.2322 | 15.0696 |
| 11 | 0 | 0 | 0 | 0.2074 | 0.8033 | 1.2545 | 2.6683 | 0.4924 | 0.8325 | 0.6883 | 2.0060 | 1.4245 | 1.4912 | 2.1303 | 1.0566 | 0.3156 | 15.3709 |
| 12 | 0 | 0 | 0 | 1.8895 | 1.2683 | 1.8777 | 0.4082 | 0.4591 | 0.9515 | 0.4220 | 1.3371 | 1.0995 | 0.2594 | 2.0763 | 1.8980 | 1.7256 | 15.6722 |
| 13 | 0 | 0 | 0 | 0.5463 | 1.5841 | 2.2741 | 0.6864 | 1.7750 | 1.0821 | 2.2638 | 1.0922 | 0.1644 | 0.9335 | 1.6846 | 1.7107 | 0.1767 | 15.9739 |
| 14 | 0 | 0 | 0 | 0.4383 | 1.4288 | 1.1083 | 1.8269 | 1.8860 | 0.6423 | 1.6620 | 1.6082 | 1.5625 | 1.7996 | 0.6303 | 0.8963 | 0.7858 | 16.2753 |
| 15 | 0 | 0 | 0 | 0.5037 | 0.1000 | 0.6569 | 1.9495 | 0.9542 | 0.6438 | 0.2341 | 2.1577 | 1.7489 | 2.0631 | 2.1289 | 1.5088 | 1.9270 | 16.5766 |
| 16 | 0 | 0 | 0 | 2.0456 | 0.7605 | 0.1306 | 1.3516 | 1.1887 | 2.1341 | 0.8891 | 1.9828 | 2.1629 | 0.7917 | 2.2242 | 0.4557 | 0.7606 | 16.8781 |

| | | | | | | | | | | | | | | | | | |
|---|---|---|---|---|---|---|---|---|---|---|---|---|---|---|---|---|---|
| 17 | 0 | 0 | 0 | 0.7070 | 0.0826 | 1.6864 | 1.1838 | 0.8458 | 2.4394 | 1.5902 | 0.8811 | 3.3324 | 1.5365 | 0.0261 | 1.6440 | 1.2242 | 17.1795 |
| 18 | 0 | 0 | 0 | 1.2119 | 0.6952 | 0.8153 | 2.0299 | 1.5422 | 1.9247 | 0.6948 | 0.8098 | 1.8347 | 0.4111 | 2.0127 | 1.5485 | 1.9501 | 17.4809 |
| 19 | 0 | 0 | 0 | 1.9635 | 1.9686 | 0.9034 | 1.7024 | 0.2937 | 1.2577 | 1.2842 | 1.3456 | 2.1236 | 1.8248 | 0.0218 | 1.4273 | 1.6658 | 17.7824 |
| 20 | 0 | 0 | 0 | 1.2682 | 1.6650 | 2.2434 | 0.6826 | 1.8813 | 2.2115 | 0.6752 | 2.2573 | 2.0808 | 0.0110 | 0.6555 | 1.1148 | 1.3370 | 18.0836 |
| 21 | 0 | 0 | 0 | 2.2957 | 0.0237 | 0.7070 | 1.2556 | 1.3247 | 2.1501 | 0.0743 | 2.5285 | 1.3749 | 2.0161 | 1.6405 | 1.4792 | 1.5148 | 18.3851 |
| 22 | 0 | 0 | 0 | 2.1653 | 1.2580 | 2.6999 | 2.5043 | 1.0203 | 2.1111 | 0.4162 | 1.6440 | 0.7509 | 0.4549 | 0.2210 | 1.3204 | 2.1200 | 18.6863 |
| 23 | 0 | 0 | 0 | 1.1219 | 0.9183 | 1.8194 | 1.6270 | 1.9885 | 1.8149 | 2.5990 | 0.5021 | 0.9366 | 0.9649 | 2.2303 | 0.6541 | 1.8107 | 18.9877 |
| 24 | 0 | 0 | 0 | 2.0444 | 2.4661 | 2.0507 | 2.2994 | 0.7644 | 2.5993 | 0.3863 | 0.3852 | 1.1334 | 1.8707 | 1.2541 | 0.1507 | 1.8847 | 19.2894 |
| 25 | 0 | 0 | 0 | 0.6409 | 0.8438 | 0.2177 | 0.5784 | 2.2501 | 2.3529 | 2.3179 | 0.6231 | 1.6545 | 1.4502 | 2.5183 | 2.6399 | 1.5029 | 19.5906 |
| 26 | 0 | 0 | 0 | 0.5821 | 0.9531 | 2.1440 | 2.2680 | 1.5909 | 1.8709 | 2.4349 | 1.7425 | 2.0821 | 1.1283 | 0.9742 | 1.7132 | 0.4078 | 19.892 |
| 27 | 0 | 0 | 0 | 2.2169 | 3.1239 | 2.7381 | 0.4016 | 0.0246 | 2.6222 | 2.9959 | 0.8905 | 0.8189 | 1.7790 | 0.2119 | 0.4395 | 1.9302 | 20.1932 |
| 28 | 0 | 0 | 0 | 0.4663 | 2.1241 | 2.7400 | 2.5618 | 2.6023 | 2.4545 | 2.1770 | 0.0687 | 1.8321 | 0.6109 | 0.1804 | 2.1564 | 0.5203 | 20.4948 |
| 29 | 0 | 0 | 0 | 1.2488 | 2.7919 | 2.0756 | 2.6304 | 1.3094 | 0.5665 | 0.4164 | 0.3068 | 1.8838 | 1.6210 | 1.4602 | 1.9741 | 1.9083 | 20.1932 |
| 30 | 0 | 0 | 0 | 0.8996 | 3.7580 | 1.3798 | 0.3606 | 0.3216 | 1.0021 | 1.3026 | 1.5300 | 2.0814 | 1.8609 | 1.0191 | 2.7299 | 1.6465 | 19.8921 |
| 31 | 0 | 0 | 0 | 1.5239 | 0.1141 | 1.1739 | 2.4293 | 0.1457 | 2.1568 | 3.1317 | 3.4734 | 1.1993 | 1.4774 | 0.2484 | 0.3433 | 2.1734 | 19.5906 |
| 32 | 0 | 0 | 0 | 2.3026 | 1.4950 | 2.4326 | 2.4597 | 1.7611 | 1.2258 | 1.2250 | 2.1842 | 0.3739 | 1.2996 | 0.8966 | 1.3183 | 0.3148 | 19.2892 |
| 33 | 0 | 0 | 0 | 4.1257 | 0.5432 | 1.7744 | 0.8215 | 4.0886 | 0.4026 | 0.8167 | 1.0990 | 0.6513 | 2.2423 | 0.8170 | 0.3277 | 1.8805 | 19.5905 |
| 34 | 0 | 0 | 0 | 1.9102 | 0.0432 | 1.2675 | 0.1617 | 0.8994 | 3.0207 | 0.9158 | 2.4585 | 1.3600 | 1.8209 | 1.4617 | 2.5847 | 1.8249 | 19.7292 |
| 35 | 0 | 0 | 0 | 2.2159 | 1.4844 | 2.1659 | 2.2738 | 1.0053 | 0.0569 | 1.0543 | 1.8255 | 1.7466 | 2.3719 | 0.1829 | 1.9473 | 1.7000 | 20.0307 |
| 36 | 0 | 0 | 0 | 1.1265 | 0.2991 | 1.6041 | 3.0534 | 0.0030 | 2.7568 | 1.0472 | 2.4452 | 1.4288 | 2.0754 | 0.5044 | 0.8035 | 3.1847 | 20.3321 |
| 37 | 0 | 0 | 0 | 0.1915 | 2.2926 | 2.6475 | 1.4293 | 0.1775 | 0.8233 | 2.3899 | 1.0847 | 2.4017 | 1.1635 | 1.9673 | 2.3662 | 1.6984 | 20.6334 |
| 38 | 0 | 0 | 0 | 2.4543 | 0.4362 | 0.7384 | 2.4974 | 1.8888 | 2.5082 | 0.3511 | 1.4479 | 0.9639 | 2.5074 | 1.0469 | 2.4242 | 1.6700 | 20.9347 |
| 39 | 0 | 0 | 0 | 1.6049 | 1.1109 | 1.5938 | 1.1353 | 3.7577 | 2.4323 | 0.5715 | 1.5289 | 0.6866 | 1.8980 | 0.4827 | 0.7317 | 3.7020 | 21.2363 |
| 40 | 0 | 0 | 0 | 2.1671 | 1.1588 | 2.1858 | 1.8001 | 0.6418 | 1.1370 | 1.3617 | 2.3871 | 1.4410 | 2.0853 | 2.0184 | 0.4490 | 2.7044 | 21.5375 |
| 41 | 0 | 0 | 0 | 0.5946 | 2.2210 | 0.4049 | 0.8262 | 2.2636 | 0.4080 | 2.6584 | 2.7751 | 1.4600 | 3.0024 | 0.6405 | 2.8612 | 1.7232 | 21.8391 |
| 42 | 0 | 0 | 0 | 1.0478 | 2.4124 | 2.7887 | 2.9245 | 0.9736 | 3.0870 | 0.5433 | 0.5053 | 0.0233 | 1.7698 | 0.5183 | 2.8867 | 2.5212 | 22.0019 |
| 43 | 0 | 0 | 0 | 1.8258 | 2.2504 | 1.4030 | 1.0525 | 1.0339 | 1.9366 | 1.5765 | 2.4385 | 2.4171 | 1.4600 | 1.8347 | 0.9783 | 1.4929 | 21.7002 |
| 44 | 0 | 0 | 0 | 2.6076 | 1.0013 | 1.6516 | 1.7464 | 2.2778 | 2.1301 | 2.0517 | 0.8275 | 2.4361 | 1.2109 | 1.7103 | 0.5574 | 1.1903 | 21.399 |
| 45 | 0 | 0 | 0 | 0.6908 | 1.2617 | 0.3366 | 2.6381 | 3.4709 | 0.2580 | 0.5585 | 1.3679 | 3.6535 | 1.9592 | 0.2251 | 3.6387 | 1.0386 | 21.0976 |
| 46 | 0 | 0 | 0 | 1.8870 | 1.8241 | 1.6376 | 1.8070 | 2.0722 | 1.3751 | 1.8877 | 0.4594 | 2.3647 | 1.1603 | 2.3263 | 0.5874 | 1.4073 | 20.7961 |
| 47 | 0 | 0 | 0 | 0.3365 | 1.3879 | 2.9764 | 2.1136 | 1.8089 | 0.1699 | 0.3885 | 2.2323 | 2.2185 | 1.9565 | 2.2354 | 0.1944 | 2.4757 | 20.4945 |
| 48 | 0 | 0 | 0 | 1.3511 | 1.8228 | 1.4061 | 0.2662 | 1.4989 | 1.4828 | 2.0651 | 2.6002 | 1.8379 | 0.6457 | 1.6961 | 2.0122 | 1.5083 | 20.1934 |
| 49 | 0 | 0 | 0 | 0.2263 | 0.1765 | 1.5076 | 1.5413 | 2.9021 | 1.5679 | 2.8861 | 0.9133 | 1.7904 | 2.6841 | 0.0255 | 1.6491 | 2.0217 | 19.8919 |
| 50 | 0 | 0 | 0 | 0.4750 | 1.6239 | 1.7090 | 1.2539 | 1.3475 | 0.9941 | 2.4920 | 1.5912 | 0.9196 | 0.1538 | 1.7669 | 1.0148 | 4.2490 | 19.5907 |
| 51 | 0 | 0 | 0 | 2.1608 | 1.3488 | 0.7983 | 0.8718 | 2.5303 | 0.0322 | 2.6791 | 1.8851 | 0.4434 | 0.3188 | 2.6023 | 1.8221 | 1.7962 | 19.2892 |
| 52 | 0 | 0 | 0 | 1.8205 | 0.5110 | 1.3852 | 1.6533 | 2.2579 | 1.7319 | 1.6604 | 1.1456 | 1.2131 | 2.7923 | 1.8155 | 0.2711 | 0.7300 | 18.9878 |
| 53 | 0 | 0 | 0 | 0.1972 | 0.2518 | 1.4921 | 1.7633 | 2.1377 | 0.0208 | 2.2148 | 0.8241 | 1.1925 | 1.2163 | 2.9704 | 2.5280 | 1.8773 | 18.6863 |
| 54 | 0 | 0 | 0 | 1.4186 | 2.3131 | 1.1473 | 1.4398 | 2.1767 | 0.3240 | 1.8681 | 2.1114 | 0.9031 | 0.9288 | 1.7613 | 1.4398 | 0.5529 | 18.3849 |
| 55 | 0 | 0 | 0 | 3.6586 | 0.3663 | 0.4502 | 0.5728 | 1.9026 | 0.2261 | 1.2454 | 0.0542 | 1.6167 | 0.3502 | 3.6262 | 3.1997 | 0.8146 | 18.0836 |
| 56 | 0 | 0 | 0 | 2.1086 | 0.1065 | 2.3945 | 0.8795 | 1.8896 | 0.1508 | 1.2052 | 0.1249 | 2.2109 | 1.8778 | 1.8537 | 1.9311 | 1.0493 | 17.7824 |
| 57 | 0 | 0 | 0 | 1.2797 | 1.1154 | 1.8290 | 1.0173 | 1.1489 | 1.4839 | 0.0722 | 1.1543 | 1.8603 | 1.9135 | 0.1147 | 2.3598 | 2.1318 | 17.4808 |

Step 1 to Step 4 from the developed sequential computation algorithm can be considered as the initialisation part of the sequential programming solution algorithm, and they consist of data preparation tasks.

The flowchart of the sequential programming algorithm to evaluate the daily performance of a distribution network with a feeder reconfiguration scheme under dynamic loading conditions is given in Figure 5.4.

The results of the sequential programming algorithm are presented in the next section.

### 5.3.3. Results of the sequential computing solution algorithm to analyse the performance of the distribution network with a feeder reconfiguration scheme under dynamic loading conditions.

The developed sequential computing solution algorithm is used to assess the performance of the 16-bus distribution system with a feeder reconfiguration scheme over a 24h period. The developed sequential algorithm is implemented in MATLAB R2016b, and the simulations are carried out in a SUPERMICRO computer with 2 Intel Xeon CPU E5-2620 v4 @ 2.10GHz processor and a 16GB RAM. The computer has 16 physical cores and 16 virtual cores, a total of 32 logical cores.

The rate of the power change threshold is 500 kW. Equations 5.1 and 5.2 are used to determine the real and reactive power at each PQ bus every time the real power demand decreases or increases by 500 kW. Therefore, for the daily real power demand profile given in Figure 5.2, there are 57 datasets to be simulated. The calculated real and reactive power at each bus is given in Table 5.3 and 5.4 respectively.

Given that the developed algorithm is sequential, all the 57 datasets are simulated consecutively, one after the other in a since processor.

The sequential computing solution for each dataset is given in Table 5.5. The real power loss profile and the minimum voltage profile for each dataset are presented in Figure 5.5 and Figure 5.6 respectively.

**Table 5.5**: **Sequential computing solutions for the feeder reconfiguration problem**

| Dataset Nº. | Before reconfiguration | | | After reconfiguration | | | | | |
|---|---|---|---|---|---|---|---|---|---|
| | Real power loss (kW) | Max voltage (p.u) | Min voltage (p.u) | Real power loss (kW) | Max voltage (p.u) | Min voltage (p.u) | Optimal topology (tie switches) | | |
| 1 | 465.5 | 1 | 0.9724 | 423.1 | 1 | 0.9750 | 7 | 8 | 16 |
| 2 | 473.9 | 1 | 0.9731 | 430.4 | 1 | 0.9766 | 7 | 8 | 16 |
| 3 | 402.2 | 1 | 0.9766 | 385.9 | 1 | 0.9766 | 7 | 14 | 16 |
| 4 | 474.3 | 1 | 0.9698 | 377.3 | 1 | 0.9822 | 8 | 13 | 15 |
| 5 | 388.6 | 1 | 0.9736 | 353.5 | 1 | 0.9793 | 4 | 7 | 8 |

| | | | | | | | | | |
|---|---|---|---|---|---|---|---|---|---|
| 6 | 343.3 | 1 | 0.9798 | 339.7 | 1 | 0.9798 | 8 | 15 | 16 |
| 7 | 335.4 | 1 | 0.9790 | 329.3 | 1 | 0.9792 | 8 | 15 | 16 |
| 8 | 385.5 | 1 | 0.9710 | 315.0 | 1 | 0.9822 | 7 | 8 | 16 |
| 9 | 337.8 | 1 | 0.9806 | 336.0 | 1 | 0.9806 | 11 | 14 | 16 |
| 10 | 320.1 | 1 | 0.9756 | 318.0 | 1 | 0.9797 | 13 | 14 | 15 |
| 11 | 375.8 | 1 | 0.9769 | 364.4 | 1 | 0.9727 | 8 | 15 | 16 |
| 12 | 358.1 | 1 | 0.9778 | 358.1 | 1 | 0.9778 | 14 | 15 | 16 |
| 13 | 358.8 | 1 | 0.9801 | 349.2 | 1 | 0.9819 | 4 | 8 | 15 |
| 14 | 393.5 | 1 | 0.9760 | 358.9 | 1 | 0.9783 | 8 | 15 | 16 |
| 15 | 479.2 | 1 | 0.9729 | 408.3 | 1 | 0.9775 | 8 | 11 | 16 |
| 16 | 486.8 | 1 | 0.9651 | 388.1 | 1 | 0.9793 | 8 | 15 | 16 |
| 17 | 576.3 | 1 | 0.9626 | 477.7 | 1 | 0.9716 | 7 | 8 | 16 |
| 18 | 458.7 | 1 | 0.9780 | 430.5 | 1 | 0.9780 | 8 | 15 | 16 |
| 19 | 451.0 | 1 | 0.9777 | 439.5 | 1 | 0.9761 | 8 | 15 | 16 |
| 20 | 588.4 | 1 | 0.9611 | 472.9 | 1 | 0.9755 | 4 | 7 | 8 |
| 21 | 541.7 | 1 | 0.9670 | 529.9 | 1 | 0.9706 | 2 | 7 | 13 |
| 22 | 564.8 | 1 | 0.9637 | 560.7 | 1 | 0.9637 | 7 | 14 | 16 |
| 23 | 519.4 | 1 | 0.9746 | 502.1 | 1 | 0.9755 | 8 | 15 | 16 |
| 24 | 529.9 | 1 | 0.9664 | 527.8 | 1 | 0.9661 | 8 | 15 | 16 |
| 25 | 690.3 | 1 | 0.9700 | 598.7 | 1 | 0.9724 | 8 | 13 | 15 |
| 26 | 685.6 | 1 | 0.9630 | 589.8 | 1 | 0.9696 | 7 | 8 | 16 |
| 27 | 592.5 | 1 | 0.9737 | 580.7 | 1 | 0.9732 | 4 | 8 | 15 |
| 28 | 694.1 | 1 | 0.9650 | 626.8 | 1 | 0.9654 | 7 | 8 | 16 |
| 29 | 618.6 | 1 | 0.9650 | 614.0 | 1 | 0.9649 | 8 | 11 | 16 |
| 30 | 589.8 | 1 | 0.9719 | 576.8 | 1 | 0.9753 | 13 | 14 | 15 |
| 31 | 776.5 | 1 | 0.9532 | 594.4 | 1 | 0.9698 | 8 | 15 | 16 |
| 32 | 561.2 | 1 | 0.9647 | 544.5 | 1 | 0.9674 | 4 | 8 | 15 |
| 33 | 455.6 | 1 | 0.9781 | 447.9 | 1 | 0.9761 | 8 | 15 | 16 |
| 34 | 707.8 | 1 | 0.9612 | 531.7 | 1 | 0.9768 | 8 | 13 | 15 |
| 35 | 577.6 | 1 | 0.9679 | 577.6 | 1 | 0.9679 | 14 | 15 | 16 |
| 36 | 719.0 | 1 | 0.9649 | 640.1 | 1 | 0.9658 | 8 | 15 | 16 |
| 37 | 652.7 | 1 | 0.9728 | 639.4 | 1 | 0.9718 | 8 | 15 | 16 |
| 38 | 629.4 | 1 | 0.9714 | 590.7 | 1 | 0.9714 | 8 | 15 | 16 |
| 39 | 672.7 | 1 | 0.9690 | 611.5 | 1 | 0.9708 | 8 | 15 | 16 |
| 40 | 674.9 | 1 | 0.9718 | 668.5 | 1 | 0.9668 | 8 | 15 | 16 |
| 41 | 799.4 | 1 | 0.9631 | 680.8 | 1 | 0.9713 | 8 | 13 | 15 |
| 42 | 790.7 | 1 | 0.9600 | 790.7 | 1 | 0.9600 | 14 | 15 | 16 |
| 43 | 744.0 | 1 | 0.9589 | 657.0 | 1 | 0.9697 | 8 | 15 | 16 |
| 44 | 684.5 | 1 | 0.9663 | 628.6 | 1 | 0.9731 | 7 | 8 | 16 |
| 45 | 728.0 | 1 | 0.9648 | 652.1 | 1 | 0.9733 | 7 | 8 | 13 |
| 46 | 596.3 | 1 | 0.9743 | 582.2 | 1 | 0.9738 | 8 | 15 | 16 |
| 47 | 644.9 | 1 | 0.9689 | 639.8 | 1 | 0.9640 | 8 | 15 | 16 |
| 48 | 679.7 | 1 | 0.9605 | 572.1 | 1 | 0.9739 | 8 | 15 | 16 |
| 49 | 685.3 | 1 | 0.9666 | 613.6 | 1 | 0.9727 | 8 | 11 | 16 |
| 50 | 636.4 | 1 | 0.9668 | 609.2 | 1 | 0.9668 | 8 | 15 | 16 |
| 51 | 538.3 | 1 | 0.9752 | 520.0 | 1 | 0.9759 | 8 | 15 | 16 |
| 52 | 493.2 | 1 | 0.9747 | 451.9 | 1 | 0.9780 | 8 | 15 | 16 |
| 53 | 596.3 | 1 | 0.9673 | 552.3 | 1 | 0.9711 | 8 | 13 | 15 |
| 54 | 468.1 | 1 | 0.9757 | 468.1 | 1 | 0.9757 | 14 | 15 | 16 |
| 55 | 487.4 | 1 | 0.9714 | 469.5 | 1 | 0.9723 | 8 | 13 | 15 |
| 56 | 429.5 | 1 | 0.9779 | 423.9 | 1 | 0.9779 | 8 | 15 | 16 |
| 57 | 464.6 | 1 | 0.9734 | 445.2 | 1 | 0.9734 | 8 | 15 | 16 |
| **Total** | 31373.9 | | | 28966.4 | | | | | |

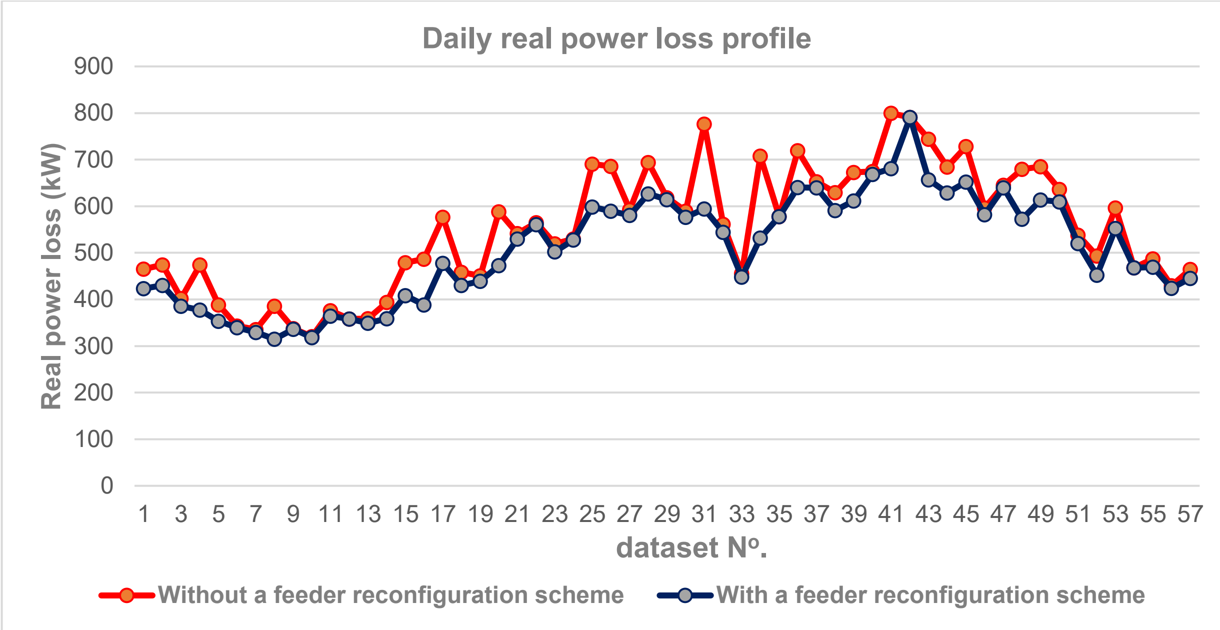


**Figure 5.5**: Daily real power loss profile using the developed sequential programming approach

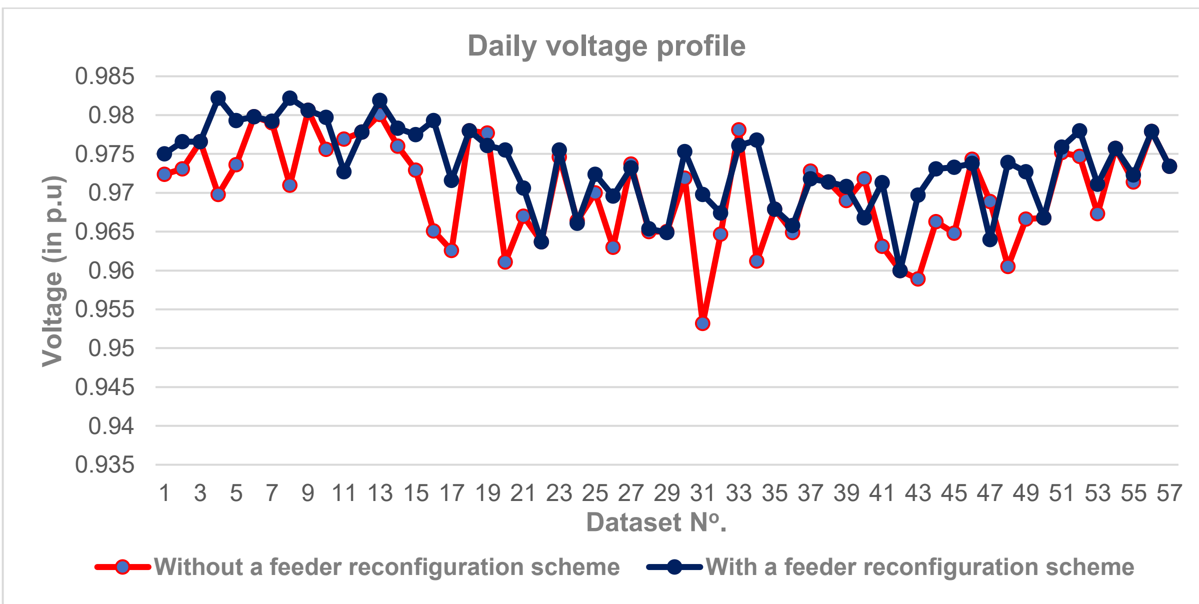


**Figure 5.6**: Daily minimum voltage profile using the developed sequential programming approach

The profile summary of the sequential programming simulations is given in Figure 5.7. The profile summary provides information about how long it takes to simulate all the datasets from Table 5.3 and 5.4. The profile summary shows that in comparison with all other functions used in the code, the Newton-Raphson power flow takes most of the computation time with about 46.373 seconds.


**Profile Summary**

*Generated 17-Feb-2018 21:00:58 using performance time.*

| Function Name | Calls | Total Time | Self Time* | Total Time Plot (dark band = self time) |
|---|---|---|---|---|
| daily_load_profil_seq_3 | 1 | 173.297 s | 0.386 s | |
| spmd1 | 57 | 170.906 s | 7.123 s | |
| runpf | 86830 | 157.411 s | 13.095 s | |
| newtonpf | 86830 | 62.191 s | 46.373 s | |
| ext2int | 86830 | 23.676 s | 22.964 s | |
| int2ext | 86830 | 18.132 s | 10.940 s | |
| dSbus_dV | 261695 | 14.026 s | 14.026 s | |
| pfsoln | 86830 | 13.537 s | 12.610 s | |
| makeYbus | 86830 | 9.142 s | 8.745 s | |
| mpoption | 86830 | 6.591 s | 6.591 s | |
| rmfield | 86830 | 6.451 s | 5.434 s | |
| rank | 102013 | 6.372 s | 6.372 s | |
| bustypes | 86830 | 3.455 s | 3.023 s | |
| makeSbus | 86830 | 3.059 s | 2.643 s | |
| angle | 435355 | 2.086 s | 2.086 s | |
| xlswrite | 3 | 1.925 s | 0.028 s | |
| loadcase | 86830 | 1.820 s | 1.820 s | |
| xlswrite>ExecuteWrite | 3 | 1.607 s | 0.601 s | |
| idx_bus | 607810 | 1.588 s | 1.588 s | |
| etime | 86830 | 1.382 s | 1.382 s | |
| idx_gen | 520980 | 1.234 s | 1.234 s | |
| cellstr | 86830 | 1.017 s | 1.017 s | |
| idx_brch | 434150 | 0.915 s | 0.915 s | |
| iofun\private\openExcelWorkbook | 3 | 0.848 s | 0.808 s | |
| deal | 173660 | 0.705 s | 0.705 s | |
| getExcelInstance | 3 | 0.235 s | 0.005 s | |
| actxserver | 1 | 0.226 s | 0.225 s | |
| idx_area | 173660 | 0.219 s | 0.219 s | |

**Figure 5.7**: Profile summary of the developed sequential programming approach for the feeder reconfiguration scheme under dynamic loading conditions

### 5.3.4. Discussion of the results of the sequential computing algorithm to analyse the performance of the distribution network with feeder reconfiguration under dynamic loading conditions

The analysis of the results of the daily performance of the distribution network with a feeder reconfiguration scheme shows that the distribution network topology is likely to change if there is a significant change in load demand at each PQ bus. As seen in Table 5.5, the distribution network topology does not remain the same for all 57 datasets. This means that the topology of the distribution network changes throughout the day, depending on the real and reactive power demand at each PQ bus.

Looking at the real power loss, it is observed that for any data set, the real power loss is reduced after the reconfiguration process. Figure 5.5 indicates that when a feeder reconfiguration scheme is present in a distribution network, the real power loss incurred in the distribution network is reduced, in comparison to a distribution network without feeder reconfiguration scheme. From Table 5.5, it can be calculated that when the distribution network is equipped with a feeder reconfiguration scheme, the total daily power is $\mathbf{28.9664\ MW}$. Otherwise, the total daily power loss would be $\mathbf{31.3741\ MW}$. Therefore, for the 16-bus distribution network, and for the real and reactive power demands provided in Table 5.3 and 5.4 respectively, the difference of total daily real power loss between the distribution network with the feeder reconfiguration scheme and the distribution network without the feeder reconfiguration scheme is $\mathbf{2.4077\ MW}$, which corresponds to a real power saving of approximately $\mathbf{7.67}\%$.

For each dataset, the distribution network has a different voltage profile, irrespective of whether a feeder reconfiguration scheme is present or not. However, when a feeder reconfiguration scheme is implemented in the distribution network, the voltage level at each bus is improved. Figure 5.6 provides the minimum voltage resulting from the simulation of each dataset. It is observed that for the distribution network with a feeder reconfiguration scheme, the minimum voltages are above $\mathbf{0.96\ p.u}$ for all 57 datasets. For the distribution network without feeder reconfiguration scheme, the minimum voltages are above $\mathbf{0.95\ p.u}$ for all 57 datasets, and voltage below $0.96\ \mathrm{p.u}$ are registered. As given in Table 5.5, for all datasets, the maximum voltage is $1\ \mathrm{p.u}$. Thus, it is concluded that the voltage levels of the 16-bus distribution network are within the recommended limit of $\pm\mathbf{6}\%$**,** for each of the datasets from Table 5.3 and 5.4.

### 5.3.5. Parallel computing solution algorithm to analyse the performance of a distribution network with a feeder reconfiguration scheme under dynamic loading conditions

#### 5.3.5.1. Introduction to parallel computing

Parallel computing may be defined as the simultaneous execution of several processes within a computational problem using multiple computer resources. Several applications are solved using codes in which segments of code are repetitive and independent of each other (Almasi & Gottlieb, 1989). Such codes are traditionally computed serially, i.e. the problem is divided into several code instructions, the instructions are executed sequentially, one after another and on a single processor (Barney, 2017). In parallel computing, the problem is divided into multiple subproblems that can be solved simultaneously. The subproblems are further divided into multiple instructions, solved on different processors, and the results are collected after all subproblems are solved (Grama et al., 2003). The concepts of parallel and sequential programming are illustrated in Figure 5.8 and 5.9, respectively. The use of parallel computing may result in a saving of time and possibly in computation memory. However, the use of parallel computing is not without limitations.

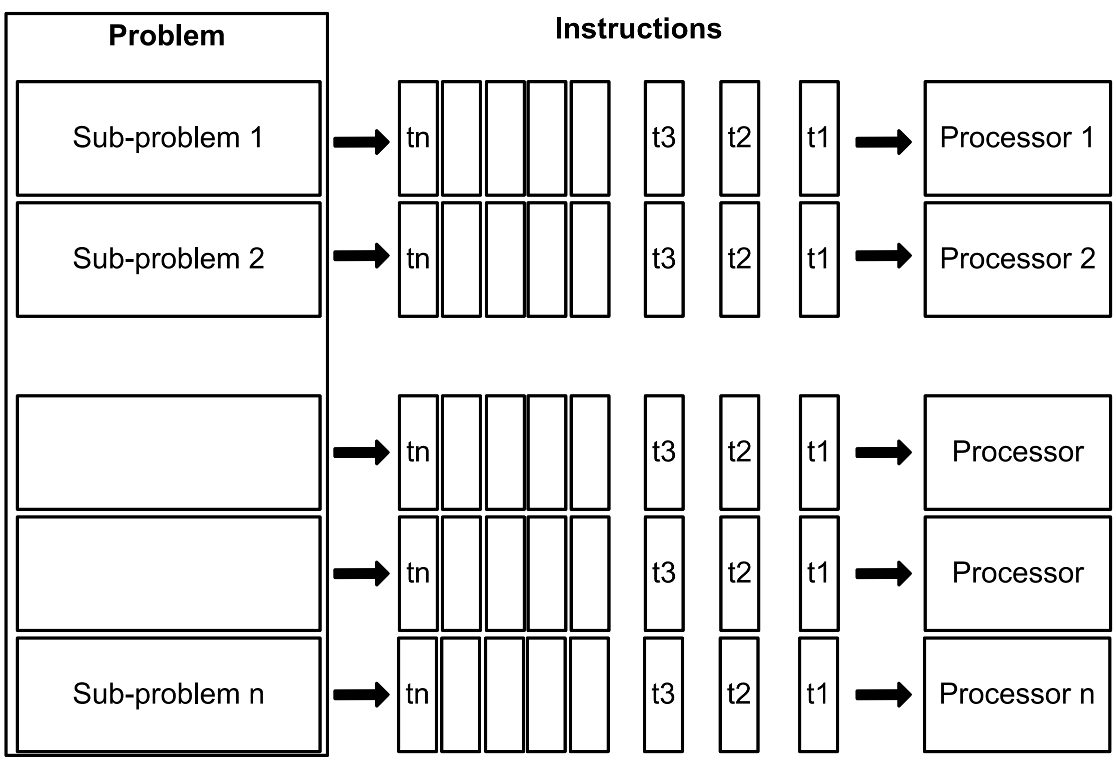


**Figure 5.8**: Illustration of Parallel computing (Barney, 2017)

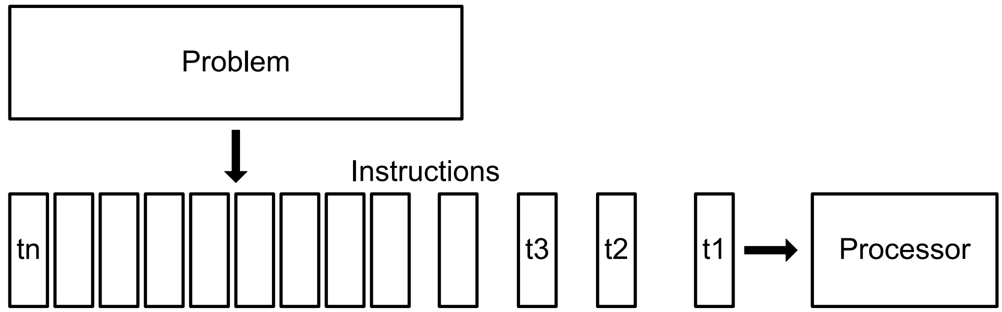


**Figure 5.9**: **Illustration of serial computing (Barney, 2017)**

The next section presents the limitations of parallel computing.

#### 5.3.5.2. Limitations of parallel computing

Parallel computing has some benefits to the programmer. However, there are limitations associated with its use. These limitations are the complexity, the speed-up, the resources requirements, the portability, and the scalability.

- **Complexity**: Compared to sequential/serial algorithms, parallel algorithms are more complicated to design, to code, to debug, to tune and to maintain (Barney,2017).

- **The speed-up**: There is a limit to the speedup that can be achieved through parallel computing. This statement is supported by Amdahl's law which states that the potential speed-up of an algorithm coding on a parallel platform is dependent on the percentage of the code that can be parallelised (Amdahl, 1967).
  Based on Amdahl's law, the potential speed-up can be calculated using Equation 5.3. Another approximation of the potential speed-up of the algorithm coding is given by Gustafson's law (Gustafson, 1988) as expressed in Equation 5.4.

$$\mathbf{speedup} = \frac{\mathbf{1}}{\frac{\mathbf{P}}{\mathbf{N}} + \mathbf{1} - \mathbf{P}} \tag{5.3}$$

Where,

$\mathbf{P}$ is the percentage of the code that can be parallelized.

$\mathbf{N}$ is the number of processors to be used.

$$\mathbf{speedup} = \mathbf{1} - \mathbf{P} + \mathbf{N} * \mathbf{P} \tag{5.4}$$

Amdahl's law assumes that the parallelizable portion of the code is independent of the number of processors used while for Gustafson's, the parallelizable portion of the algorithm coding varies linearly with the number of processors (Barney, 2017).

- **Resources requirements**: Parallel computing needs multiple processors to achieve optimal speed-up. Additionally, the memory requirements for parallel codes may be higher than in serial codes (Barney, 2017).

- **Portability:** The portability of a code refers to its use in different vendors platforms. Hardware architecture and operating systems may negatively affect the portability of parallel programs. So, reinstalling a parallel code or transferring it from one computer to another may be challenging (Grama et al., 2003).

- **Scalability:** The scalability refers to the potential of a system to be enlarged to accommodate a growing amount of work. There is a limit in the scalability of parallel computers, and they will eventually fail to meet their objectives as they amount of processes increase. Likewise, when scaling parallel computers for a constant amount of work, there is a number of processors beyond which the scalability has no or insignificant effect on the speed-up of the parallel code (Almasi & Gottlieb, 1989).

To curb the limitations of parallel computing, it is essential to adhere to good software development practices when working with parallel computing applications.

#### 5.3.5.3. Types of parallelism

The ultimate purpose of parallel computing is to save time. However, depending on the applications and the abilities of the programmers, different parallel programming approaches may be used.

- **Instruction Level Parallelism (ILP):** In Instruction Level Parallelism, multiple instructions from the same stream of instructions are executed simultaneously (Patterson & Henessy, 2014). The instructions can be reordered, grouped and executed in parallel, with no change in the result. Instruction Level Parallelism is limited in practice by data and control dependencies.

- **Data Level Parallelism (DLP):** Data Level Parallelism is achieved by performing the same operation on independent data (Patterson & Henessy, 2014). Its usage is limited by non-regular data manipulation and memory bandwidth, with the memory bandwidth being the rate at which a processor can read from or store data in a semiconductor memory.

- **Task Level Parallelism (TLP):** Task Level Parallelism consists of using multiple processors to run independent programs concurrently (Patterson & Henessy, 2014). It contrasts with data parallelism where the operations are performed on the same or independent data. Task Level Parallelism is limited in practice by communication overheads. Therefore, It is challenging to scale with the size of the problem (Patterson & Henessy, 2014).

Because of the multitude of datasets to be simulated, the data parallel computing solution is developed to assess the daily performance of the distribution network feeder reconfiguration in the 16-bus distribution network under dynamic loading conditions.

#### 5.3.5.4. Classification of parallel computers

Parallel computers are those in which the operation of calculations can be performed simultaneously. Various criteria can be used to classify parallel computers. Some of such criteria include the instructions and data streams, the structure of the computer, the way the memory is accessed and the size of the instructions to be processed. The most common classification of parallel computers includes Flynn's classification, Handler's classification, the structural classification, and the Grain size-based classification.

#### a. Flynn's classification

This classification is based on the multiplicity of instructions and data streams observed by a computer's CPU during the execution of a program. Is was introduced in 1972 by Michael Flynn and does not consider the computer's architecture (Flynn, 1972). Based on the sequence of instructions, computers can be classified into four types: SISD, SIMD, MISD, and MIMD.

- **Single Instruction Single Data (SISD)**: SISD machines are serial machines, i.e. they can only run non-parallel programs. The architecture of SISD chines is given in Figure 5.10.

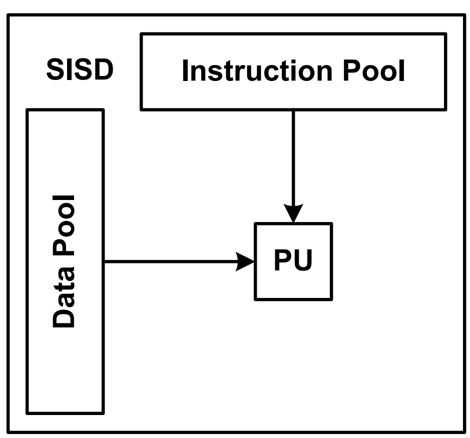


**Figure 5.10**: **Architecture of SISD computers (Barney, 2017)**

In SISD machines, only one instruction and only one data can be executed at the time (John, 2000). Moreover, SISD machines just have one processor or Processing Unit (PU).

- **Single Instruction Multiple Data (SIMD)**: SIMD machines are parallel computers. They have multiple processors, all executing the same instruction concurrently. However, the data processed may be either the same or entirely different and independent (Behrooz, 2002). The architecture of SIMD machines is given in Figure 5.11.

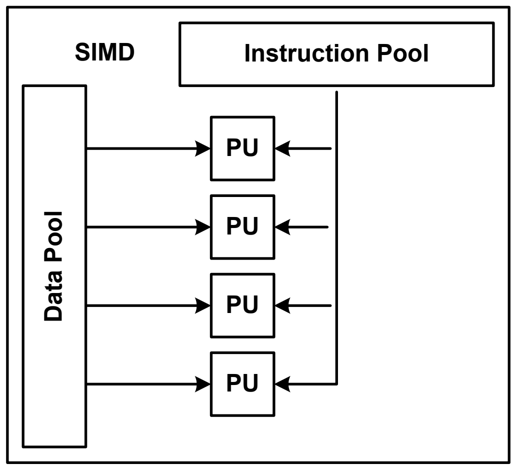


**Figure 5.11**: **Architecture of SIMD computers (Barney, 2017)**

- **Multiple Instruction Single Data (MISD)**: MISD machines are parallel computers in which a single data stream is fed into multiple processors, each processing the data independently and via a separate instruction stream (Changhun, 2002). The architecture of MISD computers is given in Figure 5.12.

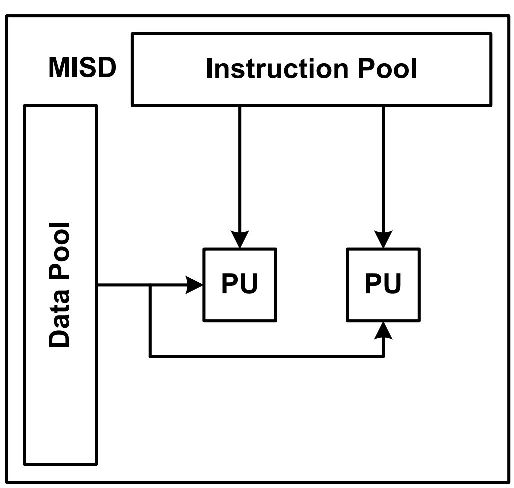


**Figure 5.12**: **Architecture of MISD computers (Barney, 2017)**

MISD Computers are not very common as a single data stream is rarely executed on multiple processors.

- **Multiple Instructions Multiple Data (MIMD)**: MIMD machines are the most common type of parallel computers. Almost all modern supercomputer, multicore PCs, and computers clusters fall under this category. The architecture of MIMD machines is given in Figure 5.13. In MIMD machines, processors may work with different data streams and execute different instruction streams (Behrooz, 2002).

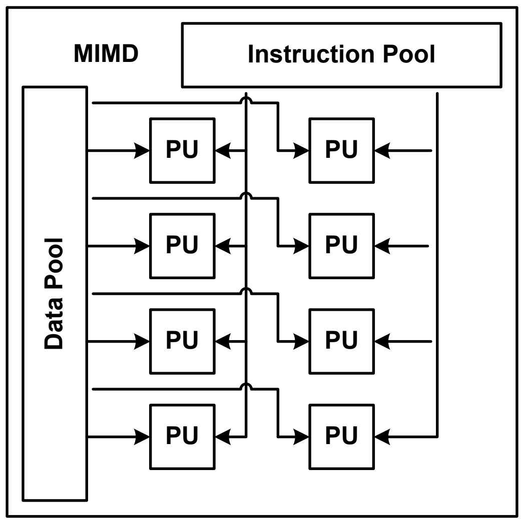


**Figure 5.13**: **Architecture of MIMD computers (Barney, 2017)**

**b. Handler's classification**

It was introduced in 1977 by Wolfgang Handler to express the parallelism type of computers. This classification is based on three different criteria:

- **The Processing Control Unit (PCU)** or **processor**, or **CPU**.
- **The Arithmetic Logic Unit (ALU)** which is the hardware that processes the arithmetic operations like "addition" and "subtraction", and logical operations like "AND" and "OR" (Patterson & Henessy, 2014).
- **The Bit Level Circuit** which is the logic circuit used to perform one-bit operations in the Arithmetic Logic Unit.

**c. Structural classification**

In the structural classification, parallel computers are classified according to the structure of their memory. So, based on the memory structure, there are two types of parallel computers: Shared Memory parallel computers and Distributed Memory parallel computers

- **Shared memory parallel computers**: They are also referred to as tightly coupled systems, they are distinguished by a common global memory for all processors/CPU. Although all the processors share the same memory, they run independently from each other. Shared memory parallel computers are subdivided into two classes, based on the access and access time to the memory: The Uniform Memory Access (UMA) and the Non-Uniform Memory Access (NUMA). The architecture of UMA and NUMA computers is shown in Figures 5.14 and 5.15, respectively.

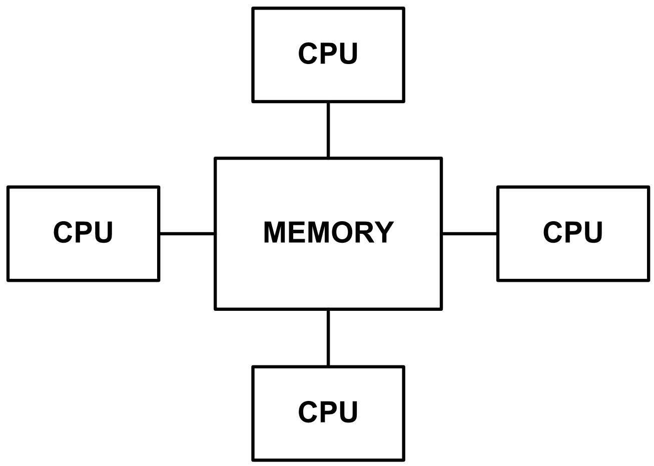


**Figure 5.14**: **Architecture of shared memory UMA (Culler et al.,1999)**

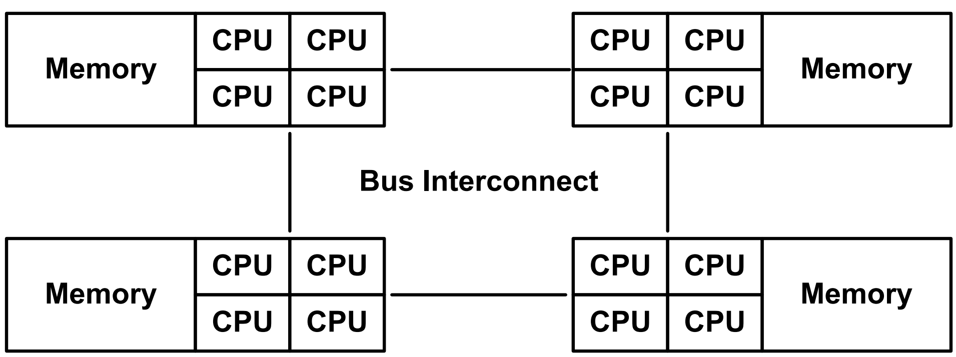


**Figure 5.15**: **Architecture of shared memory NUMA (Culler et al.,1999)**

In UMA, the processors have equal access and access time to the memory while in NUMA, the access time to the memory is not the same for all processors. Furthermore, in contrast to UMA, the memory access is slower in NUMA.

Shared memory parallel computers are ideal for applications requiring fast and uniform data sharing. They, however, suffer from a lack of scalability between the memory and the CPUs (Culler et al., 1999).

- **Distributed memory parallel computers**: In the distributed memory model, each processor has an independent memory, and no processor can access a memory other than theirs. Therefore, a Message Passing Interconnection Network is required to manage the traffic of information between the processors. The distributed memory approach alleviates the memory conflict problem known to slow down the execution of instructions in shared memory parallel computers (Culler et al., 1999). The architecture of distributed memory parallel computers is given in Figure 5.16

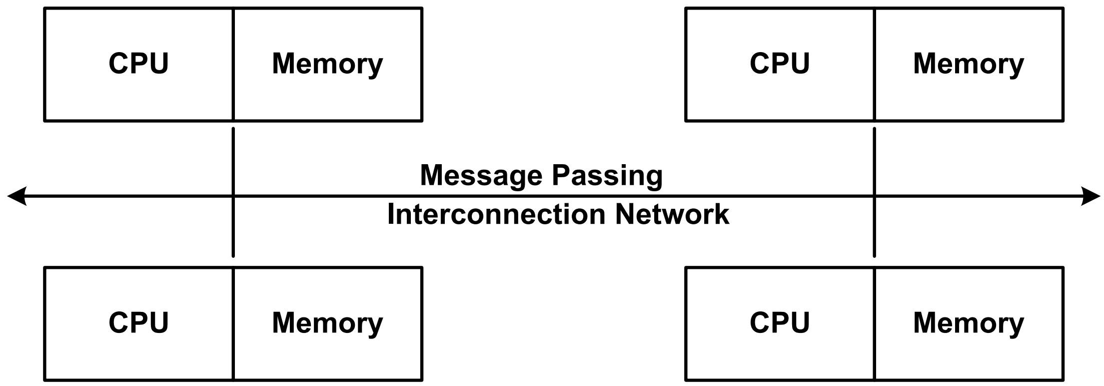


**Figure 5.16**: **Architecture of distributed memory parallel computers (Culler et al.,1999)**

**d. Grain size-based classification**

The grain size or granularity is a measure of the number of computations involved in a process. It is determined by counting the number of instructions in a segment of the program. Thus, based on the grain size, parallelism can be classified as fine grain, medium grain, and coarse grain parallelisms (Barney, 2017).

- **Fine Grain**: this type involves relatively small amounts of computations. The typical number of instructions is approximately less than 20. If the number of instructions is too small (too fine granularity), the communication overheads may take longer than the actual computation of the instructions.

- **Medium Grain**: this type consists of sub-programs and processes involving several hundreds of instructions.

- **Coarse Grain**: it consists of several independent programs involving thousands of instructions. The higher number of instruction make possible an opportunity for a performance increase. Furthermore, the communication overheads time is relatively small compared to the instructions' computation time.

#### 5.3.5.5. Parallel programming in MATLAB/SIMULINK

In MATLAB/Simulink, data and computationally expensive problems are solved through the parallel computing toolbox and the MATLAB Distributed Computing Server/Engine (MDCS/MDCE), provided that they are installed on multicores or multiprocessors computers (MathWorks, 2017). Data and task parallel algorithms can be directly implemented in MATLAB parallel computing environment using parallel processing constructs such as parallel for loops, code blocks, distributed arrays, message passing functions and more (MathWorks, 2017). Figure 5.17 shows the basic parallel computing setup.

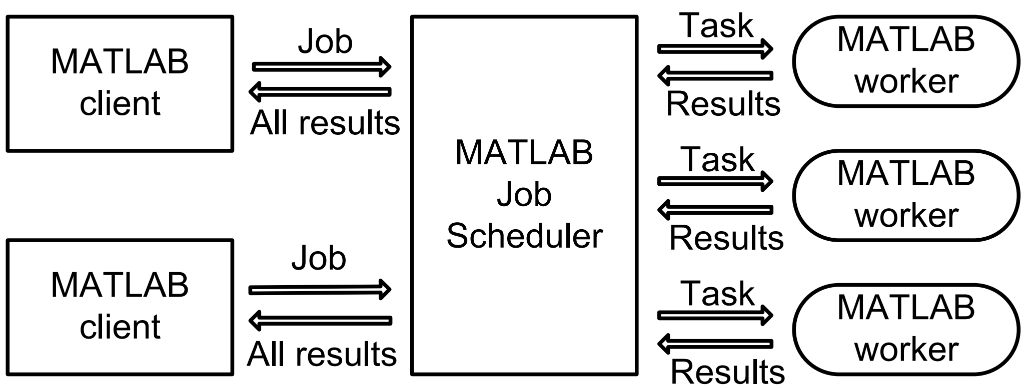


**Figure 5.17**: **Parallel computing setup and interactions between its sessions (MathWorks, 2016)**

A job is an operation that needs to be performed. Often, it is broken into smaller segments of tasks before to be processed. The MATLAB client is the machine in which the tasks to be executed are defined and programmed. The scheduler or MATLAB Job Scheduler (MJS) is the session that coordinates the execution of jobs and the evaluation of tasks. It usually processes the jobs in the order in which they are submitted. The MJS is also responsible for allocating tasks to the workers. A MATLAB worker is a session that performs the computation of tasks allocated to it by the MJS. After executing the tasks, the worker returns the result to the MJS (MathWorks, 2017).

The parallel computing toolbox allows the execution of parallel applications on a local multicores or multiprocessors computer. The MDCE is the preferred MATLAB service when parallel applications need to be executed on computers clusters, grids or clouds. In such instance, the parallel computing network might have several MJS and client sessions. Additionally, the MDCE must run on all workers in the network (MathWorks, 2017). Figure 5.18 is a representation of a computer cluster with multiple clients, MJS, and workers.

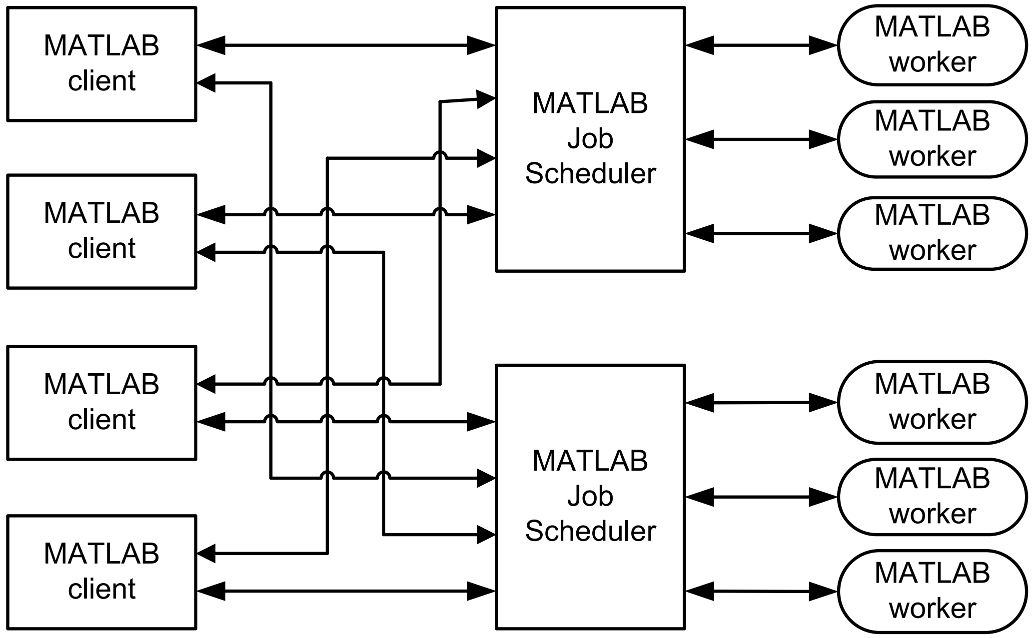


**Figure 5.18**: Computer cluster with multiple clients and MJS (MathWorks, 2017)

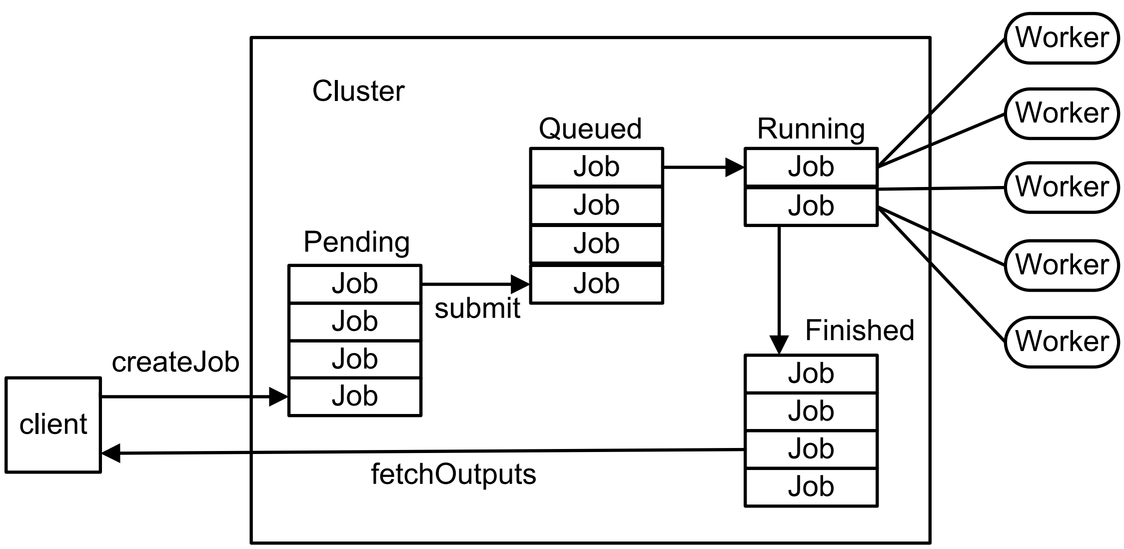


**Figure 5.19**: Diverse stages of a job (MathWorks, 2017)

From Figure 5.19, it can be inferred that a job goes through many stages from its creation to its execution. The set of stages a job undergoes, from its creation to the end of its execution is referred to as the lifecycle of the job. Jobs are categorised by their stage in the MJS. Figure 5.19 shows the different stages of a job's lifecycle. Further details on the job's lifecycle states are given in Table 5.6.

**Table 5.6**: **Details on the states of a job's lifecycle**

| Job Stage | Description |
|---|---|
| **Pending** | A job is created on the scheduler with the createJob function in the client session of Parallel Computing Toolbox software. The job's first state is pending. This is when the job is defined by adding tasks to it. |
| **Queued** | After the job has been submitted, the MJS or scheduler places the job in the queue, and the job's state is queued. The scheduler executes jobs in the queue in the sequence in which they are submitted, all jobs moving up the queue as the jobs before them are finished. |
| **Running** | When a job reaches the top of the queue, the scheduler distributes the job's tasks to worker sessions for evaluation. The job's state is now running. If more workers are available than what are required for a job's tasks, the scheduler begins executing the next job. In this way, there can be more than one job running at a time. |
| **Finished** | When all a job's tasks have been evaluated, the job is moved to the finished state. Now, the results from all the tasks in the job can be retrieved with the function fetchOutputs. |
| **Failed** | When a third-party scheduler is used, a job might fail if the scheduler encounters an error when attempting to execute its commands or access necessary files. |
| **Deleted** | When a job's data has been removed from its data location or the MJS with the delete function, the state of the job in the client is deleted. This state is available only as long as the job object remains in the client. |

#### 5.3.5.6. Parallel computing solution algorithm to analyse the performance of a distribution network with a feeder reconfiguration scheme under dynamic loading conditions

The algorithm in section 5.3.2 is a sequential algorithm. The instructions from Step 5 to Step 7 are executed as long as there are datasets for which the real power loss needs to be calculated. However, the number of data sets can be very high, especially if the threshold rate of power change **dp** as defined in Step 2 of the sequential algorithm in section 5.3.2. is small. Consequently, this results in a high computational burden and a time-consuming process. Parallel computing is used to alleviate that computational burden. Step 5 to Step 7 of the developed sequential programming algorithm is parallelizable. This portion of the code (Step 5 to Step 7) can be spread and computed on several workers, each processing a workload whose size is determined by the **pctdemo_helper_split_scalar** function. The MATLAB coding of the **pctdemo_helper_split_scalar** function is given in **Appendix F**. The **pctdemo_helper_split_scalar** function divides a non-negative number of data sets into **n_wrks** smaller non-negative numbers of data sets, where **n_wrks** is the number of workers from the parallel computer/cluster to be used to solve the parallel problem (MathWorks, 2016). A limit is imposed on the number of workers as it cannot be greater that the numbers of processors/cores in the parallel machine.

In the parallelizable portion of the code (Step 5 to Step 7), only the datasets change over the iterations. The same program is used to evaluate a high number of datasets. As such, the Single Program Multiple Data (SPMD) function in MATLAB is ideal to computerise the algorithm in a parallel manner. The Single Program aspect of the SPMD means that an identical code is run in all workers (MathWorks, 2017). The Multiple Data attribute means that each worker can have a different data set, even though the same program code runs in all workers (MathWorks, 2017). When the SPMD function is executed, it creates a pool of workers using the default cluster profile. Each worker in the pool has a unique index number referred to as "$\mathbf{labindex}$". The $\mathrm{labindex}$ allows you to specify the dataset to be used and/or the code to be executed on specific workers in the pool (MathWorks, 2017).

The parallel computing algorithm is quite similar to its sequential programming algorithm developed in section 5.3.2. Step 1 to 4 from the sequential programming algorithm remains unchanged in the parallel programming algorithm.

To obtain the parallel computing algorithm, the following instructions are added to the sequential programming algorithm, just after Step 4 and before the **SPMD** function opens the pool of workers:

- Set the number of workers $\mathbf{n\_wrks}$ to be used to solve the parallel problem. The number of workers should be less than or equal to the number of cores/processors in the parallel computer.
- Using the $\mathbf{pctdemo\_helper\_split\_scalar}$ function (see **Appendix F**), determine the number of datasets from the repertoires $\mathbf{P\_rep}$ and $\mathbf{Q\_rep}$ (given in Table 5.3 and 5.4, respectively) that is allocated to each worker.

Once the parallel pool is opened by the **SPMD** function, step 5 to step 7 run concurrently on all workers. The data sets from the repertoires $\mathbf{P\_rep}$ and $\mathbf{Q\_rep}$ are closely distributed amongst the workers.

The parallel computing solution algorithm to evaluate the daily performance of a distribution network with a feeder reconfiguration scheme and under dynamic loading conditions is as follows:

**Step 1**: Read the electrical distribution network data such as the number of nodes $\mathbf{NB}$, the number of distribution lines $\mathbf{NL}$, the number of tie lines $\mathbf{NT}$, the bus type ($\mathbf{Slack}, \mathbf{PV}, \mathbf{PQ}$), the load data ($\mathbf{Pd_i}^{\mathbf{t}}, \mathbf{Qd_i}^{\mathbf{t}}, \mathbf{Bs}, \mathbf{Load\_ID}$), the generator data ($\mathbf{Pg}, \mathbf{Qg}$) and distribution line data ($\mathbf{bus\_i}, \mathbf{bus\_j}, \mathbf{r}, \mathbf{x}, \mathbf{sw\_tie}, \mathbf{sw\_sec}$).

**Step 2**: Set the threshold rate of power change $\mathrm{dp}$ as defined in step 2 of the sequential programming algorithm in section 5.3.2

**Step 3**: Find the total load demand in the distribution network at each time interval for the 24h period. This process is the same as that of the PSO-based sequential computing algorithm developed in section 5.3.2.

**Step 4**: Determine the load demand $\mathrm{Pd_i}^{\mathrm{t}}$ and $\mathrm{Qd_i}^{\mathrm{t}}$ at each PQ bus in the distribution network. Equations 5.1 and 5.2 are used to determine the real and the reactive power demand at each PQ bus in the distribution network. The results are given in Tables 5.3 and 5.4 and saved in the repertoire $\mathrm{P\_rep}$ and $\mathrm{Q\_rep}$ for the real and reactive power demand at each PQ bus, respectively.

**Step 5:** Set the number of workers $\mathbf{n\_wrks}$ to be used to solve the parallel problem. And using the $\mathbf{pctdemo\_helper\_split\_scalar}$ function, determine the number of datasets $\mathbf{numPerTask}$ from the repertoires $\mathbf{P\_rep}$ and $\mathbf{Q\_rep}$ (given in Tables 5.3 and 5.4, respectively) that is allocated to each worker

**Step 6:** Open the pool of MATLAB workers using the **SPMD** function and allocate tasks (datasets) to each worker.

**Start the iteration process** and set the iteration counter $\mathbf{k}$ to 1 for each $\mathbf{labindex}$. The iteration counter counts the number of load bus real and reactive dataset that go through the iterative loop. The iteration process is run concurrently in all the workers.

**Step 7**: Read the real and reactive power demand $\mathbf{Pd_i}^{\mathbf{t}}$ and $\mathbf{Qd_i}^{\mathbf{t}}$ at each bus at time $\mathrm{t}$ from $\mathbf{P\_rep}$ and $\mathbf{Q\_rep}$, respectively (dataset $\mathbf{k}$), and update the load demand in the distribution network.

**Step 8**: The PSO algorithm developed in chapter three, section 3.5.2 to solve the single objective distribution network feeder reconfiguration problem is used to create a function $\mathbf{spmd1}$ which takes the distribution network data defined in step 1 as inputs and returns the solution of the distribution network feeder reconfiguration optimization process as outputs.

Using the function $\mathbf{spmd1}$, run the optimal feeder reconfiguration algorithm and determine the real power loss $\mathbf{Ploss\_in}$; the minimum voltage $\mathbf{minV_{in}}$; the maximum voltage $\mathbf{maxV\_in}$ before reconfiguration, and the real power loss $\mathbf{fitness\_Gbest}$; the minimum voltage $\mathbf{Vmin\_Gbest}$; the maximum voltage $\mathbf{Vmax\_Gbest}$ after the reconfiguration.

**Step 9**: Save the results from Step 8 in the repertoire $\mathbf{y1}$. The repertoire $\mathbf{y1}$ is created for each worker to save the results of Step 8 for each dataset.

**Step 10**: Stop the iteration or increment the iteration counter. For each worker, If Step 7 to Step 9 are performed for all the datasets allocated to the worker from Step 5, then stop the iterative process. Else, increment the iteration count and repeat step 7 to step 9 until all datasets are evaluated.

**Step 11**: Print the results of the parallel computing algorithm to evaluate the daily performance of a distribution network with a feeder reconfiguration scheme and under dynamic loading conditions. At the end of the simulations, the results from each worker saved in their respective repertoire as given in Step 9, should be retrieved and printed for analysis.

The flowchart of the parallel computing algorithm to evaluate the daily performance of a distribution network with a feeder reconfiguration scheme under dynamic loading conditions is given in Figure 5.20.

Step 1 to Step 4 can be considered as the initialisation part of the Parallel computing solution algorithm, and they consist of data preparation tasks.
To compare the results of the developed sequential programming algorithm with those of the developed parallel computing algorithm, it is necessary that the datasets obtained from Step 4 are the same for both algorithms. Step 1 and Step 4 in the sequential programming algorithm in section 5.3.2 is the same as that of the parallel computing algorithm described above. So, in the MATLAB coding of the parallel computing algorithm, Step 1 to Step 4 can be omitted and replaced with a Step that consists of retrieving datasets information from the repertoires $\mathbf{P\_rep}$ and $\mathbf{Q\_rep}$ (given in Table 5.3 and 5.4, respectively) obtained after running the developed sequential programming algorithm.

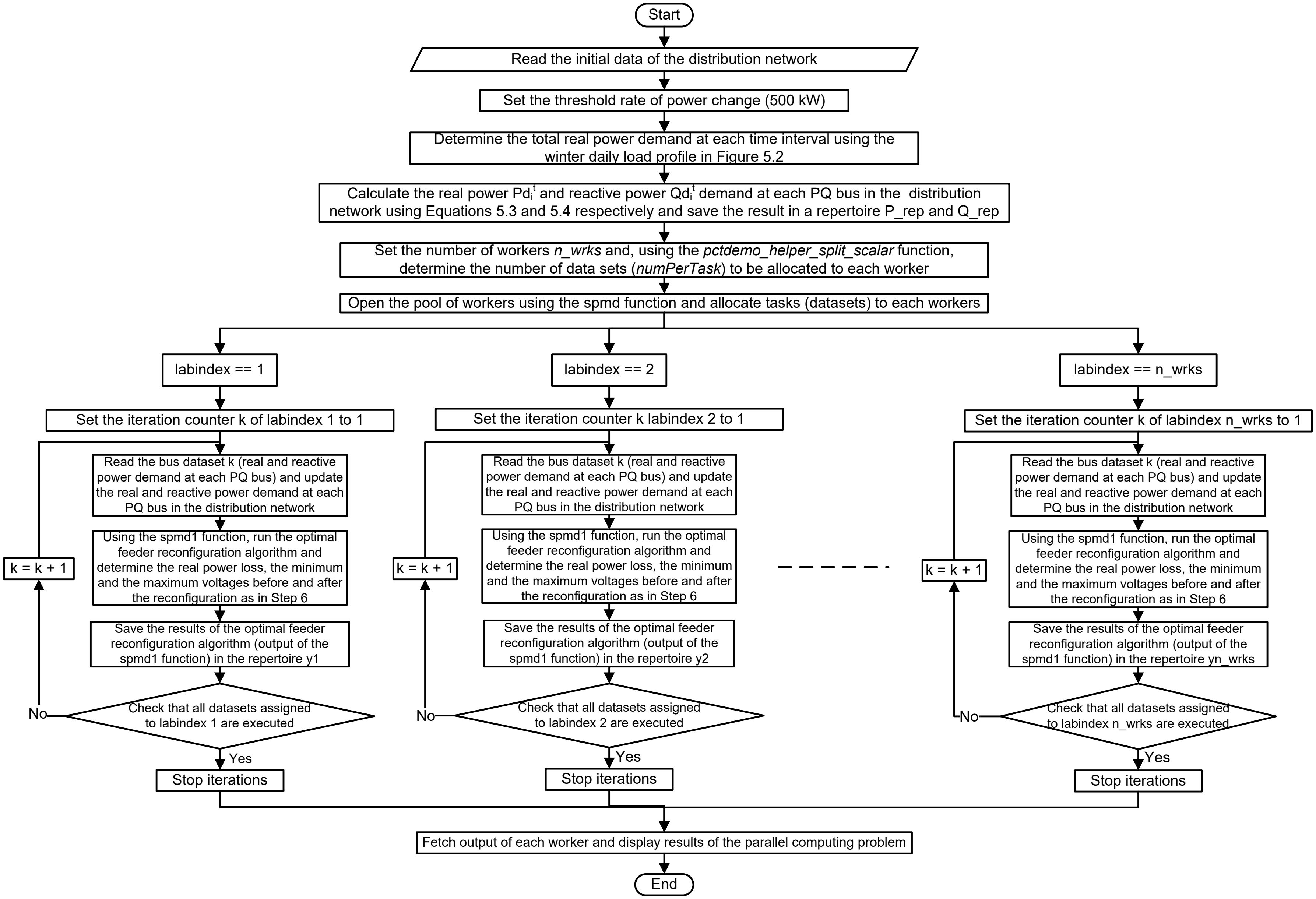


**Figure 5.20**: **Flowchart of the data-parallel computing solution to analyse the performance of the distribution network with a feeder reconfiguration scheme under dynamic loading conditions**

### 5.3.6. Results of the Parallel computing solution to analyse the performance of the distribution network with a feeder reconfiguration scheme under dynamic loading conditions

The developed parallel computing solution algorithm is used to analyse the performance of the 16-bus distribution system with a feeder reconfiguration scheme over a 24h period. The rate of the power change threshold is $500\ \mathrm{kW}$. Due to the speed-up and the scalability limits in parallel applications, the heuristic formula given in Equation 5.5 is developed to determine the optimal number of workers used in the parallel code.

$$\mathbf{n\_wrks} = \frac{\mathbf{round(n\_dataset)}}{\mathbf{10}} \tag{5.5}$$

Where,

$\mathbf{n\_dataset}$ is the number of data sets to evaluate.

$\mathbf{round(n\_dataset)}$ is the operation that rounds off the number of data sets to the nearest multiple of 10.

After the data preparation steps (Step 1 to 3) the algorithms given in sections 5.3.3.1 and 5.3.3.3., it resorts that there are 57 datasets to be simulated. Using Equation 5.5, the optimal number of workers used in the parallel code is calculated. It follows that six workers are needed for the parallel computing algorithm implementation in MATLAB. Thus, the first three workers simulate ten datasets each, and the next three workers simulate nine datasets each.

Tables 5.7 to 5.12 present the outputs of worker 1 to 6, respectively at the end of the parallel computing simulations. The results of the parallel computing algorithm are analysed in terms of real power loss, minimum voltage and maximum voltage before and after optimal network reconfiguration.

**Table 5.7**: **Data-parallel feeder reconfiguration solutions from worker 1**

| Dataset Nº. | Before reconfiguration | | | After reconfiguration | | | | | |
|---|---|---|---|---|---|---|---|---|---|
| | Real power loss (kW) | Max voltage (p.u) | Min voltage (p.u) | Real power loss (kW) | Max voltage (p.u) | Min voltage (p.u) | Optimal topology (tie switches) | | |
| 1 | 465.5 | 1 | 0.9724 | 423.1 | 1 | 0.9750 | 7 | 8 | 16 |
| 2 | 473.9 | 1 | 0.9731 | 430.4 | 1 | 0.9766 | 7 | 8 | 16 |
| 3 | 402.2 | 1 | 0.9766 | 385.9 | 1 | 0.9766 | 7 | 14 | 16 |
| 4 | 474.3 | 1 | 0.9698 | 377.3 | 1 | 0.9822 | 8 | 13 | 15 |
| 5 | 388.6 | 1 | 0.9736 | 353.5 | 1 | 0.9793 | 4 | 7 | 8 |
| 6 | 343.3 | 1 | 0.9798 | 339.7 | 1 | 0.9798 | 8 | 15 | 16 |
| 7 | 335.4 | 1 | 0.9790 | 329.3 | 1 | 0.9792 | 8 | 15 | 16 |
| 8 | 385.5 | 1 | 0.9710 | 315.0 | 1 | 0.9822 | 7 | 8 | 16 |
| 9 | 337.8 | 1 | 0.9806 | 336.0 | 1 | 0.9806 | 11 | 14 | 16 |
| 10 | 320.1 | 1 | 0.9756 | 318.0 | 1 | 0.9797 | 13 | 14 | 15 |

**Table 5.8**: Data-parallel feeder reconfiguration solutions from worker 2

| Dataset Nº. | Before reconfiguration | | | After Reconfiguration | | | | | |
|---|---|---|---|---|---|---|---|---|---|
| | Real power loss (kW) | Max voltage (p. u) | Min voltage (p. u) | Real power loss (kW) | Max voltage (p. u) | Min voltage (p. u) | Optimal topology (tie switches) | | |
| 11 | 375.8 | 1 | 0.9769 | 364.4 | 1 | 0.9727 | 8 | 15 | 16 |
| 12 | 358.1 | 1 | 0.9778 | 358.1 | 1 | 0.9778 | 14 | 15 | 16 |
| 13 | 358.8 | 1 | 0.9801 | 349.2 | 1 | 0.9819 | 4 | 8 | 15 |
| 14 | 393.5 | 1 | 0.9760 | 358.9 | 1 | 0.9783 | 8 | 15 | 16 |
| 15 | 479.2 | 1 | 0.9729 | 408.3 | 1 | 0.9775 | 8 | 11 | 16 |
| 16 | 486.8 | 1 | 0.9651 | 388.1 | 1 | 0.9793 | 8 | 15 | 16 |
| 17 | 576.3 | 1 | 0.9626 | 477.7 | 1 | 0.9716 | 7 | 8 | 16 |
| 18 | 458.7 | 1 | 0.9780 | 430.5 | 1 | 0.9780 | 8 | 15 | 16 |
| 19 | 451.0 | 1 | 0.9777 | 439.5 | 1 | 0.9761 | 8 | 15 | 16 |
| 20 | 588.4 | 1 | 0.9611 | 472.9 | 1 | 0.9755 | 4 | 7 | 8 |

**Table 5.9**: Data-parallel feeder reconfiguration solutions from worker 3

| Dataset Nº. | Before reconfiguration | | | After reconfiguration | | | | | |
|---|---|---|---|---|---|---|---|---|---|
| | Real power loss (kW) | Max voltage (p. u) | Min voltage (p. u) | Real power loss (kW) | Max voltage (p. u) | Min voltage (p. u) | Optimal topology (tie switches) | | |
| 21 | 541.7 | 1 | 0.9670 | 529.9 | 1 | 0.9706 | 2 | 7 | 13 |
| 22 | 564.8 | 1 | 0.9637 | 560.7 | 1 | 0.9637 | 7 | 14 | 16 |
| 23 | 519.4 | 1 | 0.9746 | 502.1 | 1 | 0.9755 | 8 | 15 | 16 |
| 24 | 529.9 | 1 | 0.9664 | 527.8 | 1 | 0.9661 | 8 | 15 | 16 |
| 25 | 690.3 | 1 | 0.9700 | 598.7 | 1 | 0.9724 | 8 | 13 | 15 |
| 26 | 685.6 | 1 | 0.9630 | 589.8 | 1 | 0.9696 | 7 | 8 | 16 |
| 27 | 592.5 | 1 | 0.9737 | 580.7 | 1 | 0.9732 | 4 | 8 | 15 |
| 28 | 694.1 | 1 | 0.9650 | 626.8 | 1 | 0.9654 | 7 | 8 | 16 |
| 29 | 618.6 | 1 | 0.9650 | 614.0 | 1 | 0.9649 | 8 | 11 | 16 |
| 30 | 589.8 | 1 | 0.9719 | 576.8 | 1 | 0.9753 | 13 | 14 | 15 |

**Table 5.10**: Data-parallel feeder reconfiguration solutions from worker 4

| Dataset Nº. | Before reconfiguration | | | After Reconfiguration | | | | | |
|---|---|---|---|---|---|---|---|---|---|
| | Real Power Loss (MW) | Max voltage (p. u) | Min voltage (p. u) | Real Power loss (MW) | Max voltage (p. u) | Min voltage (p. u) | Optimal topology (tie switches) | | |
| 31 | 776.5 | 1 | 0.9532 | 594.4 | 1 | 0.9698 | 8 | 15 | 16 |
| 32 | 561.2 | 1 | 0.9647 | 544.5 | 1 | 0.9674 | 4 | 8 | 15 |
| 33 | 455.6 | 1 | 0.9781 | 447.9 | 1 | 0.9761 | 8 | 15 | 16 |
| 34 | 707.8 | 1 | 0.9612 | 531.7 | 1 | 0.9768 | 8 | 13 | 15 |
| 35 | 577.6 | 1 | 0.9679 | 577.6 | 1 | 0.9679 | 14 | 15 | 16 |
| 36 | 719.0 | 1 | 0.9649 | 640.1 | 1 | 0.9658 | 8 | 15 | 16 |
| 37 | 652.7 | 1 | 0.9728 | 639.4 | 1 | 0.9718 | 8 | 15 | 16 |
| 38 | 629.4 | 1 | 0.9714 | 590.7 | 1 | 0.9714 | 8 | 15 | 16 |
| 39 | 672.7 | 1 | 0.9690 | 611.5 | 1 | 0.9708 | 8 | 15 | 16 |

**Table 5.11**: Data-parallel feeder reconfiguration solutions from worker 5

| Dataset Nº. | Before reconfiguration | | | After Reconfiguration | | | | | |
|---|---|---|---|---|---|---|---|---|---|
| | Real Power loss (MW) | Max voltage (p. u) | Min voltage (p. u) | Real Power loss (MW) | Max voltage (p. u) | Min voltage (p. u) | Optimal topology (tie switches) | | |
| 40 | 674.9 | 1 | 0.9718 | 668.5 | 1 | 0.9668 | 8 | 15 | 16 |
| 41 | 799.4 | 1 | 0.9631 | 680.8 | 1 | 0.9713 | 8 | 13 | 15 |
| 42 | 790.7 | 1 | 0.9600 | 790.7 | 1 | 0.9600 | 14 | 15 | 16 |
| 43 | 744.0 | 1 | 0.9589 | 657.0 | 1 | 0.9697 | 8 | 15 | 16 |
| 44 | 684.5 | 1 | 0.9663 | 628.6 | 1 | 0.9731 | 7 | 8 | 16 |
| 45 | 728.0 | 1 | 0.9648 | 652.1 | 1 | 0.9733 | 7 | 8 | 13 |
| 46 | 596.3 | 1 | 0.9743 | 582.2 | 1 | 0.9738 | 8 | 15 | 16 |
| 47 | 644.9 | 1 | 0.9689 | 639.8 | 1 | 0.9640 | 8 | 15 | 16 |
| 48 | 679.7 | 1 | 0.9605 | 572.1 | 1 | 0.9739 | 8 | 15 | 16 |

**Table 5.12**: Data-parallel feeder reconfiguration solutions from worker 6

| Dataset Nº. | Before reconfiguration | | | After Reconfiguration | | | | | |
|---|---|---|---|---|---|---|---|---|---|
| | Real power loss (MW) | Max voltage (p. u) | Min voltage (p. u) | Real power loss (MW) | Max voltage (p. u) | Min voltage (p. u) | Optimal topology (tie switches) | | |
| 49 | 685.3 | 1 | 0.9666 | 613.6 | 1 | 0.9727 | 8 | 11 | 16 |
| 50 | 636.4 | 1 | 0.9668 | 609.2 | 1 | 0.9668 | 8 | 15 | 16 |
| 51 | 538.3 | 1 | 0.9752 | 520.0 | 1 | 0.9759 | 8 | 15 | 16 |
| 52 | 493.2 | 1 | 0.9747 | 451.9 | 1 | 0.9780 | 8 | 15 | 16 |
| 53 | 596.3 | 1 | 0.9673 | 552.3 | 1 | 0.9711 | 8 | 13 | 15 |
| 54 | 468.1 | 1 | 0.9757 | 468.1 | 1 | 0.9757 | 14 | 15 | 16 |
| 55 | 487.4 | 1 | 0.9714 | 469.5 | 1 | 0.9723 | 8 | 13 | 15 |
| 56 | 429.5 | 1 | 0.9779 | 423.9 | 1 | 0.9779 | 8 | 15 | 16 |
| 57 | 464.6 | 1 | 0.9734 | 445.2 | 1 | 0.9734 | 8 | 15 | 16 |

The 57 datasets represent the variations of power demand throughout the day. Figure 5.21 and Figure 5.22 represent the changes of the minimum voltage and the real power loss throughout the day, respectively.

The profile summary of the simulations is given in Figure 5.23.

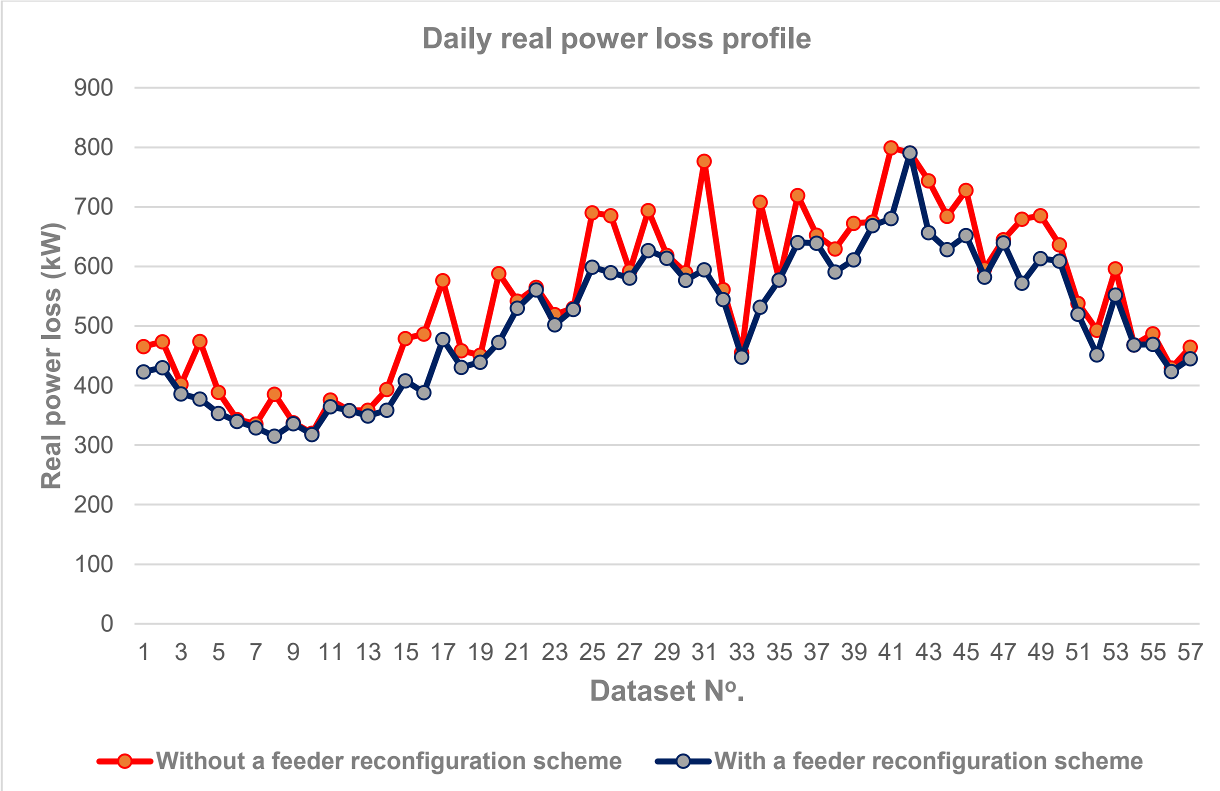


**Figure 5.21**: Daily real power loss profile using the developed data-parallel computing approach

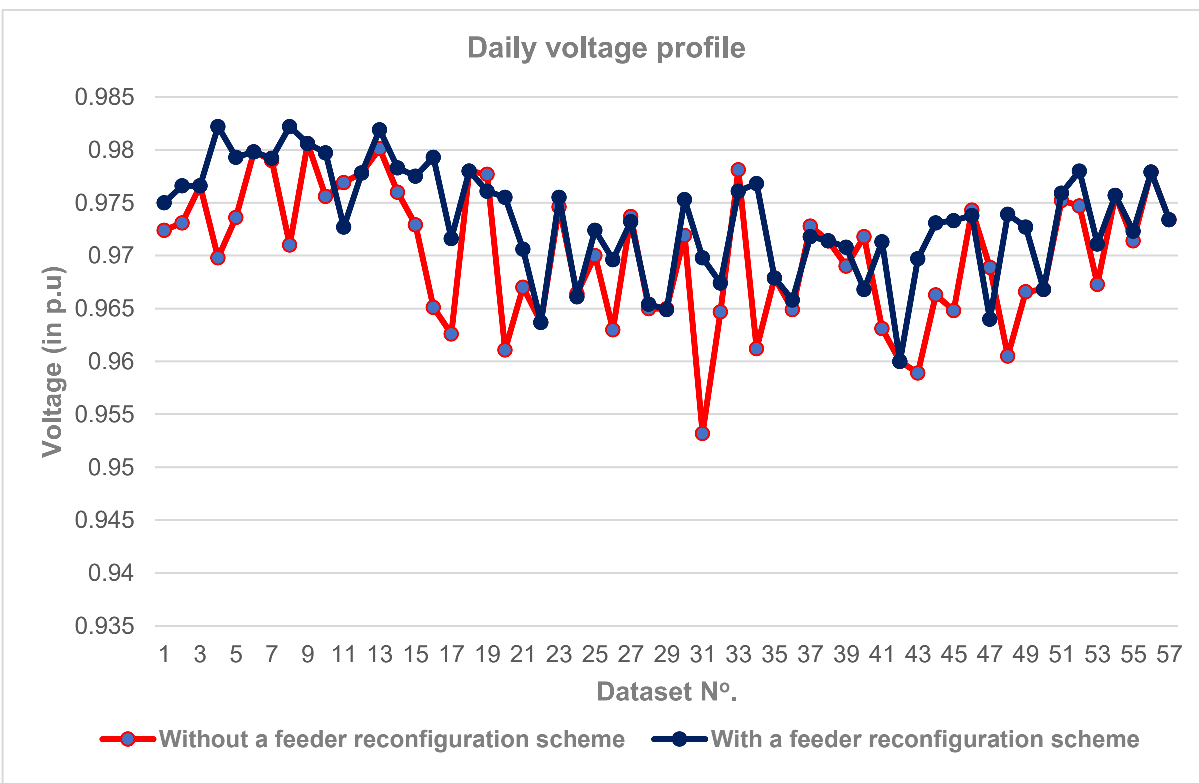


**Figure 5.22**: Daily minimum voltage profile using the developed data-parallel computing approach

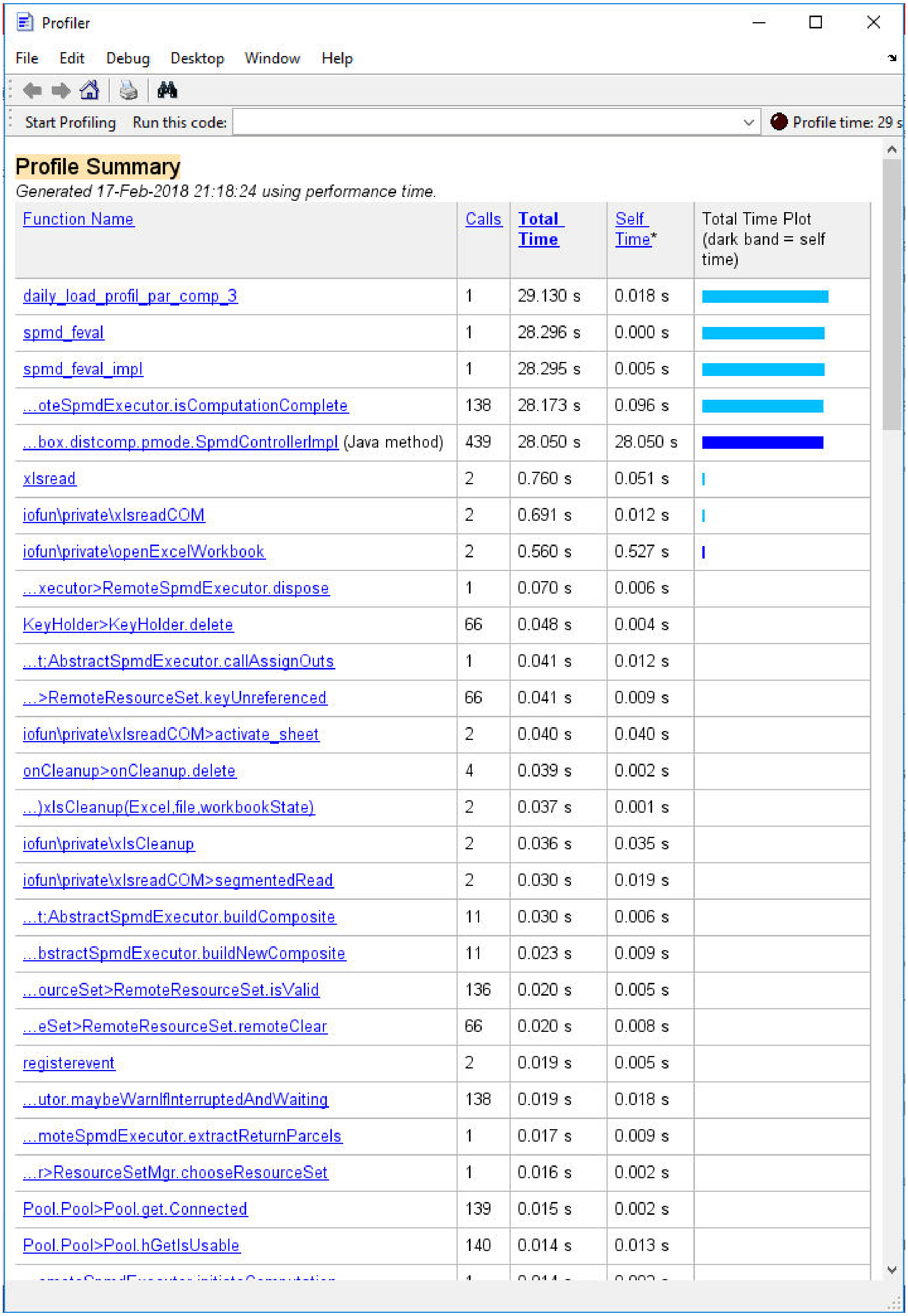

Profiler

File Edit Debug Desktop Window Help

Start Profiling Run this code: Profile time: 29 s

## Profile Summary

*Generated 17-Feb-2018 21:18:24 using performance time.*

| Function Name | Calls | Total Time | Self Time* | Total Time Plot (dark band = self time) |
|---|---|---|---|---|
| daily_load_profil_par_comp_3 | 1 | 29.130 s | 0.018 s | |
| spmd_feval | 1 | 28.296 s | 0.000 s | |
| spmd_feval_impl | 1 | 28.295 s | 0.005 s | |
| ...oteSpmdExecutor.isComputationComplete | 138 | 28.173 s | 0.096 s | |
| ...box.distcomp.pmode.SpmdControllerImpl (Java method) | 439 | 28.050 s | 28.050 s | |
| xlsread | 2 | 0.760 s | 0.051 s | |
| iofun\private\xlsreadCOM | 2 | 0.691 s | 0.012 s | |
| iofun\private\openExcelWorkbook | 2 | 0.560 s | 0.527 s | |
| ...xecutor>RemoteSpmdExecutor.dispose | 1 | 0.070 s | 0.006 s | |
| KeyHolder>KeyHolder.delete | 66 | 0.048 s | 0.004 s | |
| ...t;AbstractSpmdExecutor.callAssignOuts | 1 | 0.041 s | 0.012 s | |
| ...>RemoteResourceSet.keyUnreferenced | 66 | 0.041 s | 0.009 s | |
| iofun\private\xlsreadCOM>activate_sheet | 2 | 0.040 s | 0.040 s | |
| onCleanup>onCleanup.delete | 4 | 0.039 s | 0.002 s | |
| ...)xlsCleanup(Excel,file,workbookState) | 2 | 0.037 s | 0.001 s | |
| iofun\private\xlsCleanup | 2 | 0.036 s | 0.035 s | |
| iofun\private\xlsreadCOM>segmentedRead | 2 | 0.030 s | 0.019 s | |
| ...t;AbstractSpmdExecutor.buildComposite | 11 | 0.030 s | 0.006 s | |
| ...bstractSpmdExecutor.buildNewComposite | 11 | 0.023 s | 0.009 s | |
| ...ourceSet>RemoteResourceSet.isValid | 136 | 0.020 s | 0.005 s | |
| ...eSet>RemoteResourceSet.remoteClear | 66 | 0.020 s | 0.008 s | |
| registerevent | 2 | 0.019 s | 0.005 s | |
| ...utor.maybeWarnIfInterruptedAndWaiting | 138 | 0.019 s | 0.018 s | |
| ...moteSpmdExecutor.extractReturnParcels | 1 | 0.017 s | 0.009 s | |
| ...r>ResourceSetMgr.chooseResourceSet | 1 | 0.016 s | 0.002 s | |
| Pool.Pool>Pool.get.Connected | 139 | 0.015 s | 0.002 s | |
| Pool.Pool>Pool.hGetIsUsable | 140 | 0.014 s | 0.013 s | |

**Figure 5.23**: Profile summary of the developed data-parallel computing approach for feeder reconfiguration under dynamic loading conditions

### 5.3.7. Discussion of the results of the parallel computing solution algorithm to analyse the performance of the distribution network with feeder reconfiguration under dynamic loading conditions

The comparison of the results of the sequential programming algorithm given in Table 5.5 with the parallel computing solutions in Table 5.7 to 5.12 shows that both the developed sequential and parallel computing algorithms yield the same results. The daily real power loss profile (Figure 5.5) and the daily minimum voltage profile (Figure 5.6) for the sequential programming algorithm are identical to the daily real power loss profile (Figure 5.21) and the daily minimum voltage profile (Figure 5.22) respectively for the parallel algorithm. However, the parallel programming of the algorithm returns the results faster than the sequential programming algorithm. Figure 5.7 and Figure 5.23 represent the profile summary of the developed sequential programming and parallel computing algorithm, respectively. It is observed that the parallel computing algorithms return the solution after on average 29 seconds while the sequential programming algorithm does so in 173 seconds. This means that the parallel computing algorithm is $\frac{173}{29} = 5.9655$ times faster than the sequential programming algorithm. That is a speed-up of approximately **six times**. That is because, in the parallel code, the data sets were split amongst the six workers while in the sequential code, only one worker is responsible for evaluating all the datasets. The speed-up of the developed Single Instruction Multiple Data (SIMD) parallel computing algorithm is in line with Amdahl's law (Equation 5.3) and Gustafson's law (Equation 5.4). Given that the distribution network feeder reconfiguration algorithm in section (3.5.4) is parallelised at 100% and that six workers are used to speed up the computational process, the parallelisation of the PSO-based algorithm resulted in a significant reduction of the computation time.

The next section presents the development of a solution algorithm to analyse the daily performance of the distribution network with DG under dynamic loading conditions.

## 5.4. Development of a PSO-based solution algorithm to analyse the performance of the distribution network with DG under dynamic loading conditions

The development of a solution algorithm to analyse the performance of the distribution network with DG under dynamic loading conditions is subject to the following assumptions:

- The location and the size of the Distributed Generator are known. The optimal DG location and size is obtained by using the optimal DG placement and sizing algorithm as defined in chapter four, section 4.4.2. As such, the maximum DG capacity is

$(\mathbf{13.0456 + j1.7526})\ \mathbf{MVA}$ and the DG is located at $\mathbf{bus\ 9}$ in the 16-bus distribution network given in Figure 3.3 in section 3.5.2.

- The data measurement for the real and reactive power at each PQ bus at different time intervals are known. The algorithm uses the same set of data used in section 5.3 and given in Tables 5.3 and 5.4.

Two types of DG are considered in the performance analysis:

- dispatchable DG and
- Non-dispatchable DG.

Dispatchable DG can have their output power adjusted by the power utility or the Distribution System Operator (DSO) while non-dispatchable DG sources can't. These two DG types are considered to analyse the influence of the DG output in the distribution network with DG under dynamic loading conditions.

### 5.4.1. Solution algorithm to analyse the performance of the distribution network with DG under dynamic loading conditions

To analyse the daily performance of the distribution network with DG under dynamic loading conditions, a solution algorithm is developed and implemented as follows.

**Step 1**: Read the electrical distribution network data such as the number of nodes $\mathbf{NB}$, the number of distribution lines $\mathbf{NL}$, the number of tie lines $\mathbf{NT}$, the bus type ($\mathbf{Slack}, \mathbf{PV}, \mathbf{PQ}$), the load data ($\mathbf{Pd}, \mathbf{Qd}, \mathbf{Bs}, \mathbf{Load\_ID}$), the generator data ($\mathbf{Pg}, \mathbf{Qg}$) and distribution line data ($\mathbf{bus\_i}, \mathbf{bus\_j}, \mathbf{r}, \mathbf{x}, \mathbf{sw\_tie}, \mathbf{sw\_sec}$).

**Step 2**: Read the load profile data sets saved in the repertoires $\mathbf{P\_rep}$ and $\mathbf{Q\_rep}$, and given in Tables 5.3 and 5.4 respectively.

**Step 3**: Read the optimal Distributed Generator size $\mathbf{DG\_size}$ and location $\mathbf{DG\_loc}$ for the base case. The optimal DG location and size are found using the PSO algorithm developed in section 4.4.2 to solve the optimal DG placement and sizing in distribution networks. The optimal DG location and size for the 16-bus distribution system are given in section 4.4.3.1.

**Step 4**: Update the distribution network data and insert the DG in the network. To account for the Distributed Generator, a new generator should be placed and activated in the distribution network.

- If the DG is non-dispatchable, it will supply in the distribution network with fixed real and reactive powers equal to the optimal DG size as defined in Step 3. It is assumed that the non-dispatchable DG operates at full capacity.

- If the DG is dispatchable, it will supply the distribution network with varying real and reactive powers, depending on the load demand. The maximum DG size is $(\mathbf{13.0456 + j1.7526})\ \mathbf{MVA}$. The dispatchable DG adjusts its output power according to the change in power demand.

**Start the iteration process** and set the iteration counter $\mathbf{k}$ to 1. The iteration counter counts the number of datasets that go through the iterative process.

**Step 5**: Read the real and reactive power demand $\mathbf{Pd_i}^{\mathbf{t}}$ and $\mathbf{Qd_i}^{\mathbf{t}}$ at each bus at time $\mathbf{t}$ from $\mathbf{P\_rep}$ and $\mathbf{Q\_rep}$, respectively (dataset $\mathbf{k}$), and update the load demand in the distribution network.

**Step 6**: Find the power flow of the distribution network using the Newton-Raphson power flow approach. Then, employ the power flow results to calculate the real power loss $\mathrm{Ploss}$ for the $\mathbf{k}^{\mathbf{th}}$ data set using Equation 3.12 given in chapter three, section 3.5.1.1.

**Step 7**: Create a **repertoire** $\mathbf{y3}$ and save in the results from Step 6 for each dataset.

**Step 8**: Stop the iteration or increment the iteration counter. If step 5 to step 7 are performed for all data sets from Tables 5.3 and 5.4, then stop the iterative process. Else, increment the iteration count and repeat step 5 to step 7.

**Step 9**: Print the results of the algorithm to evaluate the daily performance of a distribution network with DG under dynamic loading conditions. At the end of the simulations, the results saved in Step 7 should be retrieved for analysis.

The flowchart of the above-described algorithm is shown in Figure 5.24.

The next section presents the results of the application of the solution algorithm developed to evaluate the daily performance of the distribution network with DG under dynamic loading conditions for the 16-bus distribution system.

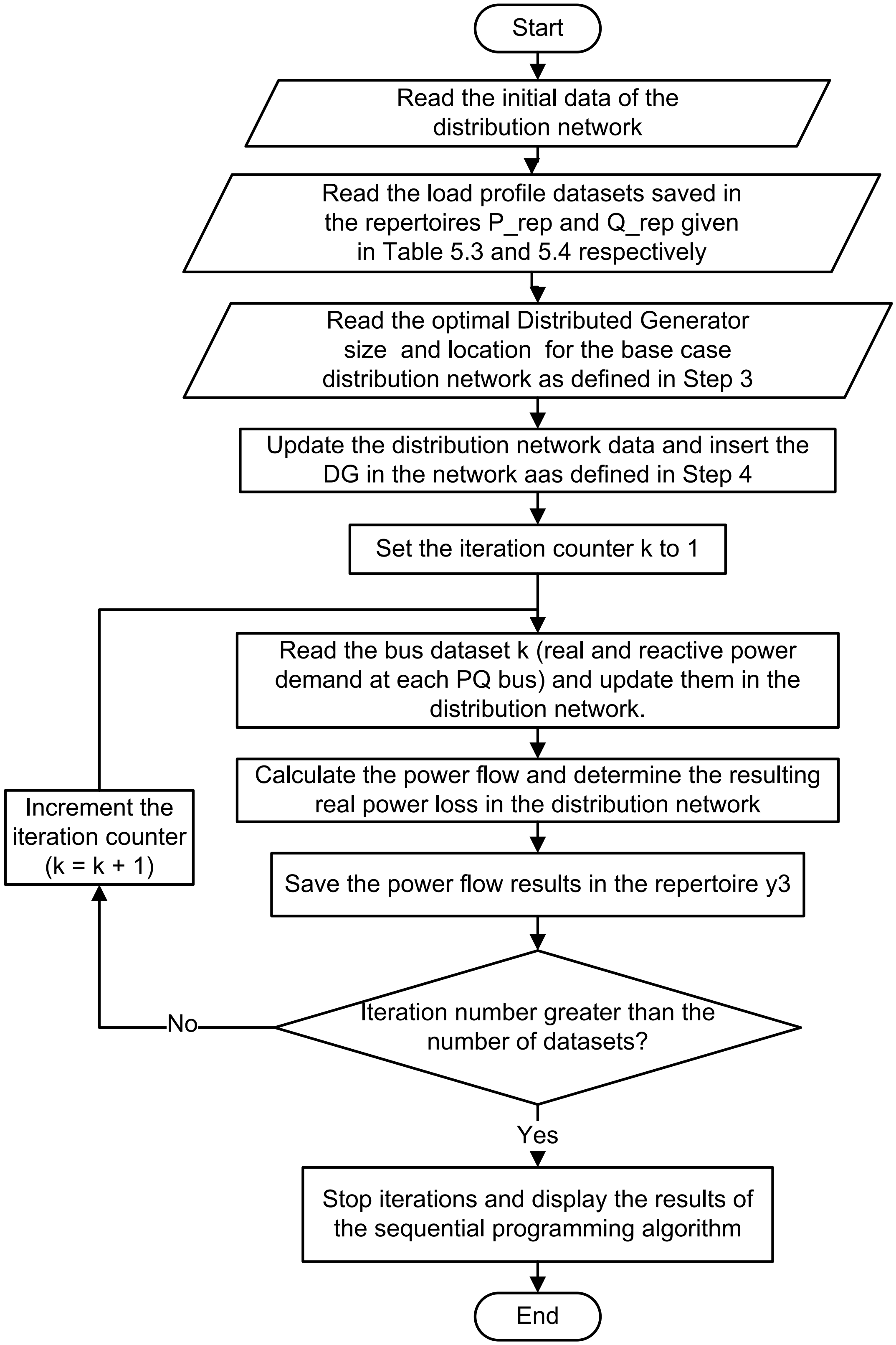


**Figure 5.124**: Flowchart of the PSO-based solution algorithm to analyse the performance of the distribution network with DG under dynamic loading conditions

### 5.4.2. Results of the solution algorithm to analyse the performance of the distribution network with DG under dynamic loading conditions

The solution algorithm developed to evaluate the daily performance of the distribution network with DG under dynamic loading conditions is applied to the 16-bus distribution system and its performance on a 24h period is evaluated.

The single line diagram of the 16-bus distribution network is given in Figure 3.3 in chapter three, section 3.5.2. Three source transformers supply the loads in the 16-bus distribution network

A comparative analysis of the distribution network with a dispatchable DG and a with non-dispatchable DG is done in this section. The results obtained from the 16-bus distribution network with a non-dispatchable DG are provided in Table 5.13. The results obtained when the DG is dispatchable are given in Table 5.14. The comparative analysis is done in terms of real and reactive power supply from the source transformers, the real power loss, the minimum and the maximum voltage of the considered distribution system.

Figure 5.25 provides the daily real power loss profiles of the 16-bus distribution network without DG, with a non-dispatchable DG, and with a dispatchable DG.

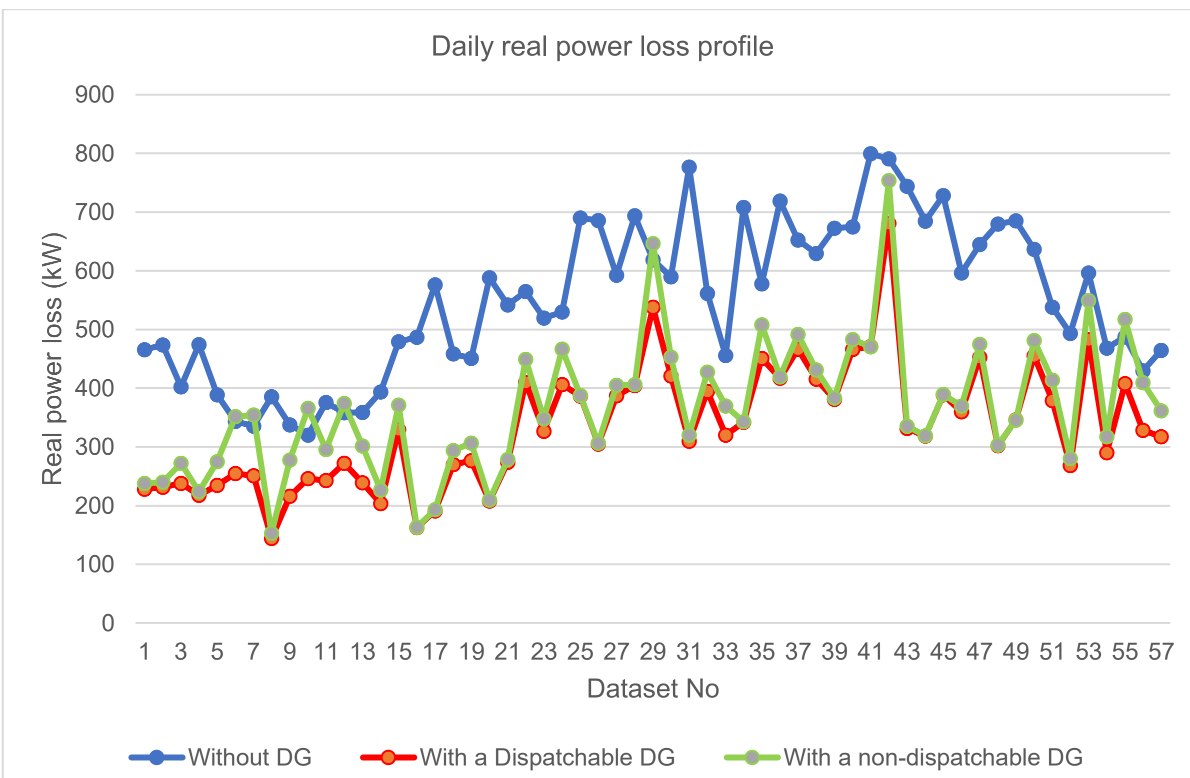


**Figure 5.25**: **Daily real power loss profiles of the distribution network without DG, with a non-dispatchable DG, and with a dispatchable DG**

Figure 5.26 provides the minimum and maximum voltage profiles of the distribution network with a non-dispatchable DG and with a dispatchable DG for all datasets.

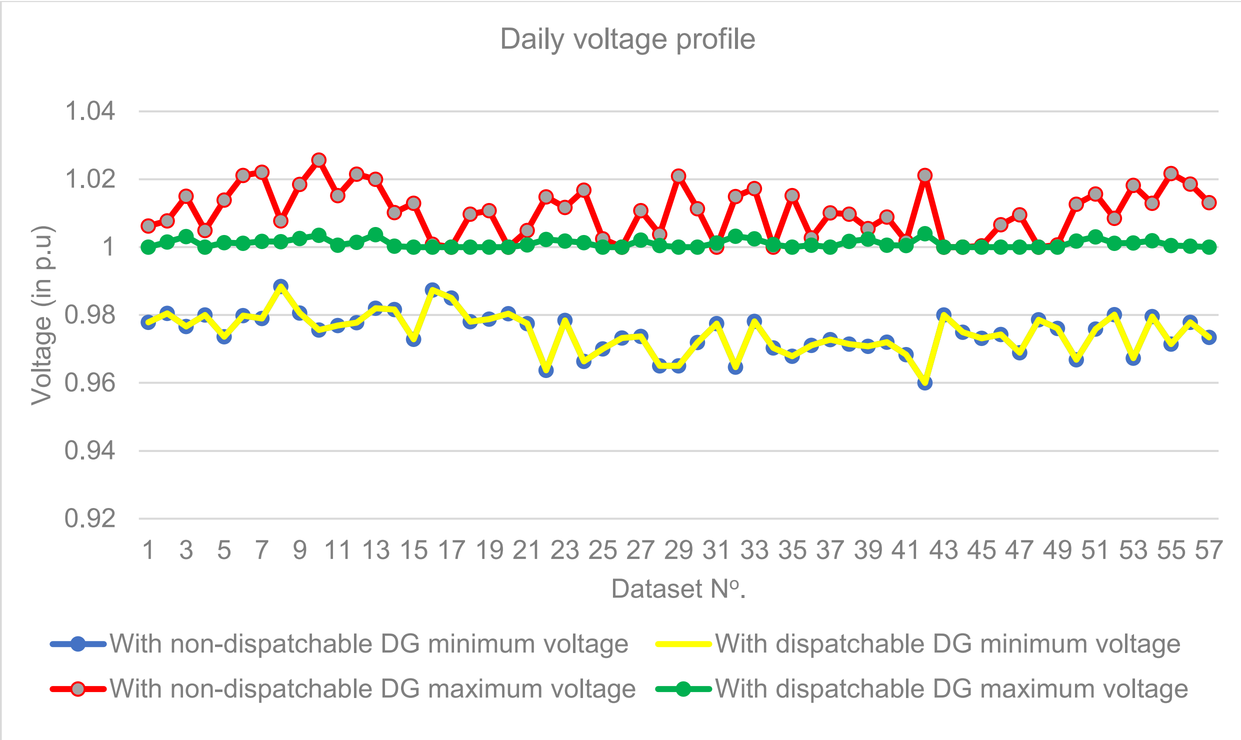


**Figure 5.262**: **Daily minimum and maximum voltage profiles of the distribution network with non-dispatchable DG and the distribution network with dispatchable DG**

**Table 5.13**: **Results of the distribution network with a non-dispatchable DG under dynamic loading conditions**

| Dataset Nº. | Source transformer 1 | | Source transformer 2 | | Source transformer 3 | | Real power loss (kW) | Max voltage (p. u) | Min voltage (p. u) |
|---|---|---|---|---|---|---|---|---|---|
| | Real power (MW) | Reactive power (MVar) | Real power (MW) | Reactive power (MVar) | Real power (MW) | Reactive power (MVar) | | | |
| **1** | 10.3354 | 4.1225 | −0.8276 | 0.0928 | 6.3848 | 0.3499 | 238.1 | 1.0062 | 0.9779 |
| **2** | 8.8337 | 3.1893 | 0.7231 | 1.0133 | 5.8375 | 0.0115 | 239.9 | 1.0077 | 0.9805 |
| **3** | 11.0519 | 4.5766 | −2.0182 | −0.7072 | 5.8927 | 0.0303 | 272.0 | 1.0150 | 0.9766 |
| **4** | 4.5118 | 0.4833 | −0.3522 | 0.3757 | 10.2187 | 2.7656 | 223.9 | 1.0049 | 0.9800 |
| **5** | 12.3896 | 5.4363 | −3.1481 | −1.3998 | 4.6876 | −0.7300 | 274.7 | 1.0139 | 0.9736 |
| **6** | 8.7713 | 3.1324 | −4.4319 | −2.2044 | 9.3302 | 2.2131 | 351.7 | 1.0211 | 0.9798 |
| **7** | 9.6220 | 3.6734 | −5.7520 | −3.0243 | 9.3027 | 2.1815 | 354.7 | 1.0221 | 0.9790 |
| **8** | 6.2522 | 1.5533 | −0.1201 | 0.4951 | 6.3389 | 0.3246 | 153.0 | 1.0077 | 0.9884 |
| **9** | 9.6716 | 3.6883 | −3.4584 | −1.5953 | 6.1192 | 0.1719 | 277.9 | 1.0185 | 0.9806 |
| **10** | 10.4704 | 4.2316 | −5.1851 | −2.6872 | 7.0349 | 0.7497 | 365.8 | 1.0257 | 0.9756 |
| **11** | 8.3022 | 2.8879 | −3.9338 | −1.8709 | 8.3817 | 1.5917 | 295.6 | 1.0152 | 0.9769 |
| **12** | 9.1202 | 3.3363 | −5.8452 | −3.0717 | 10.0534 | 2.6843 | 374.0 | 1.0215 | 0.9778 |
| **13** | 8.5390 | 2.9999 | −2.3380 | −0.9177 | 7.5548 | 1.0757 | 301.4 | 1.0200 | 0.9820 |

| | | | | | | | | | |
|---|---|---|---|---|---|---|---|---|---|
| **14** | 8.0560 | 2.6997 | −0.7589 | 0.0969 | 6.8837 | 0.6431 | 226.4 | 1.0102 | 0.9816 |
| **15** | 5.3736 | 1.0220 | −3.4534 | −1.5625 | 12.9058 | 4.4721 | 371.6 | 1.0129 | 0.9729 |
| **16** | 7.1657 | 2.1023 | 0.8572 | 1.1550 | 7.0946 | 0.7914 | 163.1 | 1.0009 | 0.9874 |
| **17** | 6.1280 | 1.4937 | 2.0827 | 1.9550 | 7.4368 | 1.0048 | 193.0 | 1 | 0.9850 |
| **18** | 7.9676 | 2.6357 | −1.7074 | −0.4879 | 9.9881 | 2.6405 | 293.9 | 1.0097 | 0.9780 |
| **19** | 10.9853 | 4.5174 | −2.5271 | −0.9824 | 8.3025 | 1.5513 | 306.3 | 1.0108 | 0.9788 |
| **20** | 9.8358 | 3.8058 | 2.1065 | 1.9419 | 5.2215 | −0.3735 | 209.4 | 1 | 0.9804 |
| **21** | 7.1591 | 2.1043 | −0.6415 | 0.2034 | 11.2157 | 3.3895 | 278.9 | 1.0049 | 0.9775 |
| **22** | 14.6105 | 6.9023 | −3.1254 | −1.3841 | 6.9188 | 0.7014 | 449.5 | 1.0148 | 0.9637 |
| **23** | 9.2165 | 3.4335 | 0.0591 | 0.5891 | 9.5267 | 2.3331 | 347.9 | 1.0117 | 0.9784 |
| **24** | 14.9900 | 7.1100 | −4.2332 | −2.0753 | 8.6644 | 1.7712 | 466.7 | 1.0168 | 0.9664 |
| **25** | 3.7983 | 0.0175 | 2.2863 | 2.0061 | 13.7573 | 5.0321 | 387.5 | 1.0025 | 0.9700 |
| **26** | 10.0246 | 3.9817 | 3.1597 | 2.5884 | 7.0764 | 0.7724 | 306.3 | 1 | 0.9732 |
| **27** | 14.3115 | 6.6380 | −0.7655 | 0.0892 | 7.3135 | 0.9236 | 405.1 | 1.0108 | 0.9737 |
| **28** | 13.3683 | 6.1374 | 2.1820 | 1.9379 | 5.8105 | −0.0120 | 406.3 | 1.0038 | 0.9650 |
| **29** | 14.8150 | 7.0249 | −5.4831 | −2.8422 | 11.7691 | 3.7573 | 646.6 | 1.0209 | 0.9650 |
| **30** | 10.7621 | 4.3855 | −2.6338 | −1.0495 | 12.2791 | 4.0836 | 453.0 | 1.0113 | 0.9719 |
| **31** | 8.8100 | 3.1843 | 3.8474 | 3.0525 | 7.1171 | 0.8059 | 320.1 | 1 | 0.9775 |
| **32** | 14.7070 | 6.9475 | −1.7327 | −0.5270 | 6.4076 | 0.3476 | 427.5 | 1.0149 | 0.9647 |
| **33** | 12.2060 | 5.2643 | −1.2282 | −0.2287 | 8.8463 | 1.8821 | 369.7 | 1.0173 | 0.9781 |
| **34** | 5.6426 | 1.1559 | 1.3529 | 1.4643 | 13.0319 | 4.5654 | 343.1 | 1 | 0.9703 |
| **35** | 13.7517 | 6.3212 | −3.5171 | −1.6133 | 10.4580 | 2.9129 | 508.3 | 1.0152 | 0.9679 |
| **36** | 10.2677 | 4.1441 | −0.2641 | 0.4526 | 11.0999 | 3.3367 | 419.1 | 1.0027 | 0.9711 |
| **37** | 11.0599 | 4.6251 | −1.5580 | −0.3743 | 12.1742 | 4.0238 | 491.6 | 1.0101 | 0.9728 |
| **38** | 10.2972 | 4.0970 | −1.1271 | −0.1365 | 12.9457 | 4.4956 | 431.4 | 1.0097 | 0.9714 |
| **39** | 9.1300 | 3.3548 | 1.9000 | 1.7434 | 11.5376 | 3.6276 | 383.2 | 1.0055 | 0.9708 |
| **40** | 12.3233 | 5.3980 | −1.4231 | −0.2986 | 12.2672 | 4.0669 | 483.0 | 1.0089 | 0.9720 |
| **41** | 6.7672 | 1.8670 | 2.9340 | 2.4299 | 13.9540 | 5.1403 | 470.7 | 1.0017 | 0.9683 |
| **42** | 15.5802 | 7.5628 | −4.4410 | −2.2259 | 13.0689 | 4.6127 | 753.7 | 1.0211 | 0.9600 |
| **43** | 10.9730 | 4.5080 | 2.6157 | 2.2801 | 9.7011 | 2.4334 | 335.5 | 1 | 0.9800 |
| **44** | 11.7894 | 5.0370 | 3.1533 | 2.5781 | 7.8307 | 1.2500 | 319.0 | 1 | 0.9749 |
| **45** | 8.2717 | 2.8354 | 2.4638 | 2.1763 | 11.6082 | 3.6594 | 389.2 | 1.0004 | 0.9731 |
| **46** | 12.0495 | 5.2108 | 0.5572 | 0.9332 | 9.2173 | 2.1312 | 369.6 | 1.0066 | 0.9743 |
| **47** | 11.5176 | 4.9539 | −1.6719 | −0.4451 | 11.5836 | 3.6298 | 474.9 | 1.0095 | 0.9689 |
| **48** | 8.1097 | 2.7004 | 2.7671 | 2.3473 | 9.8811 | 2.5662 | 303.5 | 1 | 0.9786 |
| **49** | 5.7841 | 1.2888 | 3.7516 | 2.9298 | 10.7648 | 3.1063 | 346.0 | 1.0007 | 0.9761 |
| **50** | 8.4923 | 2.9722 | −0.7657 | 0.0832 | 12.2093 | 4.0974 | 481.5 | 1.0126 | 0.9668 |
| **51** | 8.6687 | 3.0419 | −0.3506 | 0.3318 | 11.0503 | 3.3196 | 414.0 | 1.0157 | 0.9759 |
| **52** | 9.0100 | 3.2869 | 0.3046 | 0.7514 | 9.4201 | 2.2316 | 280.3 | 1.0085 | 0.9801 |
| **53** | 6.2130 | 1.5617 | −2.3128 | −0.8874 | 14.6035 | 5.5856 | 549.4 | 1.0182 | 0.9673 |
| **54** | 10.6169 | 4.2914 | −0.7012 | 0.1220 | 7.8561 | 1.2677 | 317.4 | 1.0129 | 0.9796 |
| **55** | 8.4378 | 2.8787 | −4.5328 | −2.2625 | 13.5667 | 4.9315 | 517.2 | 1.0217 | 0.9714 |
| **56** | 9.2123 | 3.4177 | −3.6696 | −1.7141 | 11.3210 | 3.4565 | 409.3 | 1.0186 | 0.9779 |
| **57** | 8.7886 | 3.1464 | −3.4954 | −1.5954 | 11.0228 | 3.2916 | 361.5 | 1.0131 | 0.9734 |
| **Total** | | | | | | | **20904.2** | | |

**Table 5.14**: Results of the distribution network with a dispatchable DG under dynamic loading conditions

| Dataset Nº. | source transformer 1 | | source transformer 2 | | source transformer 3 | | Real power loss (kW) | Max Voltage (p. u) | Min Voltage (p. u) | DG | |
|---|---|---|---|---|---|---|---|---|---|---|---|
| | P (MW) | Q (MVar) | P (MW) | Q (MVar) | P (MW) | Q (MVar) | | | | P (MW) | Q (Mvar) |
| **1** | 10.3354 | 4.1225 | 1.6173 | 0.8009 | 6.3848 | 0.3499 | 228.1 | 1 | 0.9779 | 10.5907 | 1.0984 |
| **2** | 8.8337 | 3.1893 | 3.2754 | 1.6310 | 5.8375 | 0.0115 | 231.5 | 1.0015 | 0.9805 | 10.4849 | 1.1869 |
| **3** | 11.0519 | 4.5766 | 2.1620 | 1.0722 | 5.8927 | 0.0303 | 237.8 | 1.0031 | 0.9766 | 8.8312 | 0.0571 |
| **4** | 4.5118 | 0.4833 | 1.7058 | 0.8449 | 10.2187 | 2.7656 | 217.5 | 1 | 0.9800 | 10.9811 | 1.3277 |
| **5** | 12.3896 | 5.4363 | 1.1603 | 0.5742 | 4.6876 | -0.7300 | 234.5 | 1.0013 | 0.9736 | 8.6970 | -0.1332 |
| **6** | 8.7713 | 3.1324 | 2.2223 | 1.1017 | 9.3302 | 2.2131 | 254.8 | 1.0011 | 0.9798 | 6.2946 | -1.4572 |
| **7** | 9.6220 | 3.6734 | 0.8860 | 0.4384 | 9.3027 | 2.1815 | 251.0 | 1.0017 | 0.9790 | 6.3040 | -1.6095 |
| **8** | 6.2522 | 1.5533 | 2.3199 | 1.1501 | 6.3389 | 0.3246 | 144.0 | 1.0016 | 0.9884 | 10.5965 | 1.1497 |
| **9** | 9.6716 | 3.6883 | 1.9442 | 0.9674 | 6.1192 | 0.1719 | 216.1 | 1.0026 | 0.9806 | 7.5812 | -0.7144 |
| **10** | 10.4704 | 4.2316 | 2.1282 | 1.0550 | 7.0349 | 0.7497 | 245.9 | 1.0035 | 0.9756 | 5.6124 | -1.8958 |
| **11** | 8.3022 | 2.8879 | 0.9617 | 0.4762 | 8.3817 | 1.5917 | 242.5 | 1.0006 | 0.9769 | 8.0969 | -0.4993 |
| **12** | 9.1202 | 3.3363 | 0.7171 | 0.3548 | 10.0534 | 2.6843 | 272.4 | 1.0014 | 0.9778 | 6.3817 | -1.5724 |
| **13** | 8.5390 | 2.9999 | 3.3078 | 1.6458 | 7.5548 | 1.0757 | 238.9 | 1.0037 | 0.9820 | 7.3373 | -0.7183 |
| **14** | 8.0560 | 2.6997 | 2.9005 | 1.4410 | 6.8837 | 0.6431 | 203.5 | 1.0003 | 0.9816 | 9.3634 | 0.4826 |
| **15** | 5.3736 | 1.0220 | 0.9670 | 0.4784 | 12.9058 | 4.4721 | 329.2 | 1 | 0.9729 | 8.5829 | -0.1979 |
| **16** | 7.1657 | 2.1023 | 1.6940 | 0.8396 | 7.0946 | 0.7914 | 162.5 | 1 | 0.9874 | 12.2081 | 2.0764 |
| **17** | 6.1280 | 1.4937 | 1.9902 | 0.9880 | 7.4368 | 1.0048 | 191.2 | 1 | 0.9850 | 13.1362 | 2.6930 |
| **18** | 7.9676 | 2.6357 | 1.8233 | 0.9035 | 9.9881 | 2.6405 | 270.1 | 1 | 0.9780 | 9.4910 | 0.4363 |
| **19** | 10.9853 | 4.5174 | 1.2879 | 0.6387 | 8.3025 | 1.5513 | 276.5 | 1 | 0.9788 | 9.2008 | 0.2129 |
| **20** | 9.8358 | 3.8058 | 2.0843 | 1.0332 | 5.2215 | -0.3735 | 207.9 | 1 | 0.9804 | 13.0662 | 2.6379 |
| **21** | 7.1591 | 2.1043 | 1.1386 | 0.5634 | 11.2157 | 3.3895 | 273.9 | 1.0007 | 0.9775 | 11.2605 | 1.4313 |
| **22** | 14.6105 | 6.9023 | 1.1695 | 0.5789 | 6.9188 | 0.7014 | 409.9 | 1.0023 | 0.9637 | 8.7111 | -0.1222 |
| **23** | 9.2165 | 3.4335 | 3.7616 | 1.8735 | 9.5267 | 2.3331 | 326.5 | 1.0018 | 0.9784 | 9.3218 | 0.5406 |
| **24** | 14.9900 | 7.1100 | 0.9365 | 0.4634 | 8.6644 | 1.7712 | 406.1 | 1.0013 | 0.9664 | 7.8152 | -0.6891 |
| **25** | 3.7983 | 0.0175 | 3.7426 | 1.8630 | 13.7573 | 5.0321 | 386.6 | 1.0000 | 0.9700 | 11.5883 | 1.9179 |
| **26** | 10.0246 | 3.9817 | 3.2989 | 1.6420 | 7.0764 | 0.7724 | 304.9 | 1 | 0.9732 | 12.9050 | 2.6785 |
| **27** | 14.3115 | 6.6380 | 2.4821 | 1.2374 | 7.3135 | 0.9236 | 387.2 | 1.0021 | 0.9737 | 9.7800 | 0.6729 |
| **28** | 13.3683 | 6.1374 | 3.9148 | 1.9484 | 5.8105 | -0.0120 | 404.5 | 1.0005 | 0.9650 | 11.3110 | 1.7716 |

| | | | | | | | | | | | |
|---|---|---|---|---|---|---|---|---|---|---|---|
| **29** | 14.8150 | 7.0249 | 1.4054 | 0.6959 | 11.7691 | 3.7573 | 537.9 | 1 | 0.9650 | 6.0484 | -1.6871 |
| **30** | 10.7621 | 4.3855 | 1.3258 | 0.6575 | 12.2791 | 4.0836 | 420.7 | 1 | 0.9719 | 9.0538 | 0.1289 |
| **31** | 8.8100 | 3.1843 | 2.6941 | 1.3436 | 7.1171 | 0.8059 | 309.9 | 1.0012 | 0.9775 | 14.1887 | 3.3887 |
| **32** | 14.7070 | 6.9475 | 2.4378 | 1.2097 | 6.4076 | 0.3476 | 394.5 | 1.0032 | 0.9647 | 8.8421 | 0.0988 |
| **33** | 12.2060 | 5.2643 | 4.0094 | 1.9926 | 8.8463 | 1.8821 | 319.9 | 1.0025 | 0.9781 | 7.7582 | -0.3806 |
| **34** | 5.6426 | 1.1559 | 1.4798 | 0.7333 | 13.0319 | 4.5654 | 342.1 | 1.0008 | 0.9703 | 12.9178 | 2.4678 |
| **35** | 13.7517 | 6.3212 | 1.6798 | 0.8328 | 10.4580 | 2.9129 | 450.7 | 1 | 0.9679 | 7.7911 | -0.5983 |
| **36** | 10.2677 | 4.1441 | 0.8567 | 0.4246 | 11.0999 | 3.3367 | 417.3 | 1.0006 | 0.9711 | 11.9231 | 1.8007 |
| **37** | 11.0599 | 4.6251 | 2.1045 | 1.0472 | 12.1742 | 4.0238 | 466.9 | 1 | 0.9728 | 9.3583 | 0.4076 |
| **38** | 10.2972 | 4.0970 | 1.8250 | 0.9041 | 12.9457 | 4.4956 | 415.6 | 1.0017 | 0.9714 | 10.0778 | 0.7766 |
| **39** | 9.1300 | 3.3548 | 3.5356 | 1.7558 | 11.5376 | 3.6276 | 381.3 | 1.0024 | 0.9708 | 11.4082 | 1.7684 |
| **40** | 12.3233 | 5.3980 | 1.6356 | 0.8114 | 12.2672 | 4.0669 | 466.0 | 1.0006 | 0.9720 | 9.9698 | 0.7099 |
| **41** | 6.7672 | 1.8670 | 4.0371 | 2.0113 | 13.9540 | 5.1403 | 470.8 | 1.0005 | 0.9683 | 11.9426 | 2.1817 |
| **42** | 15.5802 | 7.5628 | 1.2353 | 0.6116 | 13.0689 | 4.6127 | 680.7 | 1.0040 | 0.9600 | 7.2962 | -0.9862 |
| **43** | 10.9730 | 4.5080 | 2.1326 | 1.0587 | 9.7011 | 2.4334 | 331.6 | 1 | 0.9800 | 13.5248 | 2.9317 |
| **44** | 11.7894 | 5.0370 | 3.5443 | 1.7631 | 7.8307 | 1.2500 | 318.4 | 1 | 0.9749 | 12.6540 | 2.5556 |
| **45** | 8.2717 | 2.8354 | 3.2897 | 1.6331 | 11.6082 | 3.6594 | 389.0 | 1 | 0.9731 | 12.2195 | 2.2985 |
| **46** | 12.0495 | 5.2108 | 3.2397 | 1.6106 | 9.2173 | 2.1312 | 360.0 | 1 | 0.9743 | 10.3535 | 1.1297 |
| **47** | 11.5176 | 4.9539 | 1.7903 | 0.8869 | 11.5836 | 3.6298 | 452.5 | 1 | 0.9689 | 9.5609 | 0.4947 |
| **48** | 8.1097 | 2.7004 | 2.9168 | 1.4503 | 9.8811 | 2.5662 | 302.2 | 1 | 0.9786 | 12.8946 | 2.6303 |
| **49** | 5.7841 | 1.2888 | 4.7524 | 2.3701 | 10.7648 | 3.1063 | 346.4 | 1 | 0.9761 | 12.0452 | 2.3178 |
| **50** | 8.4923 | 2.9722 | 3.1468 | 1.5663 | 12.2093 | 4.0974 | 455.4 | 1.0018 | 0.9668 | 9.1070 | 0.3468 |
| **51** | 8.6687 | 3.0419 | 4.2736 | 2.1296 | 11.0503 | 3.3196 | 378.8 | 1.0030 | 0.9759 | 8.3862 | 0.0376 |
| **52** | 9.0100 | 3.2869 | 3.2039 | 1.5922 | 9.4201 | 2.2316 | 268.1 | 1.0011 | 0.9801 | 10.1341 | 0.9713 |
| **53** | 6.2130 | 1.5617 | 3.5647 | 1.7738 | 14.6035 | 5.5856 | 482.3 | 1.0012 | 0.9673 | 7.1010 | -0.8161 |
| **54** | 10.6169 | 4.2914 | 3.3092 | 1.6452 | 7.8561 | 1.2677 | 290.1 | 1.0019 | 0.9796 | 9.0079 | 0.3076 |
| **55** | 8.4378 | 2.8787 | 2.5704 | 1.2757 | 13.5667 | 4.9315 | 407.7 | 1.0005 | 0.9714 | 5.8329 | -1.6918 |
| **56** | 9.2123 | 3.4177 | 2.5266 | 1.2538 | 11.3210 | 3.4565 | 328.5 | 1.0003 | 0.9779 | 6.7686 | -1.1193 |
| **57** | 8.7886 | 3.1464 | 0.9936 | 0.4916 | 11.0228 | 3.2916 | 317.4 | 1 | 0.9734 | 8.5124 | -0.2436 |
| **Total** | | | | | | | **19058** | | | | |

The discussion on the results of the application of the developed algorithm to analyze the daily performance of the distribution network with DG under dynamic loading conditions is provided in the next section.

### 5.4.3. Discussion of the results of the performance of the distribution network with DG under dynamic loading conditions

The summary of the results of the application of the algorithm developed to analyse the daily performance of the 16-bus distribution network with DG under dynamic loading conditions is provided in Tables 5.13 and 5.14. From the analysis of the results in Tables 5.13 and 5.14, it follows that the integration of Distributed Generation in distribution networks results in a reduction of the real power loss, in comparison to the distribution network without DG.

Figure 5.25 uses the results in Table 5.13 and 5.14 to represent the daily real power loss in the distribution network without DG; with a non-dispatchable DG; and with a dispatchable DG. It can be seen from Figure 5.25 that for all datasets when a dispatchable DG is placed in the distribution network, the real power loss in the distribution network is lower than in the distribution network without DG. In some instances, the real power loss in the distribution network with a non-dispatchable DG is higher than the real power loss in the distribution network without DG. This situation can be observed in Figure 5.25, where the real power loss for datasets 6; 7; 10; 12; 29; and 55, the real power loss in the distribution network with a non-dispatchable DG is higher than the real power loss in the distribution network without DG. Thus, depending on the nature of the DG (dispatchable or non-dispatchable) and real and reactive power demands at the PQ buses, the integration of a DG is a distribution network can reduce or increase the real power losses in the distribution network.

The daily real power loss in the distribution network are $\mathbf{31.3741\ MW}$ (given in Table 5.5); $\mathbf{20.9042\ MW}$ (given in Table 5.13); and $\mathbf{19.058\ MW}$ (given in Table 5.14), for the distribution network without DG; with a non-dispatchable DG; and with a dispatchable DG, respectively.

Figure 5.26 is plotted using the results from Table 5.13 and 5.14, and it shows the daily minimum and maximum voltage profiles for the distribution network with a non-dispatchable and dispatchable DG. It is observed that the minimum voltage profile of the distribution network with a non-dispatchable DG is the same as the one of the distribution network with a dispatchable DG. For the whole day, the minimum voltage in the distribution network is obtained at **bus 7**. This can be explained by the fact that by placing a DG at

**bus 9** in the 16-bus distribution network in Figure 3.3 in chapter three, section 3.5.2, the DG has no effect on the load supplied by feeders 1 and 3, and consequently load bus 7. It is also observed in Figure 5.26 that when the DG is dispatchable, the daily maximum voltage profile of the distribution network is more stable at around $\mathbf{1\ p.u}$. When the DG is non-dispatchable, the daily maximum voltage profile oscillates between $\mathbf{1\ p.u}$ and $\mathbf{1.0257\ p.u}$.

The 16-bus distribution network supplies its load via three source transformers: source transformer 1, 2, and 3. The analysis of the source transformer power supply for all datasets as given in Table 5.13 and 5.14 illustrates that when the DG is non-dispatchable, the distribution system is prone to the bidirectional power flow effect. When the DG is dispatchable, the power flows from the source transformers to the loads for all datasets, as indicated by the positive values of the source transformers power supply in Table 5.14. The DG power supply is consumed by the loads. The DG and source transformers supply vary with respect to the change in the loading conditions in the distribution system. As such, the supply and the demand are balanced, and the power flows solely from the generation to the loads However, when the DG is non-dispatchable, there are occasional power flow from the load bus to source transformer 2, as indicated by the negative values of the real power supply of source transformer 2 in Table 5.13. In future smart grids, it would be acceptable to have power flows from the source transformer to the loads and vice-versa. However, the bidirectional power flow would cause problems for the current distribution networks which are not designed to withstand the bidirectional power flow.

From the analysis above, it is understood that the integration of DG may have a positive impact on the operation of distribution networks under dynamic loading conditions. However, in current distribution networks, it is necessary to pay attention to the DG type (dispatchable or not), size, and location to avoid a bidirectional power flow in the distribution networks.

The next section compares the daily performance of both the 16-bus distribution network with DG and the 16-bus distribution network with a feeder reconfiguration scheme under dynamic loading conditions.

## 5.5. Optimal feeder reconfiguration versus DG placement for minimising real power losses in distribution networks under dynamic loading conditions

Section 5.3 and 5.4 provide the developed solution algorithms to analyse the daily performance of both the 16-bus distribution network with DG and the 16-bus distribution network with a feeder reconfiguration scheme under dynamic loading conditions. The simulation results obtained in respective sections are used to compare the daily performance of both case studies, and the summary of the results is provided in Table 5.15.

**Table 5.15**: **DG placement versus feeder reconfiguration optimisation solutions of the 16-bus distribution network under dynamic loading conditions**

| Description | Base case | With a feeder reconfiguration scheme | With a non-dispatchable DG | With a dispatchable DG |
|---|---|---|---|---|
| **Tie switches** | 14 15 16 | Variable | 14 15 16 | 14 15 16 |
| **Total daily real power loss** | 31374.1 kW | 28966.4 kW | 20904.2 kW | 19058 kW |
| **Real power loss saving** | N/A | 7.6742% | 33.3712% | 39.2556% |
| **Minimum voltage recorded in the day** | 0.9532 p.u | 0.96 p.u | 0.96 p.u | 0.96 p.u |
| **Maximum voltage recorded in the day** | 1 p.u | 1 p.u | 1.0257 p.u | 1.004 p.u |
| **DG size (in MVA) and position** | N/A | N/A | 13.0456 + j1.7526 @bus 9 | Variable DG size @bus 9 |

From Table 5.15, it is understood that the topology of the distribution network only changes if a feeder reconfiguration scheme is implemented. The topology of the distribution network with a DG is the same as that of the base case, and it remains unchanged throughout the day.

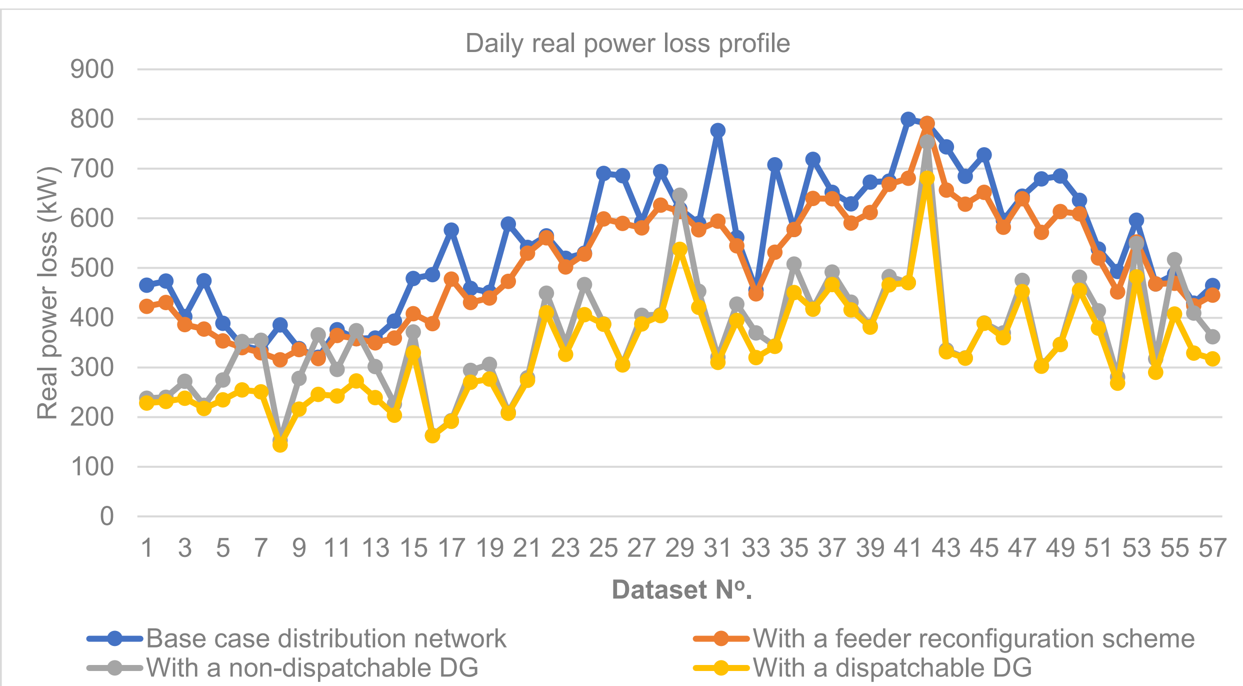

**Figure 5.27: Daily real power loss profiles of the base case distribution network, the distribution network with a feeder reconfiguration scheme, with a non-dispatchable DG, and with a dispatchable DG**

Figure 5.27 and Figure 5.28 show respectively the daily real power loss and minimum voltage profiles of the base case distribution network, the distribution network with a feeder reconfiguration scheme, with a non-dispatchable DG and with a dispatchable DG.

It is observed from Figure 5.27 that amongst the four cases, the real power loss in the distribution network is more reduced when a dispatchable DG is integrated into the distribution network. As given in Table 5.15, the total daily real power loss in the distribution network with a dispatchable DG is $\mathbf{19058\ kW}$, which corresponds to a real power loss saving of $\mathbf{39.2556\%}$ compared to the real power loss in the base case distribution network.

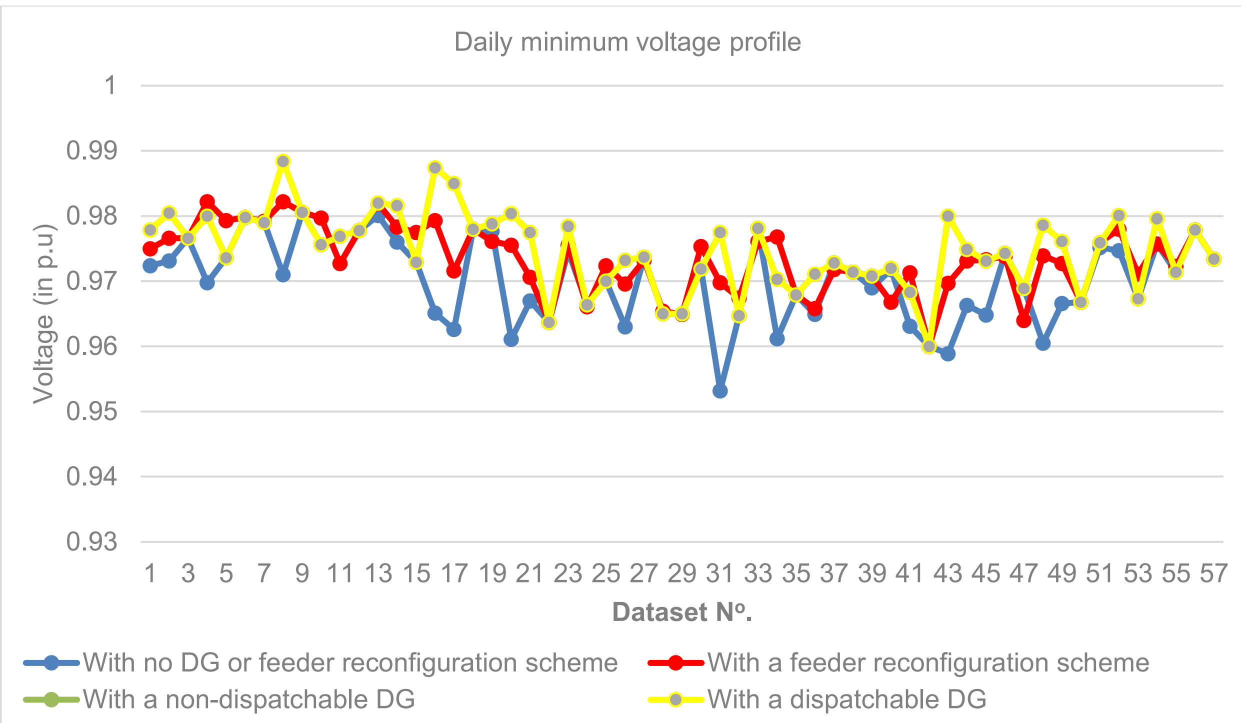


**Figure 5.28: Daily minimum voltage profiles of the base case distribution network, the distribution network with a feeder reconfiguration scheme, with a non-dispatchable DG, and with a dispatchable DG**

In term of the daily minimum voltage profiles, it is observed from Figure 5.28 that for most of the datasets, the minimum voltage of the distribution network with DG is higher than that of the base case distribution network and the distribution network with a feeder reconfiguration scheme. Therefore, from Table 5.15, Figure 5.27, and Figure 5.28, it can be concluded that the integration of dispatchable DG is a more effective way of reducing the real power loss and improving the voltage profile in the 16-bus distribution network.

## 5.6. Conclusion

This chapter presents an analysis of the daily performance of the 16-bus distribution network under dynamic loading conditions. A sequential programming algorithm has been developed to evaluate the performance of both the distribution network with a feeder reconfiguration scheme and the distribution network with a DG. The simulation results of the base 16-bus distribution network are compared with that of the 16-bus distribution network with a feeder reconfiguration scheme, and that of the 16-bus distribution network with DG.

The simulation results provide that:

- Feeder reconfiguration and DG placement are two essential approaches to reduce the real power loss of the distribution networks.
- The integration of DG in distribution networks leads to a higher reduction of real power losses and improved voltage levels, in comparison with the integration of a feeder reconfiguration scheme in the distribution network. The difference in real power saving is even more pronounced if the DG is dispatchable.
- The integration of a non-dispatchable DG may cause adverse conditions in the distribution network due to the possibility of bidirectional power flow.

The simulation of the developed PSO-based sequential algorithm to analyse the performance of the distribution network with a feeder reconfiguration scheme under dynamic loading conditions is a lengthy computation process. Thus, a data-parallel computing algorithm is developed to speed-up the simulation of the 57 datasets. The comparison of the simulation results of the developed sequential and data-parallel programming algorithms to evaluate the daily performance of the distribution network with a feeder reconfiguration scheme under dynamic loading conditions proved the simulation results to be the same.

The next chapter provides the conclusion of this thesis

# CHAPTER SIX
## CONCLUSION AND FUTURE WORKS

### 6.1. Introduction

This research work developed PSO solution algorithms to improve the operation of smart distribution networks using optimal distribution network feeder reconfiguration and optimal DG placement and sizing. However, given that the current distribution networks are not designed to handle such functionalities, the power utilities should be upgraded to handle the growing energy demand, to allow the integration of Distributed Generators, to allow the implementation of distribution feeder reconfiguration schemes, and to provide effective demand response. The developed PSO algorithms were implemented in the MATLAB R2016b platform and tested on the IEEE 16-bus, the IEEE 33-bus, and the IEEE 69-bus distribution networks. The simulations results proved that the optimal distribution network feeder reconfiguration and the optimal DG placement and sizing are two valuable tools for real power loss minimisation and the overall improvement of the operation of distribution networks.

### 6.2. Deliverables of the thesis

This research work is proof that many of the challenges faced by utilities at distribution levels can be solved through the development of innovative optimisation approaches such as the optimal distribution network feeder reconfiguration and the optimal DG deployment. The review of the research on the optimal feeder reconfiguration and DG deployment problems, the mathematical formulation of the problems, the development of PSO solution algorithms to solve of these problems, the development of a data-parallel computing approach to study the operation of a distribution network with a feeder reconfiguration scheme under dynamic loading conditions, the simulations results and analysis, constitute the significant contributions of the thesis deliverables and are grouped as follow:

#### 6.2.1. Literature review

The review investigates the concept of single and multi-objective optimisation. The review further examined the distribution networks feeder reconfiguration and optimal DG placement & sizing problems. It follows that early research works on the optimisation of feeder reconfiguration and DG placement and sizing were based on classical optimisation methods. The recent focus is now towards the use of metaheuristic optimisation approaches to solve complex problems, as metaheuristic optimisation methods are deemed more robust and efficient at providing optimal solutions. The optimal distribution network feeder reconfiguration, along with the optimal placement and sizing of DG are smart tools used to minimise the real power losses, to balance the loads, improve the voltage levels, to detect faults, and to restore the power in distribution networks.

### 6.2.2. Mathematical formulation and development of the single-objective feeder reconfiguration problem for real power loss minimisation

The distribution network feeder reconfiguration problem is a non-linear problem. The development of the PSO algorithm to solve this problem is subject to operational constraints such as voltage limits; power balance; and current limits; and technical limitations such as the topological requirement of distribution networks. The discrete variant of the Particle Swarm Optimization (PSO) algorithm is used to solve the distribution network feeder reconfiguration problem. The operating principle of the PSO and its variants are provided in detail in Chapter three. The application of the discrete PSO algorithm in solving the single-objective distribution network feeder reconfiguration problem is covered in Chapter three. The developed discrete PSO algorithm is tested on the IEEE 16-bus, the IEEE 33-bus, and the IEEE 69-bus distribution networks. The simulations results prove that the integration of a feeder reconfiguration scheme may secure a significant real power loss saving in distributions systems.

### 6.2.3. Mathematical formulation and development of the multi-objective feeder reconfiguration for the real power loss minimisation and the load balancing problem

The objectives of the multi-objective feeder reconfiguration problem are the minimisation of the real power losses and the balancing of the loads in the distribution networks. This problem is a multi-objective non-linear and constrained problem. The constraints considered are the bus voltage limits, the line current limits and the topological constraints. The discrete PSO algorithm developed to solve the multi-objective problem is quite similar to that of the single-objective problem. However, because of the multitude of objective functions, the concept of non-dominance and Pareto-optimality was introduced in the selection of the personal and global best candidate solutions in the PSO algorithm. The Pareto-dominance property ensures that the global best solution is not dominated by any other solution for all objective functions. As a consequence of the inclusion of the non-dominance concept, the application of the developed multi-objective algorithm on the IEEE 33-bus and the 69-bus distribution networks yields many Pareto-optimal solutions. The implementation of the developed multi-objective solution algorithm on the IEEE 16-bus distribution network produces a single solution.

### 6.2.4. Mathematical formulation and development of the PSO solution algorithm for the single-objective optimal DG placement and sizing problem

The aim of the single-objective optimal DG placement and sizing was to find the best DG type, the optimal DG size, and the best bus location which lead to a minimised overall real power loss in the distribution network, should the DG be integrated into the distribution network. The mathematical formulation of the single objective optimal DG placement and sizing problem is the same as that of the single-objective distribution network feeder reconfiguration problem, except that the single objective optimal DG placement and sizing problem is not subject to the topological constraint of the distribution networks. The developed algorithm is a hybrid discrete PSO (to find the optimal DG position) and continuous PSO (to find the optimal DG size) as described in Chapter Four. The developed algorithm is implemented in MATLAB R2016b, and the developed algorithm is tested for single, two and three DG placement problems.

### 6.2.5. Mathematical formulation and development of the PSO solution algorithm for the multi-objective DG placement and sizing problem

The multi-objective DG deployment problem aims to minimise the real power losses, maximise the voltage regulation and maximise the voltage stability index of the distribution networks. However, unlike in the multi-objective optimal distribution network feeder reconfiguration where the concept of Pareto-optimality was utilised to find the optimal distribution network topology, the weighted-sum approach is used to solve the multi-objective DG placement and sizing problem. The considered objectives (real power loss minimisation, voltage regulation maximisation, and voltage stability index maximisation) are aggregated into a single-objective using weight factors, where a weight factor determines the relative importance of one objective with respect of others. The PSO algorithm is developed for this scenario, and the simulations are performed in the MATLAB R2016b environment.

### 6.2.6. Development of a parallel computing approach to investigate the performance of a distribution network with a feeder reconfiguration scheme under dynamic loading conditions

The PSO algorithms developed in Chapter Three and Chapter Four consider that the loads are static (the load does not change over time). In such a case, the DG placement is better than feeder reconfiguration in minimising the real power losses in distribution networks. However, loads in power systems are dynamic in nature, and they change over time. To assess the influence of feeder reconfiguration and DG deployment on distribution networks with dynamic loading conditions, two cases studies were considered. They are:

- **Case 1**: A feeder reconfiguration scheme is implemented in the IEEE 16-bus distribution network, and the performance of the distribution network is analysed for a 24 hours period.
- **Case 2**: A DG is placed in the IEEE 16-bus distribution network, and the performance of the distribution network is evaluated for a 24 hours period.

The second case is further subdivided into two sub-cases:

- The DG inserted in the network is dispatchable.
- The DG inserted in the network is non-dispatchable.

Algorithms were developed to simulate the above case studies. The sequential computing algorithm developed to evaluate the case 1 was time-consuming due to the multitude of data sets to be simulated. Therefore, a data-parallel computing solution algorithm was developed to speed-up the computation process. Finally, the solutions of both the feeder reconfiguration and DG deployment in distribution networks with dynamic loads were examined.

## 6.3. Potential impact of the research

This research work can be beneficial to both the academia and the industry. In academia, although PSO is recognised as a robust optimisation method, there is not much detailed documentation on its application to real-world problems. As such, PSO is generally used to supplement a more known optimisation method such as Genetic Algorithm. This research work provides some insights on the application of the PSO in solving the feeder reconfiguration and DG placement and sizing problems. In many research works, the size of the DG and its location are decided in a random fashion, which leads to higher real power loss or is of minimal benefits to the distribution networks. The developed PSO algorithm provides optimal DG placement and sizing results.

The real-time implementation of the developed PSO algorithm in power utilities for the feeder reconfiguration problem will result in a significant power loss reduction in the distribution research. The use of the feeder reconfiguration scheme to balance the loads can also contribute to improved performance of the distribution network operation. The integration of DG in distribution networks may result in significant benefits such as reduced real power losses, improved voltage profile and enhanced voltage stability. Therefore, the developed PSO algorithm will help Distribution Systems Operators (DSO) and power companies to determine the best DG type, size, and location for deployment in distribution networks.

## 6.4. Future research works

Besides some minor refinements that can be undertaken to improve the developed PSO algorithms, future works based on this research may include:

- The testing of the developed PSO algorithms on real-world distribution networks. The distribution network used in this research work are IEEE distribution systems. The used IEEE distribution systems have no distribution transformers; their branches have no current rating, and they also have no protection systems in place. The testing of the developed PSO algorithms on practical distribution networks will allow for the study of their effects on transformers, branch current limits, thermal limits, protective relaying systems, and control systems. A hardware in the loop (HIL) test bench could be developed for this purpose.
- The development of the PSO solution algorithm for optimal DG deployment did not consider external factors affecting the performance of DG such as wind speed or irradiation in photovoltaic (PV) systems. Therefore, the scope of this work can be extended by considering such factors that affect the DG sizing and DG output power.

## 6.5. Conclusion

This chapter addresses the aim, objectives, and project deliverables of this thesis. It also covers the description of the approach used to achieve this research work, the potential impact of this research in both academia and the industry, and finally the future research directions. The distribution feeder reconfiguration and the optimal integration of DG can be used to solve distribution networks problems. The future work can be extended to solving optimisation problems such as the fault location; isolation and service restoration, maximisation of the DG penetration level, and more advanced topics in the framework of the smart grid.

## BIBLIOGRAPHY


Abdelaziz, A., Mekhamer, S., Mohammed, F. & Badr, M. 2009. Distribution Systems Reconfiguration using a modified particle swarm optimization algorithm. Electric Power Systems Research, Vol 79(11): pp. 1521 – 1530.

Abdi, S. & Afshar, K. 2013. Application of IPSO-Monte Carlo for optimal distributed generation allocation and sizing. International Journal of Electrical Power & Energy Systems, Vol 44(1): pp. 786 - 797.

Abedini, M. & Moradi, M. 2012. A combination of genetic algorithm and particle swarm optimization for optimal DG location and sizing in distribution systems. International Journal of Electrical Power & Energy Systems, Vol 34(1): pp. 66 - 74.

Abul'Wafa, A. 2011. A new heuristic approach for optimal reconfiguration in distribution systems. Electric Power Systems Research, Vol 81(2): pp. 282 - 289.

Abu-Mouti, F. & El-Hawary, M. 2011. Optimal Distributed Generation Allocation and Sizing in Distribution Systems via Artificial Bee Colony Algorithm. IEEE Transactions on Power Delivery, Vol 26(4): pp. 2090 - 2101.

Abur, A. 1996. A modified linear programming method for distribution system reconfiguration. International Journal of Electrical Power & Energy Systems, Vol 18(7): pp. 469 - 474.

Acharya, N., Mahat, P. & Mithulananthan, N. 2006. An analytical approach for DG allocation in primary distribution network. International Journal of Electrical Power & Energy Systems, Vol 28(10): pp. 669 - 678.

Ackermann, T., Andersson, G. & Söder, L. 2001. Distributed generation: A definition. Electric Power Systems Research, Vol 57(3): pp. 195 - 204.

Afsari, M., Rao, G., Raju, G. & Singh, S. 2009. A heuristic method for feeder reconfiguration and service restoration in distribution networks. International Journal of Electrical Power & Energy Systems, Vol 31(7–8): pp. 309 – 314.

Aghababa, P., Shotorbani, A. & Shotorbani, R. 2010. An Adaptive particle swarm optimization applied to optimum controller design for AVR power systems. International Journal of Computer Applications, Vol 11(10): pp. 22 - 29.

Alfi, A. & Modares, H. 2011. System identification and control using adaptive particle swarm optimization. Applied Mathematical Modelling, Vol 35(3): pp. 1210 – 1221.

Almasi, George S. & Gottlieb, Allan. 1989. Highly parallel computing. Redwood City, CA, USA: Benjamin Cummings Publishing Co., Inc.

Aman, M., Jasmon, G., Bakar, A. & Mokhlis, H. 2013. A new approach for optimum DG placement and sizing based on voltage stability maximization and minimization of power losses. Energy Conversion and Management, Vol 70: pp. 202 - 210.

Aman, M., Jasmon, G., Bakar, A. & Mokhlis, H. 2014. A new approach for optimum simultaneous multi-DG distributed generation Units placement and sizing based on maximization of system loadability using HPSO (hybrid particle swarm optimization) algorithm. Energy, Vol 66: pp. 202 - 215.

Amdahl, Gene M. 1967. Validity of the Single Processor Approach to Achieving Large-Scale Computing Capabilities. AFIPS Conference Proceedings. Atlantic City, New Jersey: IBM Corporation (30): pp. 483 – 485.

Angeline, P. 1998. Using selection to improve particle swarm optimization. In IEEE International Conference on Evolutionary Computation Proceedings. IEEE World Congress on Computational Intelligence. New York, USA: IEEE, pp. 84 - 89.

Aoki, K., Kitagawa, M., Kuwabara, H., Itoh, M., Satoh, T., Nara, K. & Yamanaka, K. 1990. Totally automated switching operation in distribution system. IEEE Transactions on Power Delivery, Vol 5(1): pp. 514 - 520.

Atwa, Y. & El-Saadany, E. 2010. Probabilistic approach for optimal allocation of wind-based distributed generation in distribution systems. IET Renewable Power Generation, Vol 5(1): pp. 79 - 88.

Babu, B. & Jehan, M. 2003. Differential evolution for multi-objective optimization. Differential evolution for multi-objective optimization. In: Congress on Evolutionary Computation (CEC). Canberra, Australia: IEEE, pp. 2696 - 2703.

Back, H. & Merlin, A. 1975. Search for a Minimal-Loss Operating Spanning Tree Configuration in an Urban Power Distribution System. In Proceedings of the 5th Power System Computation Conference (PSCC). Cambridge, UK: Queen Mary College, University of London, Department of Electrical & Electronic Engineering.

Back, T. 1996. Evolutionary algorithms in theory and practice: Evolution strategies, evolutionary programming, genetic algorithms. New York, NY, USA: Oxford University Press, Inc.

Baran, M. & Wu, F. 1989. Network reconfiguration in distribution systems for loss reduction and load balancing. IEEE Transactions on Power Delivery, Vol 4(2): pp. 1401 - 1407.

Barney, B. 2017. Introduction to Parallel Computing. [online] Computing.llnl.gov. Available: https://computing.llnl.gov/tutorials/parallel_comp/ [Accessed 10 Sep. 2017].

Bayat, A., Bagheri, A. & Noroozian, R. 2015. Optimal siting and sizing of distributed generation accompanied by reconfiguration of distribution networks for maximum loss reduction by using a new UVDA-based heuristic method. International Journal of Electrical Power & Energy Systems, Vol 77: pp. 360 - 371.

Behrooz, P. 2002. Introduction to Parallel Processing- Algorithms and Architectures. New York: Kluwer Academic Publishers.

Blum, C. and Roli, A. 2003. Metaheuristics in combinatorial optimization: Overview and conceptual comparison. ACM Computing Surveys, 35(3), pp. 268 - 308.

Borges, C. & Falcão, D. 2006. Optimal distributed generation allocation for reliability, losses, and voltage improvement. International Journal of Electrical Power & Energy Systems, Vol 28(6): pp. 413 - 420.

Borozan, V., Ačkovski, R. & Rajičić, D. 1997. Minimum loss reconfiguration of unbalanced distribution networks. IEEE Transactions on Power Delivery, Vol 12(1): pp. 435 - 442.

Botea, A., Rintanen, J. & Banerjee, D. 2012. Optimal reconfiguration for supply restoration with informed A* search. IEEE Transactions on Smart Grid, Vol 3(2): pp. 583 - 593.

Bratton, D. & Kennedy, J. 2007. Defining a standard for particle swarm optimization. In: IEEE Swarm Intelligence Symposium proceedings. Honolulu, HI, USA: IEEE.

Cailian, G., Jianwei, J. & Li, L. 2014. Research of Immune Algorithms for Reconfiguration of Distribution Network with Distributed Generations. In: The 26th Chinese Control and Decision Conference (CCDC). Changsha, China: IEEE, pp. 2156 - 2160.

Caramia, M. & Dell'Olmo, P. 2014. Multi-objective management in freight logistics: Increasing capacity, service level and safety with optimization Algorithms. London: Springer.

Carpaneto, E. & Chicco, G. 2004. Ant-colony search-based minimum losses reconfiguration of distribution systems. In: The 12th IEEE Mediterranean Electrotechnical Conference (MELECON 2004). Dubrovnik, Croatia: IEEE, pp. 971 - 974.

Chakradeo, S., Hendre, A. & Deshpande, S. 2014. Generalized theory for hybridization of evolutionary algorithms. In: International Conference on Computational Intelligence and Computing Research (ICCIC). Coimbatore, India: IEEE.

Changhun Lee. 2002. Distributed Shared Memory. In: Proceedings on the 15th CISL Winter Workshop, Kushu, Japan.

Charlangsut, A., Rugthaicharoencheep, N. & Auchariyamet, S. 2012. Heuristic optimization techniques for network reconfiguration in distribution system. World Academy of Science, Engineering and Technology (WASET), Vol 6(4): pp. 1 - 4.

Chen, C. & Cho, M. 1993. Energy loss reduction by critical switches. IEEE Transactions on Power Delivery, Vol 8(3): pp. 1246 - 1253.

Chidanandappa, R., Ananthapadmanabha, T. & Ranjith, H. 2015. Genetic Algorithm Based Network Reconfiguration in Distribution Systems with Multiple DGs for Time Varying Loads. Procedia Technology, Vol 21: pp. 460 - 467.

Chiou, J., Chang, C. & Su, C. 2005. Distribution network reconfiguration for loss reduction by ant colony search algorithm. Electric Power Systems Research, Vol 75(2-3): pp. 190 - 199.

Civanlar, S., Yin, H., Grainger, J. & Lee, S. 1988. Distribution feeder reconfiguration for loss reduction. IEEE Transactions on Power Delivery, Vol 3(3): pp. 1217 - 1223.

Clerc, M. & Kennedy, J. 2002. The particle swarm - explosion, stability, and convergence in a multidimensional complex space. IEEE Transactions on Evolutionary Computation, Vol 6(1): pp. 58 - 73.

Clerc, M. 2006. Particle swarm optimization. United Kingdom: Wiley-Blackwell.

Corne, D., Reynolds, A., & Bonabeau, E. 2012. Swarm Intelligence. In: Handbook of Natural Computing. Berlin Heidelberg, Germany: Springer-Verlag, pp. 1599 - 1622.

Culler, David, E., Jaswinder, Pal Singh, and Anoop, Gupta. 1999. Parallel computing architecture: a hardware/software approach. San Francisco, California, USA: Morgan Kaufmann publishers, Inc.

Dantzig, G. 1998. Linear programming and extensions. 11th ed. Princeton, NJ, USA: Princeton University Press.

Darfoun, M. 2013. Optimal distributed generation sizing and placement via single and multi-objective optimization approaches. A thesis submitted in partial fulfillment of the requirements for the degree of: Master of Applied Science. Dalhousie University.

Das, S. & Suganthan, P. 2011. Differential evolution: A survey of the state-of-the-art. IEEE Transactions on Evolutionary Computation, Vol 15(1): pp. 4 - 31.

Das, S., Das, D. & Patra, A. 2017. Reconfiguration of distribution networks with optimal placement of distributed generations in the presence of remote voltage-controlled bus. Renewable and Sustainable Energy Reviews, Vol 73: pp. 772 - 781.

De Macedo Braz, H. & de Souza, B. 2011. Distribution network reconfiguration using genetic Algorithms with Sequential Encoding: Subtractive and additive approaches. IEEE Transactions on Power Systems, Vol 26(2): pp. 582 - 593.

De Oliveira, L., Carneiro, S., De Oliveira, E., Pereira, J., Silva, I. & Costa, J. 2010. Optimal reconfiguration and capacitor allocation in radial distribution systems for energy losses minimization. International Journal of Electrical Power & Energy Systems, Vol 32(8): pp. 840 - 848.

De Oliveira, L., De Oliveira, E., Gomes, F., Silva, I., Marcato, A. and Resende, P. (2014). Artificial Immune Systems applied to the reconfiguration of electrical power distribution networks for energy loss minimization. International Journal of Electrical Power & Energy Systems, Vol 56: pp. 64-74.

De Weck, O &. Willcox, K. 2010. Multidisciplinary system design optimization. In MIT OpenCourseWare [Online]. Available: https://ocw.mit.edu/courses/institute-for-data-systems-and-society/ids-338j-multidisciplinary-system-design-optimization-spring-2010 [06 June 2018]

Deb, K. 2001. Multi-objective optimization using evolutionary Algorithms. Chichester, United Kingdom: Wiley, John & Sons.

Dehghanian, P., Hosseini, S., Moeini-Aghtaie, M. & Arabali, A. 2013. Optimal siting of DG units in power systems from a probabilistic multi-objective optimization perspective. International Journal of Electrical Power & Energy Systems, Vol 51: pp. 14 - 26.

Del Valle, Y., Venayagamoorthy, G., Mohagheghi, S., Hernandez, J. & Harley, R. 2008. Particle Swarm Optimization: Basic Concepts, Variants and Applications in Power Systems. IEEE Transactions on Evolutionary Computation, Vol 12(2): pp. 171 - 195.

Dorigo, M., Maniezzo, V. & Colorni, A. 1996. Ant system: Optimization by a colony of cooperating agents. IEEE Transactions on Systems, Man and Cybernetics, Part B (Cybernetics), Vol 26(1): pp. 29 - 41.

Dugan, R., Santoso, S., McGranaghan, M. & Beaty, W. 2012. Electrical power systems quality, Third edition. Maidenhead: McGraw-Hill Professional.

Eberhart, R. & Kennedy, J. 1995. A new optimizer using particle swarm theory. In Sixth International Symposium on Micro Machine and Human Science. Nagoya, Japan: IEEE, pp. 39 - 43.

Eberhart, R. & Shi, Y. 2000. Comparing inertia weights and constriction factors in particle swarm optimization. Proceedings of the 2000 Congress on Evolutionary Computation. (CEC), Vol 1: pp. 84 - 88.

El-Khattam, W. & Salama, M. 2004. Distributed generation technologies, definitions and benefits. Electric Power Systems Research, Vol 71(2): pp. 119 - 128.

El-Saadany, E., Mohamed, F., Badr, M., Mekhamer, S. & Abdelaziz, A. 2009. A modified particle swarm algorithm for distribution systems reconfiguration. In: IEEE Power & Energy Society General Meeting. Calgary, Canada: IEEE.

Eminoglu, U. & Hocaoglu, M. 2007. A voltage stability index for radial distribution networks. In Universities Power Engineering Conference. Brighton, UK: IEEE, pp. 407 - 413.

Enacheanu, B., Bienia, W., Devaux, O., Caire, R., Raison, B. & HadjSaid, N. 2008. Radial network reconfiguration using genetic algorithm based on the Matroid theory. IEEE Transactions on Power Systems, Vol 23(1): pp. 186 - 195.

Engelbrecht, A. 2007. Computational intelligence: An introduction. New York, USA: Wiley-Blackwell.

Enrique, L., García, L., Opazo, H. & Poloujadoff, M. 2002. Minimal loss reconfiguration based on dynamic programming approach: Application to real systems. Electric Power Components and Systems, Vol 30(7): pp. 693 - 704.

Even, G. & Even, S. 2011. Graph Algorithms. 2$^{nd}$ Ed. United Kingdom: Cambridge University Press.

Ferdavani, A., Mohd Zin, A., Khairuddin, A. and Naeini, M. 2011. A review on reconfiguration of radial electrical distribution network through heuristic methods. In: International Conference on Modeling, Simulation and Applied Optimization. Kuala Lumpur, India: IEEE, pp. 1 - 5.

Flavio, V., Carneiro, S., Pereira, J., Vinagre, M., Garcia, P., Oliveira, E. and Araujo, L. 2005. A new distribution system reconfiguration approach using optimal power flow technique and sensitivity analysis for loss reduction. In: IEEE Power Engineering Society General Meeting. San Francisco, CA, USA: IEEE, pp. 897 - 901.

Flynn, M. J. 1972. Some Computer Organizations and Their Effectiveness. IEEE Transactions on Computers, Vol C-21(9): pp. 948 - 960.

Garnier, S., Gautrais, J. & Theraulaz, G. 2007. The biological principles of swarm intelligence. Swarm Intelligence, Vol 1(1): pp. 3 - 31.

Gavrilas, M. & Asachi, G. 2010. Heuristic and Metaheuristic Optimization Techniques with Application to Power Systems. In: Proceedings of the 12th World Scientific and Engineering Academy and Society (WSEAS) international conference on Mathematical methods and computational techniques in electrical engineering. Romania: WSEAS, pp. 95 - 103.

Gers, J. 2013. Distribution system analysis and automation. London, United Kingdom: Institution of Engineering and Technology.

Glamocanin, V. 1990. Optimal loss reduction of distributed networks. IEEE Transactions on Power Systems, Vol 5(3): pp. 774 - 782.

Goldberg, D. 1989. Genetic algorithms in search, optimization, and machine learning. Reading, MA: Addison-Wesley Educational Publishers.

Gomes, F., Carneiro, S., Pereira, J., Vinagre, M., Garcia, P. & Araujo, L. 2005. A New Heuristic Reconfiguration Algorithm for Large Distribution Systems. IEEE Transactions on Power Systems, Vol 20(3): pp. 1373 - 1378.

Gopiya Naik, S., Khatod, D. & Sharma, M. 2013. Optimal allocation of combined DG and capacitor for real power loss minimization in distribution networks. International Journal of Electrical Power & Energy Systems, Vol 53: pp. 967 - 973.

Gopiya, N., Khatod, D. & Sharma, M. 2012. Optimal allocation of distributed generation in distribution system for loss reduction. In: The 2012 IACSIT Coimbatore Conferences. Singapore: IACSIT Press, pp. 42 - 46.

Gosvami, S. & Basu, S. 1992. A new algorithm for the reconfiguration of distribution feeders for loss minimization. IEEE Transactions on Power Delivery, Vol 7(3): pp. 1484 - 1491.

Grama, A., Gupta, A., Karypis, G. and Kumar, V. 2003. Introduction to Parallel Computing. 2nd Ed. Addison-Wesley Professional.

Guan, W., Tan, Y., Zhang, H. & Song, J. 2015. Distribution system feeder reconfiguration considering different model of DG sources. International Journal of Electrical Power & Energy Systems, Vol 68: pp. 210 - 221.

Gustafson, John L. 1988. Reevaluating Amdahl's Law. Communications of the Association for Computing Machinery (ACM), Vol 31(5): pp. 532 - 533.

Hao, T., Yanhan, W. & Lin, L. 2014. Research of Distribution Network Reconfiguration with Renewable Energy Power Generation Unit. In: International Conference on Power System Technology (PowerCon). Chengdu, China: IEEE, pp. 2680 - 2686.

Hossen, M., Rabbi, F. & Rahman, M. 2009. Adaptive particle swarm optimization (APSO) for multimodal function optimization. International Journal of Engineering and Technology, Vol 1(3): pp. 98 - 103.

Hu, X. & Eberhart, R. 2002. Multi-objective optimization using dynamic neighborhood particle swarm optimization. In: IEEE Congress on Evolutionary Computation. Hawaii, USA: IEEE, pp. 1677 - 1681.

Hu, Z., Gao, Y., He, X. & Liu, D. 2008. Distribution network reconfiguration based on ant colony system algorithm. In: 3rd IEEE Conference on Industrial Electronics and Applications (ICIEA). Singapore: IEEE, pp. 2470 - 2474.

Huddleston, C., Broadwater, R. & Chandrasekaran, A. 1990. Reconfiguration algorithm for minimizing losses in radial electric distribution systems. Electric Power Systems Research, Vol 18(1): pp. 57 - 66.

Hung, D., Mithulananthan, N. & Bansal, R. 2010. Analytical Expressions for DG Allocation in Primary Distribution Networks. IEEE Transactions on Energy Conversion, Vol 25(3): pp. 814 - 820.

Imran, A., Kowsalya, M. & Kothari, D. 2014. A novel integration technique for optimal network reconfiguration and distributed generation placement in power distribution networks. International Journal of Electrical Power & Energy Systems, Vol 63: pp. 461 - 472.

Jin, X., Zhao, J., Sun, Y., Li, K. and Zhang, B. 2004. Distribution Network Reconfiguration for Load Balancing Using Binary Particle Swarm Optimization. In: International Conference on Power System Technology - POWERCON. Singapore: IEEE, pp. 507 - 510.

John, E. Bentley. 2000. An introduction to Parallel Computing. System Architecture [online]. Available: http://www2.sas.com/proceedings/sugi25/25/sy/25p283.pdf [06 June 2013]

Jordehi, A. 2015. Allocation of distributed generation units in electric power systems: A review. Renewable and Sustainable Energy Reviews, Vol 56: pp. 893 – 905.

Kansal, S., Kumar, V. & Tyagi, B. 2013. Optimal placement of different type of DG sources in distribution networks. International Journal of Electrical Power & Energy Systems, Vol 53: pp. 752 - 760.

Kashem, M., Jasmon, G. & Ganapathy, V. 2000. A new approach of distribution system reconfiguration for loss minimization. International Journal of Electrical Power & Energy Systems, Vol 22(4): pp. 269 – 276.

Kashem, M., Mohamed, A., Jasmon, G. & Moghavvemi, M. 1998. Artificial neural network approach to network reconfiguration for loss minimization in distribution networks. International Journal of Electrical Power & Energy Systems, Vol 20(4): pp. 247 - 258.

Kaur, S., Kumbhar, G. & Sharma, J. 2014. A MINLP technique for optimal placement of multiple DG units in distribution systems. International Journal of Electrical Power & Energy Systems, Vol 63: pp. 609 - 617.

Kavousi-Fard, A. & Akbari-Zadeh, M. 2013. Reliability enhancement using optimal distribution feeder reconfiguration. Neurocomputing, Vol 106: pp. 1 - 11.

Kefayat, M., Lashkar Ara, A. & Nabavi Niaki, S. 2015. A hybrid of ant colony optimization and artificial bee colony algorithm for probabilistic optimal placement and sizing of distributed energy resources. Energy Conversion and Management, Vol 92: pp. 149 - 161.

Kennedy, J. & Eberhart, R. 1995. Particle swarm optimization. In: Proceedings of ICNN'95 - International Conference on Neural Networks. Perth, WA, Australia: IEEE, pp. 1942 - 1948.

Kennedy, J. & Eberhart, R. 1997. A discrete binary version of the particle swarm algorithm. In: IEEE International Conference on Systems, Man, and Cybernetics - Computational Cybernetics and Simulation. Orlando, FL, USA: IEEE, pp. 4104 - 4108.

Kennedy, J., Eberhart, R. and Shi, Y. 2001. Swarm intelligence. San Francisco, USA: Morgan Kaufmann Publishers Inc.

Khalesi, N., Rezaei, N. & Haghifam, M. 2010. DG allocation with application of dynamic programming for loss reduction and reliability improvement. International Journal of Electrical Power & Energy Systems, Vol 33(2): pp. 288 - 295.

Khalil, T. & Gorpinich, A. 2012. Reconfiguration for Loss Reduction of Distribution Systems Using Selective Particle Swarm Optimization. International journal of multidisciplinary sciences and engineering, Vol 3(6): pp. 16 - 21.

Khoa, T. & Phan, B. 2006. Ant colony search - based minimum losses reconfiguration of distribution systems. In: IEEE Power India Conference. New Delhi, India: IEEE.

Kim, H., Ko, Y. & Jung, K.1993. Artificial neural-network based feeder reconfiguration for loss reduction in distribution systems. IEEE Transactions on Power Delivery, Vol 8(3): pp. 1356 - 1366.

Kiran, K., Kamakshaiah, S. & Venkata, N. 2012. Global optimal solution for network reconfiguration problem using AMPSO algorithm. In: International Conference on Power System Technology. Auckland, New Zealand: IEEE.

Kuroda, K., Magori, H., Ichimura, T. & Yokoyama, R. 2012. A new approach for optimal location and sizing of distributed generation using an exact solution method. International Journal of Smart Grid and Clean Energy, Vol 1(1): pp. 109 - 115.

Leiserson, C., Stein, C., Cormen, T. & Rivest, R. 2009. Introduction to Algorithms. 3rd Ed. Cambridge, MA, USA: MIT Press.

Li, X. & Deb, K. 2010. Comparing Lbest PSO niching algorithms using different position update rules. In: IEEE World Congress on Computational Intelligence (WCCI). Barcelona, Spain: IEEE, pp. 1564 - 1571.

Liu, C, Lee, S. &. Vu, K. 1989. Loss minimization of distribution feeders: Optimality and algorithms. IEEE Transactions on Power Delivery, Vol 4(2): pp. 1281 - 1289.

Lopez, J., Djapic, P., Mutale, J., Hatziargyriou, N. & Jenkins, N. 2007. Integrating distributed generation into electric power systems: A review of drivers, challenges and opportunities. Electric Power Systems Research, Vol 77(9): pp. 1189 - 1203.

Luenberger, D. 1984. Linear and non-linear programming. 2nd Ed. Reading, MA, USA: Addison-Wesley.

Lukasik, S. & Kowalsk, P. 2014. Fully Informed Swarm Optimization Algorithms: Basic Concepts, Variants and Experimental Evaluation. In: Federated Conference on Computer Science and Information Systems. Warsaw, Poland: IEEE, pp. 155 - 161.

Ma, P., Cao, X., Zhao, B., Wang, X., Zhang, H., Wang, S. & Guo, Y. 2015. Reconfiguration in distribution network with distributed generations based on the improved clonal genetic algorithm with tabu characteristic. In: Fifth International Conference on Communication Systems and Network Technologies (CSNT). Gwalior, India: IEEE, pp. 288 - 291.

Maringer, D. 2005. Portfolio management with heuristic optimization. Dordrecht, Netherlands: Springer-Verlag New-York.

Marler, R. & Arora, J. 2009. The weighted sum method for multi-objective optimization: new insights. Structural and Multidisciplinary Optimization, Vol 41(6): pp. 853 - 862.

MathWorks. 2016. Incidence (Graph Incidence Matrix) [Online]. Available: http://www.mathworks.com/help/matlab/ref/graph.incidence.html [18 September 2016].

MathWorks. 2017. Getting Started with Parallel Computing Toolbox. [online] Available: https://www.mathworks.com/help/distcomp/getting-started-with-parallel-computing-toolbox.html [12 Mar. 2018].

Matona, T. 2014. Power System Status Update [Online]. Available: http://www.eskom.co.za/news/Documents/finaldecemberstatus.pdf [12 February 2017].

Mendes, R., Kennedy, J. & Neves, J. 2004. The Fully Informed Particle Swarm: Simpler, Maybe Better. IEEE Transactions on Evolutionary Computation, Vol 8(3): pp. 204 - 210.

Mendoza, J., Dessante, P., Lopez, E., Morales, D., Lopez, R. & Moraga, R. 2006. Minimal loss reconfiguration using genetic Algorithms with restricted population and addressed operators: Real application. IEEE Transactions on Power Systems, Vol 21(2): pp. 948 - 954.

Momoh, J. & Caven, A. 2003. Distribution system reconfiguration scheme using integer interior point programming technique. In: IEEE Power & Energy Society (PES) Transmission and Distribution Conference and Exposition. Dallas, TX, USA: IEEE, pp. 234 - 241.

Montes de Oca, M. & Stützle, T. 2008. Convergence behavior of the fully informed particle swarm optimization algorithm. In: Proceedings of the 10th annual conference on Genetic and evolutionary computation. Atlanta, GA, USA: ACM, pp. 71 - 78.

Moravej, Z. & Akhlaghi, A. 2013. A novel approach based on cuckoo search for DG allocation in distribution network. International Journal of Electrical Power & Energy Systems, Vol 44(1): pp. 672 - 679.

Mori, H. & Komatsu, Y. 2009. A parallel meta-heuristic method for distribution network loss reduction with network reconfiguration and capacitor control. In: Transmission & Distribution Conference & Exposition: Asia and Pacific. Seoul, South Korea: IEEE, pp. 1 - 4.

Murthy, V. & Kumar, A. 2013. Comparison of optimal DG allocation methods in radial distribution systems based on sensitivity approaches. International Journal of Electrical Power & Energy Systems, Vol 53: pp. 450 - 467.

Naka, S., Genji, T., Yura, T. & Fukuyama, Y. 2003. A hybrid particle swarm optimization for distribution state estimation. IEEE Transactions on Power Systems, Vol 18(1): pp. 60 - 68.

Nara, K., Kitagawa, M., Shiose, A. & Ishihara, T. 1992. Implementation of genetic algorithm for distribution systems loss minimum re-configuration. IEEE Transactions on Power Systems, Vol 7(3): pp. 1044 - 1051.

Niknam, T. 2009. An efficient hybrid evolutionary algorithm based on PSO and HBMO algorithms for multi-objective Distribution Feeder Reconfiguration. Energy Conversion and Management, Vol 50(8): pp. 2074 - 2082.

Niknam, T. 2011. An efficient multi-objective HBMO algorithm for distribution feeder reconfiguration. Expert Systems with Applications, Vol 38(3): pp. 2878 - 2887.

Niknam, T., Khorshidi, R. & Firouzi, B. 2010. A hybrid evolutionary algorithm for distribution feeder reconfiguration. Sadhana - Academy Proceeding in Engineering Sciences, Vol 35(2): pp. 139 - 162.

Norman, D. 1993. A primal-dual simplex method for linear programs. Operations Research Letters, 13(4), pp. 233 - 237.

Olamaei, J., Niknam, T. & Gharehpetian, G. 2008. Application of particle swarm optimization for distribution feeder reconfiguration considering distributed generators. Applied Mathematics and Computation, Vol 201(1-2): pp. 575 - 586.

Oluwole, O. 2016. Optimal allocation of distributed generation for power loss reduction and voltage profile improvement. A thesis submitted in partial fulfillment of the requirements for the degree of: Master of Science (M. Sc). University of Cape Town.

Palukuru, N., Datta, T., Halder nee Dey, S. & Paul, S. 2014. Voltage stability assessment of a power system incorporating FACTS controllers using unique network equivalent. Ain Shams Engineering Journal, Vol 5(1): pp. 103 - 111.

Parsopoulos, K. & Vrahatis, M.2002. Recent approaches to global optimization problems through Particle Swarm Optimization. Natural Computing, Vol 1(2-3): pp. 235 - 306.

Patterson, A David, and John L, Hennessy. 2014. Computer organization and design: the hardware/software interface, 3rd edition. Morgan Kaufmann, Elsevier, USA, ISBN 1-55860-428-6

Pearl, J. 1984. Heuristics: Intelligent search strategies for computer problem solving. 1st Ed. Reading, MA: Addison Wesley Longman Publishing Co.

Pepermans, G., Driesen, J., Haeseldonckx, D., Belmans, R. and D'haeseleer, W. 2005. Distributed generation: definition, benefits and issues. Energy Policy, Vol 33(6), pp. 787 - 798.

Peponis, G., Papadopoulos, M. & Hatziargyriou, N. 1995. Distribution network reconfiguration to minimize resistive line losses. IEEE Transactions on Power Delivery, Vol 10(3): pp. 1338 - 1342.

Perreira, F., Vittori, K. & Da Costa, G. 2006. Distribution system reconfiguration for loss reduction based on ant colony behavior. In: IEEE/PES Transmission & Distribution Conference and Exposition: Latin America. Caracas, Venezuela: IEEE, pp. 1 - 5.

Prakash, P. & Khatod, D. 2016. Optimal sizing and siting techniques for distributed generation in distribution systems: A review. Renewable and Sustainable Energy Reviews, Vol 57: pp. 111 - 130.

Rama Prabha, D., Jayabarathi, T., Umamageswari, R. & Saranya, S. 2015. Optimal location and sizing of distributed generation unit using intelligent water drop algorithm. Sustainable Energy Technologies and Assessments, Vol 11: pp. 106 - 113.

Rao, R. & Savsani, V. 2012. Mechanical design optimization using advanced optimization techniques. 1st Ed. Springer-Verlag London.

Rao, R., Ravindra, K., Satish, K. & Narasimham, S. 2013. Power Loss Minimization in Distribution System Using Network Reconfiguration in the Presence of Distributed Generation. IEEE Transactions on Power Systems, Vol 28(1): pp. 317 - 325.

Reinefeld, A. & Marsland, T. 1994. Enhanced iterative-deepening search. IEEE Transactions on Pattern Analysis and Machine Intelligence, Vol 16(7): pp. 701 - 710.

Rezazadeh, I., Meybodi, M. & Naebi, A. 2011. Adaptive Particle Swarm Optimization Algorithm for Dynamic Environments. In: Third International Conference on Computational Intelligence, Modelling and Simulation (CIMSiM). Langkawi, Malaysia: IEEE, pp. 74 - 79.

Sarma, N. & Prakaso, K.1995. A new 0–1 integer programming method of feeder reconfiguration for loss minimization in distribution systems. Electric Power Systems Research, Vol 33(2): pp. 125 - 131.

Savier, J. & Das, D. 2007. Impact of Network Reconfiguration on Loss Allocation of Radial Distribution Systems. IEEE Transactions on Power Delivery, Vol 22(4): pp. 2473 - 2480.

Schmidhuber, J. 2015. Deep learning in neural networks: An overview. Neural Networks, Vol 61: pp. 85 - 117.

Schmidt, H., Kagan, N., Ida, N. & Guaraldo, J. 2005. Fast reconfiguration of distribution systems considering loss Minimization. IEEE Transactions on Power Systems, Vol 20(3): pp. 1311 - 1319.

Sedighizadeh, M., Esmaili, M. & Esmaeili, M. 2014. Application of the hybrid Big Bang-Big Crunch algorithm to optimal reconfiguration and distributed generation power allocation in distribution systems. Energy, Vol 76: pp. 920 - 930.

Shariatkhah, M., Salehi, J., Haghifam, M. & Moser, A. 2012. Duration based reconfiguration of electric distribution networks using dynamic programming and harmony search algorithm. International Journal of Electrical Power & Energy Systems, Vol 41(1): pp. 1 - 10.

Shi, Y. & Eberhart, R. 1998. A modified particle swarm optimizer. In: Proceedings of the International Conference on Evolutionary Computation. Anchorage, AK, USA: IEEE, pp. 69 - 73.

Shirmohammadi, D. & Hong, H. 1989. Reconfiguration of electric distribution networks for resistive line losses reduction. IEEE Transactions on Power Delivery, Vol 4(2): pp. 1492 - 1498.

Sierksma, G. 2001. Linear & integer programming: Theory and practice (pure and applied mathematics). 2nd Ed. New York: Productivity Press.

Song, Y., Johns, A., Wang, G. & Wang, P. 1997. Distribution network reconfiguration for loss reduction using fuzzy controlled evolutionary programming., IEE Proceedings - Generation, Transmission and Distribution, Vol 144(4): pp. 345 - 350.

Su, C. & Lee, C. 2003. Network reconfiguration of distribution systems using improved mixed-integer hybrid differential evolution. IEEE Transactions on Power Delivery, Vol 18(3): pp. 1022 - 1027.

Su, C., Chang, C. &. Lee, C 2005. Distribution network reconfiguration for loss reduction by hybrid differential evolution. Electric Power Components and Systems, Vol 33(12): pp. 1297 - 1312.

Tagliarini, G., Christ, J. & Page, E. 1991. Optimization using neural networks. IEEE Transactions on Computers, Vol 40(12): pp. 1347 - 1358.

Talukder, S. 2011. Mathematical modelling and applications of Particle Swarm Optimization. A thesis submitted in partial fulfillment of the requirements for the degree of: Master of Science (M. Sc). Blekinge Institute of Technology.

Taylor, T. & Lubkeman, D. 1990. Implementation of heuristic search strategies for distribution feeder reconfiguration. IEEE Transactions on Power Delivery, Vol 5(1): pp. 239 - 246.

Technology Standardization Department (TSD). 2003. NRS 048: Electricity supply – Quality of Supply. 2nd Ed. Pretoria, South Africa: Standards South Africa.

Van Den Bergh, F. 2002. An Analysis of Particle Swarm Optimizers. A Dissertation Submitted in partial fulfillment of the requirements for the degree Philosophiae Doctor (Ph.D.) in the Faculty of Natural and Agricultural Science. University of Pretoria

Venkatesh, R. 2014. Sizing of DG Units Using Exact Loss Formula to Improve Efficiency of Radial Distribution System. International Journal of Emerging Trends in Electrical and Electronics (IJETEE), Vol 10(1): pp. 13 - 17.

Viral, R. & Khatod, D. 2012. Optimal planning of distributed generation systems in distribution system: A review. Renewable and Sustainable Energy Reviews, Vol 16(7): pp. 5146 - 5165.

Voropai, N. & Bat-Undraal, B. 2012. Multicriteria reconfiguration of distribution network with distributed generation. Journal of Electrical and Computer Engineering, Vol 2012: pp. 1 - 8.

Wagner, T., Chikhani, A. & Hackam, R. 1991. Feeder reconfiguration for loss reduction: an application of distribution automation. IEEE Transactions on Power Delivery, Vol 6(4): pp. 1922 - 1933.

Wallace, A. 1889. Darwinism: An Exposition of the Theory of Natural Selection with Some of Its Applications. London and New York: Macmillan and co.

Wang, J. & Beni, G. 1993. Swarm Intelligence in Cellular Robotic Systems. In: Robots and Biological Systems: Towards a New Bionics?. NATO ASI Series (Series F: Computer and Systems Sciences), Vol 102. Berlin Heidelberg: Springer, pp. 703 - 712.

Wright, S. & Nocedal, J. 2006. Numerical optimization (Springer series in operations research and financial engineering). 2nd Ed. United States: Springer-Verlag New York.

Wu, W. & Tsai, M. 2008. Feeder Reconfiguration Using Binary Coding Particle Swarm Optimization. International Journal of Control, Automation, and Systems, Vol 6(4): pp. 488 - 494.

Yu, W. and Pollitt, M. 2009. Does Liberalization cause more electricity blackouts? Evidence from a global study of newspaper reports [online]. Available: https://www.repository.cam.ac.uk/bitstream/handle/1810/229495/0911%26EPRG0827.pdf?sequence=2&isAllowed=y [15 March 2016].

Zeinalzadeh, A., Mohammadi, Y. & Moradi, M. 2015. Optimal multi-objective placement and sizing of multiple DGs and shunt capacitor banks simultaneously considering load uncertainty via MOPSO approach. International Journal of Electrical Power & Energy Systems, Vol 67: pp. 336 - 349.

Zeng, W. & Church, R. 2009. Finding shortest paths on real road networks: The case for A*. International Journal of Geographical Information Science, Vol 23(4): pp. 531 - 543.

Zhang, L., Fu, Z. & Zhang, D. 2007. An improved Tabu Search algorithm for loss-minimum reconfiguration in large-scale distribution systems. Electric Power Systems Research, Vol 77(s 5–6): pp. 685 - 694.

Zhang, Z., Chung, H., Li, Y. & Zhang, J. 2009. Adaptive particle swarm optimization. IEEE Transactions on Systems, Man, and Cybernetics, Part B (Cybernetics), Vol 39(6): pp. 1362 - 1381.

Zhu, J. 2002. Optimal reconfiguration of electrical distribution network using the refined genetic algorithm. Electric Power Systems Research, Vol 62(1): pp. 37 - 42.

Zhu, J. 2009. Optimization of Power System Operation (IEEE Press Series on Power Engineering). Piscataway, New Jersey, U.S.A.: IEEE.

## APPENDICES

**Appendix A**: Data of the 16-bus distribution system

```
%% This M-file gives the data of the 16 bus distribution network

function mpc = case16_3
%% MATPOWER Case Format : Version 2
mpc.version = '2';

%%-----  Power Flow Data  -----%%
%% system MVA base
mpc.baseMVA = 100;
%% bus data
%            busi type   Pd      Qd      Gs  Bs   area   Vm      Va  baseKV zone  Vmax  Vmin  Qmin  Qmax
mpc.bus =   [ 1    3     0       0       0   0      1    1.00    0   12.66   1    1.05  0.95   0    0;
              2    3     0       0       0   0      1    1.00    0   12.66   1    1.05  0.95   0    0;
              3    3     0       0       0   0      1    1.00    0   12.66   1    1.05  0.95   0    0;
              4    1     2       1.6     0   0      1    1.00    0   12.66   1    1.05  0.95   0    0;
              5    1     3       1.5     0   1.1    1    1.00    0   12.66   1    1.05  0.95   0    0;
              6    1     2       0.8     0   1.2    1    1.00    0   12.66   1    1.05  0.95   0    0;
              7    1     1.5     1.2     0   0      1    1.00    0   12.66   1    1.05  0.95   0    0;
              8    1     4       2.7     0   0      1    1.00    0   12.66   1    1.05  0.95   0    0;
              9    1     5       3       0   1.2    1    1.00    0   12.66   1    1.05  0.95   0    0;
              10   1     1       0.9     0   0      1    1.00    0   12.66   1    1.05  0.95   0    0;
              11   1     0.6     0.1     0   0.6    1    1.00    0   12.66   1    1.05  0.95   0    0;
              12   1     4.5     2       0   3.7    1    1.00    0   12.66   1    1.05  0.95   0    0;
              13   1     1       0.9     0   0      1    1.00    0   12.66   1    1.05  0.95   0    0;
              14   1     1       0.7     0   1.8    1    1.00    0   12.66   1    1.05  0.95   0    0;
              15   1     1       0.9     0   0      1    1.00    0   12.66   1    1.05  0.95   0    0;
              16   1     2.1     1       0   1.8    1    1.00    0   12.66   1    1.05  0.95   0    0;
            ];

       % type == 3 => Slack bus;
       % type == 2 => PV bus
       % type == 1 => PQ bus
```

```
%% generator data
%            bus  Pg   Qg   Qmax  Qmin   Vg    mBase  status Pmax  Pmin Pc1  Pc2  Qc1min  Qc1max  Qc2min  Qc2max  ramp_agc   ramp_10 ramp_30 ramp_q  apf
mpc.gen =  [1    0    0    0     0     1.00   100     1     0     0    0    0    0       0       0       0       0          0       0       0       0;
             2   0    0    0     0     1.00   100     1     0     0    0    0    0       0       0       0       0          0       0       0       0;
             3   0    0    0     0     1.00   100     1     0     0    0    0    0       0       0       0       0          0       0       0       0;
           ];

%% branch data
%              from_bus  to_bus  r        x      b  rateA  rateB rateC ratio angle status   weight  angmin  angmax
mpc.branch =  [  1        4     0.075    0.10   0   0      0     0     0     0     1        1      -360     360;
                 4        5     0.080    0.11   0   0      0     0     0     0     1        1      -360     360;
                 4        6     0.090    0.18   0   0      0     0     0     0     1        1      -360     360;
                 6        7     0.040    0.04   0   0      0     0     0     0     1        1      -360     360;
                 2        8     0.110    0.11   0   0      0     0     0     0     1        1      -360     360;
                 8        9     0.080    0.11   0   0      0     0     0     0     1        1      -360     360;
                 8       10     0.110    0.11   0   0      0     0     0     0     1        1      -360     360;
                 9       11     0.110    0.11   0   0      0     0     0     0     1        1      -360     360;
                 9       12     0.080    0.11   0   0      0     0     0     0     1        1      -360     360;
                 3       13     0.110    0.11   0   0      0     0     0     0     1        1      -360     360;
                13       14     0.090    0.12   0   0      0     0     0     0     1        1      -360     360;
                13       15     0.080    0.11   0   0      0     0     0     0     1        1      -360     360;
                15       16     0.040    0.04   0   0      0     0     0     0     1        1      -360     360;
                 5       11     0.040    0.04   0   0      0     0     0     0     1        inf    -360     360;
                10       14     0.040    0.04   0   0      0     0     0     0     1        inf    -360     360;
                 7       16     0.090    0.12   0   0      0     0     0     0     1        inf    -360     360;
                 1        2       inf     inf   0   0      0     0     0     0     1        1      -360     360;
                 2        3       inf     inf   0   0      0     0     0     0     1        1      -360     360;
              ];
```

**Appendix B**: Data of the IEEE 33-bus distribution system

```
%% This M-file gives the data of the 33 bus distribution network

function mpc = case33_3
%% MATPOWER Case Format : Version 2
mpc.version = '2';

%%-----  Power Flow Data  -----%%
%% system MVA base
mpc.baseMVA = 100;
%% bus data
%           busi type   Pd      Qd      Gs  Bs    area  Vm      Va  baseKV zone   Vmax  Vmin  Qmin  Qmax
mpc.bus = [  1    3      0       0      0   0      1    1.00    0   12.66   1     1.05  0.95   0     0;
             2    1    0.10    0.06     0   0      1    1.00    0   12.66   1     1.05  0.95   0     0;
             3    1    0.09    0.04     0   0      1    1.00    0   12.66   1     1.05  0.95   0     0;
             4    1    0.12    0.08     0   0      1    1.00    0   12.66   1     1.05  0.95   0     0;
             5    1    0.06    0.03     0   0      1    1.00    0   12.66   1     1.05  0.95   0     0;
             6    1    0.06    0.02     0   0      1    1.00    0   12.66   1     1.05  0.95   0     0;
             7    1    0.20    0.10     0   0      1    1.00    0   12.66   1     1.05  0.95   0     0;
             8    1    0.20    0.10     0   0      1    1.00    0   12.66   1     1.05  0.95   0     0;
             9    1    0.06    0.02     0   0      1    1.00    0   12.66   1     1.05  0.95   0     0;
             10   1    0.06    0.02     0   0      1    1.00    0   12.66   1     1.05  0.95   0     0;
             11   1   0.045    0.03     0   0      1    1.00    0   12.66   1     1.05  0.95   0     0;
             12   1    0.06   0.035     0   0      1    1.00    0   12.66   1     1.05  0.95   0     0;
             13   1    0.06   0.035     0   0      1    1.00    0   12.66   1     1.05  0.95   0     0;
             14   1    0.12    0.08     0   0      1    1.00    0   12.66   1     1.05  0.95   0     0;
             15   1    0.06    0.01     0   0      1    1.00    0   12.66   1     1.05  0.95   0     0;
             16   1    0.06    0.02     0   0      1    1.00    0   12.66   1     1.05  0.95   0     0;
             17   1    0.06    0.02     0   0      1    1.00    0   12.66   1     1.05  0.95   0     0;
             18   1    0.09    0.04     0   0      1    1.00    0   12.66   1     1.05  0.95   0     0;
             19   1    0.09    0.04     0   0      1    1.00    0   12.66   1     1.05  0.95   0     0;
             20   1    0.09    0.04     0   0      1    1.00    0   12.66   1     1.05  0.95   0     0;
             21   1    0.09    0.04     0   0      1    1.00    0   12.66   1     1.05  0.95   0     0;
             22   1    0.09    0.04     0   0      1    1.00    0   12.66   1     1.05  0.95   0     0;
             23   1    0.09    0.05     0   0      1    1.00    0   12.66   1     1.05  0.95   0     0;
             24   1    0.42    0.20     0   0      1    1.00    0   12.66   1     1.05  0.95   0     0;
             25   1    0.42    0.20     0   0      1    1.00    0   12.66   1     1.05  0.95   0     0;
             26   1    0.06   0.025     0   0      1    1.00    0   12.66   1     1.05  0.95   0     0;
```

```
    27   1   0.06   0.025    0   0    1   1.00   0   12.66   1    1.05   0.95   0   0;
    28   1   0.06   0.02     0   0    1   1.00   0   12.66   1    1.05   0.95   0   0;
    29   1   0.12   0.07     0   0    1   1.00   0   12.66   1    1.05   0.95   0   0;
    30   1   0.20   0.60     0   0    1   1.00   0   12.66   1    1.05   0.95   0   0;
    31   1   0.15   0.07     0   0    1   1.00   0   12.66   1    1.05   0.95   0   0;
    32   1   0.21   0.10     0   0    1   1.00   0   12.66   1    1.05   0.95   0   0;
    33   1   0.06   0.04     0   0    1   1.00   0   12.66   1    1.05   0.95   0   0;
   ];
  % type == 3 => Slack bus;
  % type == 2 => PV bus
  % type == 1 => PQ bus

%% generator data
%       bus  Pg  Qg  Qmax  Qmin  Vg    mBase  status  Pmax  Pmin  Pc1  Pc2  Qc1min  Qc1max  Qc2min  Qc2max  ramp_agc  ramp_10  ramp_30  ramp_q  apf
mpc.gen = [1   0   0   0     0     1.00  100    1       0     0     0    0    0       0       0       0       0         0        0        0       0
   ];

%% branch data
%          from_bus  to_bus   r                x                b  rateA  rateB  rateC  ratio  angle  status  weight  angmin  angmax
mpc.branch =  [ 1    2   0.0922*0.62393   0.0477*0.62393   0  0   0   0   0   0   1   1   -360   360;
                2    3   0.4930*0.62393   0.2511*0.62393   0  0   0   0   0   0   1   1   -360   360;
                3    4   0.3660*0.62393   0.1840*0.62393   0  0   0   0   0   0   1   1   -360   360;
                4    5   0.3811*0.62393   0.1941*0.62393   0  0   0   0   0   0   1   1   -360   360;
                5    6   0.8190*0.62393   0.0700*0.62393   0  0   0   0   0   0   1   1   -360   360;
                6    7   0.1872*0.62393   0.6188*0.62393   0  0   0   0   0   0   1   1   -360   360;
                7    8   1.7114*0.62393   1.2351*0.62393   0  0   0   0   0   0   1   1   -360   360;
                8    9   1.0300*0.62393   0.7400*0.62393   0  0   0   0   0   0   1   1   -360   360;
                9    10  1.0400*0.62393   0.7400*0.62393   0  0   0   0   0   0   1   1   -360   360;
               10    11  0.1966*0.62393   0.0650*0.62393   0  0   0   0   0   0   1   1   -360   360;
               11    12  0.3744*0.62393   0.1238*0.62393   0  0   0   0   0   0   1   1   -360   360;
               12    13  1.4680*0.62393   1.1550*0.62393   0  0   0   0   0   0   1   1   -360   360;
               13    14  0.5416*0.62393   0.7129*0.62393   0  0   0   0   0   0   1   1   -360   360;
               14    15  0.5910*0.62393   0.5260*0.62393   0  0   0   0   0   0   1   1   -360   360;
               15    16  0.7463*0.62393   0.5450*0.62393   0  0   0   0   0   0   1   1   -360   360;
               16    17  1.2890*0.62393   1.7210*0.62393   0  0   0   0   0   0   1   1   -360   360;
               17    18  0.7320*0.62393   0.5740*0.62393   0  0   0   0   0   0   1   1   -360   360;
                2    19  0.1640*0.62393   0.1565*0.62393   0  0   0   0   0   0   1   1   -360   360;
```

```
    19      20      1.5042*0.62393    1.3554*0.62393    0    0      0     0     0     0     1        1      -360    360;
    20      21      0.4095*0.62393    0.4784*0.62393    0    0      0     0     0     0     1        1      -360    360;
    21      22      0.7089*0.62393    0.9373*0.62393    0    0      0     0     0     0     1        1      -360    360;
    3       23      0.4512*0.62393    0.3083*0.62393    0    0      0     0     0     0     1        1      -360    360;
    23      24      0.8980*0.62393    0.7091*0.62393    0    0      0     0     0     0     1        1      -360    360;
    24      25      0.8960*0.62393    0.7011*0.62393    0    0      0     0     0     0     1        1      -360    360;
    6       26      0.2030*0.62393    0.1034*0.62393    0    0      0     0     0     0     1        1      -360    360;
    26      27      0.2842*0.62393    0.1447*0.62393    0    0      0     0     0     0     1        1      -360    360;
    27      28      1.0590*0.62393    0.9337*0.62393    0    0      0     0     0     0     1        1      -360    360;
    28      29      0.8042*0.62393    0.7006*0.62393    0    0      0     0     0     0     1        1      -360    360;
    29      30      0.5075*0.62393    0.2585*0.62393    0    0      0     0     0     0     1        1      -360    360;
    30      31      0.9744*0.62393    0.9630*0.62393    0    0      0     0     0     0     1        1      -360    360;
    31      32      0.3105*0.62393    0.3619*0.62393    0    0      0     0     0     0     1        1      -360    360;
    32      33      0.3410*0.62393    0.5302*0.62393    0    0      0     0     0     0     1        1      -360    360;
    21       8      2.0000*0.62393    2.0000*0.62393    0    0      0     0     0     0     0      inf      -360    360;
     9      15      2.0000*0.62393    2.0000*0.62393    0    0      0     0     0     0     0      inf      -360    360;
    12      22      2.0000*0.62393    2.0000*0.62393    0    0      0     0     0     0     0      inf      -360    360;
    18      33      0.5000*0.62393    0.5000*0.62393    0    0      0     0     0     0     0      inf      -360    360;
    25      29      0.5000*0.62393    0.5000*0.62393    0    0      0     0     0     0     0      inf      -360    360;
  ];
```

**Appendix C**: **Load flow results of the 33-bus distribution system before and after feeder reconfiguration**

**Appendix C1**: **Load flow results of the 33-bus distribution system before reconfiguration of the distribution network**

| Bus Data | | | | | | |
|---|---|---|---|---|---|---|
| Bus | Voltage | | Generation | | Load | |
| # | Mag(pu) | Ang(deg) | P (MW) | Q (MVAr) | P (MW) | Q (MVAr) |
| 1 | 1.000 | 0.000* | 3.92 | 2.41 | - | - |
| 2 | 0.997 | 0.013 | - | - | 0.10 | 0.06 |
| 3 | 0.983 | 0.089 | - | - | 0.09 | 0.04 |
| 4 | 0.976 | 0.154 | - | - | 0.12 | 0.08 |
| 5 | 0.968 | 0.216 | - | - | 0.06 | 0.03 |
| 6 | 0.956 | 0.643 | - | - | 0.06 | 0.02 |
| 7 | 0.953 | 0.414 | - | - | 0.20 | 0.10 |
| 8 | 0.939 | 0.263 | - | - | 0.20 | 0.10 |
| 9 | 0.933 | 0.189 | - | - | 0.06 | 0.02 |
| 10 | 0.927 | 0.126 | - | - | 0.06 | 0.02 |
| 11 | 0.926 | 0.133 | - | - | 0.04 | 0.03 |
| 12 | 0.925 | 0.145 | - | - | 0.06 | 0.04 |
| 13 | 0.918 | 0.053 | - | - | 0.06 | 0.04 |
| 14 | 0.916 | -0.026 | - | - | 0.12 | 0.08 |
| 15 | 0.915 | -0.064 | - | - | 0.06 | 0.01 |
| 16 | 0.913 | -0.087 | - | - | 0.06 | 0.02 |
| 17 | 0.911 | -0.165 | - | - | 0.06 | 0.02 |
| 18 | 0.911 | -0.174 | - | - | 0.09 | 0.04 |
| 19 | 0.996 | 0.002 | - | - | 0.09 | 0.04 |
| 20 | 0.993 | -0.065 | - | - | 0.09 | 0.04 |
| 21 | 0.992 | -0.085 | - | - | 0.09 | 0.04 |
| 22 | 0.992 | -0.105 | - | - | 0.09 | 0.04 |
| 23 | 0.979 | 0.058 | - | - | 0.09 | 0.05 |
| 24 | 0.973 | -0.030 | - | - | 0.42 | 0.20 |
| 25 | 0.969 | -0.074 | - | - | 0.42 | 0.20 |
| 26 | 0.954 | 0.681 | - | - | 0.06 | 0.03 |
| 27 | 0.952 | 0.737 | - | - | 0.06 | 0.03 |
| 28 | 0.940 | 0.819 | - | - | 0.06 | 0.02 |
| 29 | 0.932 | 0.896 | - | - | 0.12 | 0.07 |
| 30 | 0.929 | 0.999 | - | - | 0.20 | 0.60 |
| 31 | 0.924 | 0.916 | - | - | 0.15 | 0.07 |
| 32 | 0.924 | 0.893 | - | - | 0.21 | 0.10 |
| 33 | 0.923 | 0.886 | - | - | 0.06 | 0.04 |
| | | Total: | 3.92 | 2.41 | 3.72 | 2.30 |

| Branch Data | | | | | | | | |
|---|---|---|---|---|---|---|---|---|
| Brnch | From | To | From Bus Injection | | To Bus Injection | | Loss (I^2 * Z) | |
| # | Bus | Bus | P (MW) | Q (MVAr) | P (MW) | Q (MVAr) | P (MW) | Q (MVAr) |
| 1 | 1 | 2 | 3.92 | 2.41 | -3.91 | -2.41 | 0.012 | 0.01 |
| 2 | 2 | 3 | 3.45 | 2.18 | -3.40 | -2.16 | 0.052 | 0.03 |
| 3 | 3 | 4 | 2.37 | 1.66 | -2.35 | -1.65 | 0.020 | 0.01 |
| 4 | 4 | 5 | 2.23 | 1.57 | -2.21 | -1.56 | 0.019 | 0.01 |
| 5 | 5 | 6 | 2.15 | 1.53 | -2.11 | -1.53 | 0.038 | 0.00 |
| 6 | 6 | 7 | 1.10 | 0.53 | -1.10 | -0.53 | 0.002 | 0.01 |
| 7 | 7 | 8 | 0.90 | 0.43 | -0.89 | -0.42 | 0.012 | 0.01 |
| 8 | 8 | 9 | 0.69 | 0.32 | -0.68 | -0.32 | 0.004 | 0.00 |
| 9 | 9 | 10 | 0.62 | 0.30 | -0.62 | -0.29 | 0.004 | 0.00 |
| 10 | 10 | 11 | 0.56 | 0.27 | -0.56 | -0.27 | 0.001 | 0.00 |
| 11 | 11 | 12 | 0.52 | 0.24 | -0.51 | -0.24 | 0.001 | 0.00 |
| 12 | 12 | 13 | 0.45 | 0.21 | -0.45 | -0.21 | 0.003 | 0.00 |
| 13 | 13 | 14 | 0.39 | 0.17 | -0.39 | -0.17 | 0.001 | 0.00 |
| 14 | 14 | 15 | 0.27 | 0.09 | -0.27 | -0.09 | 0.000 | 0.00 |
| 15 | 15 | 16 | 0.21 | 0.08 | -0.21 | -0.08 | 0.000 | 0.00 |
| 16 | 16 | 17 | 0.15 | 0.06 | -0.15 | -0.06 | 0.000 | 0.00 |
| 17 | 17 | 18 | 0.09 | 0.04 | -0.09 | -0.04 | 0.000 | 0.00 |
| 18 | 2 | 19 | 0.36 | 0.16 | -0.36 | -0.16 | 0.000 | 0.00 |
| 19 | 19 | 20 | 0.27 | 0.12 | -0.27 | -0.12 | 0.001 | 0.00 |
| 20 | 20 | 21 | 0.18 | 0.08 | -0.18 | -0.08 | 0.000 | 0.00 |
| 21 | 21 | 22 | 0.09 | 0.04 | -0.09 | -0.04 | 0.000 | 0.00 |
| 22 | 3 | 23 | 0.94 | 0.46 | -0.94 | -0.46 | 0.003 | 0.00 |
| 23 | 23 | 24 | 0.85 | 0.41 | -0.84 | -0.40 | 0.005 | 0.00 |
| 24 | 24 | 25 | 0.42 | 0.20 | -0.42 | -0.20 | 0.001 | 0.00 |
| 25 | 6 | 26 | 0.95 | 0.97 | -0.95 | -0.97 | 0.003 | 0.00 |
| 26 | 26 | 27 | 0.89 | 0.95 | -0.88 | -0.95 | 0.003 | 0.00 |
| 27 | 27 | 28 | 0.82 | 0.92 | -0.81 | -0.91 | 0.011 | 0.01 |
| 28 | 28 | 29 | 0.75 | 0.89 | -0.75 | -0.88 | 0.008 | 0.01 |
| 29 | 29 | 30 | 0.63 | 0.81 | -0.62 | -0.81 | 0.004 | 0.00 |
| 30 | 30 | 31 | 0.42 | 0.21 | -0.42 | -0.21 | 0.002 | 0.00 |
| 31 | 31 | 32 | 0.27 | 0.14 | -0.27 | -0.14 | 0.000 | 0.00 |
| 32 | 32 | 33 | 0.06 | 0.04 | -0.06 | -0.04 | 0.000 | 0.00 |
| 33 | 21 | 8 | 0.00 | 0.00 | 0.00 | 0.00 | 0.000 | 0.00 |
| 34 | 9 | 15 | 0.00 | 0.00 | 0.00 | 0.00 | 0.000 | 0.00 |
| 35 | 12 | 22 | 0.00 | 0.00 | 0.00 | 0.00 | 0.000 | 0.00 |
| 36 | 18 | 33 | 0.00 | 0.00 | 0.00 | 0.00 | 0.000 | 0.00 |
| 37 | 25 | 29 | 0.00 | 0.00 | 0.00 | 0.00 | 0.000 | 0.00 |
| | | | | | | Total: | 0.208 | 0.11 |

**Appendix C2:** Load flow results of the 33-bus distribution system after reconfiguration of the distribution network

```
================================================================
|     Bus Data
================================================================
 Bus      Voltage          Generation            Load
  #   Mag(pu) Ang(deg)   P (MW)   Q (MVAr)   P (MW)   Q (MVAr)
----- ------- --------  --------  --------  --------  --------
    1  1.000    0.000*     3.85      2.39       -         -
    2  0.997    0.013       -         -        0.10      0.06
    3  0.987    0.094       -         -        0.09      0.04
    4  0.983    0.160       -         -        0.12      0.08
    5  0.978    0.225       -         -        0.06      0.03
    6  0.972    0.518       -         -        0.06      0.02
    7  0.971    0.478       -         -        0.20      0.10
    8  0.963   -0.686       -         -        0.20      0.10
    9  0.959   -0.738       -         -        0.06      0.02
   10  0.963   -0.626       -         -        0.06      0.02
   11  0.963   -0.626       -         -        0.04      0.03
   12  0.963   -0.628       -         -        0.06      0.04
   13  0.960   -0.643       -         -        0.06      0.04
   14  0.960   -0.659       -         -        0.12      0.08
   15  0.953   -0.894       -         -        0.06      0.01
   16  0.951   -0.917       -         -        0.06      0.02
   17  0.949   -1.009       -         -        0.06      0.02
   18  0.947   -1.020       -         -        0.09      0.04
   19  0.995   -0.024       -         -        0.09      0.04
   20  0.978   -0.307       -         -        0.09      0.04
   21  0.974   -0.427       -         -        0.09      0.04
   22  0.970   -0.517       -         -        0.09      0.04
   23  0.983    0.063       -         -        0.09      0.05
   24  0.977   -0.025       -         -        0.42      0.20
   25  0.973   -0.068       -         -        0.42      0.20
   26  0.970    0.555       -         -        0.06      0.03
   27  0.968    0.608       -         -        0.06      0.03
   28  0.957    0.692       -         -        0.06      0.02
   29  0.950    0.770       -         -        0.12      0.07
   30  0.946    0.868       -         -        0.20      0.60
   31  0.943    0.795       -         -        0.15      0.07
   32  0.942    0.777       -         -        0.21      0.10
   33  0.947   -1.024       -         -        0.06      0.04
                          --------  --------  --------  --------
                 Total:     3.85      2.39      3.72      2.30
```

| Branch Data

| Brnch # | From Bus | To Bus | From Bus Injection P (MW) | From Bus Injection Q (MVAr) | To Bus Injection P (MW) | To Bus Injection Q (MVAr) | Loss (I^2 * Z) P (MW) | Loss (I^2 * Z) Q (MVAr) |
|---|---|---|---|---|---|---|---|---|
| 1 | 1 | 2 | 3.85 | 2.39 | -3.84 | -2.39 | 0.012 | 0.01 |
| 2 | 2 | 3 | 2.41 | 1.68 | -2.38 | -1.67 | 0.027 | 0.01 |
| 3 | 3 | 4 | 1.35 | 1.17 | -1.35 | -1.16 | 0.007 | 0.00 |
| 4 | 4 | 5 | 1.23 | 1.08 | -1.22 | -1.08 | 0.007 | 0.00 |
| 5 | 5 | 6 | 1.16 | 1.05 | -1.15 | -1.05 | 0.013 | 0.00 |
| 6 | 6 | 7 | 0.20 | 0.10 | -0.20 | -0.10 | 0.000 | 0.00 |
| 7 | 7 | 8 | 0.00 | 0.00 | 0.00 | 0.00 | 0.000 | 0.00 |
| 8 | 8 | 9 | 0.39 | 0.15 | -0.39 | -0.15 | 0.001 | 0.00 |
| 9 | 9 | 10 | 0.00 | 0.00 | 0.00 | 0.00 | 0.000 | 0.00 |
| 10 | 10 | 11 | -0.06 | -0.02 | 0.06 | 0.02 | 0.000 | 0.00 |
| 11 | 11 | 12 | -0.11 | -0.05 | 0.11 | 0.05 | 0.000 | 0.00 |
| 12 | 12 | 13 | 0.18 | 0.12 | -0.18 | -0.12 | 0.000 | 0.00 |
| 13 | 13 | 14 | 0.12 | 0.08 | -0.12 | -0.08 | 0.000 | 0.00 |
| 14 | 14 | 15 | 0.00 | 0.00 | 0.00 | 0.00 | 0.000 | 0.00 |
| 15 | 15 | 16 | 0.27 | 0.12 | -0.27 | -0.12 | 0.000 | 0.00 |
| 16 | 16 | 17 | 0.21 | 0.10 | -0.21 | -0.10 | 0.000 | 0.00 |
| 17 | 17 | 18 | 0.15 | 0.08 | -0.15 | -0.08 | 0.000 | 0.00 |
| 18 | 2 | 19 | 1.33 | 0.65 | -1.33 | -0.64 | 0.002 | 0.00 |
| 19 | 19 | 20 | 1.24 | 0.60 | -1.22 | -0.59 | 0.018 | 0.02 |
| 20 | 20 | 21 | 1.13 | 0.55 | -1.13 | -0.54 | 0.004 | 0.00 |
| 21 | 21 | 22 | 0.44 | 0.24 | -0.44 | -0.24 | 0.001 | 0.00 |
| 22 | 3 | 23 | 0.94 | 0.46 | -0.94 | -0.46 | 0.003 | 0.00 |
| 23 | 23 | 24 | 0.85 | 0.41 | -0.84 | -0.40 | 0.005 | 0.00 |
| 24 | 24 | 25 | 0.42 | 0.20 | -0.42 | -0.20 | 0.001 | 0.00 |
| 25 | 6 | 26 | 0.89 | 0.93 | -0.88 | -0.93 | 0.002 | 0.00 |
| 26 | 26 | 27 | 0.82 | 0.90 | -0.82 | -0.90 | 0.003 | 0.00 |
| 27 | 27 | 28 | 0.76 | 0.88 | -0.75 | -0.87 | 0.010 | 0.01 |
| 28 | 28 | 29 | 0.69 | 0.85 | -0.68 | -0.84 | 0.007 | 0.01 |
| 29 | 29 | 30 | 0.56 | 0.77 | -0.56 | -0.77 | 0.003 | 0.00 |
| 30 | 30 | 31 | 0.36 | 0.17 | -0.36 | -0.17 | 0.001 | 0.00 |
| 31 | 31 | 32 | 0.21 | 0.10 | -0.21 | -0.10 | 0.000 | 0.00 |
| 32 | 32 | 33 | 0.00 | 0.00 | 0.00 | 0.00 | 0.000 | 0.00 |
| 33 | 21 | 8 | 0.60 | 0.26 | -0.59 | -0.25 | 0.006 | 0.01 |
| 34 | 9 | 15 | 0.33 | 0.13 | -0.33 | -0.13 | 0.002 | 0.00 |
| 35 | 12 | 22 | -0.35 | -0.20 | 0.35 | 0.20 | 0.002 | 0.00 |
| 36 | 18 | 33 | 0.06 | 0.04 | -0.06 | -0.04 | 0.000 | 0.00 |
| 37 | 25 | 29 | 0.00 | 0.00 | 0.00 | 0.00 | 0.000 | 0.00 |
| | | | | | | Total: | 0.139 | 0.09 |

**Appendix D**: Data of the IEEE 69-bus distribution system

```
%% This M-file gives the data of the 69 bus distribution network

function mpc = case69
%% MATPOWER Case Format : Version 2
mpc.version = '2';

%%-----  Power Flow Data  -----%%
%% system MVA base
mpc.baseMVA = 100;

%% bus data
%            bus_i   type    Pd       Qd       Gs  Bs  area  Vm  Va  baseKV  zone   Vmax  Vmin
mpc.bus =    [1      3       0        0        0   0   1     1   0   12.6    1      1     0.9;
              2      1       0        0        0   0   1     1   0   12.6    1      1     0.9;
              3      1       0        0        0   0   1     1   0   12.6    1      1     0.9;
              4      1       0        0        0   0   1     1   0   12.6    1      1     0.9;
              5      1       0        0        0   0   1     1   0   12.6    1      1     0.9;
              6      1       0.0026   0.0022   0   0   1     1   0   12.6    1      1     0.9;
              7      1       0.0404   0.03     0   0   1     1   0   12.6    1      1     0.9;
              8      1       0.075    0.054    0   0   1     1   0   12.6    1      1     0.9;
              9      1       0.03     0.022    0   0   1     1   0   12.6    1      1     0.9;
              10     1       0.028    0.019    0   0   1     1   0   12.6    1      1     0.9;
              11     1       0.145    0.104    0   0   1     1   0   12.6    1      1     0.9;
              12     1       0.145    0.104    0   0   1     1   0   12.6    1      1     0.9;
              13     1       0.008    0.0055   0   0   1     1   0   12.6    1      1     0.9;
              14     1       0.008    0.0055   0   0   1     1   0   12.6    1      1     0.9;
              15     1       0        0        0   0   1     1   0   12.6    1      1     0.9;
              16     1       0.0455   0.03     0   0   1     1   0   12.6    1      1     0.9;
              17     1       0.06     0.035    0   0   1     1   0   12.6    1      1     0.9;
              18     1       0.06     0.035    0   0   1     1   0   12.6    1      1     0.9;
              19     1       0        0        0   0   1     1   0   12.6    1      1     0.9;
              20     1       0.001    0.0006   0   0   1     1   0   12.6    1      1     0.9;
              21     1       0.114    0.081    0   0   1     1   0   12.6    1      1     0.9;
              22     1       0.005    0.0035   0   0   1     1   0   12.6    1      1     0.9;
              23     1       0        0        0   0   1     1   0   12.6    1      1     0.9;
              24     1       0.028    0.02     0   0   1     1   0   12.6    1      1     0.9;
              25     1       0        0        0   0   1     1   0   12.6    1      1     0.9;
```

```
26	1	0.014	0.01	0	0	1	1	0	12.6	1	1	0.9;
27	1	0.014	0.01	0	0	1	1	0	12.6	1	1	0.9;
28	1	0.026	0.0186	0	0	1	1	0	12.6	1	1	0.9;
29	1	0.026	0.0186	0	0	1	1	0	12.6	1	1	0.9;
30	1	0	0	0	0	1	1	0	12.6	1	1	0.9;
31	1	0	0	0	0	1	1	0	12.6	1	1	0.9;
32	1	0	0	0	0	1	1	0	12.6	1	1	0.9;
33	1	0.014	0.01	0	0	1	1	0	12.6	1	1	0.9;
34	1	0.0195	0.014	0	0	1	1	0	12.6	1	1	0.9;
35	1	0.006	0.004	0	0	1	1	0	12.6	1	1	0.9;
36	1	0.026	0.01855	0	0	1	1	0	12.6	1	1	0.9;
37	1	0.026	0.01855	0	0	1	1	0	12.6	1	1	0.9;
38	1	0	0	0	0	1	1	0	12.6	1	1	0.9;
39	1	0.024	0.017	0	0	1	1	0	12.6	1	1	0.9;
40	1	0.024	0.017	0	0	1	1	0	12.6	1	1	0.9;
41	1	0.0012	0.001	0	0	1	1	0	12.6	1	1	0.9;
42	1	0	0	0	0	1	1	0	12.6	1	1	0.9;
43	1	0.006	0.0043	0	0	1	1	0	12.6	1	1	0.9;
44	1	0	0	0	0	1	1	0	12.6	1	1	0.9;
45	1	0.0392	0.0263	0	0	1	1	0	12.6	1	1	0.9;
46	1	0.0392	0.0263	0	0	1	1	0	12.6	1	1	0.9;
47	1	0	0	0	0	1	1	0	12.6	1	1	0.9;
48	1	0.079	0.0564	0	0	1	1	0	12.6	1	1	0.9;
49	1	0.3847	0.2745	0	0	1	1	0	12.6	1	1	0.9;
50	1	0.3847	0.2745	0	0	1	1	0	12.6	1	1	0.9;
51	1	0.0405	0.0283	0	0	1	1	0	12.6	1	1	0.9;
52	1	0.0036	0.0027	0	0	1	1	0	12.6	1	1	0.9;
53	1	0.00435	0.0035	0	0	1	1	0	12.6	1	1	0.9;
54	1	0.0264	0.019	0	0	1	1	0	12.6	1	1	0.9;
55	1	0.024	0.0172	0	0	1	1	0	12.6	1	1	0.9;
56	1	0	0	0	0	1	1	0	12.6	1	1	0.9;
57	1	0	0	0	0	1	1	0	12.6	1	1	0.9;
58	1	0	0	0	0	1	1	0	12.6	1	1	0.9;
59	1	0.1	0.072	0	0	1	1	0	12.6	1	1	0.9;
60	1	0	0	0	0	1	1	0	12.6	1	1	0.9;
61	1	1.244	0.888	0	0	1	1	0	12.6	1	1	0.9;
62	1	0.032	0.023	0	0	1	1	0	12.6	1	1	0.9;
```

```
        63      1       0         0         0   0   1   1   0   12.6    1       1   0.9;
        64      1       0.227     0.162     0   0   1   1   0   12.6    1       1   0.9;
        65      1       0.059     0.042     0   0   1   1   0   12.6    1       1   0.9;
        66      1       0.018     0.013     0   0   1   1   0   12.6    1       1   0.9;
        67      1       0.018     0.013     0   0   1   1   0   12.6    1       1   0.9
        68      1       0.028      0.02     0   0   1   1   0   12.6    1       1   0.9;
        69      1       0.028      0.02     0   0   1   1   0   12.6    1       1   0.9;
        ];

    % type == 3 => Slack bus;
    % type == 2 => PV bus
    % type == 1 => PQ bus

%% generator data
%           bus Pg  Qg  Qmax    Qmin    Vg   mBase status Pmax Pmin Pc1 Pc2 Qc1min Qc1max Qc2min Qc2max ramp_agc ramp_10 ramp_30 ramp_q apf
mpc.gen =   [1  0   0   0       0       1.00  100   1      0    0    0   0    0      0      0      0       0        0       0      0    0;
];

%% branch data
%              f_bus  to_bus   r            x            b rateA  rateB rateC ratio angle status  weight  angmin  angmax
mpc.branch = [  1       2   0.000311963  0.00074871   0   0      0     0     0     0     1       1      -360     360;
                2       3   0.000311963  0.00074871   0   0      0     0     0     0     1       1      -360     360;
                3       4   0.000935888  0.002246131  0   0      0     0     0     0     1       1      -360     360;
                4       5   0.015660525  0.018343403  0   0      0     0     0     0     1       1      -360     360;
                5       6   0.228356656  0.116299674  0   0      0     0     0     0     1       1      -360     360;
                6       7   0.237777928  0.121103899  0   0      0     0     0     0     1       1      -360     360;
                7       8   0.057525912  0.029324489  0   0      0     0     0     0     1       1      -360     360;
                8       9   0.030759517  0.015660525  0   0      0     0     0     0     1       1      -360     360;
                9       10  0.510994811  0.168896576  0   0      0     0     0     0     1       1      -360     360;
                10      11  0.116798814  0.038620975  0   0      0     0     0     0     1       1      -360     360;
                11      12  0.44386045   0.146684835  0   0      0     0     0     0     1       1      -360     360;
                12      13  0.642643047  0.212134598  0   0      0     0     0     0     1       1      -360     360;
                13      14  0.651378001  0.215254225  0   0      0     0     0     0     1       1      -360     360;
                14      15  0.660112955  0.218124281  0   0      0     0     0     0     1       1      -360     360;
                15      16  0.122663712  0.040555144  0   0      0     0     0     0     1       1      -360     360;
                16      17  0.233597628  0.077241951  0   0      0     0     0     0     1       1      -360     360;
                17      18  0.002932449  0.00099828   0   0      0     0     0     0     1       1      -360     360;
```

| | | | | | | | | | | | | | |
|---|---|---|---|---|---|---|---|---|---|---|---|---|---|
| 18 | 19 | 0.204397925 | 0.067571109 | 0 | 0 | 0 | 0 | 0 | 0 | 1 | 1 | -360 | 360; |
| 19 | 20 | 0.131398666 | 0.0434252 | 0 | 0 | 0 | 0 | 0 | 0 | 1 | 1 | -360 | 360; |
| 20 | 21 | 0.213132879 | 0.070441165 | 0 | 0 | 0 | 0 | 0 | 0 | 1 | 1 | -360 | 360; |
| 21 | 22 | 0.008734954 | 0.002870056 | 0 | 0 | 0 | 0 | 0 | 0 | 1 | 1 | -360 | 360; |
| 22 | 23 | 0.099266513 | 0.03281847 | 0 | 0 | 0 | 0 | 0 | 0 | 1 | 1 | -360 | 360; |
| 23 | 24 | 0.216065327 | 0.071439446 | 0 | 0 | 0 | 0 | 0 | 0 | 1 | 1 | -360 | 360; |
| 24 | 25 | 0.467195256 | 0.154421509 | 0 | 0 | 0 | 0 | 0 | 0 | 1 | 1 | -360 | 360; |
| 25 | 26 | 0.192730522 | 0.063702772 | 0 | 0 | 0 | 0 | 0 | 0 | 1 | 1 | -360 | 360; |
| 26 | 27 | 0.10806386 | 0.035688527 | 0 | 0 | 0 | 0 | 0 | 0 | 1 | 1 | -360 | 360; |
| 3 | 28 | 0.002745271 | 0.006738393 | 0 | 0 | 0 | 0 | 0 | 0 | 1 | 1 | -360 | 360; |
| 28 | 29 | 0.039931218 | 0.097644308 | 0 | 0 | 0 | 0 | 0 | 0 | 1 | 1 | -360 | 360; |
| 29 | 30 | 0.24819748 | 0.082046175 | 0 | 0 | 0 | 0 | 0 | 0 | 1 | 1 | -360 | 360; |
| 30 | 31 | 0.043799555 | 0.014475067 | 0 | 0 | 0 | 0 | 0 | 0 | 1 | 1 | -360 | 360; |
| 31 | 32 | 0.218997776 | 0.072375333 | 0 | 0 | 0 | 0 | 0 | 0 | 1 | 1 | -360 | 360; |
| 32 | 33 | 0.523473317 | 0.175697361 | 0 | 0 | 0 | 0 | 0 | 0 | 1 | 1 | -360 | 360; |
| 33 | 34 | 1.065664393 | 0.352268218 | 0 | 0 | 0 | 0 | 0 | 0 | 1 | 1 | -360 | 360; |
| 34 | 35 | 0.919665876 | 0.304038793 | 0 | 0 | 0 | 0 | 0 | 0 | 1 | 1 | -360 | 360; |
| 3 | 36 | 0.002745271 | 0.006738393 | 0 | 0 | 0 | 0 | 0 | 0 | 1 | 1 | -360 | 360; |
| 36 | 37 | 0.039931218 | 0.097644308 | 0 | 0 | 0 | 0 | 0 | 0 | 1 | 1 | -360 | 360; |
| 37 | 38 | 0.065699333 | 0.076742811 | 0 | 0 | 0 | 0 | 0 | 0 | 1 | 1 | -360 | 360; |
| 38 | 39 | 0.018967329 | 0.022149348 | 0 | 0 | 0 | 0 | 0 | 0 | 1 | 1 | -360 | 360; |
| 39 | 40 | 0.001123066 | 0.001310243 | 0 | 0 | 0 | 0 | 0 | 0 | 1 | 1 | -360 | 360; |
| 40 | 41 | 0.454404788 | 0.530898028 | 0 | 0 | 0 | 0 | 0 | 0 | 1 | 1 | -360 | 360; |
| 41 | 42 | 0.193416839 | 0.226048132 | 0 | 0 | 0 | 0 | 0 | 0 | 1 | 1 | -360 | 360; |
| 42 | 43 | 0.025580937 | 0.029823629 | 0 | 0 | 0 | 0 | 0 | 0 | 1 | 1 | -360 | 360; |
| 43 | 44 | 0.005740113 | 0.007237533 | 0 | 0 | 0 | 0 | 0 | 0 | 1 | 1 | -360 | 360; |
| 44 | 45 | 0.067945464 | 0.085664942 | 0 | 0 | 0 | 0 | 0 | 0 | 1 | 1 | -360 | 360; |
| 45 | 46 | 0.000561533 | 0.00074871 | 0 | 0 | 0 | 0 | 0 | 0 | 1 | 1 | -360 | 360; |
| 4 | 47 | 0.002121346 | 0.005240972 | 0 | 0 | 0 | 0 | 0 | 0 | 1 | 1 | -360 | 360; |
| 47 | 48 | 0.053096042 | 0.129963638 | 0 | 0 | 0 | 0 | 0 | 0 | 1 | 1 | -360 | 360; |
| 48 | 49 | 0.180813549 | 0.442425422 | 0 | 0 | 0 | 0 | 0 | 0 | 1 | 1 | -360 | 360; |
| 49 | 50 | 0.051286659 | 0.125471376 | 0 | 0 | 0 | 0 | 0 | 0 | 1 | 1 | -360 | 360; |
| 8 | 51 | 0.057900267 | 0.029511666 | 0 | 0 | 0 | 0 | 0 | 0 | 1 | 1 | -360 | 360; |
| 51 | 52 | 0.207080803 | 0.069505277 | 0 | 0 | 0 | 0 | 0 | 0 | 1 | 1 | -360 | 360; |
| 9 | 53 | 0.108563 | 0.055279781 | 0 | 0 | 0 | 0 | 0 | 0 | 1 | 1 | -360 | 360; |
| 53 | 54 | 0.126656834 | 0.064513875 | 0 | 0 | 0 | 0 | 0 | 0 | 1 | 1 | -360 | 360; |
| 54 | 55 | 0.177319567 | 0.090281989 | 0 | 0 | 0 | 0 | 0 | 0 | 1 | 1 | -360 | 360; |

```
55	56	0.175510184	0.089408494	0	0	0	0	0	0	1	1	-360	360;
56	57	0.992041209	0.332988927	0	0	0	0	0	0	1	1	-360	360;
57	58	0.488970249	0.164092351	0	0	0	0	0	0	1	1	-360	360;
58	59	0.189798073	0.062766884	0	0	0	0	0	0	1	1	-360	360;
59	60	0.240897554	0.073124044	0	0	0	0	0	0	1	1	-360	360;
60	61	0.316642084	0.161284687	0	0	0	0	0	0	1	1	-360	360;
61	62	0.060770323	0.030946694	0	0	0	0	0	0	1	1	-360	360;
62	63	0.090469167	0.046045686	0	0	0	0	0	0	1	1	-360	360;
63	64	0.443298918	0.225798562	0	0	0	0	0	0	1	1	-360	360;
64	65	0.649506226	0.330805188	0	0	0	0	0	0	1	1	-360	360;
11	66	0.125533768	0.038121835	0	0	0	0	0	0	1	1	-360	360;
66	67	0.002932449	0.000873495	0	0	0	0	0	0	1	1	-360	360;
12	68	0.461330358	0.152487341	0	0	0	0	0	0	1	1	-360	360;
68	69	0.002932449	0.00099828	0	0	0	0	0	0	1	1	-360	360;
11	43	0.311962644	0.311962644	0	0	0	0	0	0	0	inf	-360	360;
13	21	0.311962644	0.311962644	0	0	0	0	0	0	0	inf	-360	360;
15	46	0.623925289	0.311962644	0	0	0	0	0	0	0	inf	-360	360;
50	59	1.247850577	0.623925289	0	0	0	0	0	0	0	inf	-360	360;
27	65	0.623925289	0.311962644	0	0	0	0	0	0	0	inf	-360	360;
];
```

**Appendix E**: **Load flow results of the IEEE 69-bus distribution system before and after feeder reconfiguration**

**Appendix E1: Load flow results of the 69-bus distribution system before reconfiguration of the distribution network**

```
================================================================
|     Bus Data
================================================================
 Bus      Voltage          Generation            Load
  #   Mag(pu)  Ang(deg)   P (MW)   Q (MVAr)   P (MW)   Q (MVAr)
----- ------- --------  --------  --------  --------  --------
    1  1.000    0.000*    4.03      2.80        -         -
    2  1.000   -0.001      -          -         -         -
    3  1.000   -0.002      -          -         -         -
    4  1.000   -0.006      -          -         -         -
    5  0.999   -0.019      -          -         -         -
    6  0.990    0.049      -          -       0.00      0.00
    7  0.981    0.121      -          -       0.04      0.03
    8  0.979    0.138      -          -       0.07      0.05
    9  0.977    0.147      -          -       0.03      0.02
   10  0.972    0.232      -          -       0.03      0.02
   11  0.971    0.251      -          -       0.14      0.10
   12  0.968    0.304      -          -       0.14      0.10
   13  0.965    0.350      -          -       0.01      0.01
   14  0.962    0.397      -          -       0.01      0.01
   15  0.959    0.442      -          -         -         -
   16  0.959    0.451      -          -       0.05      0.03
   17  0.958    0.465      -          -       0.06      0.04
   18  0.958    0.465      -          -       0.06      0.04
   19  0.958    0.474      -          -         -         -
   20  0.957    0.479      -          -       0.00      0.00
   21  0.957    0.488      -          -       0.11      0.08
   22  0.957    0.488      -          -       0.01      0.00
   23  0.957    0.490      -          -         -         -
   24  0.957    0.493      -          -       0.03      0.02
   25  0.956    0.496      -          -         -         -
   26  0.956    0.497      -          -       0.01      0.01
   27  0.956    0.497      -          -       0.01      0.01
   28  1.000   -0.003      -          -       0.03      0.02
   29  1.000   -0.005      -          -       0.03      0.02
   30  1.000   -0.003      -          -         -         -
   31  1.000   -0.003      -          -         -         -
   32  1.000   -0.001      -          -         -         -
   33  0.999    0.003      -          -       0.01      0.01
   34  0.999    0.009      -          -       0.02      0.01
   35  0.999    0.010      -          -       0.01      0.00
   36  1.000   -0.003      -          -       0.03      0.02
   37  1.000   -0.009      -          -       0.03      0.02
   38  1.000   -0.012      -          -         -         -
```

| | | | | | | |
|---|---|---|---|---|---|---|
| 39 | 1.000 | -0.012 | - | - | 0.02 | 0.02 |
| 40 | 1.000 | -0.013 | - | - | 0.02 | 0.02 |
| 41 | 0.999 | -0.024 | - | - | 0.00 | 0.00 |
| 42 | 0.999 | -0.028 | - | - | - | - |
| 43 | 0.999 | -0.029 | - | - | 0.01 | 0.00 |
| 44 | 0.999 | -0.029 | - | - | - | - |
| 45 | 0.998 | -0.031 | - | - | 0.04 | 0.03 |
| 46 | 0.998 | -0.031 | - | - | 0.04 | 0.03 |
| 47 | 1.000 | -0.008 | - | - | - | - |
| 48 | 0.999 | -0.053 | - | - | 0.08 | 0.06 |
| 49 | 0.995 | -0.192 | - | - | 0.38 | 0.27 |
| 50 | 0.994 | -0.211 | - | - | 0.38 | 0.27 |
| 51 | 0.979 | 0.139 | - | - | 0.04 | 0.03 |
| 52 | 0.979 | 0.139 | - | - | 0.00 | 0.00 |
| 53 | 0.975 | 0.169 | - | - | 0.00 | 0.00 |
| 54 | 0.971 | 0.195 | - | - | 0.03 | 0.02 |
| 55 | 0.967 | 0.230 | - | - | 0.02 | 0.02 |
| 56 | 0.963 | 0.265 | - | - | - | - |
| 57 | 0.940 | 0.662 | - | - | - | - |
| 58 | 0.929 | 0.864 | - | - | - | - |
| 59 | 0.925 | 0.945 | - | - | 0.10 | 0.07 |
| 60 | 0.920 | 1.050 | - | - | - | - |
| 61 | 0.912 | 1.119 | - | - | 1.24 | 0.89 |
| 62 | 0.912 | 1.122 | - | - | 0.03 | 0.02 |
| 63 | 0.912 | 1.125 | - | - | - | - |
| 64 | 0.910 | 1.143 | - | - | 0.23 | 0.16 |
| 65 | 0.909 | 1.149 | - | - | 0.06 | 0.04 |
| 66 | 0.971 | 0.252 | - | - | 0.02 | 0.01 |
| 67 | 0.971 | 0.252 | - | - | 0.02 | 0.01 |
| 68 | 0.968 | 0.310 | - | - | 0.03 | 0.02 |
| 69 | 0.968 | 0.310 | - | - | 0.03 | 0.02 |
| | | | -------- | -------- | -------- | -------- |
| | | Total: | 4.03 | 2.80 | 3.80 | 2.69 |

================================================================================

| Branch Data

================================================================================

| Brnch # | From Bus | To Bus | From Bus Injection P (MW) | From Bus Injection Q (MVAr) | To Bus Injection P (MW) | To Bus Injection Q (MVAr) | Loss (I^2 * Z) P (MW) | Loss (I^2 * Z) Q (MVAr) |
|---|---|---|---|---|---|---|---|---|
| 1 | 1 | 2 | 4.03 | 2.80 | -4.03 | -2.80 | 0.000 | 0.00 |
| 2 | 2 | 3 | 4.03 | 2.80 | -4.03 | -2.80 | 0.000 | 0.00 |
| 3 | 3 | 4 | 3.75 | 2.60 | -3.75 | -2.60 | 0.000 | 0.00 |
| 4 | 4 | 5 | 2.90 | 1.99 | -2.90 | -1.99 | 0.002 | 0.00 |
| 5 | 5 | 6 | 2.90 | 1.99 | -2.87 | -1.97 | 0.028 | 0.01 |
| 6 | 6 | 7 | 2.87 | 1.97 | -2.84 | -1.96 | 0.029 | 0.01 |
| 7 | 7 | 8 | 2.80 | 1.93 | -2.79 | -1.92 | 0.007 | 0.00 |
| 8 | 8 | 9 | 2.67 | 1.84 | -2.67 | -1.84 | 0.003 | 0.00 |

| | | | | | | | | |
|---|---|---|---|---|---|---|---|---|
| 9 | 9 | 10 | 0.78 | 0.53 | -0.78 | -0.53 | 0.005 | 0.00 |
| 10 | 10 | 11 | 0.75 | 0.51 | -0.75 | -0.51 | 0.001 | 0.00 |
| 11 | 11 | 12 | 0.57 | 0.38 | -0.56 | -0.38 | 0.002 | 0.00 |
| 12 | 12 | 13 | 0.36 | 0.24 | -0.36 | -0.24 | 0.001 | 0.00 |
| 13 | 13 | 14 | 0.35 | 0.23 | -0.35 | -0.23 | 0.001 | 0.00 |
| 14 | 14 | 15 | 0.34 | 0.23 | -0.34 | -0.23 | 0.001 | 0.00 |
| 15 | 15 | 16 | 0.34 | 0.23 | -0.34 | -0.23 | 0.000 | 0.00 |
| 16 | 16 | 17 | 0.30 | 0.20 | -0.30 | -0.20 | 0.000 | 0.00 |
| 17 | 17 | 18 | 0.24 | 0.16 | -0.24 | -0.16 | 0.000 | 0.00 |
| 18 | 18 | 19 | 0.18 | 0.13 | -0.18 | -0.13 | 0.000 | 0.00 |
| 19 | 19 | 20 | 0.18 | 0.13 | -0.18 | -0.13 | 0.000 | 0.00 |
| 20 | 20 | 21 | 0.18 | 0.12 | -0.18 | -0.12 | 0.000 | 0.00 |
| 21 | 21 | 22 | 0.06 | 0.04 | -0.06 | -0.04 | 0.000 | 0.00 |
| 22 | 22 | 23 | 0.06 | 0.04 | -0.06 | -0.04 | 0.000 | 0.00 |
| 23 | 23 | 24 | 0.06 | 0.04 | -0.06 | -0.04 | 0.000 | 0.00 |
| 24 | 24 | 25 | 0.03 | 0.02 | -0.03 | -0.02 | 0.000 | 0.00 |
| 25 | 25 | 26 | 0.03 | 0.02 | -0.03 | -0.02 | 0.000 | 0.00 |
| 26 | 26 | 27 | 0.01 | 0.01 | -0.01 | -0.01 | 0.000 | 0.00 |
| 27 | 3 | 28 | 0.09 | 0.07 | -0.09 | -0.07 | 0.000 | 0.00 |
| 28 | 28 | 29 | 0.07 | 0.05 | -0.07 | -0.05 | 0.000 | 0.00 |
| 29 | 29 | 30 | 0.04 | 0.03 | -0.04 | -0.03 | 0.000 | 0.00 |
| 30 | 30 | 31 | 0.04 | 0.03 | -0.04 | -0.03 | 0.000 | 0.00 |
| 31 | 31 | 32 | 0.04 | 0.03 | -0.04 | -0.03 | 0.000 | 0.00 |
| 32 | 32 | 33 | 0.04 | 0.03 | -0.04 | -0.03 | 0.000 | 0.00 |
| 33 | 33 | 34 | 0.03 | 0.02 | -0.03 | -0.02 | 0.000 | 0.00 |
| 34 | 34 | 35 | 0.01 | 0.00 | -0.01 | -0.00 | 0.000 | 0.00 |
| 35 | 3 | 36 | 0.19 | 0.13 | -0.19 | -0.13 | 0.000 | 0.00 |
| 36 | 36 | 37 | 0.16 | 0.11 | -0.16 | -0.11 | 0.000 | 0.00 |
| 37 | 37 | 38 | 0.13 | 0.09 | -0.13 | -0.09 | 0.000 | 0.00 |
| 38 | 38 | 39 | 0.13 | 0.09 | -0.13 | -0.09 | 0.000 | 0.00 |
| 39 | 39 | 40 | 0.11 | 0.07 | -0.11 | -0.07 | 0.000 | 0.00 |
| 40 | 40 | 41 | 0.09 | 0.06 | -0.09 | -0.06 | 0.000 | 0.00 |
| 41 | 41 | 42 | 0.08 | 0.06 | -0.08 | -0.06 | 0.000 | 0.00 |
| 42 | 42 | 43 | 0.08 | 0.06 | -0.08 | -0.06 | 0.000 | 0.00 |
| 43 | 43 | 44 | 0.08 | 0.05 | -0.08 | -0.05 | 0.000 | 0.00 |
| 44 | 44 | 45 | 0.08 | 0.05 | -0.08 | -0.05 | 0.000 | 0.00 |
| 45 | 45 | 46 | 0.04 | 0.03 | -0.04 | -0.03 | 0.000 | 0.00 |
| 46 | 4 | 47 | 0.85 | 0.61 | -0.85 | -0.61 | 0.000 | 0.00 |
| 47 | 47 | 48 | 0.85 | 0.61 | -0.85 | -0.61 | 0.001 | 0.00 |
| 48 | 48 | 49 | 0.77 | 0.55 | -0.77 | -0.55 | 0.002 | 0.00 |
| 49 | 49 | 50 | 0.38 | 0.27 | -0.38 | -0.27 | 0.000 | 0.00 |
| 50 | 8 | 51 | 0.04 | 0.03 | -0.04 | -0.03 | 0.000 | 0.00 |
| 51 | 51 | 52 | 0.00 | 0.00 | -0.00 | -0.00 | 0.000 | 0.00 |
| 52 | 9 | 53 | 1.86 | 1.28 | -1.85 | -1.28 | 0.006 | 0.00 |
| 53 | 53 | 54 | 1.85 | 1.27 | -1.84 | -1.27 | 0.007 | 0.00 |
| 54 | 54 | 55 | 1.81 | 1.25 | -1.80 | -1.25 | 0.009 | 0.00 |
| 55 | 55 | 56 | 1.78 | 1.23 | -1.77 | -1.23 | 0.009 | 0.00 |
| 56 | 56 | 57 | 1.77 | 1.23 | -1.72 | -1.21 | 0.050 | 0.02 |
| 57 | 57 | 58 | 1.72 | 1.21 | -1.70 | -1.20 | 0.024 | 0.01 |
| 58 | 58 | 59 | 1.70 | 1.20 | -1.69 | -1.20 | 0.010 | 0.00 |

| | | | | | | | | |
|---|---|---|---|---|---|---|---|---|
| 59 | 59 | 60 | 1.59 | 1.13 | -1.58 | -1.12 | 0.011 | 0.00 |
| 60 | 60 | 61 | 1.58 | 1.12 | -1.56 | -1.12 | 0.014 | 0.01 |
| 61 | 61 | 62 | 0.32 | 0.23 | -0.32 | -0.23 | 0.000 | 0.00 |
| 62 | 62 | 63 | 0.29 | 0.20 | -0.29 | -0.20 | 0.000 | 0.00 |
| 63 | 63 | 64 | 0.29 | 0.20 | -0.29 | -0.20 | 0.001 | 0.00 |
| 64 | 64 | 65 | 0.06 | 0.04 | -0.06 | -0.04 | 0.000 | 0.00 |
| 65 | 11 | 66 | 0.04 | 0.03 | -0.04 | -0.03 | 0.000 | 0.00 |
| 66 | 66 | 67 | 0.02 | 0.01 | -0.02 | -0.01 | 0.000 | 0.00 |
| 67 | 12 | 68 | 0.06 | 0.04 | -0.06 | -0.04 | 0.000 | 0.00 |
| 68 | 68 | 69 | 0.03 | 0.02 | -0.03 | -0.02 | 0.000 | 0.00 |
| 69 | 11 | 43 | 0.00 | 0.00 | 0.00 | 0.00 | 0.000 | 0.00 |
| 70 | 13 | 21 | 0.00 | 0.00 | 0.00 | 0.00 | 0.000 | 0.00 |
| 71 | 15 | 46 | 0.00 | 0.00 | 0.00 | 0.00 | 0.000 | 0.00 |
| 72 | 50 | 59 | 0.00 | 0.00 | 0.00 | 0.00 | 0.000 | 0.00 |
| 73 | 27 | 65 | 0.00 | 0.00 | 0.00 | 0.00 | 0.000 | 0.00 |
| | | | | | | Total: | 0.225 | 0.10 |

**Appendix E2:** Load flow results of the 69-bus distribution system after reconfiguration of the distribution network

| Bus Data | | | | | | |
|---|---|---|---|---|---|---|
| Bus | Voltage | | Generation | | Load | |
| # | Mag(pu) | Ang(deg) | P (MW) | Q (MVAr) | P (MW) | Q (MVAr) |
| 1 | 1.000 | 0.000* | 3.90 | 2.79 | - | - |
| 2 | 1.000 | -0.001 | - | - | - | - |
| 3 | 1.000 | -0.002 | - | - | - | - |
| 4 | 1.000 | -0.005 | - | - | - | - |
| 5 | 1.000 | -0.008 | - | - | - | - |
| 6 | 0.998 | 0.011 | - | - | 0.00 | 0.00 |
| 7 | 0.995 | 0.030 | - | - | 0.04 | 0.03 |
| 8 | 0.995 | 0.034 | - | - | 0.07 | 0.05 |
| 9 | 0.995 | 0.036 | - | - | 0.03 | 0.02 |
| 10 | 0.992 | 0.084 | - | - | 0.03 | 0.02 |
| 11 | 0.991 | 0.095 | - | - | 0.14 | 0.10 |
| 12 | 0.990 | 0.116 | - | - | 0.14 | 0.10 |
| 13 | 0.990 | 0.118 | - | - | 0.01 | 0.01 |
| 14 | 0.990 | 0.120 | - | - | 0.01 | 0.01 |
| 15 | 0.982 | -0.177 | - | - | - | - |
| 16 | 0.981 | -0.160 | - | - | 0.05 | 0.03 |
| 17 | 0.979 | -0.129 | - | - | 0.06 | 0.04 |
| 18 | 0.979 | -0.129 | - | - | 0.06 | 0.04 |
| 19 | 0.978 | -0.106 | - | - | - | - |
| 20 | 0.977 | -0.091 | - | - | 0.00 | 0.00 |

| | | | | | | |
|---|---|---|---|---|---|---|
| 21 | 0.975 | -0.067 | – | – | 0.11 | 0.08 |
| 22 | 0.975 | -0.066 | – | – | 0.01 | 0.00 |
| 23 | 0.975 | -0.057 | – | – | – | – |
| 24 | 0.974 | -0.038 | – | – | 0.03 | 0.02 |
| 25 | 0.972 | -0.001 | – | – | – | – |
| 26 | 0.971 | 0.015 | – | – | 0.01 | 0.01 |
| 27 | 0.970 | 0.023 | – | – | 0.01 | 0.01 |
| 28 | 1.000 | -0.003 | – | – | 0.03 | 0.02 |
| 29 | 1.000 | -0.005 | – | – | 0.03 | 0.02 |
| 30 | 1.000 | -0.003 | – | – | – | – |
| 31 | 1.000 | -0.003 | – | – | – | – |
| 32 | 1.000 | -0.001 | – | – | – | – |
| 33 | 0.999 | 0.004 | – | – | 0.01 | 0.01 |
| 34 | 0.999 | 0.009 | – | – | 0.02 | 0.01 |
| 35 | 0.999 | 0.011 | – | – | 0.01 | 0.00 |
| 36 | 1.000 | -0.005 | – | – | 0.03 | 0.02 |
| 37 | 0.999 | -0.039 | – | – | 0.03 | 0.02 |
| 38 | 0.998 | -0.053 | – | – | – | – |
| 39 | 0.998 | -0.058 | – | – | 0.02 | 0.02 |
| 40 | 0.998 | -0.058 | – | – | 0.02 | 0.02 |
| 41 | 0.991 | -0.155 | – | – | 0.00 | 0.00 |
| 42 | 0.989 | -0.197 | – | – | – | – |
| 43 | 0.988 | -0.203 | – | – | 0.01 | 0.00 |
| 44 | 0.988 | -0.204 | – | – | – | – |
| 45 | 0.987 | -0.221 | – | – | 0.04 | 0.03 |
| 46 | 0.987 | -0.222 | – | – | 0.04 | 0.03 |
| 47 | 1.000 | -0.010 | – | – | – | – |
| 48 | 0.996 | -0.129 | – | – | 0.08 | 0.06 |
| 49 | 0.985 | -0.526 | – | – | 0.38 | 0.27 |
| 50 | 0.983 | -0.620 | – | – | 0.38 | 0.27 |
| 51 | 0.995 | 0.034 | – | – | 0.04 | 0.03 |
| 52 | 0.995 | 0.034 | – | – | 0.00 | 0.00 |
| 53 | 0.995 | 0.037 | – | – | 0.00 | 0.00 |
| 54 | 0.994 | 0.037 | – | – | 0.03 | 0.02 |
| 55 | 0.994 | 0.038 | – | – | 0.02 | 0.02 |
| 56 | 0.959 | -0.403 | – | – | – | – |
| 57 | 0.959 | -0.403 | – | – | – | – |
| 58 | 0.959 | -0.403 | – | – | – | – |
| 59 | 0.959 | -0.403 | – | – | 0.10 | 0.07 |
| 60 | 0.955 | -0.325 | – | – | – | – |
| 61 | 0.949 | -0.275 | – | – | 1.24 | 0.89 |
| 62 | 0.965 | 0.072 | – | – | 0.03 | 0.02 |
| 63 | 0.965 | 0.072 | – | – | – | – |
| 64 | 0.965 | 0.070 | – | – | 0.23 | 0.16 |
| 65 | 0.968 | 0.049 | – | – | 0.06 | 0.04 |
| 66 | 0.991 | 0.096 | – | – | 0.02 | 0.01 |
| 67 | 0.991 | 0.096 | – | – | 0.02 | 0.01 |
| 68 | 0.990 | 0.122 | – | – | 0.03 | 0.02 |

| | | | | | | |
|---|---|---|---|---|---|---|
| 69 | 0.990 | 0.122 | - | - | 0.03 | 0.02 |
| | | | -------- | -------- | -------- | -------- |
| | | Total: | 3.90 | 2.79 | 3.80 | 2.69 |

================================================================================
| Branch Data
================================================================================

| Brnch # | From Bus | To Bus | From Bus Injection P (MW) | From Bus Injection Q (MVAr) | To Bus Injection P (MW) | To Bus Injection Q (MVAr) | Loss (I^2 * Z) P (MW) | Loss (I^2 * Z) Q (MVAr) |
|---|---|---|---|---|---|---|---|---|
| 1 | 1 | 2 | 3.90 | 2.79 | -3.90 | -2.79 | 0.000 | 0.00 |
| 2 | 2 | 3 | 3.90 | 2.79 | -3.90 | -2.79 | 0.000 | 0.00 |
| 3 | 3 | 4 | 2.94 | 2.13 | -2.94 | -2.12 | 0.000 | 0.00 |
| 4 | 4 | 5 | 0.68 | 0.49 | -0.68 | -0.49 | 0.000 | 0.00 |
| 5 | 5 | 6 | 0.68 | 0.49 | -0.68 | -0.48 | 0.002 | 0.00 |
| 6 | 6 | 7 | 0.67 | 0.48 | -0.67 | -0.48 | 0.002 | 0.00 |
| 7 | 7 | 8 | 0.63 | 0.45 | -0.63 | -0.45 | 0.000 | 0.00 |
| 8 | 8 | 9 | 0.51 | 0.37 | -0.51 | -0.37 | 0.000 | 0.00 |
| 9 | 9 | 10 | 0.43 | 0.30 | -0.43 | -0.30 | 0.001 | 0.00 |
| 10 | 10 | 11 | 0.40 | 0.29 | -0.40 | -0.29 | 0.000 | 0.00 |
| 11 | 11 | 12 | 0.22 | 0.16 | -0.22 | -0.16 | 0.000 | 0.00 |
| 12 | 12 | 13 | 0.02 | 0.01 | -0.02 | -0.01 | 0.000 | 0.00 |
| 13 | 13 | 14 | 0.01 | 0.01 | -0.01 | -0.01 | 0.000 | 0.00 |
| 14 | 14 | 15 | 0.00 | 0.00 | 0.00 | 0.00 | 0.000 | 0.00 |
| 15 | 15 | 16 | 0.67 | 0.46 | -0.67 | -0.45 | 0.001 | 0.00 |
| 16 | 16 | 17 | 0.62 | 0.42 | -0.62 | -0.42 | 0.001 | 0.00 |
| 17 | 17 | 18 | 0.56 | 0.39 | -0.56 | -0.39 | 0.000 | 0.00 |
| 18 | 18 | 19 | 0.50 | 0.35 | -0.50 | -0.35 | 0.001 | 0.00 |
| 19 | 19 | 20 | 0.50 | 0.35 | -0.50 | -0.35 | 0.001 | 0.00 |
| 20 | 20 | 21 | 0.50 | 0.35 | -0.50 | -0.35 | 0.001 | 0.00 |
| 21 | 21 | 22 | 0.38 | 0.27 | -0.38 | -0.27 | 0.000 | 0.00 |
| 22 | 22 | 23 | 0.38 | 0.27 | -0.38 | -0.27 | 0.000 | 0.00 |
| 23 | 23 | 24 | 0.38 | 0.27 | -0.38 | -0.27 | 0.000 | 0.00 |
| 24 | 24 | 25 | 0.35 | 0.25 | -0.35 | -0.25 | 0.001 | 0.00 |
| 25 | 25 | 26 | 0.35 | 0.25 | -0.35 | -0.25 | 0.000 | 0.00 |
| 26 | 26 | 27 | 0.33 | 0.24 | -0.33 | -0.24 | 0.000 | 0.00 |
| 27 | 3 | 28 | 0.09 | 0.07 | -0.09 | -0.07 | 0.000 | 0.00 |
| 28 | 28 | 29 | 0.07 | 0.05 | -0.07 | -0.05 | 0.000 | 0.00 |
| 29 | 29 | 30 | 0.04 | 0.03 | -0.04 | -0.03 | 0.000 | 0.00 |
| 30 | 30 | 31 | 0.04 | 0.03 | -0.04 | -0.03 | 0.000 | 0.00 |
| 31 | 31 | 32 | 0.04 | 0.03 | -0.04 | -0.03 | 0.000 | 0.00 |
| 32 | 32 | 33 | 0.04 | 0.03 | -0.04 | -0.03 | 0.000 | 0.00 |
| 33 | 33 | 34 | 0.03 | 0.02 | -0.03 | -0.02 | 0.000 | 0.00 |
| 34 | 34 | 35 | 0.01 | 0.00 | -0.01 | -0.00 | 0.000 | 0.00 |
| 35 | 3 | 36 | 0.87 | 0.60 | -0.87 | -0.60 | 0.000 | 0.00 |
| 36 | 36 | 37 | 0.84 | 0.58 | -0.84 | -0.58 | 0.000 | 0.00 |
| 37 | 37 | 38 | 0.81 | 0.56 | -0.81 | -0.56 | 0.001 | 0.00 |
| 38 | 38 | 39 | 0.81 | 0.56 | -0.81 | -0.56 | 0.000 | 0.00 |
| 39 | 39 | 40 | 0.79 | 0.54 | -0.79 | -0.54 | 0.000 | 0.00 |

| | | | | | | | | |
|---|---|---|---|---|---|---|---|---|
| 40 | 40 | 41 | 0.76 | 0.52 | -0.76 | -0.52 | 0.004 | 0.00 |
| 41 | 41 | 42 | 0.76 | 0.52 | -0.76 | -0.52 | 0.002 | 0.00 |
| 42 | 42 | 43 | 0.76 | 0.52 | -0.76 | -0.51 | 0.000 | 0.00 |
| 43 | 43 | 44 | 0.75 | 0.51 | -0.75 | -0.51 | 0.000 | 0.00 |
| 44 | 44 | 45 | 0.75 | 0.51 | -0.75 | -0.51 | 0.001 | 0.00 |
| 45 | 45 | 46 | 0.71 | 0.48 | -0.71 | -0.48 | 0.000 | 0.00 |
| 46 | 4 | 47 | 2.26 | 1.64 | -2.26 | -1.64 | 0.000 | 0.00 |
| 47 | 47 | 48 | 2.26 | 1.64 | -2.26 | -1.63 | 0.004 | 0.01 |
| 48 | 48 | 49 | 2.18 | 1.57 | -2.17 | -1.54 | 0.013 | 0.03 |
| 49 | 49 | 50 | 1.78 | 1.27 | -1.78 | -1.26 | 0.003 | 0.01 |
| 50 | 8 | 51 | 0.04 | 0.03 | -0.04 | -0.03 | 0.000 | 0.00 |
| 51 | 51 | 52 | 0.00 | 0.00 | -0.00 | -0.00 | 0.000 | 0.00 |
| 52 | 9 | 53 | 0.05 | 0.04 | -0.05 | -0.04 | 0.000 | 0.00 |
| 53 | 53 | 54 | 0.05 | 0.04 | -0.05 | -0.04 | 0.000 | 0.00 |
| 54 | 54 | 55 | 0.02 | 0.02 | -0.02 | -0.02 | 0.000 | 0.00 |
| 55 | 55 | 56 | 0.00 | 0.00 | 0.00 | 0.00 | 0.000 | 0.00 |
| 56 | 56 | 57 | 0.00 | 0.00 | 0.00 | 0.00 | 0.000 | 0.00 |
| 57 | 57 | 58 | 0.00 | 0.00 | -0.00 | -0.00 | 0.000 | 0.00 |
| 58 | 58 | 59 | 0.00 | 0.00 | -0.00 | -0.00 | 0.000 | 0.00 |
| 59 | 59 | 60 | 1.26 | 0.89 | -1.25 | -0.89 | 0.006 | 0.00 |
| 60 | 60 | 61 | 1.25 | 0.89 | -1.24 | -0.89 | 0.008 | 0.00 |
| 61 | 61 | 62 | 0.00 | 0.00 | 0.00 | 0.00 | 0.000 | 0.00 |
| 62 | 62 | 63 | -0.03 | -0.02 | 0.03 | 0.02 | 0.000 | 0.00 |
| 63 | 63 | 64 | -0.03 | -0.02 | 0.03 | 0.02 | 0.000 | 0.00 |
| 64 | 64 | 65 | -0.26 | -0.19 | 0.26 | 0.19 | 0.001 | 0.00 |
| 65 | 11 | 66 | 0.04 | 0.03 | -0.04 | -0.03 | 0.000 | 0.00 |
| 66 | 66 | 67 | 0.02 | 0.01 | -0.02 | -0.01 | 0.000 | 0.00 |
| 67 | 12 | 68 | 0.06 | 0.04 | -0.06 | -0.04 | 0.000 | 0.00 |
| 68 | 68 | 69 | 0.03 | 0.02 | -0.03 | -0.02 | 0.000 | 0.00 |
| 69 | 11 | 43 | 0.00 | 0.00 | 0.00 | 0.00 | 0.000 | 0.00 |
| 70 | 13 | 21 | 0.00 | 0.00 | 0.00 | 0.00 | 0.000 | 0.00 |
| 71 | 15 | 46 | -0.67 | -0.46 | 0.67 | 0.46 | 0.004 | 0.00 |
| 72 | 50 | 59 | 1.40 | 0.98 | -1.36 | -0.97 | 0.038 | 0.02 |
| 73 | 27 | 65 | 0.32 | 0.23 | -0.32 | -0.23 | 0.001 | 0.00 |
| | | | | | | | -------- | -------- |
| | | | | | | Total: | 0.099 | 0.09 |

**Appendix F**: Pctdemo_helper_split_scalar

```
%PCTDEMO_HELPER_SPLIT_SCALAR Divides a non-negative integer into a sum of
%smaller non-negative integers.

function [integerPerTask, numTasks] = pctdemo_helper_split_scalar(intVal,
numTasks)

%   [integerPerTask, numTasks] = PCTDEMO_HELPER_SPLIT_SCALAR(intVal, numTasks)
%   assigns a vector of length min(numTasks, intVal) to integerPerTask.
%   The sum of that vector is intVal.
%   The value of numTasks returned equals min(numTasks, numIntVal).
%
%   The input arguments must be integers greater than or equal to zero.  If
%   intVal is greater than zero, numTasks must be greater than zero.
%
%   The function is useful when dividing a Monte-Carlo simulation that is
%   repeated intVal times into numTasks tasks.  In that case, task i should
%   perform integerPerTask(i) simulations.
%
%   See also PCTDEMO_HELPER_SPLIT_VECTOR

%   Copyright 2007-2012 The MathWorks, Inc.

    % Validate the input arguments.
    narginchk(2, 2);
    tc = pTypeChecker();
    if ~(tc.isIntegerScalar(intVal, 0, Inf) ...
        && tc.isIntegerScalar(numTasks, 0, Inf))
        error('pctexample:splitscalar:SplitScalarInputsMustBePositive', ...
              'Input arguments must be non-negative integers');
    end
    if (intVal > 0 && numTasks == 0)
        error('pctexample:splitscalar:SplitScalarInvalidNumTasks', ...
              ['Number of tasks must be greater than 0 if the scalar is '...
               'greater than 0']);
    end
    % Input arguments have been validated.

    if (intVal < numTasks)
        numTasks = intVal;
    end
    if (intVal == 0)
        integerPerTask = [];
        return;
    end

    % At this point, both intVal and numTasks are strictly positive integers.
    split = fix(intVal / numTasks);
    remainder = intVal - numTasks * split;
    integerPerTask = zeros(numTasks, 1);
    integerPerTask(:) = split;
    integerPerTask(1:remainder) = integerPerTask(1:remainder) + 1;

end % End of pctdemo_helper_split_scalar
```